THE UNIVERSITY OF
SYDNEY

Novel antiviral strategies for feline coronavirus and feline calicivirus

Phillip McDonagh

A thesis submitted in fulfilment of the requirements
for the degree of Doctor of Philosophy

Pathobiology Group, Faculty of Veterinary Science

The University of Sydney

2014

Declaration of authorship

Apart from the assistance stated in the acknowledgements, this thesis represents the original work of the author. The results from this study have not been presented for any other degree or diploma at this or any other university.

Phillip McDonagh
BVSc (hons I)

March 2014

Dedication

For Nicki, Charlie, and Joe

Acknowledgements

The work described within these pages was only possible with the invaluable guidance and support of a large number of individuals. Whilst specific mention will be made of some of these in the paragraphs below, many others have contributed in ways which they, and perhaps I, don't fully appreciate. So to the unnamed, I also say thank you.

I was fortunate enough to be guided in my PhD studies by my supervisor Associate Professor Jacqui Norris and co-supervisor Associate Professor Paul Sheehy. To Jacqui, your infectious (pun possibly intended) enthusiasm for microbiology and virology helped inspire my interest in infectious diseases during my undergraduate studies, and it was a privilege to be able to return to complete post-graduate training under your tutelage. I am also eternally grateful to you for providing opportunities for me to expand my academic horizons outside of the laboratory during the course of my PhD. To Paul, you were roped into my PhD journey along the way, and it was an honour to work with someone with such an obvious passion for science. As supervisors, you were both a continual source of support and advice, allowing me plenty of scope to explore, but also making sure that I didn't stray too far. They say "life is what happens when you are busy making other plans". Perhaps that should be changed to "life is what happens when you are busy doing a PhD!" And so, on a personal note, your kindness and understanding as the rollercoaster of life took its twists and turns during my epic PhD journey was very much appreciated.

Thanks must also go to the staff of the McMaster building for creating an atmosphere that was both welcoming and so conducive to research. To Denise Wigney and Veronica Ventura in particular, thank you for keeping the lab running so smoothly. A number of researchers, both from within the faculty and external, shared their invaluable time, experience, not to mention their expensive equipment, which allowed me to successfully undertake the studies reported herein. I am particularly grateful to Karen Matthews (The University of Sydney) for providing what may be the most painless introduction to PCR ever That things "just worked" is a testament to your skill and experience in this field. Thanks also go to Dr Adrian Smith and Steven Allen (Centenary Institute of Cancer Medicine and Cell Biology), to Dr Louise Cole (Bosch Advanced Microscopy Facility), and to Dr Donna Lai (Bosch Molecular Biology Facility) for your expert advice and assistance. The feline calicivirus studies would not have been possible without the assistance of Professor James Gilkerson and Ms Natalie Job (The University of Melbourne) in providing the reference strain FCV F9 in addition to field isolates from Victoria, and Anne Fawcett for collecting FCV samples from cats in Sydney. Thanks also go to Mark Kelman of Virbac Australia for

donating recombinant feline interferon omega for these studies, and to Dr Chris Grant of Custom Monoclonals International for the donation of a range of antibodies for testing.

To my fellow PhD students, thank you for your companionship, support, and advice over the years – it has been a pleasure to work with like-minded people. I still however stand by my decision not to join in the "Carcassonne" tournaments lest my PhD candidature go even longer.

Thanks go to the Australian Companion Animal Health Foundation (Australian Veterinary Association) and the Dr William Richards Award in Veterinary Pathology (The University of Sydney) for providing financial support for these studies.

Quite simply none of this work would have been possible without my family. To my parents and brothers, thank you for your unwavering support over the years, not only through this PhD, but through every step of my life. To Mum, Dad, and Bill, thanks in particular for letting me turn your lives upside down just a little as Nicki, Charlie, and I took up residence in your homes for those final few "months" of lab work that dragged on for longer than anyone wanted. To my late brother Dave, I wish you were here to see the completed thesis. I imagine you would have skimmed rather than read it, but I know you would have been proud, and that means a lot.

The biggest thanks go my wife and sons – I cannot hope to express in these words what it is that you bring to my life. Nicki, you literally travelled to the other side of the world so I could indulge my intellectual curiosity, and that is something I will never forget. Along the way you have managed to keep me (relatively) sane, providing support and encouragement, all the while shouldering considerably more than your fair share of the household burden in raising two young children with a dad, sometimes physically, and often mentally, in absentia. In the almost embarrassingly long time I have spent in university as a student I have been fortunate to learn a lot, however to Charlie and Joe, in the blink of an eye you have taught me the most important lesson of all. Thank you.

Oh, and boys, as we draw this thesis to a close, it is now officially time for the study to be renamed the Lego room! Let's play…

List of publications and conference proceedings

Refereed publications

McDonagh, P, Sheehy, P.A., Norris, J.M. (2011) *In vitro* inhibition of feline coronavirus replication by small interfering RNAs. *Veterinary Microbiology*. 150 (3-4): 220-229

Conference presentations

Antiviral activity of small interfering RNAs on feline coronavirus replication in vitro. Australian Society for Microbiology Annual Scientific Meeting. Hobart, 2011

Publications not arising from this thesis

Worthing, K., Wigney, D.I., Dhand, N.K., Fawcett, A., **McDonagh, P.**, Malik, R., Norris, J.M. (2012) Risk factors for feline infectious peritonitis in Australian cats. *Journal of Feline Medicine and Surgery*. 14(6): 405-412.

Summary

Both feline coronavirus (FCoV) and feline calicivirus (FCV) are common infections in domestic cats, and are an important cause of morbidity and mortality in this species. Whilst most FCoV infections are asymptomatic, or result in mild self-limiting gastrointestinal disease, infection with virulent mutant FCoV biotypes can result in the development of feline infectious peritonitis (FIP), an invariably fatal immune mediated disease for which there is currently no effective therapy. Similarly, whilst many FCV infections result in only mild self-limiting oro-respiratory disease, more severe disease manifestations, such as the newly recognised FCV-associated virulent systemic disease, can occur with a significant impact on the health and wellbeing of affected cats. As with FCoV, a lack of effective antiviral agents limits treatment of FCV-associated disease to supportive therapy. The aim of the studies described in this thesis was to begin to address this therapeutic shortfall by identifying effective antiviral therapeutics for the treatment of these two important feline viruses.

Chapter 1 reviews the pertinent literature on the inherent difficulties associated with antiviral chemotherapy across all animal species, the different classes of antiviral therapeutics, with a particular emphasis on nucleic acid based therapies, and the process of antiviral drug development. The chapter culminates in a systematic review of the two viruses which are the focus of this work in terms of their importance in feline medicine, aspects of their physical structure and biology relevant to therapeutics, and places into context the unmet need for effective and safe treatments.

Chapter 2 describes some of the general methods used throughout the studies in this thesis, including general cell and viral culture methods, molecular biology methods, and imaging methods.

Veterinary practice, and in particular feline therapeutics, has a long history of therapeutic ‘trial and error’ in which drugs with proposed or theoretical benefit have been trialled in patients, with variable success. Advances in available *in vitro* methods, higher expectations of the profession and the public, industry support for the companion animal sector, and the concerns regarding ‘off label’ use of drugs has seen a shift towards a more rigorous and structured approach to drug development and testing. In light of this, Chapter 3 describes the development of cytopathic effect inhibition assays for screening compounds for antiviral efficacy against FCoV and FCV. Two different assay formats were optimised and tested for each virus, a resazurin-based assay which detects viable cells through their reduction of the substrate resazurin to fluorescent resorufin, and a sulforhodamine B-based assay which provides a measure of cell biomass, and thus an indirect indication of cell viability. Both

assay formats demonstrated excellent performance for FCoV and FCV, and based on the calculated Z'-factors would be suitable in their current form for high throughput screening. Although the SRB-based assay resulted in slightly higher Z'-factors for both viruses, the resazurin-based assay was selected for subsequent screening due to significant practical advantages, including low cost and assay simplicity. The development of this economical, robust, and reliable screening assay opens up avenues for small and large scale compound screening, allowing a physiologically relevant assessment of the efficacy of potential antiviral compounds.

Chapter 4 describes the use of the optimised resazurin-based CPE inhibition assay to screen a focused panel of nineteen compounds for antiviral activity against FCoV. Compounds were selected for inclusion in the panel based on published demonstration of antiviral effects against coronaviruses or other RNA viruses. Three compounds, chloroquine, mefloquine, and hexamethylene amiloride were demonstrated to markedly inhibit CPE (> 75% inhibition) in the screening assay and were confirmed to be potent antiviral agents at low micromolar concentrations in orthogonal confirmatory assays. Preliminary investigation into the mechanism of action of the compounds demonstrated chloroquine and hexamethylene amiloride were effective only when present in the early stages of viral replication, while mefloquine remained effective when added as late as 5 h post infection suggesting a different mechanism of action. As replication of virulent biotypes of FCoV is a triggering and perpetuating factor in the pathogenesis of FIP, the successful clinical application of these results would likely provide a critical missing piece of the therapeutic puzzle. Given two of the compounds identified, mefloquine and chloroquine, are commonly available antimalarial compounds with a long history of prophylactic and therapeutic use in humans, if demonstrated effective *in vivo* these treatments should be rapidly accessible and eminently affordable, avoiding some the practical barriers seen with the introduction of a therapeutic based on a new molecular entity.

RNA interference (RNAi) provides a promising new approach to antiviral therapy. Preliminary studies on the efficacy of this approach against FCoV, using synthetic small interfering RNAs (siRNAs), are presented in Chapter 5. All of the eight designed siRNAs had some inhibitory effect on FCoV replication, two of which were highly effective, resulting in > 95% reduction in extracellular viral titre. Further characterisation of these demonstrated them to be effective at low nanomolar concentrations, when used in combination, and when used against high viral challenge. Serial passage of virus through siRNA treated cells highlighted a weakness of the RNAi-based approach, with antiviral resistance rapidly emerging; however combination therapy with three siRNAs was able to considerably delay

this. A structural siRNA variant, Dicer-substrate siRNA, was tested and shown to provide similar or better efficacy, depending on the target, over canonical siRNAs targeted at the same motif. In addition to demonstrating the efficacy of an antiviral RNAi approach for inhibiting FCoV, the results of this study also informs its potential therapeutic application, with combinatorial therapy with a minimum of three siRNAs needed to minimise the development of viral resistance when used *in vivo*. The successful therapeutic application of these results for FIP however, will require an appropriate and affordable systemic delivery system. Based on the results reported, the benefits of this potent and specific antiviral approach should encourage further research to enable the translation of the results into a clinical setting for further evaluation.

Chapter 6 reports the identification and characterisation of a small molecule antiviral effective against feline calicivirus. Antiviral screening of the compound panel used in Chapter 4 with the optimised resazurin-based CPE inhibition assay identified only a single compound, mefloquine, displaying marked inhibitory effects against FCV. Orthogonal testing with virus yield reduction assays and plaque reduction assays confirmed the antiviral effects at low micromolar concentrations. Mefloquine, a commonly available antimalarial, was shown to be effective against a panel of recent Australian FCV isolates, with greater potency demonstrated against these field isolates than the reference strain. The seven field isolates tested were taken from cats with a range of typical FCV-associated clinical disease and from two geographically distinct regions, and thus represent an unbiased sample of circulating viruses. Demonstration of efficacy against a broad range of circulating viruses is important when considering the therapeutic application of mefloquine against a virus as genetically diverse as FCV, as treatment will only be clinically useful if effective against relevant field viruses. Combination treatment with mefloquine and recombinant feline interferon omega demonstrated additive effects and may be a clinically useful approach. Based on these data, consideration should be given to *in vivo* trials of mefloquine in cats with severe FCV-associated disease. Given the paucity of antiviral treatments available for caliciviruses in other species, the identification of a well characterised pharmaceutical with antiviral properties against feline calicivirus should prompt further investigation into its use against other related viruses.

The final experimental chapter (Chapter 7) reports on the use of RNAi against FCV. Despite the small length and highly variable nature of the FCV genome, four short highly-conserved regions were identified as suitable target regions for siRNA design. Three of the eight siRNAs designed demonstrated a marked antiviral effect with a greater than 99% reduction in extracellular viral titre. Titration of these effective siRNAs demonstrated a clear

concentration-response relationship, with IC50 values of approximately 1 nM, and combination treatment with multiple siRNAs demonstrated additive or synergistic effects. To assess the likely usefulness of the compounds in a clinical setting, siRNAs were screened against a panel of six recent Australian FCV isolates. Efficacy against currently circulating viruses was broadly reflective of that demonstrated against the reference strain FCV F9, although pre-existing resistance was noted for one isolate. The results presented in this chapter, support the further investigation into antiviral RNAi for treating severe FCV-associated disease.

The findings and limitations of the studies presented in this thesis are discussed in Chapter 8. Avenues for future research, including both *in vitro* studies and the *in vivo* therapeutic application of the antivirals identified in the previous chapters are proposed.

Table of contents

List of tables

List of figures

Abbreviations

aa	Amino acid
ACE2	Angiotensin-converting enzyme 2
ADE	Antibody-dependent enhancement
ATP	Adenosine triphosphate
BLAST	Basic local alignment search tool
BP	Band pass
bp	Base pair
BRM	Biological response modifier
CC50	50% cytotoxic concentration
CDV	Canine distemper virus
CMC	Carboxymethylcellulose
CMI	Cell mediated immunity
CNS	Central nervous system
CPE	Cytopathic effect
CRFK	Crandell Rees feline kidney cells
CSF	Cerebrospinal fluid
CV	Coefficient of variation
DAPI	4',6-diamidino-2-phenylindole
DMEM	Dulbecco’s modified Eagle’s medium
DMSO	Dimethyl sulfoxide
DNA	Deoxyribonucleic acid
DsiRNA	Dicer-substrate small interfering RNA
dsRNA	Double stranded RNA
Em	Emission

Ex	Excitation
FA	Formaldehyde agarose
fAPN	Feline aminopeptidase N (CD13)
FBS	Foetal bovine serum
FCGS	Feline chronic gingivostomatitis syndrome
FCoV	Feline coronavirus
FCV	Feline calicivirus
FCV-VSD	FCV-associated virulent systemic disease
Fcwf-4	Felis catus whole fetus cells
fDC-SIGN	Feline dendritic cell-specific intracellular adhesion molecule grabbing non-integrin
FECV	Feline enteric coronavirus
FeLV	Feline leukemia virus
FIP	Feline infectious peritonitis
FIPV	Feline infectious peritonitis virus
FITC	Fluorescein isothiocyanate
FIV	Feline immunodeficiency virus
fJAM-A	Feline junctional adhesion molecule A
GAPDH	Glyceraldehyde 3-phosphate dehydrogenase
GFP	Green fluorescent protein
HAART	Highly active antiretroviral therapy
HBV	Hepatitis B virus
HCS	High content screening
HCV	Hepatitis C virus
HIV	Human immunodeficiency virus
HMA	Hexamethylene amiloride
hpi	Hours post infection

HTS	High throughput screening
IBV	Infectious bronchitis virus
IC50	50% inhibitory concentration
IFA	Immunofluorescence assay
IL	Interleukin
INF	Interferon
JC virus	John Cunningham virus
kDa	Kilodalton
LC	Leader of the capsid
LP	Long pass
MDA-5	Melanoma differentiation-associated protein 5
MERS-CoV	Middle East Respiratory syndrome coronavirus
MHC	Major histocompatibility complex
MHV	Mouse hepatitis virus
MOI	Multiplicity of infection
NSC	Non-silencing control
nsp	Non-structural protein
nt	nucleotide
OD	Optical density
ON	Oligonucleotide
ORF	Open reading frame
PBS	Phosphate buffered saline
PCR	Polymerase chain reaction
pfu	Plaque forming units
PKR	Protein kinase R
PML	Progressive multifocal leukoencephalopathy
PMO	Phosphorodiamidate morpholino oligomers

PRA	Plaque reduction assay
qRT-PCR	Quantitative reverse transcriptase PCR
R/O	Reverse osmosis
rFeINF-ω	Recombinant feline interferon omega
RFS	Ribosomal frameshift
RFU	Relative fluorescence units
RHDV	Rabbit haemorrhagic disease virus
RIG-I	Retinoic acid inducible gene
RISC	RNA-induced silencing complex
RNA	Ribonucleic acid
RNAi	RNA interference
RSV	Respiratory syncytial virus
RTC	Replication transcription complex
S/B	Signal to background ratio
SARS-CoV	Severe acute respiratory syndrome coronavirus
SC	Subcutaneous
SD	Standard deviation
SE	Standard error
shRNA	Short hairpin RNA
SI	Selectivity index
siRNA	Small interfering RNA
SRB	Sulforhodamine B
TAE	Tris-acetate-EDTA
TCA	Trichloroacetic acid
TCID50	50% tissue culture infective dose 50%
TE	Tris-EDTA
TGEV	Transmissible gastroenteritis virus

TLR	Toll-like receptor
TNF	Tumour necrosis factor
TRS	Transcription regulatory sequence
TURBS	Termination upstream ribosomal-binding site
UTR	Untranslated region
UV	Ultraviolet
VPg	Viral protein genome-linked
VSD	Virulent systemic disease

1

Literature review

1.1. INTRODUCTION

Viral diseases are a significant cause of morbidity and mortality in domestic cats. The two primary approaches in managing viral diseases are vaccination and antiviral chemotherapeutics. Vaccination is, and will remain the most important weapon in the feline practitioner's antiviral armamentarium, and whilst it has proven effective at controlling or minimising the impact of a number of important feline viral diseases, there remain significant pathogens, such as feline coronavirus, that have thus far proved intractable to the development of a disease preventing vaccine (Pedersen, 2009). Furthermore some vaccines, such as those used for feline calicivirus, provide variable protection in the face of a heterogeneous population of circulating strains (Radford et al., 2006). Whilst the development of suitable vaccines is clearly the optimal long term solution, there exists an unmet need for safe and efficacious antiviral drugs for use in cats. Even with effective vaccines, antiviral drugs would be of benefit to treat the inevitable cases that arise in unvaccinated cats, or those in which vaccination has failed.

1.2. ANTIVIRAL THERAPEUTICS

1.2.1. The challenges of antiviral therapeutics

A recent review listed approximately 50 approved antiviral drugs for use in humans in the United States (De Clercq, 2010). Despite this impressive number, collectively they are effective against only a limited number of viruses, with over half being antiretroviral drugs for the treatment of human immunodeficiency virus (HIV) infections, and the remainder effective for the treatment of influenza virus, hepatitis B virus (HBV), hepatitis C virus (HCV), or several herpesvirus infections. Consequently, many viral infections in humans have no effective treatments. In feline medicine the situation is more pressing with no direct acting antivirals approved for clinical use, although a number of human antivirals are used off-label with variable success (Hartmann et al., 1995; Thomasy et al., 2011).

The limited number of antivirals available reflects the difficulties of developing therapeutics to treat viral diseases, both at a practical and financial level. As obligate intracellular parasites,

the replication of viruses is intricately linked to normal cell processes and thus many compounds that interfere with viral replication are inherently toxic to host cells and present a low therapeutic index. The timely administration of treatment also poses a problem for antiviral therapeutics, particularly for treating acute infections. Such a challenge is likely greater in veterinary medicine where non-specific prodromal clinical signs associated with acute viral infections in humans (e.g. headache, malaise, myalgia) are less likely to be noticed by pet owners, delaying the possibility of therapeutic intervention until after viral replication has peaked, and therefore limiting the potential efficacy of treatment. Advances in rapid cage-side diagnostics may go some way in overcoming this obstacle; however it will likely remain a significant challenge.

Another challenge encountered is the development of drug resistance during treatment, a problem so inherent with antiviral chemotherapy that Herrmann and Herrmann (1977) proposed the development of resistance to be an indicator of specific antiviral activity. The combination of short replication cycles, large numbers of progeny, and error prone replication provides a pool of mutant viruses, allowing for the rapid emergence of resistant phenotypes under the selection pressure imposed by antiviral drug treatment. The problem of resistance is particularly acute for RNA viruses owing to the poor fidelity of viral RNA dependent RNA polymerase (Domingo et al., 1996; Figlerowicz et al., 2003). The rapidity with which resistance can develop is demonstrated by the antiretroviral drug nevirapine, where resistance is seen in 35% of mothers and 52% of infected children following a single peripartum dose given to HIV positive pregnant women (Arrive et al., 2007). Combination therapy using two or more mechanistically distinct antiviral drugs can delay or prevent the emergence of resistance (Ribeiro and Bonhoeffer, 2000) and may also work synergistically, enhancing the clinical outcome and reducing host toxicity and associated side effects (Govorkova and Webster, 2010). The benefits of combination antiviral therapy are well documented for HIV and HCV infections in humans (Kanda et al., 2013; Shafer and Vuitton, 1999).

The difficulty facing antiviral drug development is a pragmatic one. From a financial perspective, the development of antiviral drugs for treating acute infections may not have the same potential windfall as those involved in treating chronic diseases, both infectious and non-infectious, as treatment is of short duration. This limits the chance for a return on the significant investment required to bring a drug to market, making them less financially attractive than other therapeutic categories.

1.2.2. Classes of antiviral therapeutics

Antiviral therapeutics can be divided into three groups based on their broad mechanism of action: virucides, biological response modifiers, or direct acting antivirals. Virucides are

chemical or physical agents that are capable of physically inactivating a virus. Owing to problems with toxicity, agents in this class are used primarily as disinfectants for inanimate objects, although virucides with more acceptable toxicity profiles, such as nonoxynol-9 or sodium dodecyl sulfate, have been investigated as a prophylactic therapy in humans for a number of sexually transmitted diseases including HIV and herpes simplex virus type 2 (Cutler and Justman, 2008; Howett et al., 1999).

Biological response modifiers (BRMs) are a diverse group of agents with the common property of modulating the host immune response. BRMs include substances produced naturally in the body like cytokines, other non-endogenous biologicals such as bacterial cell wall extracts, or synthetically produced compounds (Ford, 1986). These drugs can also have an indirect antiviral effect by stimulating the host's innate or adaptive immune response. Type I interferons are the most commonly used BRM for antiviral therapy in humans (Bergman et al., 2011). Interferons modulate the transcription of hundreds of interferon stimulated genes (ISG), the translation products of which activate intrinsic cellular pathways to inhibit viral replication by blocking transcription and translation and degrading viral RNA (recently reviewed by Sadler and Williams, 2008). Interferons can also promote apoptosis in infected cells (Clemens and Jeffrey, 2006) and have immunomodulatory effects that enhance other aspects of the innate and adaptive immune response and therefore facilitate viral clearance (Guidotti and Chisari, 2001). In small animal medicine, interferons have a long history of use with variable success. The mixed results seen with veterinary use of interferons may in part be due to the necessary use of human interferon owing, until recently, to the lack of available appropriate animal interferons. Although cross reactive, interferons are species specific (Gifford, 1963), and the use of heterologous interferons is associated with the production of neutralising antibodies which limit the longevity of their effectiveness (Zeidner et al., 1990). A recombinant feline type I interferon, interferon omega (rFeINF-ω) is now available and has reported clinical efficacy in controlled trials in treating canine parvovirus (Martin et al., 2002; Minagawa et al., 1999) and feline retroviruses (FIV/FeLV) (Doménech et al., 2011; Mari et al., 2004).

The largest and most important class of antiviral therapeutics are the direct acting antivirals. These drugs exert their antiviral effect by targeting essential viral or cellular factors involved in replication (De Clercq, 2002). Traditionally the former has been the primary focus, however an increased appreciation and understanding of the role of specific host factors in viral replication has resulted in the development of antivirals directed against host cell targets (Liang, 2008; Maeda et al., 2004). This approach is appealing in the context of minimising the development of viral resistance; however drugs targeting host factors are more likely to be intrinsically toxic due to the potential interruption of essential host cell functions. A further potential benefit is that a drug targeting cellular factors may provide a broader spectrum of

activity if the target pathway is utilised by diverse virus families. Conversely, drugs targeting virus specific factors, particularly those with no cellular homologue, are less likely to be toxic to the host, but are more likely to rapidly select for resistant viral mutants and be active against a narrow spectrum of viruses. Due to the specificity of the molecular interaction between the drug and target, the currently available antivirals, with the exception of ribavirin, all have a narrow spectrum of activity. Small molecule drugs comprise the bulk of the current antiviral armamentarium, however a number of promising novel antiviral approaches have recently emerged. At this time, many of these have not progressed beyond *in vitro* proof of principle studies, and it remains to be seen whether such success can be translated into a viable therapeutic.

1.2.2.1. Small molecule antivirals

The replication cycle of the virus and its reliance on host cell factors determine the potential targets for a small molecule antiviral. Whilst, theoretically at least, it is possible to block replication at each stage from viral attachment and entry through to assembly and release, most of the currently available small molecule antivirals target a small number of specific viral enzymes, primarily viral polymerases and proteases (De Clercq, 2010). Antiviral molecules directed against non-enzymatic targets have also demonstrated efficacy, such as the drug pleconaril which inhibits viral replication by binding to specific sites on the capsid of picornaviruses to prevent attachment and uncoating (McKinlay et al., 1992).

1.2.2.2. Oligonucleotide antivirals

Oligonucleotide (ON) antivirals are a diverse class of therapeutic agents with differing mechanisms of action but which share the common structural feature of being composed of nucleic acids. Drugs within this class have demonstrated excellent antiviral efficacy in cell culture, and in some cases animal models. Thus far their clinical application in human or veterinary medicine has been limited however, with only fomivirsen, used for the treatment of cytomegalovirus retinitis, being approved for clinical use in humans (de Smet et al., 1999). ON-based drugs can interact with proteins and nucleic acids, and can be broadly categorised based on whether that interaction is by virtue of the specific nucleotide sequence of the ON, or due to its three-dimensional shape.

The largest group of ON antivirals function by interacting with viral or cellular transcripts via Watson-Crick base pairing and, through a variety of pathways, result in transcriptional arrest or a degradation of the targeted genomic or messenger RNA. Included in this group are antisense oligonucleotides, ribozymes, and the RNA interference (RNAi)-based mechanisms of short interfering RNAs (siRNAs), Dicer-substrate siRNAs (DsiRNAs), short hairpin RNAs (shRNAs) and short interfering DNAs (siDNAs). Although these different technologies share the same underlying targeting mechanism, they have different effector mechanisms as

illustrated in Figure 1.1. Of relevance to this thesis are the RNAi-based mechanisms, in particular synthetic siRNA mediated RNAi, discussed further below.

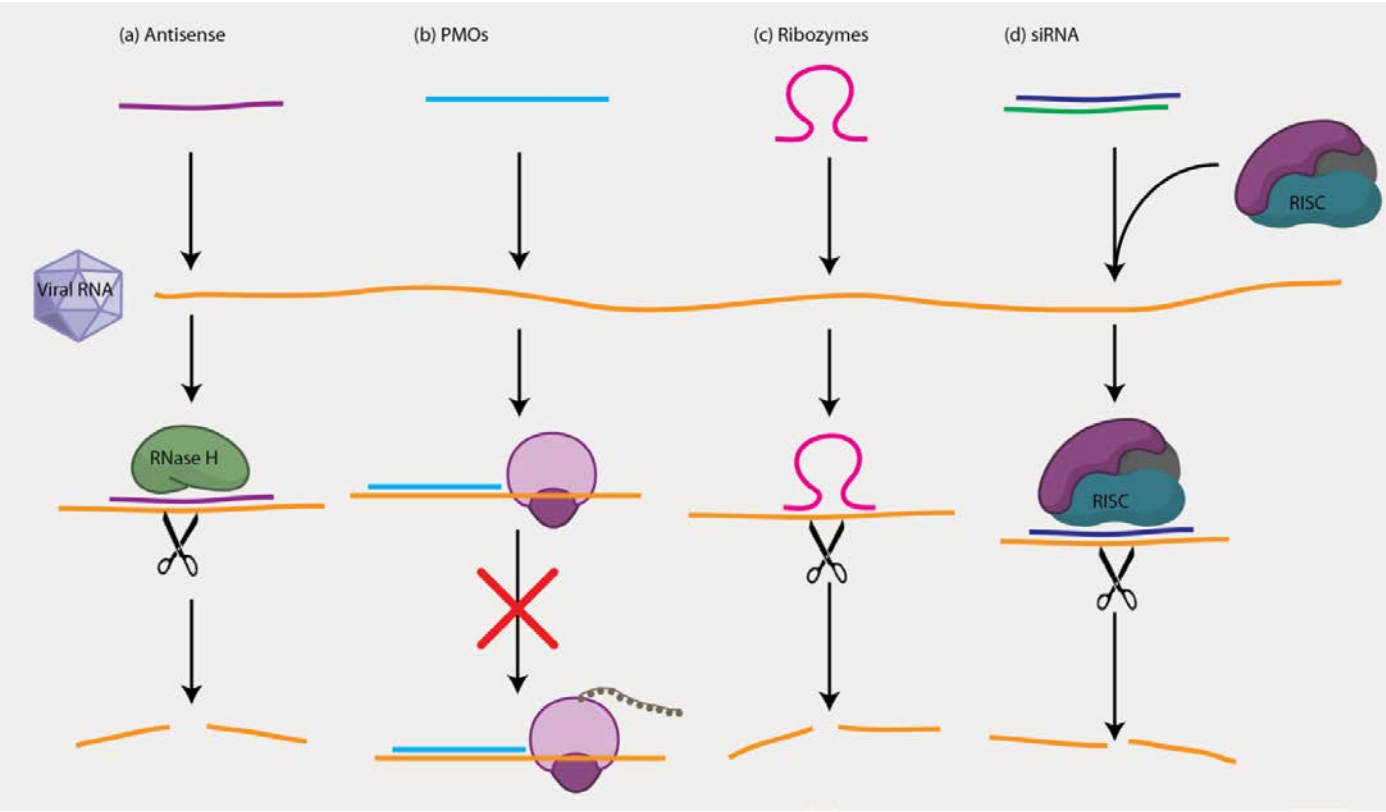

Figure 1.1: Mechanism of action of oligonucleotide antivirals interacting via Watson-Crick base pairing. (a) Antisense and (b) phosphorodiamidate morpholino oligomers (PMOs) are single-stranded DNA oligomers with sequence complementary to the target mRNA. Binding of antisense oligomers results in the RNase H-mediated degradation of the target. PMOs are modified antisense reagents in which the deoxyribose ring of the nucleotide backbone is replaced by a morpholine ring. The modified backbone of PMOs is unable to interact with RNase H, and hence the target is not degraded. Instead PMOs work through steric hindrance of mRNA translation or processing. (c) Ribozymes are catalytic RNAs capable of cleaving target RNA by virtue of their intrinsic enzymatic properties. (d) RNA interference involves the incorporation of siRNAs into RISC (RNA induced silencing complex). Binding of the activated RISC to the complementary sequence results in target cleavage.

1.2.2.2.1. RNA interference (RNAi)

The mechanism of RNAi was first described by Fire et al. (1998) as a highly potent gene silencing mechanism in the nematode *Caenorhabditis elegans*. Such silencing, thought previously to act via the antisense mechanism of a single-stranded RNA hybridising with its target, was shown instead to be mediated by double-stranded RNA. Subsequent to this initial finding in worms it was demonstrated that the RNAi mechanism is an evolutionarily conserved pathway found in most eukaryotes (Cerutti and Casas-Mollano, 2006). RNAi is involved in cellular gene regulation via the action of short endogenous non-coding RNAs known as microRNAs (miRNAs) (He and Hannon, 2004). Additionally, in some organisms RNAi plays a role as an innate antiviral defence mechanism via short interfering RNAs (siRNAs), ≈ 21 nt RNA duplexes with characteristic 2 nt 3' overhangs (Figure 1.2) derived from the cleavage of longer double-stranded RNA molecules by the cellular enzyme Dicer. Although the question is not completely resolved, the general consensus is that RNAi does not play a role in the innate antiviral defences of veterbrates. The prevailing hypothesis is that the antiviral function of RNAi in vertebrates was supplanted by the interferon response during the course of evolution, with dsRNA recognised instead by sequence independent pattern recognition receptors such as TLR3 and RIG-I triggering a cascade of cellular events to create an antiviral state (Parameswaran et al., 2010; Sidahmed and Wilkie, 2010; Umbach and Cullen, 2009). Recent results in embryonic stem cells and neonatal mice appear to challenge the hypothesis that RNAi plays no role in antiviral responses in vertebrates, however these results remain to be validated (Li et al., 2013; Maillard et al., 2013). Regardless of whether RNAi is an innate defence mechanism in mammals, the demonstration by Elbashir et al. (2001a) that this pathway could be harnessed in mammalian cells by the direct introduction of exogenous siRNAs triggered considerable interest in the therapeutic potential of RNAi.

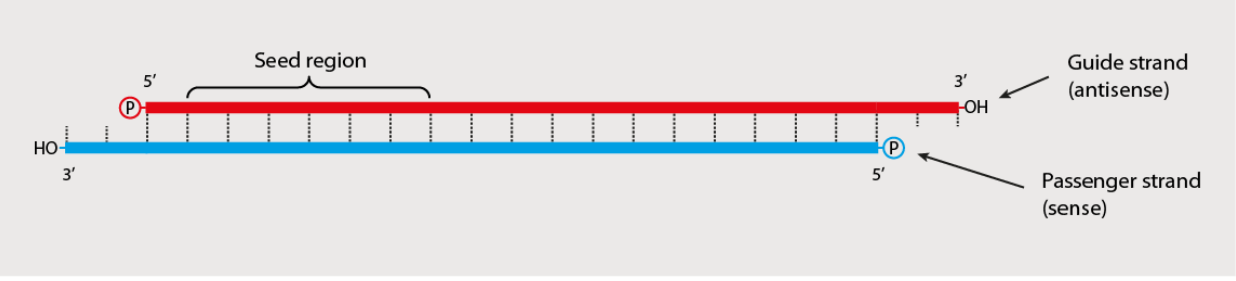

Figure 1.2: Structure of a canonical short interfering RNA (siRNA). Upon incorporation in a RNA induced silencing complex (RISC) the passenger strand is cleaved. Watson-Crick base paring between the guide strand in the activated RISC and its complimentary RNA target provides exquisite sequence specificity to this gene silencing mechanism.

The RNAi pathway is shown in Figure 1.3. A key step involves the assembly of the multiprotein RNA-induced silencing complex (RISC) incorporating a siRNA. In mammalian cells the incorporated siRNAs may be directly introduced into the cell, or they may be derived from Dicer mediated cleavage of endogenously expressed shRNAs or exogenously introduced DsiRNAs. Activation of RISC involves the cleavage and subsequent removal of one of the strands of the duplex (Leuschner et al., 2006). The preferential retention of the guide (or antisense) strand over the passenger (sense) strand in the activated RISC is based on the relative thermodynamic stability of their 5' ends (Khvorova et al., 2003). The activated RISC binds complementary RNA sequences via Watson-Crick base pairing between the guide strand and the target site and mediates cleavage of the target RNA.

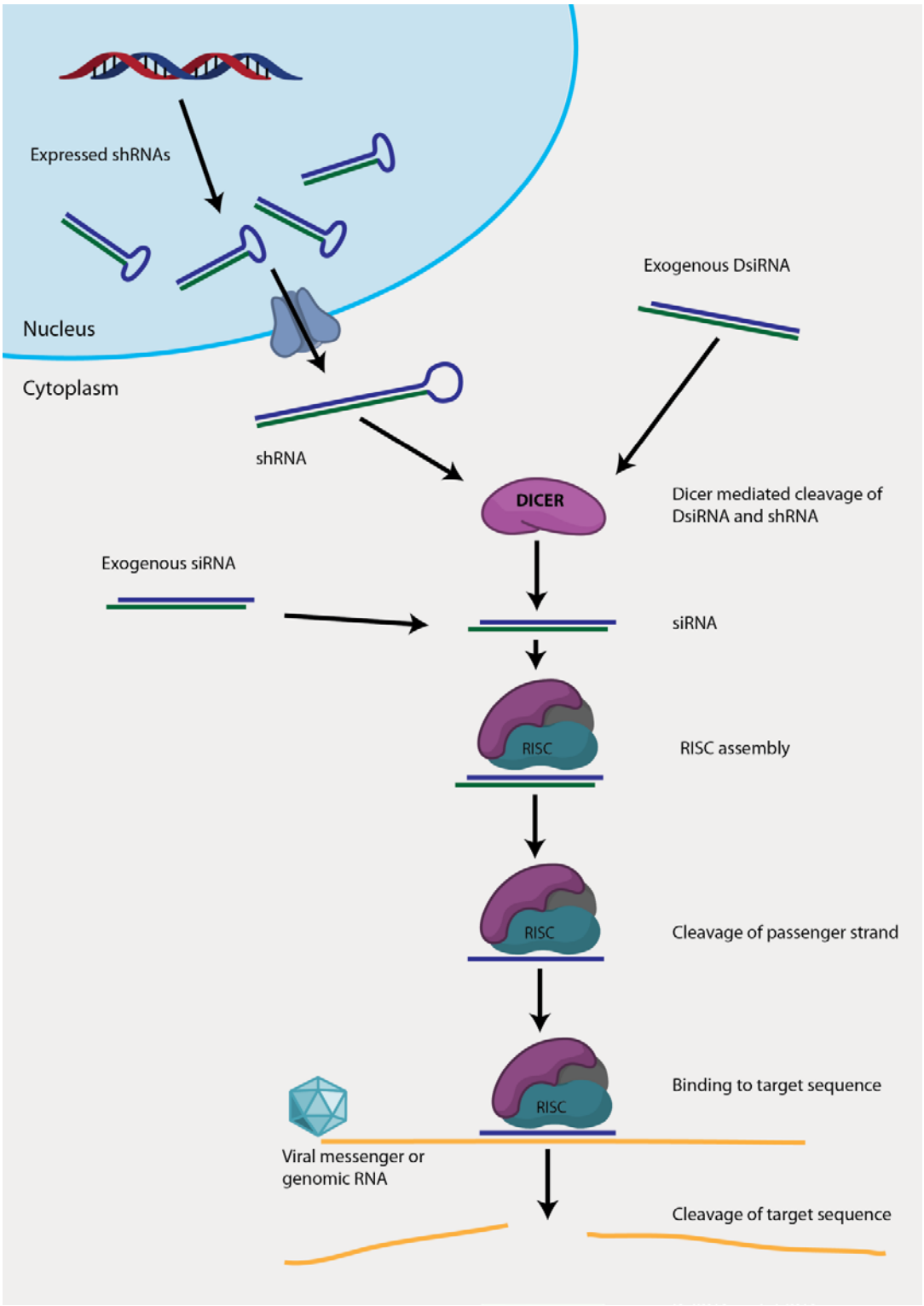

Figure 1.3: Antiviral RNAi mechanism of action. Exogenous siRNAs can be introduced directly into the cytoplasm. Alternatively siRNAs can be produced endogenously via the cleavage action of Dicer on exogenously introduced Dicer-substrate siRNAs (DsiRNAs) or on endogenously expressed short hairpin RNAs (shRNA). Irrespective of their origin, siRNAs are incorporated into RISC. The passenger strand is cleaved allowing the guide strand to bind the target sequence. The targeted viral RNA is subsequently cleaved by the endonuclease activity of RISC.

The potential antiviral application of sequence specific RNA cleavage afforded by RNAi was quickly realised. Multiple studies have demonstrated the viability of an RNAi-based antiviral strategy *in vitro* against a range of viruses of medical and veterinary significance from diverse viral families including *Retroviridae*, *Picornaviridae*, *Flaviviridae*, *Orthomyxoviridae*, *Paramyxoviridae*, *Herpesviridae*, and *Coronaviridae* (Hu et al., 2002; Jun et al., 2008; Kahana et al., 2004; Kapadia et al., 2003; McSwiggen and Seth, 2008; Shi et al., 2011; Wilkes and Kania, 2009; Wu et al., 2011). For a few viruses, such as hepatitis B virus, SARS coronavirus (SARS-CoV), influenza A virus, and HCV this success has been extended to *in vivo* models (Hean et al., 2010; Li et al., 2005a; Tompkins et al., 2004; Wang et al., 2005). Despite these early promising results, no antiviral RNAi-based therapeutic has been approved for clinical use. The failure to translate the *in vitro* success of RNAi into a practical therapeutic is mostly due to difficulties associated with delivery, stability, off-target effects, and viral escape from inhibition, however solutions to these problems are currently being actively researched and determined.

The ubiquitous presence of ribonucleases in serum and in cells rapidly results in the degradation of naked single- or double-stranded RNA and is a significant barrier to the use of synthetic siRNAs *in vivo* (Hong et al., 2010). Two main approaches have been considered to address the problem of the short serum half-life of siRNAs. Encapsulation of siRNAs in a nanoparticle delivery vehicle can provide protection by providing a physical barrier to serum nucleases (Buyens et al., 2008; Katas and Alpar, 2006). Alternatively, siRNAs can be made intrinsically more resistant to nucleases through the use of chemical modifications to the base, sugar, or backbone of the RNA (Choung et al., 2006). Unfortunately chemical modification of siRNAs may reduce efficacy and increase toxicity, however such reductions in efficacy appear to be related to the type, location, and number of modified bases, with the guide strand showing less tolerance to significant modifications (Bramsen et al., 2009). Although chemical modifications are generally thought to reduce the efficacy of the modified siRNA, a few studies have demonstrated an increase in potency, which in most cases relates to an alteration in the thermodynamic properties of the siRNA such that the guide strand is preferentially incorporated into the RISC (Allerson et al., 2005; Bramsen et al., 2009; Elmen et al., 2005).

To be effective, siRNAs must reach their target cells and enter the cytoplasm; however naked unmodified siRNAs are polar and too large (approximately 13 kDa) to cross cell membranes (Whitehead et al., 2009). *In vitro*, this problem is relatively easily overcome, most commonly using lipid-based transfection reagents. For *in vivo* use similar approaches have been successful for topical applications (Li et al., 2005a), however successful systemic delivery of siRNAs to distant sites poses additional challenges. Systemically delivered siRNA must avoid serum degradation and uptake and clearance by non-target tissues prior

to reaching their desired site of action (Huang et al., 2011). Furthermore, to minimise off-target effects it is desirable to direct siRNAs to specific target cells rather than more widespread uptake. Chemical modifications, conjugation to small molecules or peptides, or encapsulation in nanoparticle delivery vehicles have successfully increased the half-life of injected siRNAs and facilitated cell entry (Geisbert et al., 2006; Shim and Kwon, 2010). Furthermore conjugation of the siRNAs or their delivery vehicles with antibodies (Kumar et al., 2008), aptamers (Zhou and Rossi, 2011), or peptides (Kim et al., 2010) has been shown to selectively biodistribute siRNAs to a particular cell type.

Although RNAi can provide specific gene silencing, there is an increasing recognition that it is also associated with a range of off-target effects. Three types of off-target effects are recognised: (1) sequence dependent regulation of non-target transcripts, (2) activation of immune responses, and (3) effects on microRNAs due to saturation of the RNAi machinery (Jackson and Linsley, 2010). Sequence dependent off-target effects primarily occur as a result of partial complementarity, often but not exclusively between 5' end of the siRNA guide strand and the 3' UTR of the "off-target" transcripts (Jackson et al., 2006b; Tschuch et al., 2008). Given that this can occur with as little as 8 nucleotides of complementarity within the seed region (Tschuch et al., 2008) it is likely impossible to avoid this type of off-target effect, although it can be minimised by using pools of multiple siRNAs such that the concentration of each individual siRNA is minimised (Kittler et al., 2007) or by introducing position specific chemical modifications into the siRNA guide strand (Jackson et al., 2006a). Although the magnitude of sequence specific off-target effects is usually less than twofold (Jackson et al., 2006b), they may produce phenotypically relevant effects in experimental systems and *in vivo*.

Saturation of RNAi machinery by highly expressed shRNAs has the potential to cause significant off-target effects by interfering with the normal processing and function of endogenous microRNAs (Grimm et al., 2006). It is unclear whether this type of off-target effect occurs with exogenous siRNAs, as the interference in the case of highly expressed shRNAs is thought due to saturation of a nuclear export factor, a point upstream of the entry of siRNAs into the RNAi pathway (Grimm et al., 2006). It is known that transfection of multiple siRNAs may antagonise each other, suggesting competition between the siRNA species for the RNAi machinery (Bitko et al., 2005), however there is conflicting data as to whether this competition has a significant effect on endogenous microRNA function (John et al., 2007; Khan et al., 2009).

The presence of dsRNA within mammalian cells is considered a hallmark of viral infection (Jacobs and Langland, 1996), and consequently the immune system has evolved a complex network of intrinsic mechanisms to detect and respond the presence of foreign RNA

(Koyama et al., 2008). Activation of endosomal (TLR3, 7, 8) or cytoplasmic (PKR, RIG-I, MDA-5) innate immune sensors by foreign double- or single-stranded RNA triggers a cellular signalling cascade resulting in the production of cytokines that mediate acute inflammatory and antiviral responses (Koyama et al., 2008). Early studies utilising synthetic siRNAs in mammalian cells suggested these short RNA duplexes were non-immunostimulatory (Elbashir et al., 2001a) as they were shorter than the 30 nucleotides thought needed to stimulate an interferon response (Manche et al., 1992; Minks et al., 1979). It is now clear however that siRNAs are able to activate the innate immune response in both a sequence specific (Judge et al., 2005) and a non-sequence specific manner (Marques et al., 2006). Furthermore it has been demonstrated that the choice of siRNA delivery system can influence the degree of immunostimulation (Judge et al., 2005), with systems that require endosomal processing, such as liposomes, potentially triggering enhanced immune responses due to activation of TLRs (Sioud, 2005).

Several strategies have been devised to abrogate immunological off-target effects. Chemical modifications to the siRNA can reduce structurally mediated immune system activation (Sioud and Furset, 2006), however as with chemical modifications to address other off-target effects, these have the ability to significantly reduce siRNA potency. Reducing sequence-dependent immunostimulation can be achieved by designing siRNAs that do not include specifically identified immunostimulatory motifs (Hornung et al., 2005; Judge et al., 2005) or by chemical modification of the siRNAs (Hornung et al., 2005; Kariko et al., 2005). Whilst stimulation of the innate immune response has the capacity to complicate the interpretation of experimental data (Robbins et al., 2008), and may cause deleterious toxic effects for many *in vivo* gene silencing applications, this “off-target” effect may actually be beneficial for antiviral RNAi *in vivo* where the induction of an interferon response may enhance viral clearance and hence the therapeutic effect of the treatment (Gantier et al., 2010; Stewart et al., 2011).

Of specific concern to the antiviral application of RNAi is the emergence of viral resistance during treatment. Whilst this is a concern with any antiviral regimen, the exquisite sequence specificity of RNAi means that a single nucleotide mutation in the seed region of the target site can dramatically reduce the efficacy of RNAi-based viral inhibition by impairing base pairing between the guide strand and its target (Boden et al., 2003; Gitlin et al., 2005). An analogous problem is encountered in designing siRNAs against highly divergent viruses that exist as multiple circulating strains. Targeting highly conserved regions of the viral genome may help to reduce the chance of viral escape mutants developing, as mutations in these structurally or functionally constrained regions are more likely to compromise viral function and thus be deleterious. Unfortunately, mutations at sites distant to the target may allow for viral escape by altering the secondary or tertiary structure of viral RNA in such a way as to

sterically hinder RISC access (Berkhout et al., 2005). Alternatively, a mutation in a viral promoter or enhancer element distant from the target site may also allow for viral escape if such a mutation results in increased transcription of the siRNA target which can overwhelm the RNAi machinery (Schaffer et al., 2008). Combinatorial therapy with two or more siRNAs targeting distinct sites can minimise the chance of escape mutants by increasing the size of the evolutionary leap required for the resistant phenotype (Liu et al., 2009b; Schubert et al., 2005). As with traditional small molecule antivirals, an alternative approach to minimise the development of resistance is to target more genetically stable cellular genes encoding factors essential for viral replication (Novina et al., 2002; Zhang et al., 2004), however this approach has an increased potential for host related toxicity.

Despite these substantial challenges to the *in vivo* application of antiviral siRNA therapeutics, they do offer a number of advantages over conventional small molecule drugs. Theoretically at least, the specificity of RNAi allows for the specific knockdown of viral genes without affecting cellular genes and without the cellular toxicity that is often associated with traditional small molecule antivirals. The ease and speed of design is a considerable advantage of RNAi-based antiviral approaches. Effective siRNAs can be designed with no more information than a viral sequence, which with the advent of advanced sequencing methodologies is becoming less expensive and simpler (Seto, 2010), particularly when contrasted to the degree of structural, biological, and chemical knowledge required for the rational design of small molecule antivirals (see Section 1.2.3.1). For this reason RNAi-based antivirals may be particularly useful in treating emerging and less well studied viruses. The number of potential targets is also significantly greater for RNAi-based drugs compared to small molecule antivirals. Targets for traditional antivirals are primarily limited to the functional domains of viral, and to a lesser extent cellular proteins. In contrast, as RNAi-based antivirals target only short regions of viral RNA, there are many potential targets, including non-coding regions, even in viruses with the smallest of genomes.

1.2.3. Antiviral drug development

The process of antiviral drug discovery consists of a number of sequential phases as shown in Figure 1.4 (Kramer et al., 2007). The initial preclinical stage begins with the process of identifying “hit” compounds that demonstrate antiviral effects in *in vitro* screening assays. Initial hits are validated (the so called “hits to leads” stage), before suitable lead compounds are further optimised and developed to improve their efficacy, safety profile, and pharmacokinetics. Suitable candidates that emerge from this process can enter the clinical development stage to assess safety and efficacy in the target species. This process is both expensive and time consuming, with the estimated cost of developing a new molecular entity for humans, from initial screening through clinical trials to final market approval being

approximately US $1.8 billion and taking 13.5 years (Paul et al., 2010). Whilst no similar figures are available for the development of veterinary therapeutics, it is likely that the costs and time involved, although considerably lower, would be nonetheless substantial. Given the high cost of the drug discovery process, particularly as it relates to the clinical development phases, an attractive alternate strategy is drug repurposing, that is the development of novel uses for existing drugs. In addition to the obvious cost savings, identifying efficacious lead compounds with known pharmacokinetic and toxicity profiles, particularly drugs with a well-established safety profile in the field, can shorten the drug development time, giving greater potential for improved health outcomes in veterinary and human medicine. This is particularly important when dealing with a viral diseases for which there are no alternate therapies.

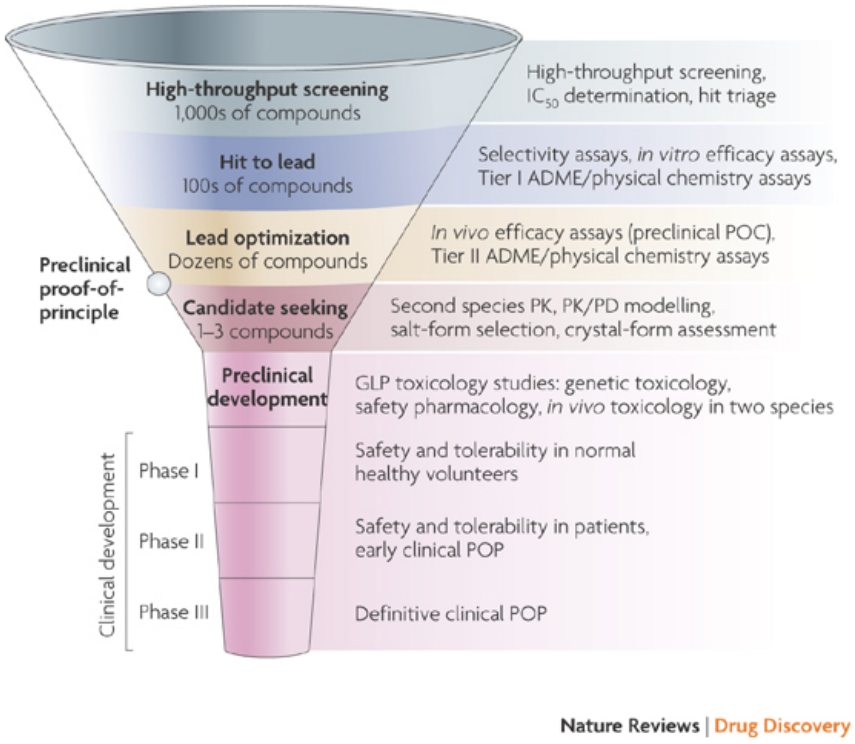

Figure 1.4: Outline of drug discovery testing scheme. Reprinted by permission from Macmillan Publishers Ltd: Nature Reviews: Drug discovery, (Kramer et al., 2007), copyright 2007.

1.2.3.1. Empirical or rational antiviral drug development

There are two general approaches to the development of drugs: empirical screening or rational, or targeted drug design (Adam, 2011). These approaches are not mutually exclusive and are in many cases complementary. The empirical approach is an unbiased one, making no assumptions and requiring no prior knowledge of molecular targets or the mechanism of action of potential lead compounds. Historically, antiviral drug discovery was

based on the empirical screening approach, from which emerged drugs that are still in clinical use today (Bauer, 1985). In contrast, rational drug design is a directed process to identify drugs interacting with a specific molecular target. Inherent in this definition is a requirement for an in depth knowledge of the viral replication cycle, the structure and function of specific viral proteins, and their interactions with host cell factors to enable identification of an appropriate target. This process has resulted in the development of a number of important antiviral molecules, including HIV protease inhibitors (Wlodawer and Vondrasek, 1998) and influenza virus neuraminidase inhibitors (von Itzstein, 2007). These rational design success stories target two of the most intensively studied human viruses. Clearly, our current level of knowledge for most companion animal viruses is vastly lower than that for HIV and influenza. Given this, and the complexities of the rational design process, the use of this methodology may be prohibitively costly for the comparatively modest funding available for companion animal antiviral research.

1.2.3.2. Antiviral drug screening

Irrespective of the drug development paradigm involved, an antiviral screening system of some type is required to assess efficacy in a specific context. The different assay formats utilised in antiviral screening can be broadly grouped into target based biochemical or *in silico* assays, and cell-based assays.

Biochemical assays are a more reductionist approach and require the identification, isolation, and purification of a suitable viral target, and thus, almost by definition can only be used as part of a rational drug design program. This approach requires considerable background knowledge of the viral replication cycle to identify a suitable target, in addition to advanced molecular biology techniques to produce sufficient quantities of pure, stable, and enzymatically active protein for screening. Biochemical-based screening allows for an uncomplicated assessment of the interaction between a drug and a target protein, resulting in assays that are highly reproducible and amenable to miniaturisation and automation. The downside of the reductionist approach is that biochemical efficacy may not translate into efficacy in a cell model or *in vivo* due to problems associated with membrane permeability, cytotoxicity, and the requirement for cellular cofactors (An and Tolliday, 2010). An alternative or adjunct to biochemical screening in the rational drug design process is the *in silico* approach of ligand-based or receptor-based virtual screening (Sousa et al., 2010). Advances in computational power now make it possible to virtually screen antiviral targets against molecular libraries containing millions of compounds. This process can identify likely lead candidates for subsequent biochemical or cell-based screens, thus reducing the cost and time involved in the random screening approach. In addition the *in silico* approach, using appropriate models, can be used to predict pharmacokinetic and toxicological

properties of candidate drugs, allowing unsuitable leads to be eliminated and thus minimise an important cause of potentially costly late stage drug failure (van de Waterbeemd and Gifford, 2003).

Cell-based screening, whilst still several steps removed from the complexities of *in vivo* studies, provides a more physiologically relevant model for assessing antiviral molecules. A significant benefit of cell-based antiviral screens is that a precise knowledge of mechanism of inhibition is not needed, as is exemplified in the case of the anti-influenza drug amantadine, for which the antiviral mechanism of action was elucidated almost 30 years after its discovery and following many years of clinical use (Davies et al., 1964; Pinto et al., 1992). Cell-based approaches are therefore suitable for less well studied viruses, a group which includes most of the viruses affecting companion animals, in addition to newly emerged human pathogens. Additional advantages of cell-based assays are the ability to screen for compounds affecting all stages of the replication cycle and the facility to gather concurrent data regarding the cytotoxicity of tested compounds.

The choice of assay system for a cell-based antiviral screen is in large part dependent on the nature of the virus. For viruses that induce cytopathic effect (CPE), the simplest determination of antiviral activity in cell culture is protection from virus induced CPE. Assessment of protection from CPE can be based on a simple qualitative morphological assessment of cell monolayers or can be a quantitative measure such as cell number, plaque number reduction, or cell viability / cytotoxicity measurements (Green et al., 2008). This latter approach, utilising a variety of different assay formats is the most commonly used due to its sensitivity, relative simplicity, and its suitability for medium to high throughput screening. Additionally, these assays are generally based on a gain-of-signal endpoint which can help to minimise false positive hits caused by toxic compounds, an important factor to consider when screening large numbers of compounds with limited replicates (Green et al., 2008). Alternative readouts of efficacy, which can also be used for non-cytopathic viruses, include quantification of infected cells using antiviral antibodies (Shum et al., 2010) or reporter viruses / cell lines (Li et al., 2009; White et al., 2007), or the measurement of viral genetic material or viral enzyme activity (Tanabe and Yamamoto, 2001). For viruses that do not grow in culture, a surrogate virus (Buckwold et al., 2003), pseudotyped virus (Larson et al., 2008), or a replicon system (Horscroft et al., 2005) may be used for screening. These approaches can also be used to alleviate biosecurity concerns when performing antiviral screening for highly pathogenic viruses that would ordinarily require PC3 or PC4 containment (Talekar et al., 2012).

1.3. FELINE CORONAVIRUS

> *"A peculiar entity with a definite predilection for cats is chronic fibrinous peritonitis, in which the fibrin deposited on the abdominal organs, especially the liver and the spleen, gradually organises into a tough, pale fibrous coating. The liver and spleen may become contracted into barely recognisable forms. Clinical signs are persistent fever, gradual loss of weight and appetite, and enlarging of the abdomen with a more or less clear fluid. The condition is seen most often, but not invariably in young cats, often several in a household or cattery. Respiratory infections and lavish dosing with various antibiotics appear in many of the histories. To date no causative organism has been isolated or any effective treatment found."* (Holzworth, 1963)

The above quote, taken in entirety from a paper entitled "Some important disorders of cats" is the first recorded reference to feline infectious peritonitis (FIP), an invariably fatal immune mediated disease. Unknown at the time, this condition is triggered by infection with virulent, mutant forms of feline coronavirus (FCoV), an extremely common viral infection of cats. True to the title of this initial paper, FIP is arguably one of the most important diseases of both domestic and wild felids, and is a common cause of infectious disease mortality in pet cats (Rohrbach et al., 2001). Since its first description as a 'peculiar entity' almost 50 years ago, considerable research effort has gone into understanding this unique disease and its causative virus, and yet despite significant advances, FIP remains somewhat of an enigma, thus far eluding any satisfying unifying description of its pathogenesis (Kipar and Meli, 2014). Perhaps more importantly, treatment options for this devastating disease remain extremely limited, and in most cases are at best palliative (Hartmann and Ritz, 2008). The development of effective antiviral therapeutic against FCoV may provide hope in treating this devastating disease.

1.3.1. Virology of feline coronavirus

1.3.1.1. Taxonomy – groups, serotypes, and biotypes

The family *Coronaviridae* includes a number of important human and veterinary pathogens. A recent taxonomic reorganisation of this family has placed feline coronavirus, along with canine coronavirus, porcine respiratory coronavirus, and porcine transmissible gastroenteritis virus, in the species *Alphacoronavirus 1*, the type species of the genus *Alphacoronavirus*, subfamily *Coronavirinae*, family *Coronaviridae*, order *Nidovirales* (see Table 1.1) (de Groot et al., 2012). The grouping of these coronaviruses with disparate hosts into a single species is based upon analysis showing greater than 96% amino acid sequence homology in

conserved regions of replicase polyprotein 1ab, a value significantly higher than the species demarcation threshold of 90% (Carstens and Ball, 2009).

Table 1.1: *Coronaviridae* taxonomy adapted from the Ninth Report of the International Committee on Taxonomy of Viruses (de Groot et al., 2012). * indicates type species.

Taxonomy of the order *Nidovirales*

- **Family** *Arteriviridae*
- **Family** *Roniviridae*
- **Family** *Coronaviridae*
    - **Subfamily** *Torovirinae*
    - **Subfamily** *Coronavirinae*
        - **Genus** *Alphacoronavirus*
            - Alphacoronavirus 1 *
                - **Feline coronavirus**, canine coronavirus, porcine transmissible gastroenteritis virus
            - Porcine epidemic diarrhoea virus
            - Human coronavirus 229E
            - Human coronavirus NL63
        - **Genus** *Betacoronavirus*
            - Betacoronavirus 1
            - Severe acute respiratory syndrome associated coronavirus (SARS-
            - Human coronavirus OC43
            - Murine coronavirus *
        - **Genus** *Gammacoronavirus*
            - Avian coronavirus *
            - Beluga whale coronavirus

1.3.1.1.1. FCoV serotypes

Feline coronaviruses cluster in two distinct serotypes (type I and type II) distinguished on the basis of virus neutralisation assays with type-specific sera (Pedersen et al., 1984) or spike protein monoclonal antibodies (Hohdatsu et al., 1991b), or on sequence analysis of the spike protein open reading frame (ORF) (Herrewegh et al., 1998). The two serotypes differ in their origin and relation to canine coronavirus (CCoV), *in vitro* growth characteristics, and natural distribution (see Table 1.2). Type I FCoV is considered a wholly feline virus, while type II FCoV most likely arose through a double recombination event between type I FCoV and CCoV (Herrewegh et al., 1998). Because of this, type II FCoV are neutralised by CCoV

specific antibodies, while type I FCoV are not neutralised, or poorly neutralised by CCoV antibodies (Pedersen, 1995).

The serotypes differ markedly in their *in vitro* growth characteristics (Pedersen et al., 1984). Type I FCoVs grow poorly in cell culture and produce a slowly developing cytopathic effect, while type II FCoVs grow well in culture and show a pronounced cytopathic effect (Pedersen, 1995). The difference in *in vitro* growth characteristics has been shown, at least in part, to be due to differences in receptor utilisation (see 1.3.1.4.1) (Dye et al., 2007; Regan and Whittaker, 2008; Tekes et al., 2010; Van Hamme et al., 2011).

The worldwide distribution of type I versus type II FCoV has been shown to vary, however in all reported studies type I FCoV is clearly the most prevalent (Addie et al., 2003b; Benetka et al., 2004; Hohdatsu et al., 1992; Kummrow et al., 2005). Despite this, type II viruses are the more intensively studied due primarily to the ease with which they can be cultured.

Table 1.2: Comparison of type I and type II feline coronavirus (FCoV).

	Serotype I	**Serotype II**
Origin	Feline virus	Recombinant FCoV/CCoV
Neutralisation by CCoV antibodies	No / poor neutralisation	Neutralise to high titres
Cellular receptor(s)	fDC-SIGN (CD209), ?	fAPN (CD13), fDC-SIGN, ?
Growth in cell culture	Poor	Good
Optimal cell line	Fcwf-4	CRFK
CPE in cell culture	Slowly developing CPE	Marked CPE (24-38 hours)
Worldwide prevalence	High	Low
Isolated from cases of FIP	Yes	Yes
Examples isolates	UCD1 Black	FIPV-1146 FECV-1683

1.3.1.1.2. FCoV biotypes

In addition to the two serotypes, two biotypes or pathotypes of FCoV have been demonstrated. These biotypes are referred to as feline enteric coronavirus (FECV) and feline infectious peritonitis virus (FIPV). Infection with FECV typically results in subclinical or mild enteritis (Addie and Jarrett, 1992b; Hickman et al., 1995; Mochizuki et al., 1999; Pedersen et al., 1981). In contrast, infection with FIPV biotypes is associated with significant disease, which for the more virulent strains, such as FIPV WSU 79-1146 (FIPV1146), is invariably fatal (Pedersen, 2009). A number of studies have confirmed both type I and II FCoVs can cause FIP as well as mild or inapparent enteric infections (Benetka et al., 2004;

Hohdatsu et al., 1992). The clear *in vivo* difference in the behaviour of the biotypes is mirrored in *in vitro* studies in primary feline monocytes and macrophages where FECV strains demonstrate a reduced ability to infect and replicate (Dewerchin et al., 2005; Stoddart and Scott, 1989). The difference in *in vitro* properties of the biotypes is not seen in continuous cell lines, where the growth characteristics of the biotypes are similar (Dewerchin et al., 2005; McKeirnan et al., 1987).

Two alternative hypotheses have been proposed to explain the origin of virulent biotypes and hence the development of FIP – the internal mutation hypothesis and the circulating virulent / avirulent hypothesis. The internal mutation hypothesis is the more widely accepted and supported, and postulates that virulent viruses arise within an infected cat during the replication of avirulent biotypes (Chang et al., 2011; Pedersen et al., 2009; Poland et al., 1996; Vennema et al., 1998). It is posited that mutations arise during the error prone replication of FCoV that enhance its macrophage tropism, resulting in the FIPV biotype, and that the manifestation of FIP is dependent upon the subsequent immune response to the increased replication of the macrophage tropic virus (Groot-Mijnes et al., 2005). If true, an obvious corollary of the internal mutation theory is that virulent coronaviruses isolated from individual cats with FIP should be unique, a feature challenged by the alternative hypothesis of circulating virulent / avirulent strains proposed by Brown et al. (2009). This alternative hypothesis was based on phylogenetic analysis of FCoVs from 46 healthy cats and 8 cats with FIP in a small geographically localised study that showed viral sequences clustered by disease state, with viruses from healthy cats distinct from those from cats with FIP. Subsequent studies from different locales, and which included a greater number of FIPV sequences, have failed to show similar clustering by biotype (Chang et al., 2011; Pedersen et al., 2012).

A number of different mutations have been suggested as being responsible for the acquisition of virulence. Mutations in the spike gene (Rottier et al., 2005) or the accessory genes 3c (Chang et al., 2010; Pedersen et al., 2009; Vennema et al., 1998), 7a (Kennedy et al., 2001), and 7b (Vennema et al., 1998) have all been suggested. Loss of function mutations in the 3c gene are found in a majority, but not all FIPVs suggesting its role as a contributor to or alternatively as a marker of virulence (Chang et al., 2010; Pedersen et al., 2012). Loss of function mutations in the 3abc ORF have been demonstrated to result in enhanced replication in primary feline monocytes, suggesting it is more likely to be the former (Bálint et al., 2012). More recent studies by this group examined the *in vivo* effects of loss of function mutations in ORF 3abc and showed that restoration of an intact 3abc ORF in FIPV DF-2 (a virulent type II FCoV) through targeted recombination is associated with *in vivo* biological behaviour similar to that of a FECV, with an attenuated clinical phenotype, absence of viraemia, and high titre faecal shedding (Bálint et al., 2014). Recently, it has also

been reported that mutations in the spike ORF are frequently identified in FCoV isolates from cats with FIP (Chang et al., 2012; Licitra et al., 2013). These findings may account for the enhanced macrophage tropism and support the earlier results of Rottier et al. (2005) which demonstrated, using a chimeric viruses, that enhanced macrophage replication *in vitro* is associated with mutations in the spike protein. From these combined results it appears likely that multiple mutations may be involved in the acquisition of the FIPV biotype. If multiple mutations are required, this may provide an explanation for the discrepancies previously reported between the internal mutation hypothesis and the circulating virulent / avirulent hypothesis (O'Brien et al., 2012). The result of Brown et al. (2009), interpreted in a different light, would support the hypothesis that some circulating strains may be more prone to mutations or be closer to acquiring the critical mutations required for the FECV to FIPV transition. A modified version of the circulating virulent / avirulent hypothesis may therefore be compatible with the internal mutation hypothesis, and the weight of data that support it.

1.3.1.2. Coronavirus structure and morphology

Morphologically, coronaviruses are enveloped, spherical or pleomorphic in shape, between 80-120 nm in size, with a helical nucleocapsid (Masters, 2006). Projecting from the surface of the virion are large (approximately 20 nm) club shaped peplomers responsible for its characteristic “crown-like” appearance in electron micrographs (Neuman et al., 2006), and from which they derive their name (de Groot et al., 2012). Coronaviruses have a monopartite linear positive-sense single-stranded RNA genome that encodes four major structural proteins, S, M, E, and N, in addition to a number of non-structural proteins (Masters, 2006).

1.3.1.2.1. Non-structural proteins

1.3.1.2.1.1. Replicase protein

Translation of the replicase gene is the initial step in viral replication. In common with other coronaviruses (and all known members of the order *Nidovirales*) the replicase gene of FCoV consists of two large ORFs (1a and 1b) which overlap, and which contain a ribosomal frameshift element consisting of a “slippery” sequence and an adjacent downstream pseudoknot structure (Brierley, 1995; Dye and Siddell, 2005, 2007). The ribosomal frameshifting element results in a proportion of the ribosomes translating ORF1a to shift into the -1 reading frame, resulting in a failure of protein synthesis to terminate at the ORF1a stop codon. Continued translation beyond the ORF1a stop codon results in the production of the large pp1ab replicase polyprotein, in addition to the smaller pp1a polyprotein produced without the frameshift. Extensive post translational proteolytic processing of pp1a/ab by three autoproteinases encoded by ORF1a result in a predicted 16 mature non-structural proteins (Figure 1.5) (Dye and Siddell, 2005, 2007; Tekes et al., 2008; Ziebuhr and Snijder, 2007).

1.3.1.2.1.2. **Accessory proteins**

The number and configuration of the coronavirus accessory protein ORFs is highly variable among the genera (Masters, 2006). FCoV encodes for five accessory proteins – 3abc and 7ab in two clusters (Dye and Siddell, 2005). The FCoV accessory protein genes have been demonstrated to be non-essential *in vitro* (Haijema et al., 2003; Haijema et al., 2004), as is the case for all other examined coronaviruses (Masters, 2006). The role of the FCoV accessory proteins remains to be determined. An intact 3c gene appears important for intestinal but not systemic replication, however the mechanism through which it acts is unclear (Chang et al., 2010; Pedersen et al., 2012). It has been suggested that mutations in the accessory genes is associated with increased virulence however complete deletion of the 3abc and 7ab gene clusters resulted in an attenuated phenotype *in vivo* (Haijema et al., 2004).

1.3.1.2.2. Structural proteins

1.3.1.2.2.1. **Spike protein (S)**

The spike protein, a class 1 fusion protein with a large ectodomain and a small endodomain, is the largest coronavirus structural protein (Dye and Siddell, 2005). Heavily glycosylated spike protein monomers combine to form a mature homotrimers, which protrude from the surface of the viral envelope to form the distinctive petal shaped peplomers (Masters, 2006). The coronavirus S protein is divided into two domains, S1 and S2. S1 comprises the amino terminal globular head at the tip of the peplomer and is responsible for cellular attachment and therefore cell tropism. Supporting this is data showing murine, but not feline cells are permissive to recombinant FCoV bearing the S protein ectodomain of mouse hepatitis virus (MHV) (Haijema et al., 2003). The S2 subunit includes the stalk of the peplomer, in addition to the transmembrane and endodomains. A fusion peptide located on S2 mediates and virus-cell and cell-cell fusion (Wentworth and Holmes, 2007). The peplomers present important humoral (Gonon et al., 1999) and cell mediated antigenic determinants (Groot-Mijnes et al., 2005) involved in viral clearance.

1.3.1.2.2.2. **Envelope protein (E)**

The E protein is the smallest and least abundant of the coronavirus structural proteins (Masters, 2006). For several coronaviruses this protein has been shown to form ion channels (viroporins) in cell membranes (Wilson et al., 2006a). The envelope protein mediates viral assembly and morphogenesis, although the mechanism through which it achieves this is unclear (Fischer et al., 1998; Vennema et al., 1996; Ye and Hogue, 2007). The E protein is poorly conserved across coronavirus genera (Masters, 2006).

1.3.1.2.2.3. **Membrane protein (M)**

The M protein is the most abundant viral protein and is thought to play the primary role in virion assembly through both homotypic and heterotypic interactions (de Haan et al., 2000; Masters, 2006). It is a multispanning integral membrane protein, with a small amino-terminus ectodomain located on the outside of the virion, three transmembrane domains, and a large endodomain in the interior of the virion. The M protein is moderately well conserved among coronaviruses, with the most highly conserved region being a stretch of approximately 25 aa comprising the end of the third transmembrane domain and the start of the endodomain (Masters, 2006). The amino terminal ectodomain expressed on the virion surface is the least conserved region (Lai and Cavanagh, 1997; Masters, 2006), likely owing to increased selection pressure from host immune responses.

1.3.1.2.2.4. **Nucleocapsid protein (N)**

The N protein is a multifunctional protein that has both structural and non-structural roles. As a structural element, the N protein binds to the single-stranded RNA genome, in both a sequence-specific and non-specific manner (Cologna et al., 2000), to form a helical nucleocapsid, that is packaged to form an infectious virion in a process mediated by interactions with the M protein (Narayanan et al., 2000). Additional to this structural role, there is considerable evidence that the N protein serves functions in viral replication, transcription, and translation. A proportion of the N protein co-localises with the membrane bound replication-transcription complexes (RTCs) in the early stages of infection, supporting the idea of its role in RNA replication (Denison et al., 1999). It has been demonstrated using TGEV replicons that the presence of the nucleocapsid protein is required for efficient coronavirus replication (Almazan et al., 2004), and using anti-nucleocapsid antibodies it was demonstrated that synthesis of genome sized RNA was decreased by greater than 90% using an *in vitro* MHV replication system (Compton et al., 1987). Although the N protein has a significant effect on the viral replication and transcription, the concentration of free nucleocapsid proteins in MHV infected cells is relatively high, suggesting it is unlikely to be a rate-limiting factor for RNA synthesis (Perlman et al., 1986). The overall N protein homology between coronavirus groups is low however there are stretches of high amino acid homology within the N protein, suggesting the presence of structurally or functionally constrained elements (Lapps et al., 1987).

1.3.1.3. Genome

At 27.3 to 31.3 kb in size, the coronavirus genome is the largest RNA genome yet identified, being approximately 3 to 4 times larger than other typical RNA viruses (Masters, 2006). This increased coding capacity has enabled the evolution of considerable genomic complexity within the coronaviruses. The genome of FCoV is approximately 29 kb in size (Dye and

Siddell, 2005, 2007), and in common with all other coronaviruses the genome contains multiple ORFs as depicted in Figure 1.5. The replicase gene, at over 20 kb, consists of two ORFs (ORF1a and ORF1b), and occupies the proximal two-thirds of the 5' end of the genome. The remaining structural and accessory genes are located in the 3' one-third. As with all other known coronaviruses, the spatial organisation of the FCoV genome shows the four canonical structural genes are fixed in the order S,E, M, and N (de Groot et al., 2012). Located between the structural genes are the genes encoding the accessory proteins – 3abc located between S and E, and 7ab located at the 3' most end of the genome downstream from N ORF. FCoV possesses a 5' untranslated region (UTR) of approximately 300 nt, and a 3' UTR of a similar size, followed by a poly(A) tail. Both the 5' and 3' UTRs contain putative *cis*-acting structures (Dye and Siddell, 2005). The 5' UTR contains the leader sequence, a 92 nt sequence that is important for viral transcription and translation (Dye and Siddell, 2005). Immediately downstream of the leader sequence is the transcription-regulatory sequence (TRS) [5'-CUAAAC-3'] (De Groot et al., 1988; Dye and Siddell, 2005), sometimes referred to as the intergenic sequence. Identical "body" TRS motifs are located at the 5' end of most ORFs (Dye and Siddell, 2005), and are responsible for determining the fusion sites of the 5'-leader and 3'-body segments during the discontinuous transcription process (Sawicki et al., 2007) .

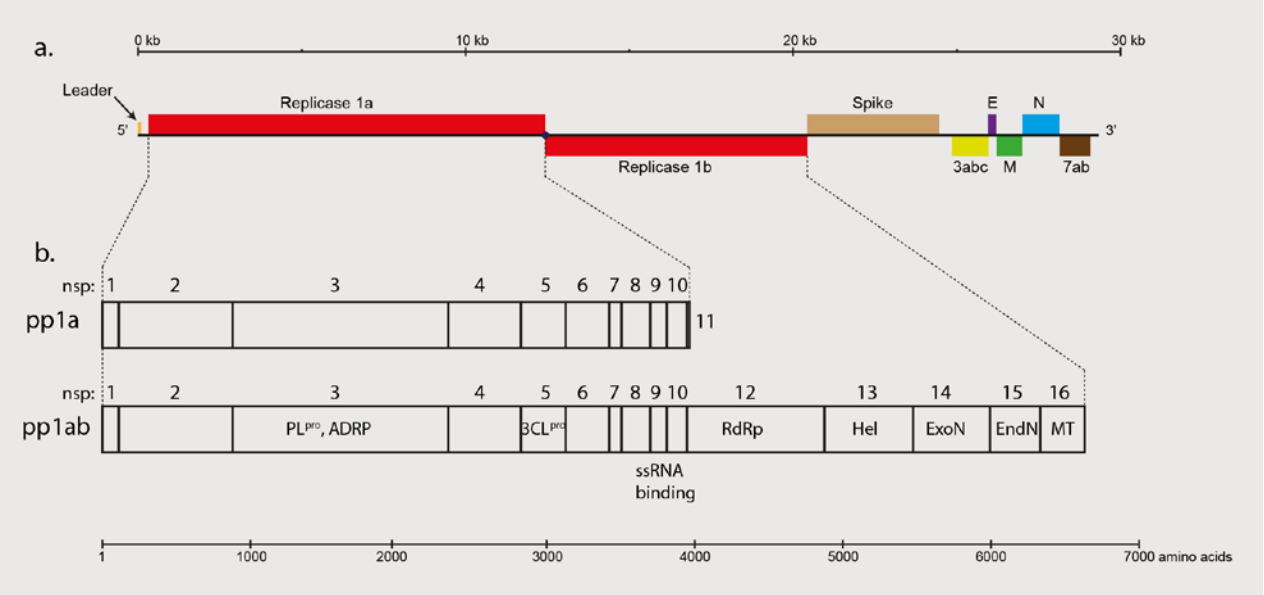

Figure 1.5: Feline coronavirus genome. Schematic of FCoV genome (a) and predicted cleavage map of FCoV replicase polyproteins (b) according to Dye and Siddell (2005). Proteolytic processing of replicase polyprotein 1a (pp1a) gives rise to non-structural proteins (nsp) 1 to 11 while processing of replicase polyprotein 1ab (pp1ab) produced by ribosomal frameshifting gives rise to nsp 1 to 10 and nsp 12 to 16. Putative functions have been ascribed to a number of the nsp which are listed in the figure. E, envelope; M, membrane; N, nucleocapsid; PL^{pro}, papin-like proteinase; ADRP, ADP-ribose 1"-phosphatase; $3CL^{pro}$, 3C-like proteinase; ssRNA, single-stranded RNA; RdRp, RNA-dependent RNA polymerase; HEL, helicase; ExoN, exonuclease; EndN, endonuclease; MT, 2'-O-methyltransferase.

Like all RNA viruses, coronaviruses are prone to high mutation rates due to the inherent low fidelity of the RNA dependent RNA polymerase (Domingo et al., 1996; Holland et al., 1982). Unlike other known RNA viruses however, coronavirus nsp14 likely functions with a proofreading mechanism that can regulate replication fidelity (Denison et al., 2011; Minskaia et al., 2006). It is speculated that this improved fidelity may have allowed for the evolution of the exceptionally large coronavirus genome (Holmes, 2009). In addition to deletions and mutations contributing to genetic diversity, homologous recombination occurs frequently in coronaviruses (Lai, 1996) and has been demonstrated in FCoV (Herrewegh et al., 1998). The resulting high levels of genetic diversity result in a heterogeneous population of viruses, a feature which has been demonstrated for FCoV *in vitro* and *in vivo* (Gunn-Moore et al., 1999; Kiss et al., 1999). The quasispecies nature of FCoV replication is thought to have important implications for viral persistence and pathogenesis, as the resultant swarm of mutant viruses provides a large reservoir of potentially advantageous phenotypes in the face of external change, including the development of resistance to antiviral therapeutics (Lauring and Andino, 2010). The error prone replication of FCoV also increases the likelihood of virulent macrophage tropic mutants arising, and thus the occurrence of FIP.

1.3.1.4. FCoV life cycle

1.3.1.4.1. Attachment and entry

Details of interactions between FCoV and host cells are only partly understood and differ between serotype I and II viruses. *In vitro* studies have identified two potential receptors involved in FCoV attachment and entry, although it is clear from these results that additional factors are involved. The first receptor identified, feline aminopeptidase N (fAPN) [CD13] (Tresnan et al., 1996), is a glycoprotein expressed on the surface of numerous cell types, including granulocytic and monocytic haematopoetic cells and epithelial cells of the intestinal brush border, and highly expressed on the commonly used CRFK cell line (Van Hamme et al., 2011). Using immortalised cell lines and primary feline monocytes/dendritic cells fAPN has been demonstrated to act as a receptor for serotype II viruses but not type I viruses (Dye et al., 2007; Hohdatsu et al., 1998; Regan and Whittaker, 2008; Tekes et al., 2010; Van Hamme et al., 2011). The second identified receptor, feline dendritic cell specific intracellular adhesion molecule grabbing non-integrin (fDC-SIGN) [CD209] (Regan et al., 2010; Regan and Whittaker, 2008; Van Hamme et al., 2011), is involved in viral entry for both type I and II viruses (Regan et al., 2010; Van Hamme et al., 2011), but for type I FCoV it is thought to be involved in the replication cycle at a point after virus binding (Van Hamme et al., 2011). Following receptor binding, cell entry for both type I and II FCoVs in primary monocyte cultures occurs via endocytosis (Van Hamme et al., 2007). Using the serotype II FCoV FIPV1146, this receptor mediated endocytic pathway was shown to be dependent on dynamin, but independent of both caveolae and clathrin (Van Hamme et al., 2008).

In addition to these classical mechanisms of cell entry, FCoV can also enter monocytes / macrophages via Fc receptor mediated uptake (Hohdatsu et al., 1991a). This process, known as antibody-dependent enhancement (ADE) of infection occurs following opsonisation of viral particles by non-neutralising antibodies directed towards the S or M proteins (Corapi et al., 1995; Hohdatsu et al., 1991a). ADE has been documented to occur *in vitro* (Olsen et al., 1992; Takano et al., 2008a) and experimentally *in vivo* (Scott et al., 1995; Takano et al., 2008b; Weiss and Scott, 1981b), however its occurrence in natural infections has been questioned (Addie et al., 2003b; Addie et al., 1995b).

1.3.1.4.2. Viral RNA synthesis

The coronavirus genome performs a dual role, functioning as a mRNA for the translation of viral replicative proteins and as a template for genomic and mRNA synthesis. RNA synthesis takes place in double membrane vesicles via the action of virally induced replication-transcription complexes (RTCs) (Gosert et al., 2002). Non-structural proteins (nsp) produced by cleavage of the large polyproteins 1a/1ab, viral nucleocapsid protein, and viral RNA have been demonstrated to co-localise in RTCs (van der Meer et al., 1999).

Coronavirus transcription produces a set of mRNAs that have a common 3' end followed by a poly(A) tail, a defining feature of viruses in the order *Nidovirales* (de Groot et al., 2012). FCoV produces a set of seven mRNAs which by convention are named mRNA1 to 7 in order of decreasing size, as shown in Figure 1.6 (Dye and Siddell, 2005). mRNA1 is a full length genome transcript, while the remainder are subgenomic in size. The mRNA species are produced in different quantities throughout the course of infection, however their molar ratio remains constant, with a relative abundance that is in general inversely proportional to their length (Van Marle et al., 1995). All coronavirus mRNAs, in addition to 3' nesting, also contain an identical 5' leader sequence derived from the 5' end of the genome. To achieve this, coronaviruses possess a unique discontinuous transcription mechanism. It was initially hypothesised that discontinuous transcription was a leader-primed mechanism that occurred during positive-sense RNA transcription (Lai, 1986). There is now a general, although not unanimous, consensus that the discontinuous transcription takes place during the synthesis of subgenomic negative-sense intermediates (Sawicki et al., 2007). In this model, proposed by Sawicki and Sawicki (1995), transcription of the negative-sense strand begins at the 3' end of the positive-sense genome template and progresses until a body TRS is encountered. Through mechanisms unknown, a fixed proportion of RTCs suspend transcription at the TRS, while the remainder continue through to the next body TRS, where a similar "decision" is made. If transcription is suspended at a body TRS, the nascent negative-sense strand is relocated to the 5' end of the template, where transcription is resumed and the leader sequence is synthesised. The negative-sense subgenomic and genomic mRNA strands produced are used as templates for the synthesis of functioning positive-sense subgenomic mRNAs and full genome copies respectively.

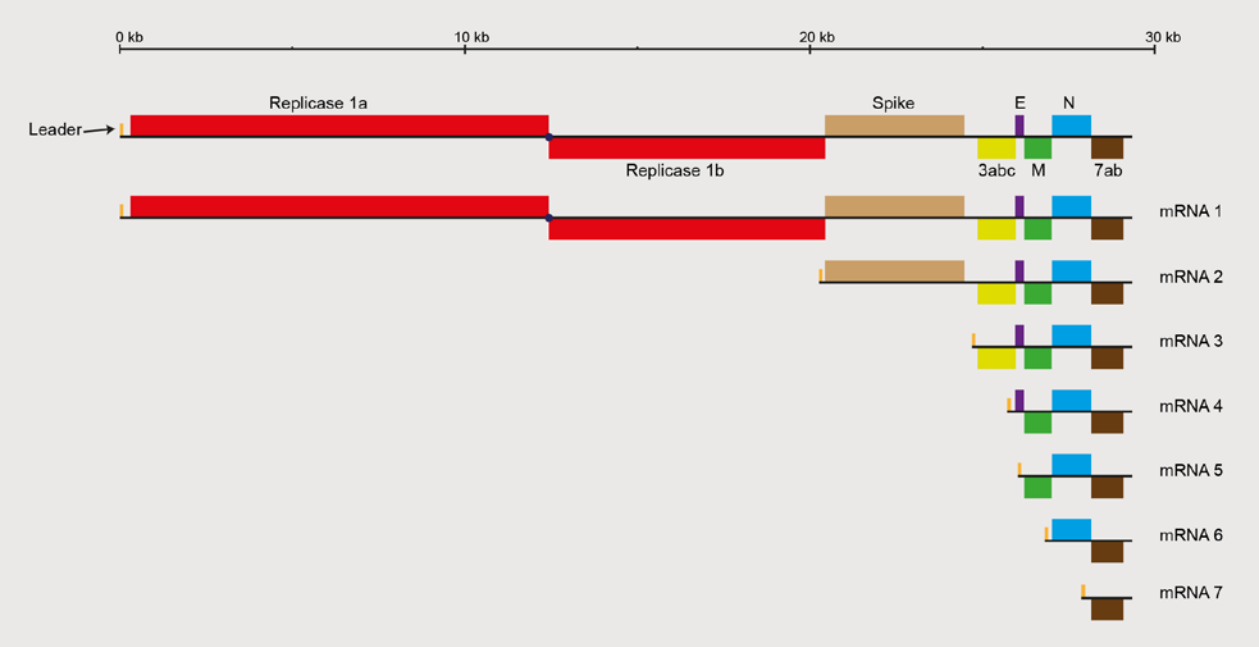

Figure 1.6: Schematic of FCoV genome and subgenomic mRNA species. The discontinuous nature of FCoV transcription results in the production of a nested set of seven subgenomic mRNA species with a common 5' leader sequence and 3' UTR.

1.3.1.4.3. Translation of viral proteins

Although coronavirus mRNAs are structurally polycistronic, in most cases they are functionally monocistronic, with only the 5' terminal ORF translated. However, as not all coronavirus genes are located 5'-terminal on an mRNA species, some mRNAs must act as polycistronic messengers. In the case of FCoV, multiple ORFs are translated from mRNA 1 (ORF1a and b), mRNA3 (ORF3a, 3b, and 3c), and mRNA7 (ORF7a and b) (Dye and Siddell, 2005). Translation of the 5' most ORF of an mRNA is thought to occur by a standard cellular 5' cap-dependent ribosome entry mechanism (Lai et al., 1982), with several non-structural viral proteins identified as being involved in the capping process (Decroly et al., 2011; Decroly et al., 2008). Alternative mechanisms of translation are utilised for internal ORFs. Translation of the internal ORF1b of mRNA1 occurs via a programmed -1 ribosomal frameshift (Brierley, 1995; Dye and Siddell, 2005, 2007). The mechanism of translation for other FCoV internal ORFs (3b, 3c, and 7b) is unknown, although a cap-independent internal ribosomal entry mechanism and a leaky scanning mechanism have been demonstrated for similar internal ORFs in IBV, TGEV, and MHV (reviewed by Lai and Cavanagh, 1997).

Translation of coronavirus proteins has been shown to be positively regulated by the common 5' leader sequence which acts in *cis* to enhance translation of viral mRNA and the nucleocapsid protein with which it interacts (Tahara et al., 1994; Tahara et al., 1998). This enhancement, although incompletely understood occurs in the face of a generalised shutdown of host cell protein synthesis (Hilton et al., 1986; Raaben et al., 2007).

1.3.1.4.4. Virus assembly and release

Assembly of coronavirus virions occurs in the endoplasmic reticulum and the vesicular-tubular cluster in a process driven primarily by the M protein (de Haan et al., 2000; Neuman et al., 2011). The S protein has been shown to be non-essential for the production of virus-like particles, however such particles are unable to bind cellular receptors and are therefore non-infectious (Bos et al., 1996). The E protein, although a minor structural component, appears to play an important role in determining the site of viral assembly and budding, and along with the M protein have been shown to be the minimum necessary elements for the production of virus like particles (Vennema et al., 1996). Selective encapsidation and packaging of viral genomic RNA over viral and cellular mRNAs present in the cytoplasm is mediated via a packaging signal present only on the genomic RNA. For porcine transmissible gastroenteritis virus (another alphacoronavirus) the packaging signal maps to the 5' most end of the genome, incorporating the 5' UTR and the start of ORF1a (Escors et al., 2003). Interactions between the M protein and the encapsidated genome result in its selective incorporation into virions (Narayanan and Makino, 2007). The process of viral budding and exit has not been fully elucidated, however it is thought the virus is released by exocytosis (Masters, 2006).

1.3.2. Epidemiology of FCoV

FCoV has a worldwide distribution, affecting both domestic and wild felids. Infection is extremely common in domestic cats, and is considered enzootic in areas with high feline population densities, such as catteries and animal shelters. In multicat environments it is estimated that greater than 80% of cats will have FCoV antibodies (Herrewegh et al., 1997; Pedersen, 1976; Sparkes et al., 1992), while in single cat households seropositivity is estimated at between 10-50% (Addie and Jarrett, 1992a; Bell et al., 2006; Holst et al., 2006; Kiss et al., 2000; Kummrow et al., 2005; Pedersen, 1976).

The high rate of seropositivity seen, particularly in situations of high population density, likely results from a number of factors: (1) husbandry conditions that promote the spread of the virus between susceptible animals (Foley et al., 1997a), (2) the relative environmental resilience of the virus under certain conditions (Scott, 1988), (3) the presence of asymptomatic carrier cats which act as a continuous source of infection and reinfection (Foley et al., 1997a), and (4) and the tenuous nature of the immune response to FCoV (Pedersen et al., 2008). FCoV is transmitted primarily through direct contact with faeces, or faecally contaminated fomites, so husbandry conditions that impose close contact between cats, especially where litter trays or toileting areas are shared, greatly facilitate the spread of the virus through a susceptible population. In these situations, infection and reinfection with FCoV is extremely common, and the virus becomes enzootic. The fastidious grooming

habits of cats also likely facilitate continued faeco-oral cycling. The ease with which FCoV transmission takes place in areas with high feline population density was highlighted in a study by Pedersen et al. (2004) in which over half of cats initially PCR-negative upon entering an animal shelter were found to be shedding FCoV within a week of entry. Conversely, feral cats, which typically live in small colonies and have a more expansive toileting area, or in households with one, or a few cats, there is less exposure to FCoV infected faeces resulting in a correspondingly lower seroprevalence (Bell et al., 2006; Luria et al., 2004).

Despite the high prevalence of FCoV infection, the occurrence of FIP is relatively rare. Addie et al. (1995a) have suggested that between 5-10% of FCoV infected cats will go on to develop FIP based on longitudinal survey that followed 820 cats in 73 households over a period of 6 years. The reported 10% incidence of FIP is somewhat controversial and may be artificially elevated by high number of multicat households, a known risk factor for FIP, included in this study, and a figure of less than 5% is quoted by many, including the original author (Addie, 2012). Multiple risk factors have been identified for the development of FIP. FIP most frequently occurs in young cats (Foley et al., 1997b; Kass and Dent, 1995; Norris et al., 2005; Pesteanu-Somogyi et al., 2006; Rohrbach et al., 2001; Worthing et al., 2012). In general FIP is more common in purebred cats compared to outbred animals (Norris et al., 2005; Pesteanu-Somogyi et al., 2006; Rohrbach et al., 2001; Worthing et al., 2012). Whilst part of this increased susceptibility is undoubtedly related to environmental factors such as domicile in a multicat household and increased risk of FCoV exposure when young (Foley et al., 1997b; Kass and Dent, 1995), a number of studies have demonstrated specific breeds are overrepresented, whilst others are underrepresented among FIP cases suggesting additional factors, most likely genetic are involved (Foley and Pedersen, 1996; Norris et al., 2005; Pesteanu-Somogyi et al., 2006; Worthing et al., 2012). This is supported by a study by Foley and Pedersen (1996) which showed that susceptibility to FIP was a partially heritable trait in Persians, with close relatives of FIP affected cats significantly more likely to die of FIP than unrelated cats. Further evidence of a genetic component to FIP susceptibility is the reported increased occurrence of FIP in cheetahs (Evermann et al., 1988) most likely due to a loss of genetic diversity, particularly at the MHC loci, following natural population bottlenecks (O'Brien et al., 1985; O'Brien et al., 1987). A recent genome wide association study with Birman cats, known to be overrepresented among FIP cases, identified five candidate genes which may influence the susceptibility to FIP (Golovko et al., 2013). Male (Norris et al., 2005; Pesteanu-Somogyi et al., 2006; Rohrbach et al., 2001; Worthing et al., 2012) and sexually intact animals (Pesteanu-Somogyi et al., 2006; Rohrbach et al., 2001) have been reported at greater risk in some studies.

1.3.2.1. Transmission

FCoV is transmitted horizontally by the faecal-oronasal route with cats exposed through contact with FCoV infected faeces or faecally contaminated fomites. For enveloped viruses, FCoV are relatively stable in the environment, with dried virus remaining infectious for up to seven weeks (Scott, 1988).

1.3.2.2. Shedding of FCoV

FCoV is primarily shed via the faeces. Transient shedding of FCoV in saliva and respiratory secretions has been documented early in the course of infection (Addie and Jarrett, 2001; Stoddart et al., 1988) however transmission via this route is thought to be uncommon, likely due to the short time in which virus is shed in these secretions. Faecal shedding of FCoV has been extensively investigated under both experimental laboratory conditions and also within natural environments (Addie and Jarrett, 2001; Addie et al., 2003b; Foley et al., 1997a; Harpold et al., 1999; Herrewegh et al., 1997; Stoddart et al., 1988). In these studies faecal shedding can be detected as soon as 2 days post infection, and faecal shedding can, and typically does precede seroconversion. Three distinct groups of cats can be identified based on their faecal shedding pattern: resistant cats, transiently infected cats, or chronically infected (carrier) cats.

Only a small percentage of cats appear to be resistant to infection and never shed FCoV. In the study by Addie and Jarrett (2001), 4 of 136 cats living in different multicat households and mixing freely with FCoV shedding cats, either failed to seroconvert or else had very low FCoV antibody titres, and never shed virus in their faeces. The mechanism of intrinsic resistance is unknown. *In vitro* host related differences in monocyte permissivity have been previously demonstrated (Dewerchin et al., 2005) and it is possible similar host related differences in enterocyte permissivity could explain the existence of these resistant cats. Addie and Jarrett (2001) suggested the innate resistance may be due to the lack of, or the presence of mutant coronavirus receptors, as has been reported for some laboratory mice strains resistant to MHV infection (Yokomori and Lai, 1992).

The majority of cats naturally exposed to FCoV are transiently infected and shed virus in their faeces, continuously or intermittently, for a variable period of time before clearing the infection. The duration of faecal shedding is typically in the order of several months, with 95% of cats that eventually stop shedding, doing so within nine months of the primary infection (Addie and Jarrett, 2001). Immunity to FCoV following viral clearance is transitory, with recovered cats susceptible to re-infection with the same, or different viral strain (Addie et al., 2003b; Pedersen et al., 2008).

Approximately 13% of FCoV infected cats fail to mount a sterilising immune response and remain persistently infected, shedding virus continuously or intermittently for a prolonged period, and in some cases for life (Addie and Jarrett, 2001; Addie et al., 2003b). Utilizing highly sensitive RT-PCR techniques, viral RNA has been demonstrated in various organs in asymptomatic carrier cats (Herrewegh et al., 1997; Kipar et al., 2010) however immunohistochemical demonstration of FCoV infected cells is restricted primarily to the distal gastrointestinal tract, suggesting that this is likely the primary site of viral persistence.

FCoV RNA has been detected in the faeces and intestinal contents of cats with naturally occurring FIP (Addie et al., 1996; Chang et al., 2010; Pedersen et al., 2009). It has long been thought that virus shed by cats with FIP is of the parental enterotropic biotype in line with the observation that FIP is infrequently spread horizontally (Hartmann, 2005). Pedersen et al. (2012) recently demonstrated faecal shedding of FIPVs containing an intact 3c gene from cats with FIP, however this shed virus was not infectious for other cats via natural routes of exposure. Although this study involved a limited number of cats the results suggest that even for virulent viruses containing an intact 3c gene, and thus capable of intestinal replication and faecal shedding, additional changes associated with virulence reduce the infectivity of these viruses and therefore the chance of horizontal spread. Clearly, as faecal shedding of infective virulent virus is an essential precondition for the circulating virulent / avirulent theory as proposed by (Brown et al., 2009), these findings cast further doubt over that hypothesis.

1.3.3. Pathogenesis and clinical disease

1.3.3.1. Non-FIP FCoV disease

Infection with FECV is typically asymptomatic, or may result in mild self-limiting gastroenteritis, mild upper respiratory tract signs, or stunted growth in kittens (Addie and Jarrett, 1992b; Hickman et al., 1995; Mochizuki et al., 1999; Pedersen et al., 1981). Clinical manifestations of FECV infection, including the FECV to FIPV mutation are more likely to occur in kittens (Addie and Jarrett, 1992b; Foley et al., 1997b; Hickman et al., 1995). Rarely more severe disease associated with FECV has been reported (Kipar et al., 1998b; McKeirnan et al., 1981), however despite this, the significance of FECV infection lies not in its inherent pathogenicity, but rather in its ability to mutate to more virulent FIP-causing biotypes.

The primary site of viral replication of FECV is within enterocytes, principally in mature columnar epithelial cells in the upper third of the villi (Pedersen et al., 1981). Viral replication occurs in the cytoplasm, and can result in destruction of infected cells. Histopathological changes in acutely infected kittens with enteritis were present from the distal duodenum to the terminal ileum and consisted of patchy areas of villous atrophy, commonly with fusion of

adjacent epithelial cells (Pedersen et al., 1981). Mature enterocytes on the tips of the villi frequently become separated from the underlying basement membrane resulting in sloughing of the villous tip. Similar histopathological changes were reported in a case series of five older cats with severe coronaviral enteritis (Kipar et al., 1998b). Histopathological changes seen in kittens with asymptomatic FCoV infection are limited to generalised T and B cell hyperplasia in the spleen and mesenteric lymph nodes (Haagmans et al., 1996; Kipar et al., 1999; Kipar et al., 2001; Meli et al., 2004). Changes in lymphatic tissue are thought due to generalised activation of the immune system, although the demonstration of FCoV RNA in the bone marrow, spleen, and mesenteric lymph nodes of asymptomatic FCoV infected cats by Meli et al. (2004) suggest some of the changes may be due to a direct effect of FCoV replication.

It was initially hypothesised that FECV was restricted to the intestine, and possibly regional lymph nodes, and that systemic spread was seen only with, and was a defining feature of infection with the more virulent FIPVs (Pedersen et al., 1981). It is now clear that intestinal compartmentalisation is not absolute, with systemic spread is seen in 80-90% of cats infected with FCoV and viral RNA detectable in almost all parenchymal organs (Gunn-Moore et al., 1998; Herrewegh et al., 1997; Kipar et al., 2006a; Meli et al., 2004). Systemic spread of FCoV is thought to occur via a monocyte-associated and cell-free viraemia (Meli et al., 2004). *In vitro* studies have shown that FCoV virions are released from the basolateral surface (away from the intestinal lumen) of polarised epithelial cells (Rossen et al., 1995; Rossen et al., 2001), a finding if representative of natural infection, suggests systemic spread is an inevitable consequence of FCoV infection and replication. Although genomic RNA is detected in a high proportion of healthy FCoV infected cats, quantitatively, the viral load of these healthy asymptomatically infected cats is significantly lower than seen in cats with FIP (Kipar et al., 2006a), indicative of reduced or inhibited viral replication. Supporting this are the findings of Simons et al. (2005) who detected viral mRNA in blood samples of approximately 5% of healthy FCoV infected cats, compared to 93% of cats with histologically confirmed FIP. Thus it would appear that there are qualitative and quantitative differences in FCoV replication in cats with FIP compared to healthy infected cats.

1.3.3.2. Feline infectious peritonitis

FIP manifests clinically as either the effusive (wet) or non-effusive parenchymatous (dry) form (Pedersen, 2009). The characteristic finding in the more common effusive form of the disease is the accumulation a protein rich exudate in the peritoneal space, (approximately 60% of cases), thoracic cavity (pleural and/or pericardial space) (approximately 20%), or both (approximately 20%) (Figure 1.7) (Hartmann, 2005). Non-specific signs such as mild pyrexia, anorexia, and weight loss are often the first manifestation of the disease. Signs

referrable to fluid accumulation in wet FIP vary depending on the location and volume of the effusion, and can include dyspnoea, tachypnoea, muffled heart sounds, and abdominal and scrotal enlargement (Addie, 2012). Non-effusive FIP is more variable in its presentation, with specific clinical signs referrable to the presence of granulomatous lesions within tissues. Ocular or CNS involvement is common in non-effusive disease, with over 60% of cats showing signs referrable to involvement of these systems (Pedersen, 2009). Irrespective of the form of the disease and the nature of the clinical signs, FIP is generally considered a terminal disease.

a.

b.

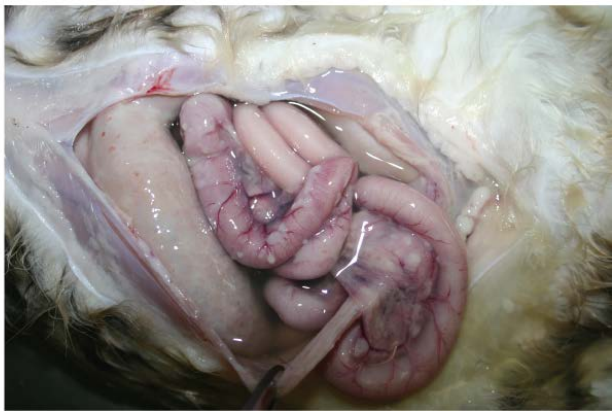

Figure 1.7: Cat with effusive FIP. Note the pot-bellied appearance typical of the effusive form of the disease (a). The opened abdominal cavity (b) reveals an accumulation of yellow tinged fluid.

The histopathological changes in FIP are heterogeneous, consisting of diffuse inflammation on serosal surfaces, granulomas (with or without areas of necrosis), focal and perivascular lymphoplasmacytic infiltrates, and granulomatous necrotising vasculitis (Berg et al., 2005; Kipar et al., 1998a). Despite the obvious clinical demarcation between effusive or non-effusive forms of FIP, the distinction is not as clear at the cellular level, with vasculitis lesions typically associated with effusive FIP being seen in non-effusive cases, and similarly demarcated granulomas more commonly associated with non-effusive FIP present in effusive cases (Berg et al., 2005).

Monocytes and macrophages are the primary target cell for virulent FCoV biotypes (FIPV), playing an important role in systemic viral dissemination and the immunopathological processes associated with FIP. To enable replication in these cells FIPV have evolved a number of strategies to avoid or negate the host's innate and adaptive immune response. Dewerchin et al. (2005) demonstrated that approximately 50% of FIPV infected monocytes do not display viral antigens on the plasma membrane, and those that do, internalise these proteins in the presence of antiviral antibodies (Dewerchin et al., 2006), making them essentially invisible to the immune system. Further experiments have shown that FIPV infected cells are resistant to antibody-dependent complement-mediated lysis, even in cells in which antigen internalisation has been blocked (Cornelissen et al., 2009). The formation of viral quasispecies during error prone viral replication is an important immune evasion mechanism for some viruses through the process of antigenic drift (Domingo et al., 1998). Given the short clinical course of FIP the role of quasispecies as an immune evasion strategy may be more significant for persistent FECV infections compared to FIPV infections. Virus induced lymphopaenia seen in FIP is a further mechanism through which FIPVs can minimise the hosts adaptive immune response (Dean et al., 2003; Takano et al., 2007a).

FIP is an immunopathological disease, the pathogenesis of which is complex and incompletely understood. A necessary step in the pathogenesis of FIP is infection by a FIPV, however the development of disease and its clinical manifestation is critically dependent on the nature of the host immune response to that infection. The nature of the immune response to non-virulent biotypes also likely influences the risk of FIP, as increased viral replication associated with a suboptimal immune response to FECV will increase the likelihood of a virulent mutant being generated.

It is generally accepted that cell mediated immunity (CMI) is essential for control and clearance of the virus and that a humoral immune response is ineffective and possibly deleterious (Pedersen, 2009). Evidence for the protective role of CMI in the development of FIP is demonstrated by the increased incidence of FIP in cats concurrently infected with FIV, a known suppressor of CMI (Poland et al., 1996). *In vitro* production of the Th1 cytokine INF-γ is greater in peripheral blood mononuclear cell (PBMC) cultures from healthy FIPV infected cats compared to cats with FIP when stimulated with inactivated FIPV (Satoh et al., 2011). Furthermore it has been shown that thymectomised cats develop more severe disease (Hayashi et al., 1983) and that cats with a strong delayed-type hypersensitivity response against FCoV antigen have prolonged survival times (Weiss and Cox, 1989).

FIPV replication in macrophages results in increased expression of B-cell differentiation and survival factors (IL-6, CD40L, B-cell-activating factor) which promote the differentiation of B-cells into antibody secreting plasma cells (Takano et al., 2009), contributing to the robust

humoral response and hypergammaglobulinaemia seen in FIP (Paltrinieri et al., 1998). In contrast to CMI, the humoral immune response is generally considered ineffectual at controlling the disease, as evidenced by the high FCoV antibody titres often seen in cats with FIP (Pedersen, 1976) and the lack of significant differences between the kinetics and titres of antiviral antibody responses in surviving and non-surviving cats following experimental exposure to FIPV (Groot-Mijnes et al., 2005). This blanket statement however belies the complexity and heterogeneity of the antibody response to FCoV, as it has been shown that antibody responses to specific viral targets may be involved in viral clearance (Gonon et al., 1999), and it is known that maternally derived antibodies provide some protection in kittens (Addie and Jarrett, 1992b). There is evidence that the humoral response may be deleterious by contributing to the immunopathological lesions seen in effusive FIP through the formation and deposition of immune complexes and a subsequent type III hypersensitivity reaction (Jacobse-Geels et al., 1980; Pedersen and Boyle, 1980). The humoral response may also contribute to the disease process by facilitating viral entry in monocytes/macrophages through the process of ADE of infection (see 1.3.1.4.1).

Two general mechanisms have been proposed for the development of disease following infection with a virulent biotype (Hartmann, 2005). Historically, the pathogenesis of FIP has been attributed primarily to a classical type III hypersensitivity reaction based on the demonstration of viral antigen, antiviral antibody, and complement proteins associated with lesions (Jacobse-Geels et al., 1980; Pedersen and Boyle, 1980) and the accelerated onset of disease in seropositive compared to seronegative kittens in experimental studies (Weiss and Scott, 1981a). More recently a study by Kipar et al. (2005) has shown that whilst an Arthus type reaction almost certainly plays a role in the development of FIP vasculitis, the morphology, distribution, and cellular composition of vasculitis lesions in FIP differ significantly from reported type III hypersensitivity vasculitidies. The authors propose a model whereby infected activated monocytes are the primary trigger for the development of FIP. FIPV infection of monocytes results in the rapid activation of the p38 mitogen-activated protein kinase (MAPK) pathway resulting in an upregulation of proinflammatory cytokines TNF and IL-1β (Regan et al., 2008a). According to the model proposed by Kipar et al. (2005) the adhesion of activated monocytes to endothelial cells results in a positive feedback cycle whereby cytokines elaborated by the adhering monocytes act in an autocrine and paracrine fashion to promote further adhesion and activation. Endothelial cells also play an active part in the development of FIP vasculitis with venous, and to a lesser extent arterial endothelial cells, displaying an activated morphology and upregulation of MHCII independent of the presence of local inflammatory lesions, most likely as a result of a systemic tumour necrosis factor α (TNF- α) cytokine response (Kipar et al., 2005).

Pan-lymphopaenia is a common finding in cats with FIP, particularly in the terminal stages of the disease (Groot-Mijnes et al., 2005; Paltrinieri et al., 2003). Lymphoid depletion is also prominent in both primary and secondary lymphoid organs (Dean et al., 2003; Kipar et al., 2001). Lymphopaenia and lymphoid depletion in FIP occurs as a result of apoptosis (Dean et al., 2003; Haagmans et al., 1996; Kipar et al., 2001; Takano et al., 2007a), most likely induced indirectly by increased TNF-α from virally infected macrophages, as FCoV does not infect lymphocytes (Dean et al., 2003; Takano et al., 2007a; Takano et al., 2007b). A longitudinal infection study by Groot-Mijnes et al. (2005) demonstrated reductions in circulating CD4+ and CD8+ T-cells is temporally correlated with viral replication and the occurrence of non-specific clinical signs such as fever and weight loss, while the converse was true during periods of apparent clinical recovery. As proposed by the authors, these findings suggest the pathogenesis and outcome of FIPV infection is determined by the opposing forces of virally induced T-cell depletion and antiviral T-cell responses.

1.3.4. Current treatment options

> *"You may know the intractability of a disease by its long list of remedies"*
> (Garrison, 1925)

In reviewing the literature pertaining to the treatment of FIP, the above quote, attributed to 19th century physician Dr Alonzo Clark, seems particularly relevant. The impressive roll call of drugs listed in Table 1.3 and detailed in a recent review of FIP treatment by Hartmann and Ritz (2008) is testament to this. Despite a multitude of reportedly successful treatments, FIP remains for the most part a fatal disease. This apparent contradiction can be reconciled by examining the quality of the studies supporting these treatments, many of which contain serious methodological flaws, including inadequate controls, poor case definitions, and a failure to definitively diagnose the condition. For this reason much of the literature regarding the treatment of FIP should be interpreted with caution.

With a lack of antiviral drugs, treatment of FIP has traditionally focused on the use of immunomodulatory agents, primarily immunosuppressive therapies. In light of the immunopathological nature of FIP there is a clear rationale for the use of immunomodulating agents to control clinical signs, however these treatments fail to address the underlying problem of viral replication, a triggering and perpetuating factor in disease pathogenesis. It is unsurprising therefore that these treatments provide at best little more than short term symptomatic relief. In fact, given that a robust cell-mediated immune response is essential for viral clearance and that FIP is associated with profound T-cell depletion (Groot-Mijnes et al., 2005), the use of immunosuppressive agents that cause further T-cell suppression may actually be deleterious.

The use of biological response modifiers and immunostimulatory drugs has been considered a promising approach to the treatment of FIP; unfortunately however results have generally been disappointing. As an example, recombinant feline interferon-ω (rFeINF-ω) generated considerable interest after demonstrating efficacy *in vitro* against FCoV (Mochizuki et al., 1994; Truyen et al., 2002) and beneficial effects in a small scale clinical trial conducted in Japan (Ishida et al., 2004). Ishida et al. (2004) reported complete remission (survival over 2 years) in four of 12 cats treated with rFeINF-ω and prednisolone, and partial remission (2 to 5 months) in a further four cases. A subsequent randomised placebo controlled study conducted in Germany failed to demonstrate any difference in survival time or quality of life between rFeINF-ω treated cats or their placebo treated cohorts (Ritz et al., 2007). Although a number of potential explanations have been put forward to account for the discrepancy between the results of the two studies, it appears that rFeINF-ω provides little or no benefit for the majority of cats with FIP.

Polyprenyl immunostimulant is a mixture of phosphorylated, linear polyisoprenols which according to US patent 6,525,035 has been demonstrated *in vitro* to upregulate mRNA expression for IL-1 and IL-2 and inhibit the constitutive transcription of TNF mRNA (Danilov et al., 2003). This patent also claims an efficacy of 50% in treating FIP in twelve kittens, however there is no additional data to support this claim and it therefore must be treated with scepticism. A recent peer reviewed publication has reported the use of polyprenyl immunostimulant as a treatment for non-effusive FIP in three cats (Legendre and Bartges, 2009). Definitive diagnosis of FIP was made in only one cat; however clinicopathological findings were strongly suggestive in the remaining cases. Two cats, including the cat definitively diagnosed with FIP, remained alive and well 2 years after diagnosis, while the third cat survived for 14 months. Although no control group is available for comparison, the survival times reported with polyprenyl immunostimulant exceed those typically associated with non-effusive FIP (Addie, 2012). Although promising results have been demonstrated with dry FIP, the authors report that “treatment of wet form FIP with Polyprenyl Immunostimulant has been dismal” (Legendre and Bartges, 2009). More recently preliminary data published on the use of polyprenyl immunostimulant in a larger number of cats with non-effusive FIP was less impressive, with only 25% of cats surviving for more than 6 months (Legendre, 2012). Given its purported mechanism of action of promoting a Th1 cytokine profile and inhibiting TNF it is feasible that this drug may still find a role as an adjunct treatment for FIP in conjunction with appropriate antiviral therapy.

There are currently no direct acting antivirals used in the treatment of FIP, despite a number of compounds demonstrating *in vitro* inhibitory effects against FCoV (Barlough and Scott, 1990; Barlough and Shacklett, 1994; Hsieh et al., 2010; van der Meer et al., 2007). For most of these potential antiviral compounds it is unknown whether the reported *in vitro* inhibitory

activity would translate to clinical efficacy as appropriate trials have not been conducted or reported. Ribavirin is an exception, being the only direct acting antiviral drug reported to be tested in cats with FIP thus far. Ribavirin is a synthetic nucleoside analogue of guanine which has demonstrated a broad spectrum of *in vitro* and *in vivo* activity against a variety of DNA and RNA viruses (Snell, 2001). The mechanism of action of ribavirin is not fully understood but may be the result of (1) inhibition of cellular inosine monophosphate dehydrogenase resulting in decreased viral protein synthesis, (2) immunomodulation through the inhibition of IL-10, (3) inhibition of viral capping, or (4) effects as an RNA mutagen resulting in lethal mutagenesis (Crotty et al., 2002; Leyssen et al., 2005). The existence of multiple alternate antiviral mechanisms may explain the broad spectrum of activity of ribavirin.

Ribavirin is known to be inhibitory to FCoV replication in cell culture, albeit with a small selectivity index (SI) (Barlough and Scott, 1990; Weiss and Oostrom-Ram, 1989). The small SI is reflected *in vivo*, and is of particular concern in cats as they are especially sensitive to the haematological adverse effects of the drug (Weiss et al., 1993a). To assess the efficacy of ribavirin in treating FIP, Weiss et al. (1993b) used a free form of the drug as well as a liposome-encapsulated form in 50 kittens following experimental exposure to FIPV. Liposome encapsulation was performed to enable targeting of the drug directly to the mononuclear phagocytes, and therefore reduce the drug dose needed and associated toxicity. Neither the free nor encapsulated ribavirin protected cats against the development of FIP. High doses of ribavirin resulted in more severe clinical signs and reduced survival times suggestive of toxicity. Cats treated with the lower doses had slightly longer survival times indicating the drug may have had some antiviral effects *in vivo*. Whilst ribavirin is clearly not an appropriate treatment for FIP, the demonstration of a positive, albeit small, effect *in vivo* suggests safe and efficacious antiviral drugs may be of use in treating this disease.

Most recently, following the completion of the studies described in this thesis, a small *in vivo* experimental study on the efficacy of chloroquine in treating FIP was reported by Takano et al. (2013). In this study treatment of cats infected with the highly virulent FCoV FIPV1146 with chloroquine was associated with an improvement in clinical scores and a slightly increased, but not statistically significant, survival time compared with control cats. In this case it is unclear whether the small *in vivo* benefits of chloroquine are derived from a direct antiviral effect or from its immunomodulatory properties (Savarino et al., 2003). Again this study provides tantalising evidence that effective antiviral therapy would be beneficial in treating FIP.

Table 1.3: Antiviral and immunomodulatory agents evaluated against feline infectious peritonitis (FIP).

Drug	Comments	References
Ribavirin	Good efficacy demonstrated *in vitro*. *In vivo* use associated with significant toxicity and poor efficacy.	(Weiss et al., 1993b)
Prednisone / dexamethasone	Immunosuppressive doses are current treatment of choice with anecdotal evidence of improved survival time and quality of life. Published studies on use as a monotherapy limited to control groups in two placebo controlled studies which demonstrated a median survival time of approximately 8 days.	(Fischer et al., 2011; Ritz et al., 2007)
Propentofylline	Randomised placebo controlled trial demonstrated no beneficial effect. Single published case report of efficacy of related drug pentoxifylline in combination therapy with rHuINF-α and prednisolone in treating FIP. FIP likely in this case but not definitively diagnosed.	(Fischer et al., 2011; Kang et al., 2011)
Ozagrel hydrochloride	Thromboxane synthetase inhibitor. Case report detailing two cats treated with improved survival time in one cat and apparent cure in the other. FIP likely based on case description but not definitively diagnosed.	(Watari et al., 1998)
Cyclophosphamide	Alkylating agent. Use reported in combination with glucocorticosteroids and antibiotics in a large study involving 151 “suspect” FIP cases. Of these, 76 were reported as healthy following therapy. FIP not definitively diagnosed and no control group.	(Bilkei, 1988)
rFeINF-ω	Uncontrolled study with 12 cats showed complete response (>2 year survival) in 33% and partial response (2- 5 month survival) in 33%. Cases not definitively diagnosed as FIP. Subsequent placebo controlled trial demonstrated no effect on survival time or quality of life. Single long term survivor (200 days) in treatment group.	(Ishida et al., 2004; Ritz et al., 2007)
Melphalan	Alkylating agent. Reported to increase survival time in a single case report but FIP not definitively diagnosed.	(Madewell et al., 1978)
Tylosin	Macrolide antibiotic with immunomodulatory properties. Improved survival times reported in two of three cats treated but FIP not confirmed.	(Colgrove and Parker, 1971)
Promodulin	Biological response modifier. Uncontrolled trial in 52 cats reported favourable response in 38 cats. No details on inclusion criteria or follow up provided.	(Ford, 1986)

Table 1.3 cont.: Antiviral and immunomodulatory agents evaluated against feline infectious peritonitis (FIP).

Drug	Comments	References
Polyprenyl immunostimulant	Single report of treatment of 3 cats with non-effusive FIP. Prolonged survival in all three cats (14 months, and two cats > 2 years). Ineffective in treating non-effusive FIP. FIP definitively diagnosed in one (long term survivor) cat. Preliminary data from larger study showed approximately 25% of treated cats survived for greater than 6 months.	(Legendre and Bartges, 2009; Legendre, 2012)
Levamisole	Anthelminthic with immunostimulatory properties. No beneficial effect seen in pilot study.	(Weiss, 1995)
Recombinant human INF-α	*In vitro* efficacy against FCoV. Experimental trial with control group demonstrated no reduction in mortality. Slight increase in mean survival time when given with Propionibacterium acnes.	(Weiss et al., 1990; Weiss and Oostrom-Ram, 1989)
Chloroquine	Antimalarial compound. Experimental trial with control group. Cats infected with highly virulent FCoV FIPV1146. Improvement in clinical signs and slight increase in survival time (not statistically significant) reported.	(Takano et al., 2013)

1.4. FELINE CALICIVIRUS

Feline calicivirus (FCV), previously feline picornavirus, was first reported by Fastier (1957) wherein it was described as “a filterable agent in search of a disease” in reference to its apparent apathogenic nature in experimental studies. Whilst it is now well recognised that FCV often results in inapparent infections in cats, sadly the virus is no longer “in search of a disease”, with a number of important, and in some cases fatal, disease syndromes associated with infection. Although FCV vaccination has been widely practiced for several decades, it continues to be a significant cause of disease in cats due to the limitations of currently available vaccines, and due to the inherent genetic plasticity of the virus allowing the emergence of more virulent strains.

1.4.1. Virology of feline calicivirus

1.4.1.1. Taxonomy

Feline calicivirus belongs to the genus *Vesivirus*, family *Caliciviridae* (Clarke et al., 2012). Despite high levels of sequence diversity amongst FCV isolates, all belong to a single diverse serotype (Radford et al., 2007). Two genotypes of FCV have been identified based on phylogenetic analysis of capsid sequences of isolates from diverse geographical locations around the world (Sato et al., 2002). Genotype I predominates worldwide while genotype II has only been identified to date in Japan (Ohe et al., 2006; Sato et al., 2002). Recently a second calicivirus belonging to the genus *Norovirus* has been isolated from faecal samples from kittens with diarrhoea, however the pathological significance of this virus is unclear (Pinto et al., 2012).

Table 1.4: *Caliciviridae* taxonomy adapted from the Ninth Report of the International Committee on Taxonomy of Viruses (Clarke et al., 2012). * indicates type species.

Taxonomy of the Family *Caliciviridae*
Family *Caliciviridae*
• Genus *Vesivirus*
o Vesicular exanthema of swine virus *
o **Feline calicivirus**
• Genus *Lagovirus*
o Rabbit haemorrhagic disease virus *
o European brown hare syndrome virus
• Genus *Norovirus*
o Norwalk virus *
o Feline Norovirus (not an official species designation)
• Genus *Sapovirus*
o Sapporo virus *
• Genus *Nebovirus*
o Newbury-1 virus *

1.4.1.2. Structure and morphology

Viruses in the family *Caliciviridae* have a monopartite linear positive-sense single-stranded RNA genome surrounded by a small (27-40 nm) non-enveloped icosahedrally symmetrical capsid (Clarke and Lambden, 1997). The virion presents characteristic cup-shaped depressions on its surface, a unique morphology from which the viral family derives its name (from the Latin *calix* meaning cup or goblet) (Clarke et al., 2012). The capsid is assembled from 180 copies (90 homodimers) of the main structural protein VP1 (Prasad et al., 1994). A second protein, VP2 is present in smaller numbers (1 to 8 copies per virion) (Luttermann and Meyers, 2007; Sosnovtsev and Green, 2000).

1.4.1.3. Genome

The RNA genome of FCV has a 5' covalently bound protein, VPg (viral protein, genome linked), and a polyadenylated 3' terminus (Herbert et al., 1997). The genome is approximately 7.7 kb and encodes three ORFs as shown in Figure 1.8 (Carter et al., 1992a; Carter et al., 1992b). ORF1 encompasses the proximal two-thirds of the genome and encodes a large polyprotein that is processed to produce the non-structural proteins involved in viral replication. ORF2 encodes the major capsid protein (VP1) precursor and ORF3 encodes the minor capsid protein (VP2). ORF2 is separated from ORF 1 by a two nucleotide

non-coding region (GC), while ORF2 and ORF3 overlap by four nucleotides. A 19 nt UTR precedes ORF1 at the 5' end, and a 3' UTR of approximately 50 nt follows ORF3. Overall FCV isolates exhibit significant genetic variability, with different isolates showing approximately 80% homology (Thumfart and Meyers, 2002).

The FCV genome contains two identified *cis*-acting elements. Sosnovtsev et al. (2005) reported a *cis*-acting sequence overlapping with the 3' end of ORF3 important for viral replication, possibly through promoting RNA-protein interactions. The second sequence, the termination upstream ribosomal binding site (TURBS), a 69 nt sequence located at the 3' end of ORF 2, is needed for efficient translation of VP2 from the bicistronic subgenomic mRNA (Herbert et al., 1996; Luttermann and Meyers, 2007).

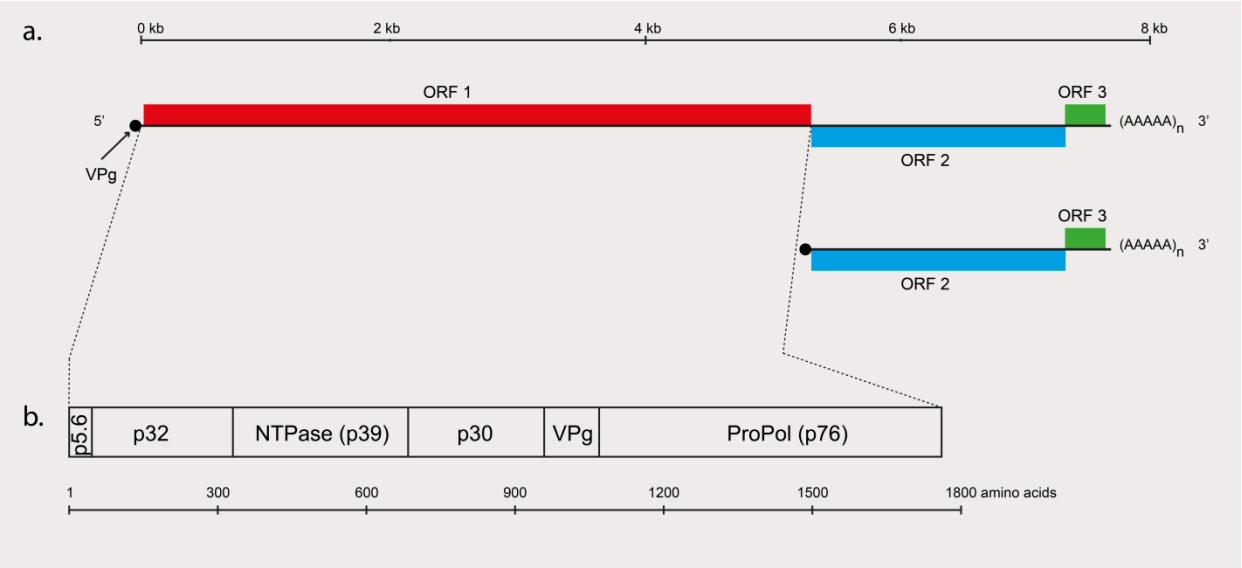

Figure 1.8: Feline calicivirus genome. (a) Schematic of FCV genome and subgenomic mRNA. (b) Non-structural proteins produced by co- and post-translational cleavage of replicase polyprotein. NTPase, nucleoside triphosphatase; VPg, viral protein genome linked; ProPol, proteinase polymerase.

1.4.1.4. Replicase protein

The replicase polyprotein is translated from ORF1 of full length genomic RNAs. The protein is co- and post-translationally cleaved by a virus-encoded proteinase to yield six mature proteins: named from the amino terminus, p5.6, p32, p39, p30, p13, and p76, and shown in Figure 1.8 (Sosnovtsev et al., 2002). The functions of p5.6, p32, and p30 are unknown. p39 is thought to possess NTPase activity analogous to that of the p37 protein of rabbit haemorrhagic disease virus with which it shows significant sequence homology (Meyers et al., 2000). p13, also known as VPg, is a 13 kDa protein found covalently linked to the 5' end of genomic and subgenomic viral RNA. VPg likely has a role as a "cap analogue" to initiate translation of viral RNA, as proteinase treatment to destroy VPg reduces the translatability of

viral RNA (Herbert et al., 1997). The C-terminal end of the ORF1 polyprotein gives rise to a large 76 kDa protein (ProPol) that includes both proteinase and polymerase domains, similar to the 3CD Pro-Pol precursor of picornaviruses. Unlike the picornavirus 3CD ProPol and the ProPol of some caliciviruses, the ProPol precursor of FCV is a bifunctional proteinase-polymerase complex and is the primary active form (Sosnovtsev et al., 2002; Wei et al., 2001).

1.4.1.5. Major capsid protein (VP1)

Translation of ORF2 from the 5' end of the subgenomic mRNA produces the 73 kDa major capsid protein precursor (Carter et al., 1992b; Neill et al., 1991). The overall nucleotide sequence homology of ORF2 between FCV isolates is approximately 78% while the homology of deduced amino acid sequences is 89% (Thumfart and Meyers, 2002). Based on the degree of amino acid conservation, this protein has been divided into six regions, A to F (Neill, 1992; Seal et al., 1993). Region A, also known as the leader of the capsid protein (LC), is cleaved by a viral encoded protease to produce the mature VP1 capsid protein (Sosnovtsev et al., 1998). The cleaved 125 aa LC protein may act in *trans* to enhance viral replication (Chang et al., 2008).

The mature VP1 protein consists of two defined domains: the shell (S) domain which forms the inner shell of the capsid and the protruding (P) domain which projects from the surface of the capsid giving rise to the characteristic morphology of caliciviruses (Bhella and Goodfellow, 2011). Region B makes up the S domain, while regions C to F make up the P domain, which is further divided into two subdomains, P1 and P2. The P2 subdomain, which contains regions C, D, and F, is inserted into the P1 domain, containing region E. The P1 subdomain (region E) is the least conserved region of the protein, encoding two hypervariable regions thought to contain important neutralising epitopes (Geissler et al., 2002; Radford et al., 1999).

1.4.1.6. Minor capsid protein (VP2)

Translation of the 3' terminal ORF produces the 106 aa minor capsid protein VP2. This translation occurs from the bicistronic subgenomic RNA through a termination/reinitiation mechanism (Luttermann and Meyers, 2007). It is unclear whether VP2 has a structural role in FCV, however it has been demonstrated to be involved in the formation of virus like particles (Di Martino and Marsilio, 2010) and is necessary for the formation of infectious viral progeny (Sosnovtsev et al., 2005).

1.4.1.7. Viral replication cycle

1.4.1.7.1. Attachment and entry

Feline junctional adhesion molecule A (fJAM-A) is a functional receptor for FCV as demonstrated by studies showing productive infection in non-susceptible cells transfected with the fJAM-A gene and successful blocking of infection in susceptible cells using fJAM-A antibodies (Makino et al., 2006). Binding of the P2 domain of VP1 to the membrane distal D2 region of fJAM-A induces conformational changes in the FCV capsid resulting in a loss of icosahedral symmetry that may be important in uncoating of the viral genome (Bhella et al., 2008; Bhella and Goodfellow, 2011; Ossiboff et al., 2010). fJAM-A is widely distributed in feline tissues, being present on feline endothelial and epithelial cells, particularly concentrated around tight intercellular junctions, as well as on platelets and leukocytes (Pesavento et al., 2011). With the exception of some virulent FCV strains, FCV-associated disease is typically restricted to the oral cavity/upper respiratory tract, meaning the tissue distribution of fJAM-A is not the sole determinant of viral tropism. Tissue distribution of α2,6-sialic acid may play a role in determining tropism in the natural host as studies have demonstrated binding of FCV to α2,6-sialic acid, suggesting it may serve as a co-receptor for viral attachment (Stuart and Brown, 2007). Furthermore, sequential treatment of susceptible cells with neuraminidase and O-glycanase to remove O-linked glycans results in a 30% reduction in FCV binding supporting the hypothesis that carbohydrate moieties may act as co-receptors to enhance interaction between FCV and fJAM-A (Kreutz et al., 1994). Following attachment the virus is taken into the cell via receptor mediated endocytosis in clathrin-coated vesicles (Stuart and Brown, 2006). Release of the viral genome into the cytoplasm requires acidification of the endosome as shown by blocking of the process using endosomal acidification inhibitors (Stuart and Brown, 2006).

1.4.1.7.2. Viral RNA synthesis

As a Baltimore group IV virus, FCV replication takes place within the cytoplasm associated with intracellular membranes (Green et al., 2002). Translation and proteolytic cleavage of ORF1 from viral genomic RNA produces the non-structural replicase proteins involved in RNA synthesis. Using genomic RNA, a negative-sense RNA strand is produced by the viral replicase enzymes in concert with host cellular factors (Green, 2007; Karakasiliotis et al., 2006). The negative-sense strand in turn serves as a template for the production of full length genomic and a 2.4 kb subgenomic mRNA (Herbert et al., 1996).

1.4.1.7.3. Translation of viral proteins

Translation of mRNA is dependent on the presence of *cis*-acting factors, most commonly a 5' cap and a 3' poly(A) tail, involved in recruiting and assembling the translation initiation

complex (Kapp and Lorsch, 2004). For FCV, which lacks a 5' cap, VPg covalently linked to the 5' end of genomic and subgenomic RNA acts as a cap substitute to enable initiation of translation of ORF1 from genomic RNA and ORF2 from subgenomic mRNA (Goodfellow et al., 2005). ORF3 is translated from the 3' end of the subgenomic mRNA through a termination/reinitiation process (Luttermann and Meyers, 2007). TURBS, located at the 3' end of ORF2, is essential for translation of ORF3, acting to bind the post-termination ribosome following translation of ORF2 and therefore increase the chance of reinitiation (Luttermann and Meyers, 2007, 2009).

1.4.1.7.4. Assembly and release

The major capsid protein VP1 has been demonstrated to assemble spontaneously into virus like particles (VLPs) in the absence of other viral proteins, however these particles often lack cup shaped surface depressions (Di Martino et al., 2007). Co-expression of VP2 with VP1 results in the formation of VLPs with a similar size and morphology to native FCV virus particles (Di Martino and Marsilio, 2010). Isopycnic separation of purified virus demonstrates a dual population of morphologically identical virus particles with differing densities with the higher density population consisting of viral particles containing the full length genome while the low density particles contain the sub-genomic mRNA (Neill, 2002). The sequence directing RNA packaging is unknown, however given the encapsidation of subgenomic RNA it likely located within ORF2, ORF3 or the 3' UTR. The mechanisms of viral release are likewise incompletely understood.

1.4.2. Epidemiology

FCV is a ubiquitous viral pathogen of domestic cats, with a prevalence reported to range from 10 to 75% depending on the nature of the study population (Bannasch and Foley, 2005; Binns et al., 2000; Coutts et al., 1994; Coyne et al., 2006a; Zicola et al., 2009). Although there are some conflicting epidemiological associations, FCV prevalence, as determined by virus isolation and/or PCR, has been shown to be higher in young animals (Coutts et al., 1994; Coyne et al., 2006a; Pedersen et al., 2004; Porter et al., 2008; Wardley et al., 1974), conditions of poor husbandry or (Bannasch and Foley, 2005; Harbour et al., 1991; Helps et al., 2005) high population density, (Bannasch and Foley, 2005; Porter et al., 2008; Wardley et al., 1974), and in animals with upper respiratory tract infections. (Binns et al., 2000; Helps et al., 2005; Porter et al., 2008). Additionally, FCV is also more prevalent in healthy cats from environments (e.g. catteries) with a recent history of upper respiratory tract disease (Helps et al., 2005). Breed related differences in FCV prevalence have been reported, however these studies did not take into account potential confounding factors such as environment and management practices (Coutts et al., 1994; Wardley et al., 1974). Several studies have shown vaccination status does not have a significant effect on whether FCV is

isolated (Binns et al., 2000; Coyne et al., 2006a), findings consistent with data showing prevalence prior to the introduction of vaccination is comparable to modern prevalence rates (Coutts et al., 1994; Wardley et al., 1974).

1.4.2.1. Transmission

Transmission of FCV is primarily via the oral, nasal, or conjunctival route through direct contact with infected cats or indirectly via contaminated fomites (Radford et al., 2007). The virus is relatively hardy in the environment and has been demonstrated to remain infectious for several weeks in a dried state (Doultree et al., 1999). A study by Wardley and Povey (1977a) failed to detect infectious aerosols from acutely infected cats suggesting that, under conditions of normal respiration, true aerosol transmission of FCV is unlikely. A potential role for fleas as mechanical vectors of FCV was reported by Mencke et al. (2009) as infectious virus was recovered from fleas and their faeces after feeding on blood spiked with FCV. It is unclear whether this is a significant route of exposure as the magnitude and duration of FCV viraemia in naturally affected cats may be insufficient for effective transmission.

1.4.2.2. Shedding

FCV is shed primarily in oronasal and ocular secretions where it can be detected as early as 24 hours post infection (Wardley and Povey, 1977b). Analysis of shedding patterns show most cats shed virus for at least 30 days following infection after which the proportion of viral carriers follows an exponential decline with a half-life of approximately 75 days (Wardley and Povey, 1977b). The primary site of viral persistence in FCV infected cats is the mucosa of the tonsil and adjacent fossa (Dick et al., 1989). A longitudinal study of FCV shedding in multiple catteries revealed shedding patterns of individual cats similar to those of FCoV, with some cats shedding consistently, some intermittently, and others never shedding the virus (Coyne et al., 2006a). Although Coyne et al. (2006a) identified continually shedding cats, it is unclear whether these are true persistent infections or a consequence of continual infection and reinfection with the same or different strain of FCV, a situation that would not be unexpected given the tenuous nature of immunity to FCV. FCV has also been isolated from urine (Rice et al., 2002) and faeces (Mochizuki, 1992), however shedding via these routes is not thought to be epidemiologically important.

1.4.3. Pathogenesis and clinical disease

Infection with FCV typically involves the oral cavity and upper respiratory tract and is associated with disease of moderate morbidity and low mortality (Gaskell et al., 2012). Many infected cats remain asymptomatic, while in those that do display clinical signs the most common finding is fever, oropharyngeal ulceration, and mild upper respiratory tract disease. In addition to the classical presentation of FCV infection, a number of distinct disease

syndromes have been associated with FCV. In some cases these syndromes have been experimentally reproduced using specific FCV isolates, suggestive of the existence of distinct biotypes. In addition to strain variations, the type and severity of clinical manifestations following FCV infection have also been shown to be dependent on the route of infection (Poulet et al., 2000; TerWee et al., 1997), challenge dose (Povey and Hale, 1974), and the age of infection, with more severe disease typically being seen in kittens.

1.4.3.1. Oral and upper respiratory tract disease

Clinical signs of oral and upper respiratory disease are commonly reported in cats with FCV, particularly in young animals. Oral lesions can be present anywhere within the oral cavity (Figure 1.9a and b) but are most common on the margins of the tongue. Lesions may appear as vesicles, however they are most often visualised as ulcers/erosions following necrosis of the overlying epithelium (Radford et al., 2007). Histologically the ulcers show marked inflammatory cell infiltrate with a fibrinopurulent exudate (Povey and Hale, 1974). Clinical signs of upper respiratory disease such as sneezing and nasal discharge may be seen in infected cats, however the severity of these signs is typically less than that associated with feline herpesvirus infection (Gaskell et al., 2012).

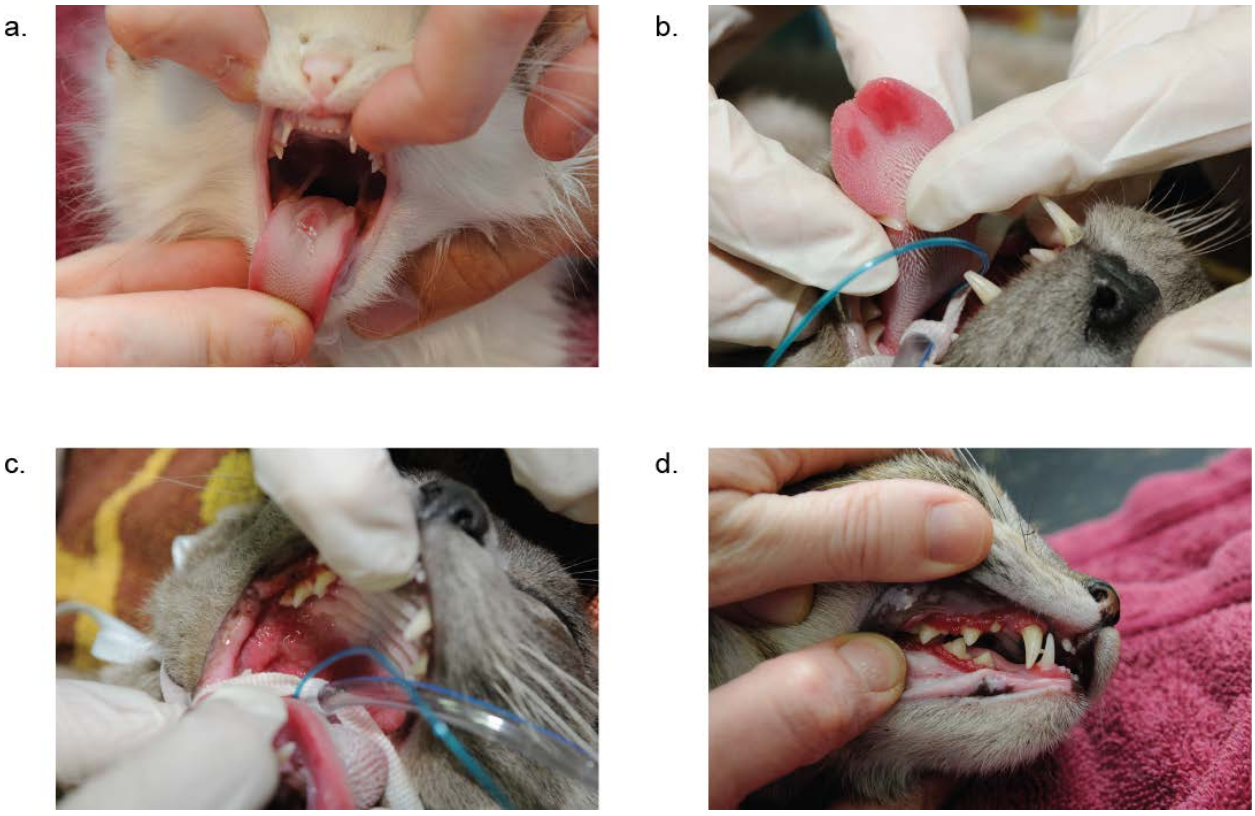

Figure 1.9: Oral lesions associated with feline calicivirus infection. Asymptomatic uncomplicated tongue ulcer in a kitten (a). Tongue ulcer (b) and inflamed palatoglossal folds (c) in a cat with FCGS. Severe gingivitis (disproportionate to the amount of tartar on the teeth) associated with a FCV infection (d). Images courtesy of Dr Anne Fawcett.

1.4.3.2. Lower respiratory tract disease

FCV has been documented to cause lower respiratory tract disease alone, or in combination with other pathogens (Foley et al., 2002; Hoover and Kahn, 1975). Experimental studies have demonstrated FCV stains of different virulence vary greatly in their ability to cause pneumonia using aerosol challenge (Hoover and Kahn, 1973, 1975). These studies utilising artificially generated aerosols have likely overestimated the significance of FCV induced pneumonia in natural infections where true aerosol transmission of high titres of FCV is unlikely due to the cats limited ability to produce infectious aerosols during normal respiration (Wardley and Povey, 1977a). The significance of FCV as a cause of lower respiratory tract disease under field conditions, where oronasal exposure is likely, is unclear.

1.4.3.3. Limping syndrome

FCV has been associated with a transient acute febrile lameness syndrome in cats following natural or experimental infection, and following modified live virus vaccination (Bennett et al., 1989; Dawson et al., 1994; Pedersen et al., 1983; Willoughby, 1989). FCV-associated lameness was the most commonly reported adverse vaccine reaction according to a study by Dawson and colleagues (1993), however as reporting of adverse vaccine reactions in cats is typically dependent on owners observing and recognising the problem, an outwardly obvious clinical sign such as lameness may be overrepresented when compared to more subtle or difficult to observe changes such as pyrexia or oral ulceration. The condition is classically described as a shifting leg lameness that occurs contemporaneous with the onset of fever with a typical duration of 48 to 72 h (Pedersen et al., 1983). No long term adverse sequelae have been reported.

An early study by Pedersen et al. (1983) failed to demonstrate any histopathological changes or immunohistochemical evidence of virus in affected joints, however later work demonstrated gross and microscopic evidence of acute synovitis (Dawson et al., 1994). Immunohistochemistry of affected joints has demonstrated the presence of viral antigen within macrophage like cells in the synovium (Bennett et al., 1989; Dawson et al., 1994), and infectious virus has been isolated from the joints of affected cats following natural contact exposure (Dawson et al., 1994). The presence of IgG, IgM, and complement within synovial macrophages as reported by Bennett et al. (1989) suggests that viral antigen may be present in the joints in the form of immune complexes. No evidence of synovial membrane vasculitis has been reported however, making it unlikely that a type III hypersensitivity is responsible for the reported clinicopathological changes (Dawson et al., 1994).

1.4.3.4. Virulent systemic disease

Pedersen and colleagues reported an outbreak of FCV-associated haemorrhagic-like fever in cats in Northern California (Pedersen et al., 2000). This clinical syndrome, now referred to as FCV-associated virulent systemic disease (FCV-VSD), has subsequently been reported from a number of geographically isolated regions (Hurley et al., 2004; Meyer et al., 2011; Schorr-Evans et al., 2003; Schulz et al., 2011). Analysis of FCV isolates from different epizootics has shown each to be genetically unique suggesting they evolved locally from less pathogenic viruses (Abd-Eldaim et al., 2005; Foley et al., 2006; Hurley et al., 2004; Ossiboff et al., 2007; Schulz et al., 2011). Most reported cases have occurred as outbreaks in a shelter or veterinary hospital setting, however sporadic individual cases have been reported (Meyer et al., 2011). It is unclear whether FCV-VSD represents a recent emergence of more virulent biotypes into the cat population, or whether the increased incidence of epizootics is simply a reflection of increased recognition of severe manifestations of FCV disease which have previously been reported to occur sporadically (Ellis, 1981; Love and Baker, 1972). If it is the former it remains to be determined what has changed in the host-pathogen-environment balance to allow the sudden and continued emergence of VSD strains.

Clinically, FCV-VSD commonly manifests with signs typical of those associated with oral/respiratory FCV disease, usually with a more marked and prolonged pyrexia. Additional signs may include facial and limb oedema, jaundice, coagulopathies, pneumonia, and a crusting or alopecic dermatoses primarily involving the face, feet, or ears (Radford et al., 2007). Case mortality rates of greater than 50% has been reported in naturally and experimentally infected cats, and ominously vaccination with the current generation FCV vaccines provides little or no protection (Coyne et al., 2006b; Hurley et al., 2004; Pedersen et al., 2000; Schulz et al., 2011). Adult cats are more severely affected than kittens (Coyne et al., 2006b; Hurley et al., 2004; Pedersen et al., 2000; Reynolds et al., 2009; Schulz et al., 2011), a finding reminiscent of another calicivirus, rabbit haemorrhagic disease virus, that has a mortality rate greater than 90% in adult European rabbits, but which causes asymptomatic or mild disease in young kits (Ward et al., 2010). Recent studies have implicated differences in the innate immune response between adult rabbits and kits to viral infection as the cause of the age related resistance, based on the finding that immunosuppressed kits died from RHDV infection similarly to naïve adult rabbits (Marques et al., 2014). These findings may provide clues to unravelling the pathogenesis of FCV-VSD.

The molecular basis for increased virulence in VSD isolates is not known. Sequence analysis of VSD isolates has shown all to be genetically distinct and has failed to identify consistent mutations associated with increased virulence (Abd-Eldaim et al., 2005; Foley et al., 2006; Hurley et al., 2004; Ossiboff et al., 2007; Schulz et al., 2011). A limited study of the

antigenic properties of two VSD isolates based on virus neutralisation assays revealed they shared a degree of homology at the neutralising epitope level (Abd-Eldaim et al., 2005). *In vitro*, VSD isolates demonstrate more rapid cytopathic effect and higher viral yields indicating more efficient infection and replication in CRFK cells (Ossiboff et al., 2007). These findings may in part account for the increased virulence seen *in vivo* with these viruses.

1.4.3.5. Feline chronic gingivostomatitis syndrome (FCGS)

Feline chronic gingivostomatitis syndrome (FCGS), estimated to account of up to 0.7% of all first opinion feline cases (Healey et al., 2007), is characterised by chronic and often marked inflammatory lesions affecting both gingival and non-gingival oral mucosa (White et al., 1992). The aetiopathogenesis of FCGS is incompletely understood, however it is generally considered multifactorial. Alterations in local cytokine expression (Harley et al., 1999) and salivary and serum immunoglobulin concentrations (Harley et al., 2003) are seen in cats with FCGS suggesting an immunological basis to the condition. A number of viral and bacterial agents have also been implicated in the pathogenesis of FCGS, along with non-infectious factors such as diet, breed predisposition, and stress (Diehl and Rosychuk, 1993). Increased $CD8^+$:$CD4^+$ ratio is seen in lesions, a finding consistent with a cell-mediated antiviral response (Harley et al., 2011). Of the viruses suggested to be involved in the pathogenesis of FCGS, the greatest evidence, albeit circumstantial, is for a role of FCV. Numerous studies have shown a higher prevalence of chronic FCV infections amongst cats with FCGS compared to control cats (Belgard et al., 2010; Dowers et al., 2010; Knowles et al., 1989; Lommer and Verstraete, 2003; Martijn, 2009; Reubel et al., 1992; Thompson et al., 1984). Cessation of FCV shedding has been reported to be coincident with a complete resolution of clinical signs in two case reports, providing further circumstantial support for a role of FCV in FCGS (Addie et al., 2003a; Southerden and Gorrel, 2007). Experimental infection of cats with FCV isolated from cats with FCGS can result in acute gingivitis/stomatitis, however chronic disease reminiscent of FCGS has not been experimentally recreated (Knowles et al., 1991; Reubel et al., 1992; Truyen et al., 1999). Given these results, it is likely that for FCV to be a primary cause of FCGS requires additional cofactors, for example a genetic predisposition or an environmental trigger. Alternatively, it may be that the chronicity of FCV infection in cats with FCGS is attributable to the virus exploiting the altered microenvironment created by the mucosal inflammation triggered by another disease process. In this case FCV may represent a perpetuating factor for the disease rather than a primary cause.

1.4.4. Current management and treatment options

Prophylactic vaccination is the most important tool in the control of FCV disease in domestic cats. The vaccination guidelines group of the World Small Animal Veterinary Association currently list the FCV vaccine as a core vaccine (Day et al., 2010). FCV vaccines, both

modified live and inactivated, generally provide protection against or reduce the severity of clinical disease, but do not prevent infection nor the development of a carrier state (Kahn et al., 1975; Knowles et al., 1991; Pedersen and Hawkins, 1995). Antigenic variability of FCV is problematic for vaccine design, although some strains such as F9 or 255 are more broadly cross protective than others (Porter et al., 2008).

Treatment of FCV disease is symptomatic, consisting primarily of nutritional and fluid support and good nursing care (Gaskell et al., 2012). In severe cases of FCV-associated respiratory disease prophylactic antibacterial therapy may be indicated to control or prevent secondary bacterial infection (Gaskell et al., 2012). Specific antiviral treatment options for FCV are extremely limited despite several agents demonstrating *in vitro* efficacy against FCV replication (Fulton and Burge, 1985; McCann et al., 2003; Povey, 1978b; Taira et al., 2005; Truyen et al., 2002). In many cases of FCV infection the lack of effective antiviral therapeutics is not a significant concern due to the mild and self-limiting nature of the associated disease. For more severe FCV disease manifestations however, such as virulent systemic disease, lower respiratory tract disease, and perhaps FCGS, the lack of efficacious antiviral drugs is problematic.

Ribavirin was demonstrated to markedly inhibit FCV replication in culture (Povey, 1978b) however *in vivo* use of this drug in a challenge experiment was associated with a lack of clinical efficacy (Povey, 1978a). Ribavirin treatment did not alter the clinical course of disease, nor did it shorten the duration of viral shedding. Additionally the use of ribavirin in cats is associated with significant toxicity, particularly haematologic toxicity resulting in thrombocytopaenia, leukopaenia, and anaemia (Povey, 1978a; Weiss et al., 1993a).

McCann et al. (2003) reported an antiviral activity of bovine lactoferrin on FCV replication *in vitro*. There are no controlled *in vivo* clinical studies of lactoferrin on FCV disease, although there are anecdotal reports of its use in cats. Addie and colleagues (2003a) reported a single case study in which topical bovine lactoferrin was used as part of a treatment regimen, along with dietary modification, antioxidant supplementation, and thalidomide treatment, for a cat with chronic gingivostomatitis. Long term treatment in this case resulted in complete resolution of clinical signs which was coincident with cessation of FCV shedding. Given the uncertain role of FCV in the pathogenesis of FCGS, the multiple simultaneous therapeutic interventions, and the natural history of FCV clearance, it is difficult to ascribe any effect of lactoferrin on FCV replication in this case.

Both feline and human interferons have demonstrated *in vitro* antiviral effects against FCV (Fulton and Burge, 1985; Taira et al., 2005; Truyen et al., 2002). A small experimental study showed some benefit in terms of reducing the duration and severity of typical oral/respiratory FCV disease in cats treated intravenously with recombinant feline interferon omega (rFeINF-

ω) (Ninomiya et al., 1991), however the expense of rFeINF-ω and the typically mild and acute nature of oral/respiratory FCV disease will likely preclude the widespread use of this treatment for this disease manifestation. A recently conducted randomised double-blinded study demonstrated an improvement in clinical parameters (lesions scores and pain reduction) in FCV positive cats with refractory stomatitis treated with oral rFeINF-ω compared to prednisolone treated control cats (Hennet et al., 2011). Unfortunately, despite current FCV infection being an inclusion criterion, this study did not perform follow up viral testing, leaving open the possibility that clinical improvement was due to the immunomodulatory effects of interferon treatment rather than an antiviral effect. Southerden and Gorrel (2007) reported the successful resolution of refractory chronic gingivostomatitis associated with clearance of FCV in a cat following SC and oral rFeINF-ω treatment. Clarification of the role of FCV in the pathogenesis of FCGS is needed to expound the mechanism, be that immunomodulatory or antiviral effects, through which rFeINF-ω may benefit affected cats.

The emergence and continued appearance of virulent systemic feline calicivirus disease in the last decade has spurred the development of a novel ON-based anti-calicivirus therapeutic. Smith et al. (2008) recently reported on the use of a feline calicivirus specific antiviral phosphorodiamidate morpholino oligomers (PMO) in three naturally occurring outbreaks of FCV-VSD. PMOs were highly efficacious; with 47/59 PMO treated cats surviving compared to only 3/31 non-PMO treated cats. PMO treatment cats also demonstrated reduced viral shedding and a more rapid clinical recovery. Therefore the use of PMO in VSD shows considerable promise as a first line treatment for future outbreaks to minimise morbidity and mortality, and also highlights the potential benefits of the timely administration of efficacious antivirals for FCV-associated disease.

1.5. SCOPE OF THIS THESIS

Feline coronavirus and feline calicivirus are two important viral pathogens of domestic cats. In many cases infection with either of these viruses results in mild or sub-clinical disease, however more severe, and potentially fatal disease manifestations are seen. As discussed, there are currently no specific antiviral therapeutics for FCoV or FCV-associated disease. The overriding aim of the work presented in this thesis was to address this shortfall by identifying antiviral compounds capable of inhibiting FCoV and FCV *in vitro*, as the first step towards developing therapeutic options that are clinically useful for treating these common infections of cats.

To achieve this aim we tested two antiviral strategies. The first of these was to identify and characterise small molecule compounds capable of inhibiting FCoV or FCV *in vitro*, from a

panel of compounds previously demonstrated to have antiviral properties against other viruses. To perform the screening required the development and optimisation of robust and reliable cell-based CPE inhibition assays suitable for assessing the antiviral efficacy of compounds against FCoV and FCV. Whilst the primary goal was to develop an assay for low to medium throughput screening, a secondary objective of assay development was to develop a “high throughput ready” assay for potential future studies. The antiviral effects of the candidate compounds identified during screening were confirmed with orthogonal testing and their antiviral effects further characterised with a series of studies to examine features relevant to their *in vivo* application, including efficacy against different strains (FCoV and FCV), the effect of time of addition (FCoV), and the effect of combination therapy with rFeINF-ω (FCV).

The second strategy tested was antiviral RNA interference. siRNAs targeting conserved regions of the FCoV and FCV viral genomes were designed and tested for antiviral efficacy. Again effective candidate siRNAs were further characterised to inform their potential *in vivo* use. The effect of siRNA concentration and combination therapy was examined for both FCoV and FCV. For FCoV, experiments were conducted to investigate the ability of combination therapy to delay or prevent the emergence of resistant variants during treatment. A structural siRNA variant, Dicer-substrate siRNAs, were also tested to determine if they provided benefits in terms of potency and duration of action over canonical siRNAs targeted at the same motif for FCoV. For FCV experiments were performed using a panel of recent field isolates to determine if they are likely to be useful against currently circulating viruses.

2

General materials and methods

2.1. BUFFERS AND SOLUTIONS

The following reagents were used within experiments described throughout this thesis and are noted in the text by their abbreviated name in the left hand column below. Further details of reagent preparation are provided in Appendix A for those reagents marked with an asterisk (*).

Agarose plaque assay overlay media *	1% (w/v) agarose (Amresco, Salon, OH, USA) and 2% (v/v) FBS (Sigma-Aldrich, Castle Hill, NSW, Australia) in DMEM (Sigma-Aldrich)
CMC plaque assay overlay media *	0.9% (w/v) high viscosity (1500 ± 400 cP) carboxymethylcellulose (BDH Lab Reagents, Poole, England) and 2% (v/v) FBS in DMEM
Cryopreservation media	20% (v/v) FBS, 10% (v/v) glycerol (Sigma-Aldrich) in DMEM
DMEM	Dulbecco's modified eagles medium, with 1000 $mg.L^{-1}$ glucose, L-glutamine and sodium bicarbonate (Sigma-Aldrich)
DMEM-10	10% FBS (v/v) in DMEM
DMEM-2	2% FBS (v/v) in DMEM
FA gel running buffer	20 mM 2-[N-morpholino] propanesulfonic acid (Sigma-Aldrich), 5 mM sodium acetate (Sigma-Aldrich), 1 mM EDTA (Sigma-Aldrich), 2% (v/v) formalin (Sigma-Aldrich) in nuclease-free water (Amresco)

FBS	Foetal bovine serum (Sigma-Aldrich)
Methanol-free 10% formalin *	4% (w/v) paraformaldehyde (Polysciences, Warrington, PA, USA) in PBS
PBS *	Calcium and magnesium free phosphate buffered saline: 136.9 mM NaCl, 2.7 mM KCl, 10.1 mM Na_2HPO_4, 1.8 mM KH_2PO_4, pH 7.4 (Sigma-Aldrich)
Plaque assay fixation media	20% (v/v) formalin (Sigma-Aldrich) in PBS, pH 7.4
Plaque assay staining solution	1% (w/v) crystal violet (Merck, Kilsyth, Australia) in R/O water
Resazurin stock solution (4 x)	1.76 mM resazurin sodium salt (Sigma-Aldrich) in DMEM
SRB destain solution	10 mM tris (Sigma-Aldrich) in R/O water, pH 10
SRB fixation solution	10% (w/v) trichloroacetic acid (Univar, Auburn, Australia) in R/O water

SRB staining solution	0.2% (w/v) sulforhodamine B (Sigma-Aldrich) in 1% (v/v) acetic acid in R/O water
SRB wash solution	1% (v/v) acetic acid (Biolab Scientific, Australia) in R/O water
TAE buffer *	0.04 M Tris-acetate (Sigma-Aldrich), 0.001 EDTA (Sigma-Aldrich) in nuclease-free water
TE buffer	10 mM tris; 1 mM EDTA, pH 7.4 (Sigma-Aldrich)
Trypan blue	0.4% (w/v) trypan blue (Sigma-Aldrich) in PBS
Trypsin/EDTA	0.25 % (w/v) Trypsin, 0.02% (w/v) EDTA in PBS (Sigma-Aldrich)
Ultrapure water	Generated with a MilliQ PF plus ultrapure water purification system (Millipore) with the following specifications: resistivity = 18.2 MΩ-cm at 25°C; total organic carbons < 10 parts per billion; endotoxin log reduction = 5log; bacteria , < 1 colony forming unit.ml^{-1}
Viral transport media	1% (v/v) FBS, 100 IU penicillin (Sigma-Aldrich), 0.5 mg.ml^{-1} streptomycin (Sigma-Aldrich) in DMEM

2.2. CELL CULTURE METHODS

2.2.1. Cell line

Crandell Rees Feline Kidney cell line (CRFK) was acquired from the Faculty of Veterinary Science, The University of Melbourne at passage number 35. CRFK cell line, initiated in 1964, is a immortalised epithelial-like cell line derived from renal cortical tissue of a healthy 10 to 12 week old female domestic shorthaired kitten (Crandell et al., 1973). For routine passaging cells were grown in standard tissue culture treated plastic flasks (Sarstedt,

Numbrecht, Germany) in DMEM-10, a growth/maintenance medium consisting of low glucose Dulbecco's Modified Eagles Medium (Sigma-Aldrich, Castle Hill, NSW, Australia) supplemented with 10% FBS (Sigma-Aldrich). Cells were cultured in a humidified incubator at 37°C in 5% CO_2 in air. All sterile manipulations were performed in a class II biosafety cabinet using sterile dedicated cell culture glassware and pipettes or sterile disposable plastic consumables. To minimise the risk of contamination, the biosafety cabinet was disinfected with 70% (w/v) ethanol in water and exposed to UV radiation for 20 min before and after use. As a further precaution against viral contamination the biosafety cabinet was disinfected with 1% solution of Virkon S (DuPont, Sudbury, Suffolk, UK) with a 10 minute contact time following cell culture work involving viruses or clinical samples.

2.2.2. Cell bank

To ensure a ready supply of healthy low passage cells, a cell bank system consisting of master and working stocks was implemented. The initial aliquot of cells was extended by routine passage in 75 cm^2 flasks and cells subsequently cryopreserved as described in Section 2.2.5 to produce the master cell stock. Aliquots of master cell stock were similarly expanded and cryopreserved as required to produce aliquots of working cell stocks. The expanded working cell stocks were designated as working passage zero. All experiments were conducted with cells between working passage 4 and 15.

2.2.3. Cell propagation

Cells were harvested and passaged when approximately 90 to 95% confluent. To harvest cells, culture media was discarded and the monolayers washed with calcium- and magnesium-free phosphate buffered saline (PBS) (1 ml per 5 cm^2). PBS was discarded and 0.25% trypsin / 0.02% EDTA solution (Sigma-Aldrich) (0.5 ml per 25 cm^2) added and allowed to stand for 30 s. Trypsin / EDTA solution was subsequently discarded and the flasks incubated at room temperature for approximately 2 min. Once the cells had rounded up and detached they were resuspended in fresh DMEM-10 and the solution gently triturated several times with a graduated pipette to ensure a single cell suspension. For routine passaging, cells were split at a ratio of 1:3-1:8 depending on experimental requirements. For experiments requiring seeding with precise cell numbers the harvested cells were quantified as detailed in Section 2.2.4 and diluted to the appropriate concentration in DMEM-10.

2.2.4. Cell quantification and assessment of viability

Cells were quantified and assessed for viability using the trypan blue exclusion method and manual counting with a haemocytometer. To perform this test an equal volume of cell suspension and 0.4% trypan blue were mixed and 10 µl of this suspension was loaded onto an improved Neubauer haemocytometer (Weber, England). Cells were visualised using an

Olympus BH2 light microscope (Olympus, Melville, NY, USA) with 100 x magnification, and the number of viable (bright refractile cells) and non-viable (non-refractile blue cells) counted in the four 1 mm^2 corner squares (volume = 0.1 µl per square). To improve the accuracy of counting, the original cell suspension was diluted in PBS as required to result in approximately 50 to 100 cells per large corner square. The concentration of the original cell suspension was then calculated according to the following formula:

$$Cell\ concentration\ (cells.ml^{-1}) = \frac{total\ cells\ counted}{4} \times\ dilution\ factor \times 10{,}000$$

The viability of the cell suspension was calculated as follows:

$$\%\ viability = \frac{viable\ cells\ counted}{total\ cells\ counted} \times\ 100$$

2.2.5. Cryopreservation

For cryopreservation cells were harvested in the log phase of growth. Prior to cryopreservation the quantity and viability of harvested cells was determined as in Section 2.2.4 to ensure greater than 90% viability prior to freezing. The cell suspension was centrifuged at 400 x g for 5 min and the pellet resuspended in cryopreservation media consisting of 20% FBS and 10% glycerol in DMEM to a concentration of 4 x 10^6 cells.ml^{-1}. Aliquots were frozen at controlled cooling rate of approximately -1°C.min^{-1} by placing cryovials (Corning Inc., Corning, NY, USA) in a 5100 Cryo 1°C Freezing Container, “Mr Frosty”, (Nalgene, Penfield, NY, USA) at -80°C overnight. Cryovials were subsequently transferred to the vapour phase of liquid nitrogen for long term storage. For quality control, a vial of cryopreserved cells from each batch was revived as detailed below after 24 h storage in liquid nitrogen to test viability of cryopreserved cells.

To recover cells, cryovials were removed from liquid nitrogen storage and transferred immediately to a water bath at 37°C for rapid thawing. The cell suspension was transferred to a sterile 10 ml centrifuge tube (Sarstedt) and diluted with pre-warmed DMEM-10. To minimise osmotic shock, 2 ml DMEM-10 was added dropwise, with stirring of the suspension between each drop. A further 7 ml DMEM-10 was added to suspension, and sample centrifuged at 200 x g for 8 min at room temperature. The supernatant was discarded, the cells resuspended in fresh DMEM-10, and transferred to a tissue culture flask. Post-thawing trypan blue cell viability staining was performed as in Section 2.2.4 and only samples with post-thaw viability >80% were used for subsequent experiments.

2.3. VIROLOGICAL METHODS

2.3.1. Feline coronavirus (FCoV)

Two strains of FCoV, FIPV WSU 79-1146 (FIPV1146) and FECV WSU 79-1683 (FECV1683), acquired from the American Type Culture Collection (Virginia, USA), were used in this study. FCoV FECV1683 was originally isolated from mesenteric lymph nodes and intestinal washes of a 1 ½ year old female domestic shorthaired cat that died of acute haemorrhagic gastroenteritis (McKeirnan et al., 1981). FCoV FIPV1146 was originally isolated from the liver, spleen, and lungs from a case of neonatal death in a 4-day-old male Persian kitten (McKeirnan et al., 1981). Pathogenicity studies of these two isolates have shown that FIPV1146 is highly virulent and reliably causes signs of classic FIP in cats following oronasal inoculation, while FECV1683 causes a low grade fever and, in some cats, mild enteritis, but no signs of FIP (Pedersen, 2009; Pedersen et al., 1984). Despite the dissimilar *in vivo* biological properties of the two isolates, a number of studies have shown that the two have quite similar *in vitro* properties in immortalised cell lines (Boyle et al., 1984; Dewerchin et al., 2005; McKeirnan et al., 1987).

2.3.1.1. Propagation of FCoV

Working stocks of FCoV were produced in CRFK using 75 cm^2 or 175 cm^2 tissue culture flasks (Sarstedt). Tissue culture media was removed prior to addition of viral inoculum to 80 to 90% confluent CRFK cells. Virus was allowed to adsorb for 90 min prior to adding fresh DMEM-10. Flasks were incubated at 37°C until monolayers showed > 80% CPE, wherein virus was harvested by scraping the remaining adherent cells and collecting the cell suspension. The cell suspension was centrifuged at 1000 x g for 5 min and the supernatant transferred to a sterile centrifuge tube (Sarstedt) and temporarily stored at 4°C. The cell pellet was resuspended in residual media and subjected to three freeze-thaw cycles. The lysed cell pellet suspension and reserved supernatant were combined and centrifuged at 2000 x g for 20 min at 4°C. The clarified viral media was aliquoted to sterile 1.5 ml microtubes (Sarstedt) and stored at -80°C until use. Fourth passage virus stocks of both FCoV FIPV1146 and FECV1683 were used in this study.

2.3.1.2. Quantification of FCoV

2.3.1.2.1. Plaque assay

Plaque assays were performed in either 6- or 12-well plates (Sarstedt; Corning). Plates were prepared by seeding 2 x 10^5 cells.well^{-1} in 2 ml DMEM-10 (6-well plate) or 6 x 10^4 cells.well^{-1} in 1 ml DMEM-10 (12-well plate) and incubating for approximately 60 h at 37°C in 5% CO_2 in air. Serial log dilutions of virus prepared in DMEM were added to approximately 90% confluent monolayers of CRFK cells following the aspiration of culture media from the wells.

Virus was allowed to adsorb for 90 min, during which time the plates were gently rocked every 15-20 min to ensure an even spread of the viral inoculum and to prevent the monolayers from drying out. After 90 min the viral inoculum was removed and cells overlaid with DMEM containing 2% FBS and either 0.9% carboxymethylcellulose (1 ml.well^{-1} in 12-well plates) or 1% agarose (2 ml.well^{-1} in 6-well plates). After 48 h cells were fixed by adding 1 ml (12-well plate) or 2 ml (6-well plate) per well of 20% formalin in PBS for one hour at room temperature. Following fixation the overlay media/formalin was discarded and the monolayers gently rinsed with tap water and immediately stained with 500 µl (12 well plate) or 1 ml (6 well plate) of 0.1% (w/v) crystal violet for 10 min. Plates were thoroughly rinsed in tap water and air dried at room temperature prior to manual counting of plaques. An example of a FCoV FIPV1146 plaque assay is shown in Figure 2.1.

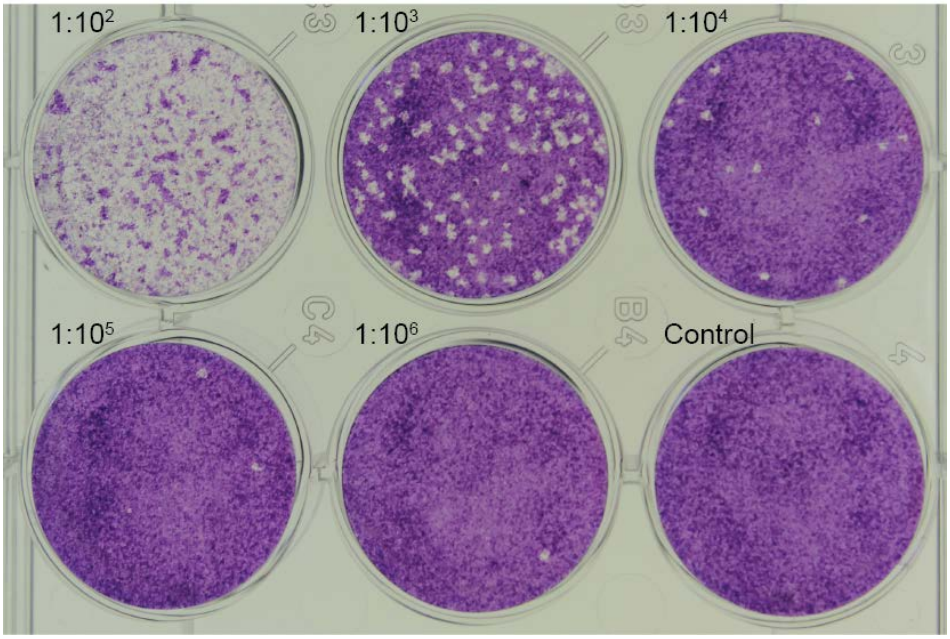

Figure 2.1: Example plaque assay of FCoV FIPV1146 using a carboxymethylcellulose overlay in 12-well plates. The titre for this plate was based on the 1:10^4 well and was calculated at 1.4 x 10^6 pfu.ml^{-1}.

2.3.1.2.2. Tissue culture infective dose 50% (TCID50) assay

Cell culture supernatant stored at -80°C was thawed at 37°C in a water bath and centrifuged at 1000 x g for 3 min to pellet cells/debris prior to performing the assay. Serial log dilutions of clarified supernatant in DMEM were added to subconfluent monolayers of CRFK cells in 96-well plates (Sarstedt), with four or six replicate wells per dilution. Wells were scored for the presence of absence of CPE 72 hpi using an Olympus CKX41 inverted phase-contrast microscope. Wells showing any evidence of CPE were scored as positive. TCID50 endpoint values were calculated according to the method of Reed and Muench (1938). Examples of positive and negative wells are shown in Figure 2.2.

a. b.

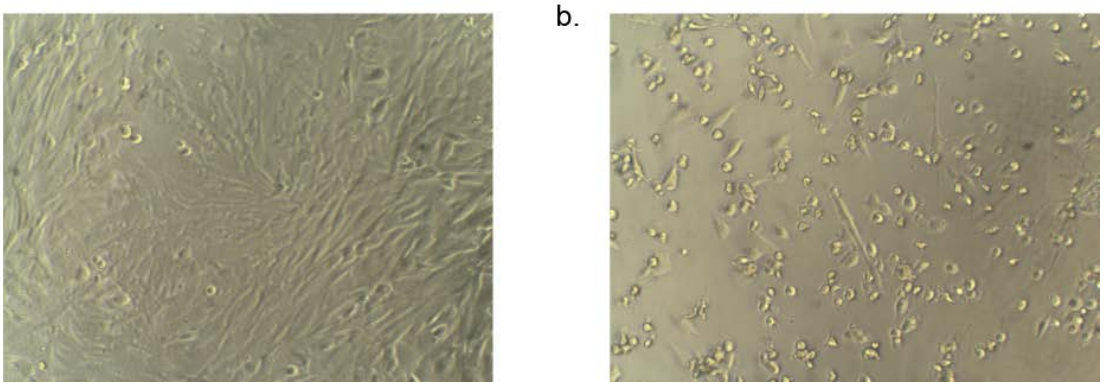

Figure 2.2: Feline coronavirus TCID50 assay. Examples of (a) negative and (b) positive wells. Obvious CPE consisting of cell rounding and detachment, as well as the formation of multinucleated syncytia are seen in positive wells. [100 x magnification].

2.3.2. Feline calicivirus (FCV)

Three field isolates of feline calicivirus and the vaccine strain F9 were kindly provided as a gift from Professor James Gilkerson of The University of Melbourne, Faculty of Veterinary Science. The field isolates were provided as a second passage while strain F9 was provided at an unknown passage number. The field isolates from Melbourne have been shown to be phylogenetically distinct with regards to their capsid sequences (personal communication: Ms Natalie Job, The University of Melbourne). Additional field isolates from Sydney, Australia, were collected as described in Section 2.3.2.1. Details of the FCV isolates used in this study are shown in Table 2.1.

Table 2.1: Details of FCV isolates used in experimental studies in this thesis. * indicates passage 2 within our laboratory, as original passage number unknown.

Strain	Disease manifestation / site of isolation	Location of isolation	Passage	Stock titre
F9	Vaccine strain	USA	P2 *	8.85×10^8
83E	Conjunctival swab from cat with oro-respiratory disease	Melbourne, Australia	P3	2.60×10^9
131M	Oropharyngeal swab from cat with oro-respiratory disease	Melbourne, Australia	P3	5.25×10^8
178N	Nasal swab from cat with oro-respiratory disease	Melbourne, Australia	P3	3.55×10^9
IW1E	Pharyngeal swab from cat with FCGS	Sydney, Australia	P2	4.50×10^8
IW10	Pharyngeal swab from cat with oro-respiratory disease	Sydney, Australia	P2	4.35×10^8
IW16	Swab from tongue ulcer noted as incidental finding during pre-general anaesthetic examination	Sydney, Australia	P2	3.05×10^8
IW25	Oropharyngeal swab from a cat with stomatitis	Sydney, Australia	P2	4.55×10^8

2.3.2.1. Isolation of FCV from clinical samples

Oral or oropharyngeal samples were taken using sterile cotton tipped swabs moistened with a sterile isotonic crystalloid solution (0.9% saline or Hartmann's solution). Swab tips were immediately placed into cryovials containing 1 ml viral transport media. Samples were stored at 4°C if a delay of less than 24 h occurred prior to transport to the lab, otherwise they were stored at -20°C until submission. The maximum storage time at -20°C was less than one month, which we have previously demonstrated in our lab does not result in a loss of infectivity for FCV.

Cryovials containing swab tips were vortexed for 1 min and the transport media transferred to a sterile 1.5 ml microtube. Samples were centrifuged at 1000 x g for 3 min and the supernatant (approximately 1 ml) added to subconfluent monolayers of CRFK cells in 6- or 12-well plates (Sarstedt / Corning). Virus was allowed to adsorb for 2 h. Viral inoculum was subsequently removed and replaced with fresh DMEM-10 supplemented with 100 units.ml^{-1} penicillin and 0.1 mg.ml^{-1} streptomycin (Sigma-Aldrich). Wells were monitored daily for five days for the development of CPE.

To confirm FCV as the causative agent in wells showing CPE, an indirect immunofluorescence assay was performed. Cells were harvested by scraping and trituration and 100 µl of cell suspension was used to make cytospin preparations on untreated glass slides using a Shandon Cytospin® 2 Cytocentrifuge (Shandon Southern Products, Cheshire,

UK) at 63 x g (750 rpm) for 5 min. Slides were subsequently air-dried for 30 min and the cell deposit outlined using a hydrophobic slide marker pen (PAP pen, Sigma-Aldrich). Cells were fixed in methanol-free 10% formalin (Polysciences) in PBS for 10 min, permeabilised in 0.2% Triton X-100 (Sigma-Aldrich) in PBS for 5 min, and blocked with 10% FBS in PBS for 30 min prior to staining, with slides rinsed two times in PBS between each step. The primary mouse anti-FCV monoclonal antibody clone S1-9 (Custom Monoclonals International, Sacramento, USA) was used at a concentration of 2 $\mu g.ml^{-1}$ and the secondary antibody goat anti-mouse IgG (H/L):FITC (AbD Serotec, Kidlington, UK) used at a concentration of 6.6 $\mu g.ml^{-1}$. Both antibody staining steps were performed at 37°C in a humid chamber for 30 min with the slides washed three times with PBS between each step. Finally cells were counterstained with 2 $\mu g.ml^{-1}$ 4',6-diamidino-2-phenylindole (DAPI) (Invitrogen, Mulgrave, VIC, Australia) in PBS for 60 s, washed three times with PBS, and the slides mounted with a coverslip using Citifluor AF1 antifadent (Citifluor Ltd, London, UK). Images were acquired using a BX-60F-3 epifluorescence microscope (Olympus) with attached DP70 camera (Olympus) at 200-400 x magnification. To serve as a negative control a well of mock infected CRFK cells was harvested and processed in parallel to the clinical isolates. An example IFA showing (a) negative control cells and (b) FCV clinical isolate IW1E is shown in Figure 2.3.

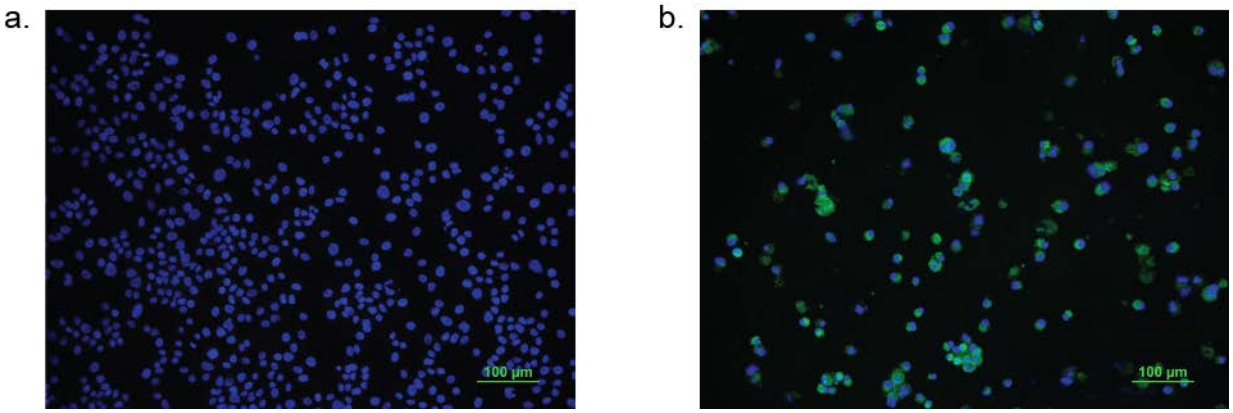

Figure 2.3: IFA for clinical isolates of FCV. Panel (a) shows uninfected negative control cells. Panel (b) shows FCV clinical isolate IW1E with infected cells displaying diffuse green (FITC) cytoplasmic staining. Cell nuclei counterstained with DAPI are blue and appear normal in panel (a) while in (b) there is evidence of nuclear degeneration associated with viral infection [bar = 100µm].

2.3.2.2. Propagation of FCV

Working stocks of FCV were prepared as described for FCoV in Section 2.3.1.1. The passage number of the FCV strains used in this study is shown in Table 2.1.

2.3.2.3. Quantification of FCV

2.3.2.3.1. Plaque assay

FCV plaque assays were performed as described for FCoV in Section 2.3.1.2.1 with the exception that assays were only performed in 6-well plates (Sarstedt) with CMC overlays and the plates were fixed and plaques visualised at 36 hpi. An example FCV plaque assay is shown in Figure 2.4.

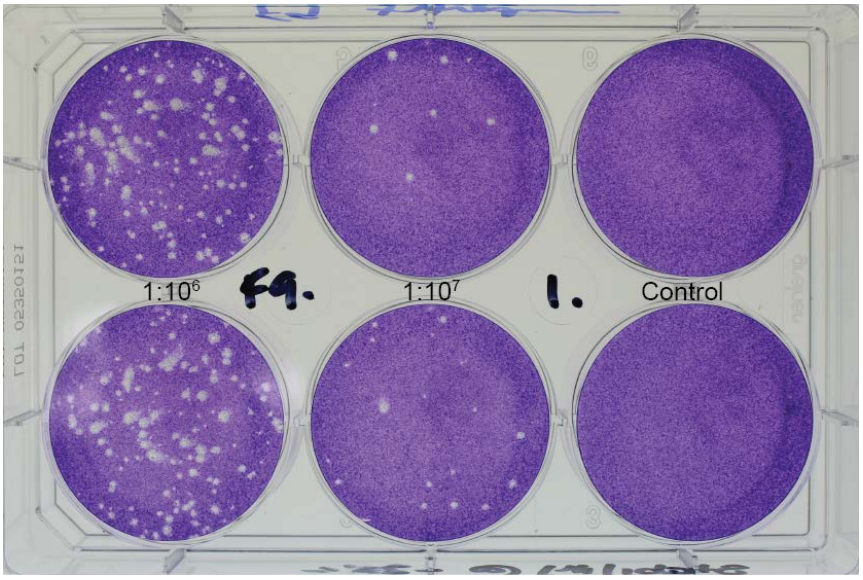

Figure 2.4: Example plaque assay for FCV strain F9. Considerable variability in plaque size was seen for all FCV isolates tested. In this case viral titre was determined using the $1:10^7$ wells. Calculated viral titre for this plate was 8.0×10^8 pfu.ml^{-1} (mean 16 plaques.well^{-1} in $1:10^7$ dilution wells, 200 µl virus suspension added).

2.3.2.3.2. Tissue culture infective dose 50% assay

FCV TCID50 assays were performed as described for FCoV in Section 2.3.1.2.2. Examples of positive and negative wells are shown in Figure 2.5.

a. b.

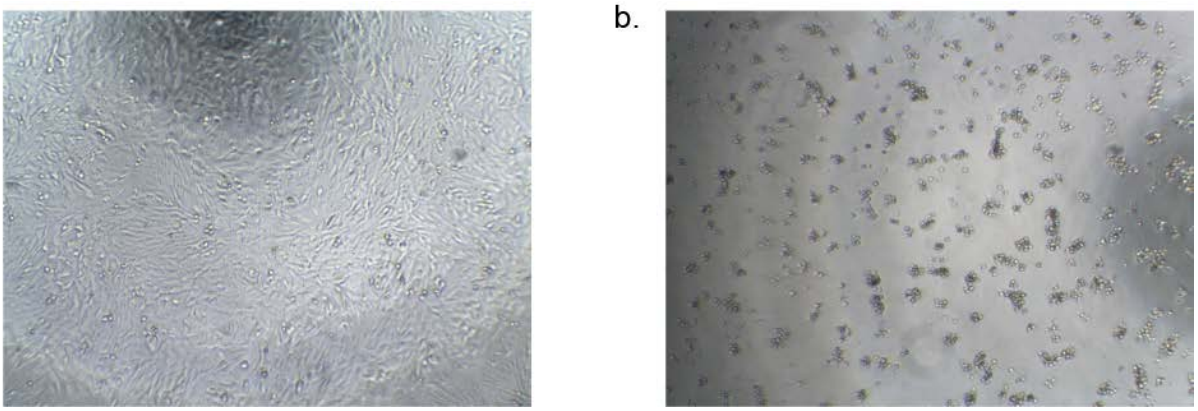

Figure 2.5: Feline calicivirus TCID50 assay. Examples of (a) negative and (b) positive wells. Obvious CPE was seen in positive wells and consisted in most cases of widespread destruction of the monolayer with floating dead cells often forming large aggregates [40 x magnification].

2.4. MOLECULAR BIOLOGY METHODS

2.4.1. siRNA\DsiRNA transfection

siRNAs were transfected into CRFK cells using the cationic lipid based transfection reagent Lipofectamine 2000 (Invitrogen). Both forward and reverse transfection methods were utilised in this study.

For forward transfection 6 x 10^4 cells.well^{-1} were added to 12-well tissue culture plates (Corning) 24 h prior to transfection. For experiments involving immunofluorescence studies and for monitoring transfection efficacy, cells were plated into wells containing preplaced sterile 13 mm glass coverslips (ProSciTech, Thuringowa, QLD, Australia). Transfection of the approximately 40-50% confluent cells was performed as per the manufacturer's protocol. Briefly, using the reagent volumes detailed in Table 2.2, Lipofectamine 2000 was diluted in Opti-MEM I (Invitrogen) and allowed to stand for 5 min. The dilute Lipofectamine 2000 was mixed with siRNAs diluted to the appropriate concentration in Opti-MEM I and the resulting mixture incubated at room temperature for 15 min to allow complex formation. After 15 min the siRNA complexes were added to the wells and mixed by gently rocking the plate. Cells were incubated at 37°C for the 6 h transfection period, following which the culture media was removed and the cells washed once with DMEM prior to infection.

Reverse transfection was conducted in both 24- and 96-well plates (Sarstedt, Greiner Bio-One) essentially as per the manufacturer's guidelines. siRNA / Lipofectamine 2000 complexes were prepared as for forward transfection using the optimised reagent volumes detailed in Table 2.2. The pre-prepared complexes were added to wells followed immediately by 1 x 10^4 cells.well^{-1} in 100 µl (96-well plate) or 8 x 10^4 cells.well^{-1} in 500 µl (24-

well plate) cell suspension. Plates were rocked gently to ensure mixing and even distribution of cells and incubated at room temperature for 30 min to minimise edge effect prior to being placed in an incubator at 37°C for a further 6 h. At the end of the transfection period the culture media was removed by decanting (96-well) or aspiration (24-well) and the cells washed once with DMEM prior to infection. The transfection protocol for DsiRNA was identical to that for siRNAs.

Table 2.2: Reagent volumes per well for forward and reverse transfection protocols**.**

Method	Plate format	Final well volume (µl)	Lipofectamine 2000 (µl)	OptiMEM (µl)	Dilute siRNA
Forward	12-well	1000	2	98	100
Reverse	24-well	1000	1.25	48.75	50
Reverse	96-well	150	0.3	24.7	25

Experiments were conducted to examine the effect of siRNA transfection on cell viability. Cell viability was assessed 24 h post transfection for both forward and reverse transfection methods using the trypan blue viability assay (Section 2.2.5) and a modification of the resazurin-based cell viability assay (Section 4.3.2) respectively. For both methods the transfection of 100 nM siRNA was associated with no significant reduction in cell viability compared to mock transfected cells.

2.4.2. Quantitative real time reverse transcriptase PCR (qRT-PCR)

2.4.2.1. Cellular RNA extraction

Cells were lysed *in situ* in Buffer RLT (QIAGEN, Doncaster, VIC, Australia), homogenised by vortexing for 60 s, and stored at -80°C prior to extraction. Total RNA was extracted using RNeasy Mini spin columns (QIAGEN) as per manufacturer's protocol, including an on-column RNase-free DNase I (QIAGEN) treatment. An aliquot of extracted RNA was diluted 1:25 in TE buffer (Sigma-Aldrich) and optical density measured at 260 and 280 nm using a Beckman DU640 spectrophotometer (Beckman Coulter, Fullerton, CA, USA). Sample purity was assessed via OD280/OD260 ratio, and RNA yield was calculated according to the following formula:

$$[RNA]\, ng.\mu l^{-1} = OD260 \times dilution\ factor \times 40$$

RNA integrity was assessed by formaldehyde agarose (FA) denaturing gel electrophoresis. Horizontal slab gels were prepared at a concentration of 1.2% agarose in FA running buffer. To prepare the gel, agarose was added to FA running buffer without formalin and dissolved by heating in a microwave for approximately 1 min. After cooling to approximately 65°C formalin was added (2% v/v) and the gel cast. Samples (approximately 1 µg RNA) were

mixed with RNA sample loading buffer containing ethidium bromide (Sigma Aldrich) and incubated at 70°C for 10 min, and placed on ice for 1 min prior to loading. RNA markers (Promega, Alexandria, NSW, Australia) were processed in an identical manner to the samples and included in each run. Electrophoresis was carried out at 90 V for 60 to 90 min. Samples were visualised and imaged using a UV transilluminator (Geldoc XR, Biorad, Hercules, CA, USA). Non-degraded samples demonstrate two sharp bands representing the 28S and 18S ribosomal subunits, with the 28S/18S intensity ratio approximately two.

2.4.2.2. Reverse transcription

cDNA was generated from purified RNA using Superscript® III (Invitrogen), a modified Moloney Murine Leukemia Virus reverse transcriptase in a final reaction volume of 20 µl. For cellular RNA the reaction consisted of 1 µg purified RNA, 100 ng random hexamer primers (Promega), 2.5 µM of each dNTP (Promega), and RNase-free water (Amresco) to a final volume of 14.5 µl. Samples were incubated at 65°C for 5 min to denature the RNA and cooled on ice for 1 min. To this was added 5.5 µl of a mix consisting of 4.5 µl First Strand Buffer (Invitrogen), 20 units RNasin Plus RNase Inhibitor (Promega), and 100 units of Superscript III. Using a thermal cycler (Eppendorf), tubes were incubated at 50°C for 60 min followed by 15 min at 70°C to inactivate the reverse transcriptase. cDNA was stored at -80°C until use.

2.4.2.3. PCR primers

Primers were designed using Primer3 software (Rozen and Skaletsky, 2000) using the published sequences of FCoV FIPV1146 (Accession number DQ010921) and feline GAPDH mRNA (Accession number AB038241) and are shown in Table 2.3. Desalted oligonucleotide primers were purchased from Sigma-Aldrich in the lyophilised form. Primers were reconstituted as 50 µM solutions in nuclease-free water (Amresco) and stored at -20°C. Working stocks of forward and reverse primers were made up as 2.5 µM solutions in nuclease-free water and stored at -20°C.

Table 2.3: Primers for FCoV qRT-PCR. FCoV primers designed based on reported sequence of FCoV FIPV1146 (accession number DQ010921). GAPDH primers designed based on sequence of feline GAPDH mRNA (accession number AB038241).

Target	Primer Sequence	Product size (bp)
GAPDH		
Forward	5'- GCGTGAACCACGAGAAGTATG-3'	236
Reverse	5'- GCCAGTAGAAGCAGGGATGA-3'	
FCoV Genome		
Forward	5'- CGGACACCAACTCGAACTAAA-3'	171
Reverse	5'- GAACCGCCGCAGCTAATAC-3'	
Membrane mRNA		
Forward	5'- CTTCGGACACCAACTCGAAC-3'	274
Reverse	5'- GCCATAAACGAGCCAGCTAA-3'	
Nucleocapsid mRNA		
Forward	5'- CTTCGGACACCAACTCGAAC-3'	202
Reverse	5'- GGAACAAGGTCTCTCGGACAT-3'	

2.4.2.4. Quantitative real time PCR

Each unknown sample or standard was amplified in a separate 10 µl reaction in quadruplicate. The PCR reaction consisted of 1 µl of a 1:10 dilution of cDNA, 2 µl 5 x GoTaq Colorless Reaction Buffer (Promega), 2.5 pmol forward and reverse primers, 2.5 nmol of each dNTP, 0.25 units GoTaq DNA polymerase (Promega), 1 µl 1:1000 SYBR Green (Invitrogen), and 25 µmol (GAPDH and FCoV genome targets) or 10 µmol (membrane and nucleocapsid mRNA targets) $MgCl_2$. qRT-PCR reactions were performed using a Rotor-Gene 3000 cycler (Corbett Life Science, Mortlake, NSW, Australia) with SYBR green signal acquisition using 470/20 (excitation) and 510/10 (emission) band-pass filters. Cycling conditions for GAPDH, FCoV genome, and nucleocapsid mRNA were as follows: initial denaturation of DNA at 95°C for 2 min, 30 cycles of 30 s at 95°C, 30 s at 62°C, and 30 s at 72°C, followed by a final extension at 75°C for 30 s. Cycling conditions for amplifying membrane mRNA were identical with the exception of a 45 s annealing time during cycling. A post amplification melt curve analysis was performed from 74°C to 96°C at 10 s per degree to confirm product specificity for all reactions.

2.4.2.5. Preparation of PCR standards for quantification

PCR products were produced in 50 µl reactions using the optimised conditions described in Section 2.4.2.4 with the exception that SYBR Green was replaced by additional nuclease-

free water. Amplified products were purified using the QIAquick PCR purification kit (QIAGEN) according to the manufacturer's protocol. A 2% (w/v) horizontal gel slab, containing 0.25 µg.ml^{-1} ethidium bromide (Sigma-Aldrich), was prepared in TAE buffer. A sample of the purified PCR product and a 100 bp DNA ladder (Promega) was electrophoresed for 60 to 90 min at 100 V to confirm a single band of the appropriate size. The concentration and purity of the PCR standards was determined spectrophotometrically (Beckman DU640). DNA concentration was calculated according to the following formula:

$$[DNA]\, ng.\mu l^{-1} = OD260 \times 50$$

Individual PCR products were diluted in nuclease free water to give a stock concentration of 50 ng.µl^{-1} and stored in aliquots at -20°C until use.

For absolute quantification the starting copy number of the standards, prior to serial dilution, was calculated according to the equation.

$$Copy\ number.\mu l^{-1} = \frac{N_A \times DNA\ concentration}{number\ of\ base\ pairs \times 660}$$

Where N_A is the Avogadro constant which equals 6.022 x 10^{23} and the DNA concentration, determined from spectrophotometric analysis is given in g.µl^{-1}. The constant 660 in the denominator represents the average weight (in Daltons) of a single base pair of double-stranded DNA.

Five serial log dilutions of purified PCR product were amplified in quadruplicate under identical conditions during each PCR run. To minimise the risk of cross contamination the standard PCR reactions were prepared in a separate laboratory space to unknown and no-template control samples. To minimise the risk of PCR product degradation, fresh standard dilutions were produced daily.

2.4.2.6. qRT-PCR data analysis

Absolute quantification of viral genomic or messenger RNA copy number was performed using the inbuilt functions of Rotor-Gene software (Version 6.1). Briefly a standard curve was produced by plotting starting template copy number against Ct using the "auto-find threshold" function to maximise R^2. For reactions with appropriate R^2 (>0.98) and efficiency values (>90% <110%) the copy number of experimental samples was interpolated from the standard curve.

Viral copy number was divided by the copy number of the endogenous reference gene GAPDH to give a normalised target value for each sample. Outliers within the PCR quadruplicates, defined as values > 3 standard deviations from the mean of the remaining replicates, were excluded from analysis. To calculate the relative inhibition due to treatment

effects this normalised value was divided by the normalised mean of the untreated sample and expressed as percentage inhibition.

2.4.3. Viral sequencing

2.4.3.1. RNA extraction

Tissue culture supernatant was thawed at 37°C in a water bath and clarified by centrifugation at 2000 x g for 3 min. RNA was extracted using the QIAamp Viral RNA mini kit (QIAGEN) as per the manufacturer's protocol. RNA was eluted in 60 µl Buffer AVE (QIAGEN) and stored at -80°C prior to use.

2.4.3.2. RT-PCR

Primers were designed using Primer3 software (Rozen and Skaletsky, 2000) to flank the target sites of siRNAs L2 and N1 (Table 2.4). Reverse transcription was as described in Section 2.4.2.2 with the exception that a fixed volume (13 µl) of RNA was used instead of a fixed mass. Conventional PCR was performed in an Eppendorf Mastercycler Gradient thermal cycler in 50 µl reactions containing 10 µl 5 x GoTaq Colorless Reaction Buffer, 12.5 nmol of each dNTP, 12.5 pmol forward and reverse primers, 125 µmol $MgCl_2$, 1.25 units GoTaq DNA polymerase, 2 µl cDNA, 22.75 µl nuclease-free water. Cycling conditions were as follows: initial denaturation of DNA at 95°C for 5 min, 35 cycles of 30 s at 95°C, 45 s at 58°C, and 60 s at 72°C, followed by a final extension at 72°C for 5 min.

2.4.3.3. DNA Sequencing

PCR products were purified prior to sequencing using the Wizard® SV Gel and PCR Clean-Up System (Promega) as per the manufacturer's protocol. Prior to purification 1 µl of PCR product was electrophoresed for 60 to 90 min at 100 V on a standard 2% (w/v) agarose horizontal gel slab, containing 1 µl.100 ml^{-1} GelRed (Biotium, Hayward, CA, USA), in TAE buffer. Gels were visualised by UV transillumination (Dolphin View, Wealtec, Sparks, NV, USA) to confirm a single band of the appropriate size. The optical density of the purified product was measured at 260 and 280 nm using a NanoDrop ND-1000 spectrophotometer (Thermo Fisher Scientific, Waltham, MA, USA). Sample purity was assessed via OD280/OD260 ratio (target range 1.8-2.0) and DNA concentration was calculated according to the formula in Section 2.4.2.5. Purified PCR products resuspended to 50 $ng.\mu l^{-1}$ in nuclease-free water were submitted to Macrogen Inc. (Seoul, South Korea) for sequencing in both directions using an ABI *3730xl* DNA Analyser. Resultant electropherograms were aligned and edited using Geneious (Version 4.6 Biomatters Ltd, Auckland, NZ) and Bioedit Sequence Alignment Editor (Version 7.2.0, http://www.mbio.ncsu.edu/bioedit/bioedit.html) software.

Table 2.4: Primers for sequencing L2 and N1 target sites. FCoV primers designed based on reported sequence of FCoV FIPV1146 (accession number DQ010921).

Target	Primer sequence	Product size (bp)
Leader2		
Forward	AAAGTGAGTGTAGCGTGGCTAT	452
Reverse	AGGTCACGACGGTATTCAGG	
Nucleocapsid1		
Forward	TCGCTGAGAGGTGGTTCTTT	461
Reverse	CTTGCCTGCAGTTTTCTTCC	

2.5. FLUORESCENT IMAGING METHODS

2.5.1. Antibodies, secondary detection reagents, and cell stains

Details of the antibodies, secondary detection reagents, and cells stains used in this thesis are shown in Table 2.5.

Table 2.5: Antibodies, secondary detection reagents, and cell stains used in this thesis.

Description	Supplier	Specificity
FITC conjugated anti-FCoV antiserum (feline and porcine origin)	VMRD (Pullman, WA, USA)	FCoV
Biotinylated mouse anti FCoV monoclonal antibody (Clone CCV2-2)	Custom Monoclonals International (Sacramento, CA, USA)	FCoV
Mouse anti FCV monoclonal antibody (Clone S-19)	Custom Monoclonals International	FCV
Streptavidin Alexa Fluor 555	Invitrogen (Mulgrave, VIC, Australia)	Biotin
Goat anti-mouse IgG (H/L):FITC	AbD Serotec, (Kidlington, UK)	Mouse IgG (H/L)
DAPI	Invitrogen	DNA
HCS CellMask Blue	Invitrogen	Whole cell stain

2.5.2. FCoV IFA on glass coverslips

2.5.2.1. Fixation and staining protocol

For some experiments imaging was performed on cells grown directly on glass coverslips. Glass coverslips (13 mm diameter) were sterilised by dry heat (161°C for 90 min) prior to use and pre-placed into 12-well plates prior to cell seeding. Details of fixation, permeabilisation, and staining for intracellular FCoV antigen is shown in Table 2.6.

Table 2.6: Details of immunofluorescence staining protocol for FCoV antigen in cells grown on glass coverslips (all steps at room temperature unless otherwise indicated).

Step	Details
Fixation	10% methanol-free formalin in PBS for 10 min (coverslips fixed in situ)
Washing	x 1 in PBS
Permeabilisation	0.2% Triton X-100 (Sigma-Aldrich) in PBS for 5 min
Washing	x 2 in PBS, stand for 5 min between rinses
Blocking	10% FBS in PBS for 30 min at room temperature
Primary antibody	Transfer coverslips to new 12 well plates. FITC conjugated anti-FCoV antiserum (50 µl.coverslip^{-1}) for 30 min at 37°C in humid chamber
Washing	x 2 in PBS, stand for 5 min between rinses
Nuclear staining	2 µg.ml^{-1} DAPI in PBS for 60 s
Washing	x 2 in PBS, stand for 5 min between rinses
Preparation for imaging	Add 10 µl Citifluor AF1 antifadent (Citifluor Ltd, London, UK) and mount coverslip on glass slide. Seal coverslip with nail varnish

2.5.2.2. Image acquisition

Mounted coverslips were imaged using a Zeiss LSM 510 Meta Confocal microscope (Carl Zeiss, Jena, Germany) in multi-track mode at 200 x magnification using the 488 nm line of an argon laser (excitation) with a 505 nm long pass filter (emission) for FITC and a 405 nm diode laser (excitation) with a 420-480 nm band-pass filter (emission) for DAPI as shown in Figure 2.6.

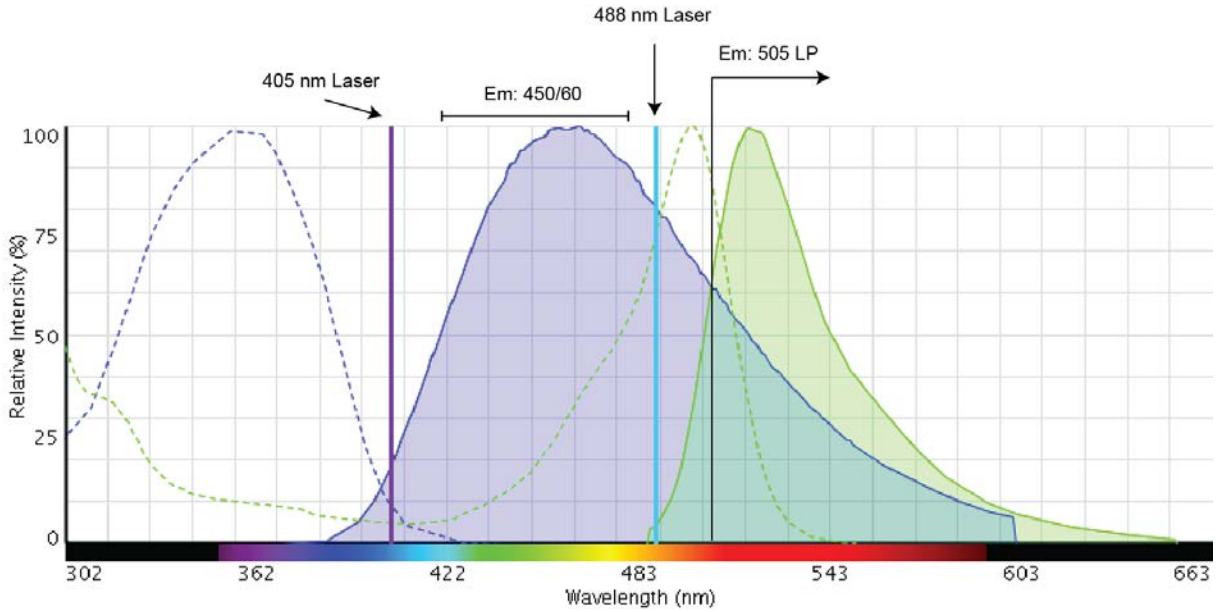

Figure 2.6: Excitation and emission spectra of fluorochromes used for imaging FITC/DAPI stained cells. Blue dotted and solid lines represent excitation and emission spectra of DAPI respectively. Green dotted and solid lines represent excitation and emission spectra of FITC. Laser source and emission optics for each fluorochrome are shown. Image produced using Fluorescence Spectraviewer (Life Technologies, Mulgrave, VIC, Australia. Em, emission; LP, long-pass.

2.5.3. FCoV IFA in 96-well plates

2.5.3.1. Fixation and staining protocol

For some experiments cells grown in 96-well plates were fixed and stained *in situ* for FCoV antigen expression. Imaging of 96-well plates was performed using a BD Pathway 855 Bioimager (BD Bioscience, Franklin Lakes, NJ, USA).

Preliminary experiments identified problems with cell loss during staining. An experiment was conducted to optimise fixation and permeabilisation methods. Fixation methods tested were 10% methanol-free formalin in PBS, 20% formalin in PBS, and 100% methanol. Permeabilisation methods tested were Triton X-100 (0.2% and 0.1% in PBS) and 100% ice-cold methanol. The effect of drying cells at room temperature between fixation and permeabilisation/staining was also tested. As shown in Figure 2.7 different fixation/permeabilisation methods resulted in significant differences in cell loss. The optimal method was determined to be fixation with 20% formalin for 30 min at 4°C followed immediately by permeabilisation with 100% ice-cold methanol for 5 min. The different fixation/permeabilisation methods were demonstrated not to have a significant effect on antibody staining with anti-FCoV monoclonal antibody clone CCV2-2.

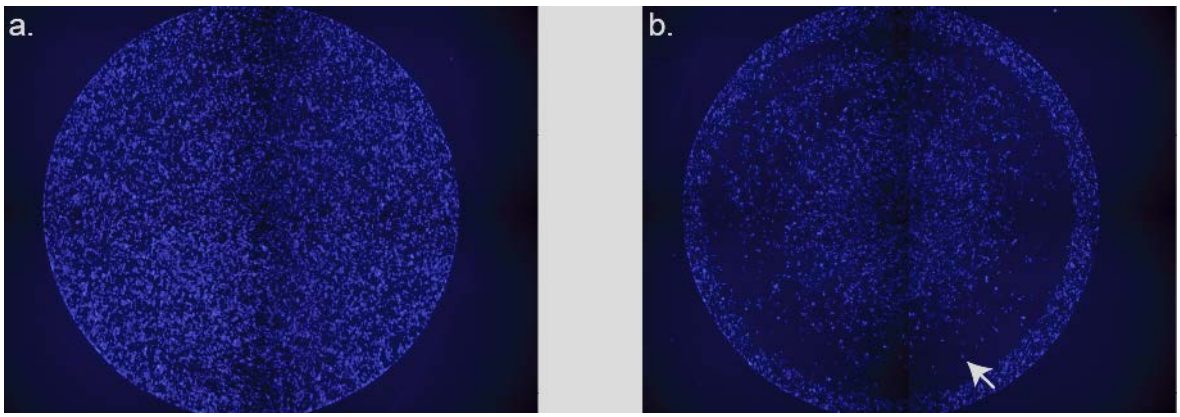

Figure 2.7: Comparison of fixation methods for staining in 96-well plates: (a) fixation with 20% formaldehyde/permeabilisation with 100% ice-cold methanol, (b) fixation with 20% formaldehyde/permeabilisation with 0.2% Triton X-100. Following fixation cells were mock treated with the multiple staining/washing steps to simulate the final staining procedure. Finally cells were stained with DAPI and imaged as a 2x2 montage with a 4 x objective using the BD Pathway 855 Bioimager. Wells permeabilised with Triton X-100 (b) displayed significant cell loss in a peripheral ring (white arrow). The annular nature of the cell loss likely reflects the effect of fluid shear forces on cells poorly fixed to the plate during the staining / washing procedures.

The FCoV staining protocol for 96-well plates is detailed in Table 2.7. To enable accurate cell segmentation, cells were stained with HCS CellMask Blue, a whole-cell stain, in addition to the nuclear stain DAPI. Although DAPI and HCS CellMask Blue have similar excitation and emission spectra (Figure 2.8a) and were imaged in the same channel, differentiation of nuclei and cytoplasm was possible due to clear differences in staining intensity (Figure 2.8b).

Table 2.7: Details of immunofluorescence staining protocol for FCoV antigen in cells grown in 96-well plates (all steps were performed at room temperature unless otherwise indicated).

Step	Details
Fixation	20% formaldehyde in PBS for 30 min at 4°C (100 µl.well^{-1})
Permeabilisation	100% ice-cold methanol for 5 min (100 µl.well^{-1})
Washing	x 2 in PBS, stand for 5 min between rinses (200 µl.well^{-1})
Blocking	10% FBS in PBS for 30 min (30 µl.well^{-1})
Primary antibody	Biotinylated CCV2-2 at 3 µg.ml^{-1} in 10% FBS in PBS (30 µl.well^{-1}) for 1 h
Washing	x 2 in PBS, stand for 5 min between rinses (200 µl.well^{-1})
Detection reagent	Streptavidin conjugated Alexa Fluor 555 10% FBS at 5 µg.ml^{-1} in PBS (30 µl.well^{-1}) for 1 h
Washing	x 1 in PBS, stand for 5 min between rinses (200 µl.well^{-1})
Whole cell staining	1 µg.ml^{-1} HCS Cell Mask Blue stain (50 µl.well^{-1}) in PBS for 1 h, with 50 µl of 4 µg.ml^{-1} DAPI in PBS (for final concentration in well of 2 µg.ml^{-1}) added for the final 1 min
Washing	x 2 in PBS, stand for 5 min between rinses (200 µl.well^{-1})
Preparation for imaging	100 µl PBS added per well – store plates at 4°C prior to imaging

a.

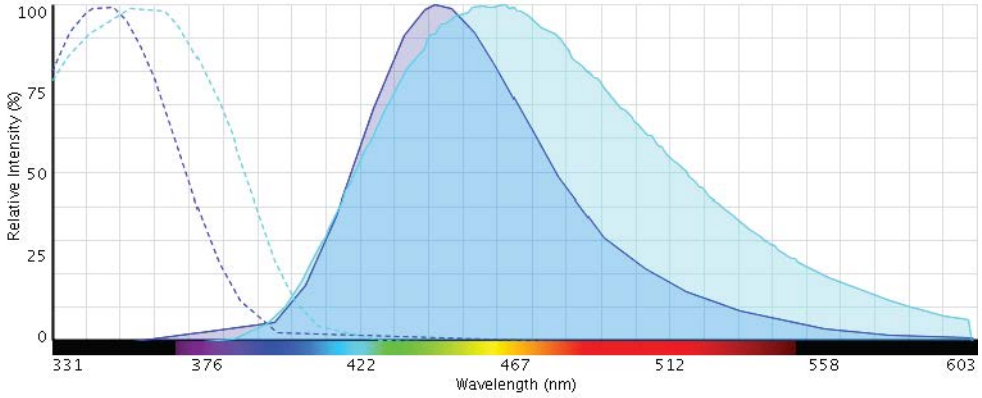

b.

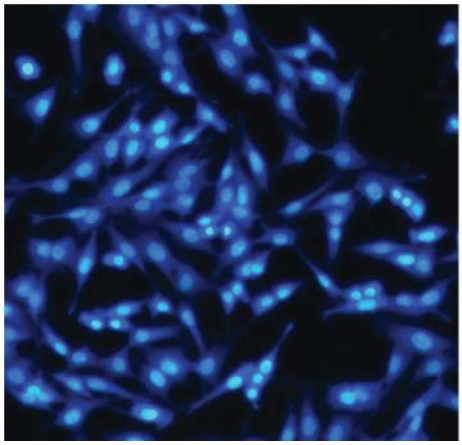

Figure 2.8: Nuclear/cytoplasmic staining for image segmentation. Cells were stained with HCS CellMask Blue and DAPI. Panel (a) shows the excitation (dotted lines) and emission (solid lines) spectra of HCS CellMask Blue (dark blue) and DAPI (light blue). Despite imaging in the same channel, identification of nuclei and cytoplasm was possible due to clear differences in intensity between these cellular compartments, as shown in Panel (b). Panel (a) produced using Fluorescence SpectraViewer (Life Technologies).

2.5.3.2. Image acquisition

Fluorescent imaging of cells in 96-well plates was performed using the BD Pathway 855 Bioimager. Images of wells were acquired using a 10 x objective (NA 0.4) using a 3 x 3 or 4 x 4 montage with laser autofocus performed for each montage frame. HCS Cell Mask Blue / DAPI, images were acquired with Ex 380/10 BP and Em 435 LP filters, and Alexa Fluor 555 images acquired with Ex 548/20 BP and Em 570 LP filters as shown in Figure 2.9.

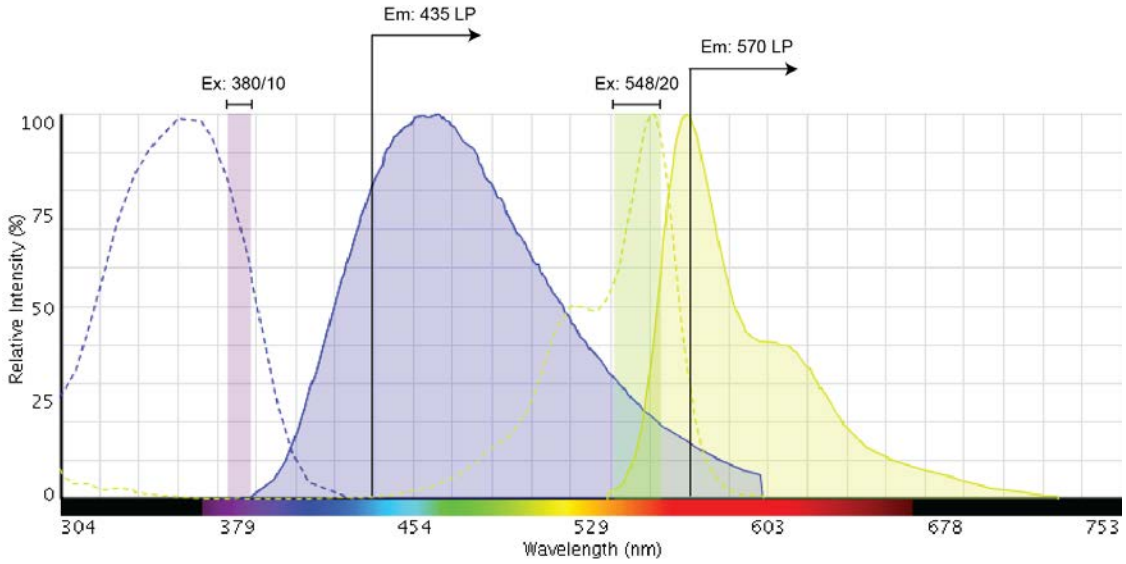

Figure 2.9: Excitation and emission spectra of fluorochromes used for imaging in 96-well plates. Blue dotted and solid lines represent excitation and emission spectra of DAPI/HCS Cell Mask Blue respectively. Yellow dotted and solid lines represent excitation and emission spectra of Alexa Fluor 555. Excitation and emission optics for each fluorochrome are shown. Image produced using Fluorescence SpectraViewer (Life Technologies). Ex, excitation; Em, emission; LP, long pass.

2.5.3.3. Post-acquisition image analysis

Image analysis was performed using the free open-source image analysis software CellProfiler (R11710, www.cellprofiler.org) (Carpenter et al., 2006). Using the available computer resources, memory errors were encountered using CellProfiler to process the large montage images acquired. To overcome this, original images were reduced in size using Adobe Photoshop CS5 12.0.3 x32 (Adobe, San Jose, California, USA) to a maximum X-Y dimension of 1500 pixels, and saved using the lossless tif format prior to analysis.

A CellProfiler pipeline was constructed to measure whole cell fluorescent intensity, the outline of which is shown schematically in Figure 2.10. Accurate cell segmentation was achieved with a two-step process using images acquired in the DAPI/HCS CellMask Blue channel. Firstly, nuclei were identified with the “IdentifyPrimaryObjects” module using manual thresholding and separation of adjacent nuclei based on shape. As each primary object is associated with a single secondary object, accurate segmentation of the nuclei in the first step was essential. Using the identified nuclei as seeds, the cytoplasmic boundaries for each cell were identified using the “IdentifySecondaryObjects” module, with manual thresholding and an image based watershed method to separate connecting cells. The final step of the pipeline was to measure fluorescence intensity in the Alexa Fluor 555 channel within the previously determined cell boundaries. CellProfiler data was exported to FCS

Express Image Cytometry (De Novo Software, Los Angeles, CA, USA) for analysis. Calculation of the percentage of infected cells was performed by placing a region marker on fluorescence intensity histograms to exclude negative cells as defined by uninfected control samples.

Segmentation of multinucleated syncytia, as can occur with FCoV infection is challenging. For syncytia, accurate identification of the nuclei resulted in cytoplasm being divided into a number of individual “cells”. In this way, calculations involving the number of infected cells remain accurate, and given the intensity of staining throughout a syncytium is relatively homogenous, calculations involving mean intensity also likely remain valid. An example of segmentation of syncytium is shown in Figure 2.11.

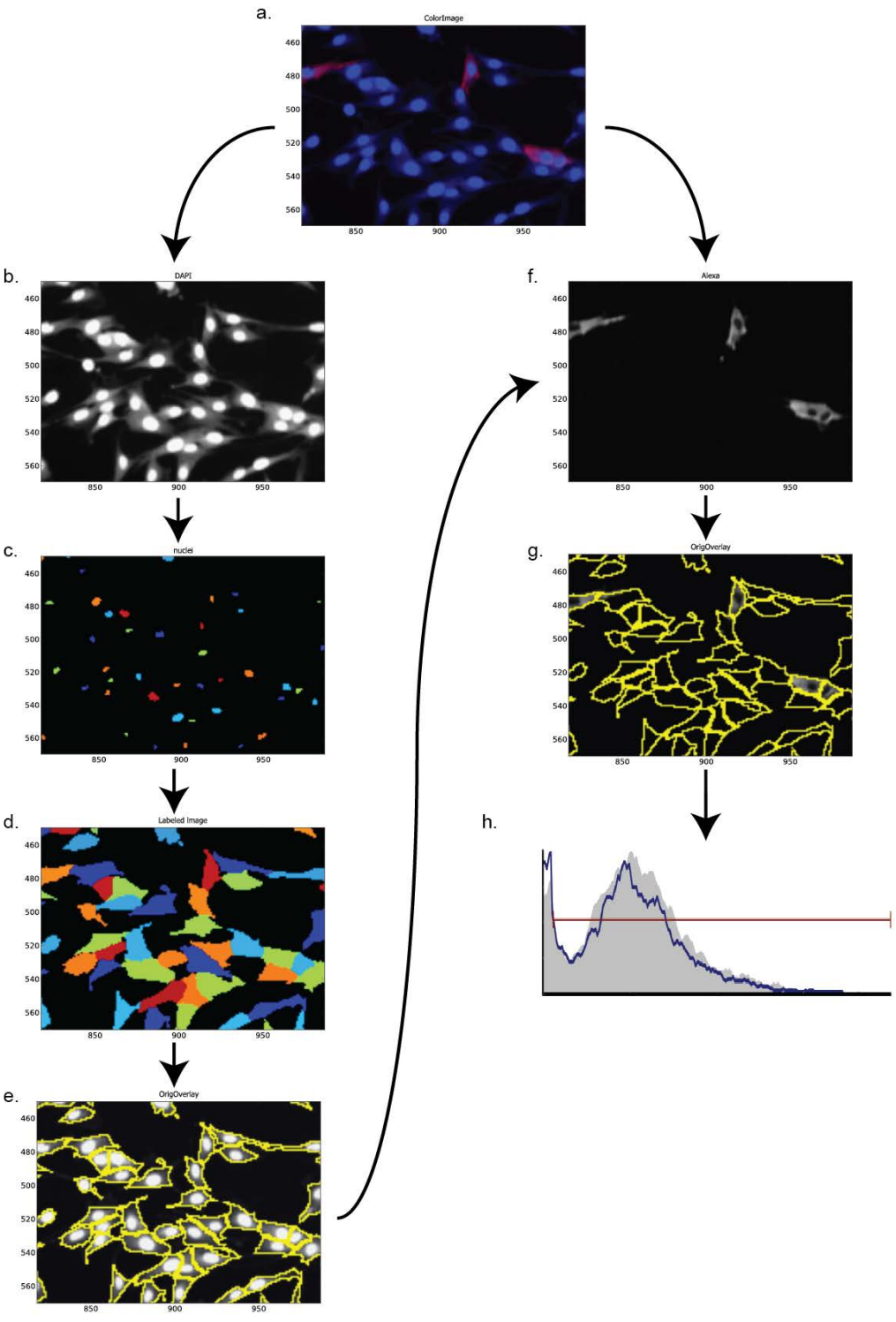

Figure 2.10: Schematic of CellProfiler pipeline used for image analysis. Panel (a) shows the merged images from DAPI / CellMask Blue (b) and Alexa Fluor 555 (f) images. Image segmentation was performed using the DAPI / CellMask Blue image (b). The initial step involved identifying nuclei (c) to act as seeds for the subsequent identification of whole cell boundaries (d and e). Fluorescent intensity measurements were made using the Alexa Fluor 555 images (f) within the cell boundaries previously identified (g). Fluorescent intensity data for each identified cell was exported to for analysis using FCS Express Image Cytometry (h).

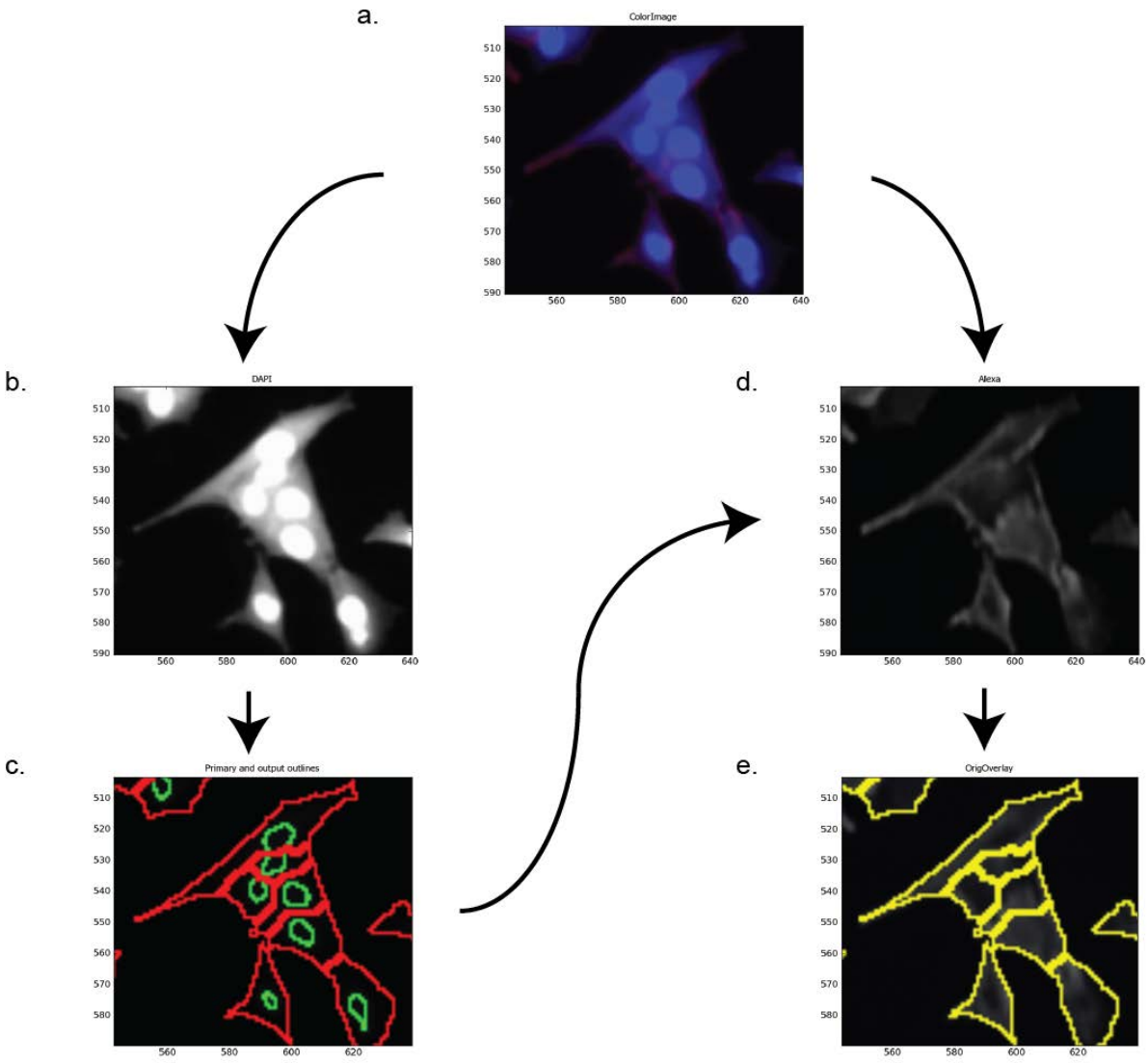

Figure 2.11: Segmentation of images containing feline coronavirus associated syncytia. Panel (a) shows the merged image of a syncytium containing five nuclei. Segmentation performed on the DAPI/CellMask Blue image (b) results in the identification of all five nuclei and the segmentation of the syncytium into five individual cells (c), with red lines showing the cytoplasmic boundaries. The Alexa Fluor 555 image (d) showing viral antigen staining is overlain with the cytoplasmic boundaries of the identified cells (e).

3

Development and optimisation of antiviral screening assays for feline coronavirus and feline calicivirus

3.1. ABSTRACT

Cell-based antiviral assays are commonly used for the initial screening of potential antiviral drugs. Demonstration of inhibitory properties in a cell-based system is an essential step prior to animal testing. Such assays provide not only an indication of antiviral properties, but can also provide important information about the potential toxicity of a candidate compound. This chapter describes the development of low to medium throughput resazurin- and sulforhodamine B-based (SRB) cytopathic effect inhibition assays for feline coronavirus and feline calicivirus. Both assays were shown to be robust and suitable in their current form for high throughput screening, with Z'-factors for FCoV of 0.70 (resazurin) and 0.86 (SRB) and for FCV of 0.76 (resazurin) and 0.91 (SRB). This study also demonstrates that these assays can be performed sequentially, with the SRB-based assay performed following the resazurin-based assay without any loss in performance.

3.2. INTRODUCTION

Cell-based screening assays are commonly performed in the initial stages of the antiviral drug discovery process to identify effective candidate compounds for further study. Such tests offer advantages over assays utilising isolated viral proteins or enzymes, as compounds can be identified that interfere with viral replication at all stages of the replication cycle. Cell-based assays may also provide a first screen to identify and eliminate compounds that display undesirable pharmacological properties, such as cytotoxicity or poor membrane permeability at the tested concentrations. Elimination of these compounds in the initial phases of screening prevents the unnecessary allocation of resources on further investigation of compounds unlikely to be of clinical use due to unacceptable pharmacokinetic properties.

A range of cell-based assays are available for antiviral screening. The most suitable approach for a specific virus depends both on the inherent biological properties of the virus, in addition to practical considerations including the number of compounds to be tested, and the facilities and equipment available. For viruses displaying *in vitro* cytopathic effect, plaque reduction assays (PRA) have long been considered the gold standard in assessing inhibition due to antiviral compounds. Whilst technically simple, PRA are time consuming and laborious, and thus are not well suited for screening purposes. Similarly, virus yield reduction assays, requiring initial incubation of cells with test compounds followed by titration of harvested culture media for viral infectivity, are impractical for screening even modest numbers of compounds. These tests are therefore primarily used for testing small numbers of compounds or for confirmatory testing of compounds identified using alternative assays.

For screening large numbers of compounds, assays amenable to use in a microtitre plate format (96-well or higher density plates) are preferred. The cytopathic effect (CPE) inhibition assay is a commonly used screening test for cytopathic viruses. The simple premise of a CPE inhibition assay is that an effective antiviral compound will result in a reduction in virus-induced CPE within the culture system, an effect that is quantifiable using various detection systems. Simple visual morphological assessment of the degree of CPE can be performed (Tan et al., 2004), however frequently additional biochemical assays are used (Baba et al., 2005; Green et al., 2008; Paragas et al., 2004). The endpoints and markers used in these assays vary, however they can be broadly categorised as assays that detect viable cells (viability assays) and those that detect dead and/or damaged cells (cytotoxicity assays).

Viability assays are generally based on detecting the metabolic activity of living cells, such as their ability to reduce substances including tetrazolium salts (e.g. MTT, XTT) or resazurin, to accumulate substances (e.g. neutral red assay), or produce ATP. Assays that measure total biomass with a protein binding dye (e.g. sulforhodamine B assay) or a DNA intercalating dye (e.g. bisbenzimide) detect both dead and live cells, however when used with adherent cell lines such assays can perform as functional viability assays as non-viable cells typically detach and are removed during washing and fixation steps prior to staining. Cytotoxicity assays on the other hand measure substances such as lactate dehydrogenase which are released from dead or dying cells or increased concentrations of proteins such as caspase enzymes associated with cell death. In this study two commonly used viability assays, utilising resazurin and sulforhodamine B, were investigated for their suitability as detection reagents for FCoV and FCV CPE inhibition assays.

Resazurin (7-Hydroxy-3H-phenoxazin-3-one-10-oxide) is a redox dye which has been used in biological research for over 80 years for applications such as assessing milk and semen quality, and more recently for cellular toxicity and proliferation studies (Niles et al., 2008;

Twigg, 1945). Resazurin-based assays have been used to screen for bioactive compounds effective against a variety of microorganisms including bacteria (Sarker et al., 2007), fungi (Monteiro et al., 2012), protozoa (Bowling et al., 2012), and viruses (Cruz et al., 2013). The assay is based on the principle that living cells metabolise resazurin, a blue, weakly-fluorescent substrate into resorufin, a highly fluorescent product via the reaction shown in Figure 3.1. The reduction reaction occurs intracellularly, most likely via the action of a number of different mitochondrial, cytosolic, and microsomal redox enzymes (O'Brien et al., 2000). The rate and extent of enzymatic conversion is dependent on the metabolic activity of the cell and has been shown to be cell line dependent (Nakayama et al., 1997).

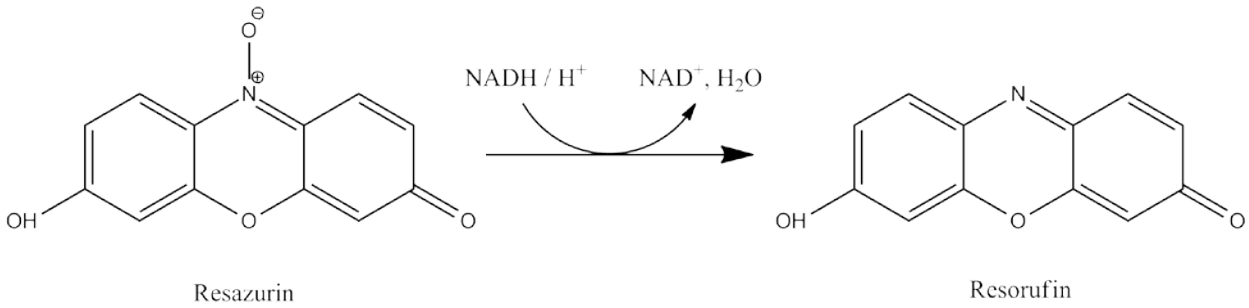

Figure 3.1: Mechanism of reduction of resazurin to resorufin. The reduction reaction occurs intracellularly most likely via the action of a number of different mitochondrial, cytosolic, and microsomal redox enzymes (O'Brien et al., 2000).

The sulforhodamine B (SRB) assay was originally developed by Skehan et al. (1990) for large scale anti-cancer drug discovery screening, and since this time the SRB assay has been used extensively for cytotoxicity testing. Sulforhodamine B (2-(3-diethylamino-6-diethylazaniumylidene-xanthen-9-yl)-5-sulfo-benzenesulfonate: Figure 3.2) is an anionic dye that binds electrostatically in a pH dependent manner to basic amino acid residues of cellular proteins. Under mildly acidic conditions SRB binds to basic amino acids in fixed cells. Following washing and drying, bound dye can be solubilised with a weak base. The optical density of the unbound dye has been shown to be proportional to cell number for a number of cell types and over a broad range of cell concentrations (Skehan et al., 1990). In addition to cytotoxicity screening, SRB has been used in CPE inhibition assays for a number of different viruses (Choi et al., 2009b; Park et al., 2011; Rocha Martins et al., 2011).

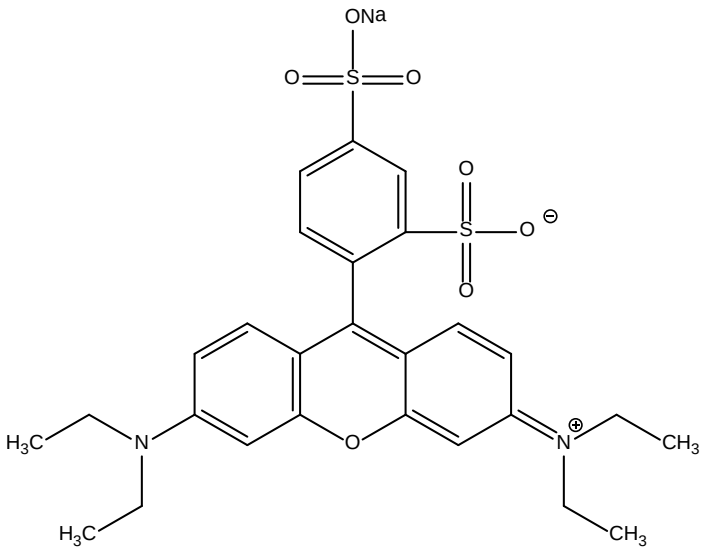

Figure 3.2: Chemical structure of sulforhodamine B (SRB). SRB binds electrostatically to basic amino acid residues in cellular proteins under acidic conditions. Measurement of optical density following solubilisation of bound SRB under basic conditions provides an assessment of the cellular protein content, and by extension cell number (chemical structure taken from Sigma-Aldrich).

The aim of the studies detailed in this chapter was to optimise and assess the performance of resazurin- and SRB-based CPE inhibition assays to screen compounds for antiviral activity against FCoV and FCV. Assay optimisation is critical for the success of a screening program to ensure reliable and reproducible results. Whilst this is particularly the case with high throughput screening (HTS), where there is usually just a single measurement of each compound's activity, it is also important for lower throughput screens. Due to the limited number of compounds required to be tested in this thesis, the primary goal was to develop an assay suitable for low to medium throughput, with multiple replicates per compound. In light of potential future studies however, a secondary goal was to develop a high-throughput capable assay for screening large chemical libraries for effective compounds.

3.3. MATERIALS AND METHODS

3.3.1. Optimisation of a resazurin-based CPE inhibition assay

3.3.1.1. Cell distribution

Uneven distribution of cells between or within wells can increase experimental variability. Preliminary experiments showed a non-uniform distribution of cells, particularly in the peripheral wells of 96-well plates. Initial incubation of plates at room temperature for a short period has been suggested as a simple method of minimising this edge effect (Lundholt et al., 2003). To investigate this, two 96-well plates (Sarstedt) were seeded with CRFK cells at

6.0 x 10^4 cells.well^{-1} in 150 µl DMEM-10. One plate was incubated at 37°C in 5% CO_2 in air immediately following seeding, while the other plate was kept at room temperature for 30 min prior to placing in the incubator. Plates were subsequently incubated for 6 h, the culture media discarded, and cells fixed with 100 µl.well^{-1} 20% (v/v) formalin in PBS for 20 minutes. Fixed cells were stained with 1% crystal violet for 10 min, rinsed in tap water, and allowed to air dry. Assessment of cell distribution was made both macroscopically, with stained plates placed on a light box and images acquired using a Canon EOS 600D digital camera (Canon, Tokyo, Japan), and microscopically using an Olympus CX41 inverted microscope at 100 x magnification.

3.3.1.2. Optimisation of resazurin incubation time and method of detection

Prolonged incubation with resazurin is associated with an increased signal-to-background (S/B) ratio and provides greater sensitivity at low cell numbers; however it can result in a loss of signal linearity due to further reduction of pink fluorescent resorufin to the non-fluorescent colourless substrate hydroresorufin (O'Brien et al., 2000). The optimal incubation time of resazurin in culture therefore is a trade-off between maintaining a linear correlation between signal and cell number and reduced assay sensitivity, and must be determined experimentally for each cell type and culture system.

To determine the optimal resazurin incubation time and method of detection, CRFK cells were plated at 11 different initial seeding densities from 1.25 x 10^3 to 6.0 x 10^4 cells.well^{-1} in 150 µl DMEM-10, with eight replicates per density, in duplicate 96-well plates. To minimise autofluorescence and fluorescent signal crosstalk between adjacent wells, clear-bottomed black-walled 96-well plates (µClear ®, Greiner Bio-One, Frickenhausen, Germany) were used for all experiments involving fluorometric data acquisition. Eight wells containing media only were included on each plate as blanks. Plates were incubated at room temperature for 30 min and then at 37°C in 5% CO_2 in air for a further 1 h prior to the addition of 50 µl of a 1:10 dilution of 4 x stock resazurin in DMEM (final resazurin concentration in media of 44 µM). Plates were subsequently incubated at 37°C in 5% CO_2 in air and data acquired at various time points from 2 to 24 h post seeding, both fluorometrically (535(25) $_{Ex}$ / 590(20) $_{Em}$) using a Tecan Polarion fluorescent microplate reader (Tecan Group Ltd., Mannedorf, Switzerland) and colorimetrically (OD_{570}-OD_{600}) using a SpectraMax 250 microplate reader (Molecular Devices, Sunnyvale, CA, USA). Data was exported to Microsoft Excel (Microsoft, Seattle, WA, USA) and the linearity of response with cell number was determined by performing a linear regression analysis in GraphPad Prism (GraphPad Prism V5.03 for Windows, GraphPad Software, San Diego, CA, USA). The signal-to-background ratio was calculated according to the following formula:

$$S/B = \frac{RFU_{Signal}}{RFU_{Blank}}$$

where RFU_{Signal} is the mean signal value (relative fluorescence units) at a particular cell density and RFU_{Blank} is the mean value of the background signal measured in wells containing no cells. The theoretical limit of detection, defined as the cell number giving a signal equal to the zero cell (media only) signal plus three standard deviations, was calculated by manual interpolation.

3.3.1.3. Cell seeding density optimisation

The initial seeding density is an important variable to optimise in cell-based assays. Seeding at too low a cell density may result in poor cell growth and reduced signals, leading to a correspondingly low S/B ratio. Conversely, seeding cells at too high a density may lead to cell overgrowth which may result in a plateauing of the signal, obscuring the true results. To determine the optimal seeding density for different incubation times, 96-well plates (µClear ®, Greiner Bio-One) were seeded with nine different cell densities from 2.5 x 10^3 to 3.0 x 10^4 cells.well^{-1} in 150 µl DMEM-10, with six replicates per density. Due to the lengthy incubation time and the associated excessive evaporation from outer wells, only the centre 60 wells were used for experimental samples, with the outer wells containing 200 µl PBS. Plates were incubated at 37°C in 5% CO_2 in air for 6, 18, 30, 54, or 78 h prior to analysis, with 50 µl of 1:10 dilution of 4 x stock resazurin in DMEM (final well concentration of resazurin 44 nM) added for the final 3.5 h. Plates were removed from the incubator for the final 30 min to allow the plates and media to equilibrate to room temperature. Fluorescent signals were measured with a FLUOstar Omega microplate reader (BMG Labtech, Mornington, VIC, Australia) using a 544 nm excitation filter and 590 nm emission filter with 8 flashes per well in bottom reading mode. Data were exported to Microsoft Excel and GraphPad Prism for analysis. Data represent Mean ± SD from a single experiment.

3.3.1.4. Optimisation of infection conditions

The primary variables to assess in optimising the infection conditions are the infective dose of virus and the incubation time. The aim of this stage of optimisation is to achieve a suitable separation band between the infected and uninfected cells, a function of the degree of virus induced CPE and the assay detection system. The degree of CPE is dependent on the MOI and incubation time, the optimal values for which depend on the virus and culture system. In general a low MOI is preferable for CPE inhibition based antiviral assays as it allows for multiple rounds of viral replication, and therefore enables the identification of compounds that act at any stage of the replication cycle. Consequently incubation times corresponding to several replication cycles are typically used.

3.3.1.4.1. Feline coronavirus

To determine the optimal infective dose and incubation time, CRFK cells were infected with FCoV FIPV1146 at MOIs ranging from 1 to 3.2 x 10^{-4} for a period of 24, 48, or 72 h. The initial cell seeding density varied with the duration of infection. For 24 h infection, 96-well plates (µClear ®, Greiner Bio-One) were seeded with 2.5 x 10^4 cells.well^{-1} in 100 µl of DMEM-10, while for 48 h and 72 h infection periods the initial seeding density was reduced to 1.25 x 10^4 and 5.0 x 10^3 cells.well^{-1} respectively. All plates were initially incubated at room temperature for 30 min to reduce edge effects and then incubated at 37°C in 5% CO_2 in air for 6 h prior to infection. Serial half-log dilutions of FCoV FIPV1146 were made in DMEM and added to the wells in 50 µl, with six replicates per MOI per infection time. Cells mock infected with DMEM were included in each plate as negative controls. Plates were incubated for 24, 48, or 72 hpi prior to analysis. Addition of resazurin and data acquisition, and data analysis were as previous described in Section 3.3.1.3. Cell viability was calculated according to the following formula:

$$Cell\ viability\ (\%) = \frac{(RFU_{V(+)} - RFU_{Blank})}{(RFU_{V(-)} - RFU_{Blank})} \times 100$$

Where $RFU_{V(+)}$ and $RFU_{V(-)}$ are the fluorescent signals from the virus infected and mock infected cells respectively, and RFU_{Blank} is the mean signal from control wells containing media only. Data represent Mean ± SD of a single experiment.

3.3.1.4.2. Feline calicivirus

Optimisation of infection conditions for FCV was performed as described for FCoV in Section 3.3.1.4.1 except plates were read at 24, 36, and 48 hpi due to the more rapid CPE induced by FCV. The seeding density for the 24 h and 48 h plates were as reported in Section 3.3.1.4.1, while the seeding density for the 36 h infection plate was 2.0 x 10^4 cells.well^{-1} in 100 µl. Cells were infected with FCV F9 in half-log dilutions from MOI 1 to MOI 3.2 x 10^{-4}, with six replicates per MOI per infection time. Data represent Mean ± SD of a single experiment.

3.3.1.5. Effect of DMSO

DMSO is an amphipathic solvent frequently used to dissolve chemicals for drug screening assays. Despite its usefulness as a solvent it is well recognised that even at low concentrations DMSO can be cytotoxic or have a significant effect on cell structure and function (Yu and Quinn, 1994). It is therefore important to minimise the effects of DMSO on an assay system. To assess any cytotoxic or cytostatic effects of DMSO on CRFK cells, cell viability was assessed following 72 h exposure to various concentrations of DMSO. Cells were seeded at 5.0 x 10^3 cells.well^{-1} in 100 µl DMEM-10 in 96-well plates (µClear ®, Greiner

Bio-One). Plates were incubated at room temperature for 30 min and then at 37°C in 5% CO_2 in air for 5 h prior to the addition of 50 µl of various concentrations of DMSO, from 4.5% to 0% (v/v) in DMEM, resulting in a final in well concentration of DMSO from 1.5% to 0% (mock treated cells). Plates were incubated for a further for 72 h at 37°C in 5% CO_2 in air prior to analysis. Addition of resazurin, data acquisition, and data analysis were as previous described in Section 3.3.1.3. Data represent Mean ± SD of a single experiment.

The effect of DMSO on virus replication was also investigated. Cells were seeded at 5.0 x 10^3 cells.well^{-1} (for FCoV) and 1.25 x 10^4 cells.well^{-1} (for FCV) in 96-well plates (µClear ®, Greiner Bio-One) for 5 h prior to the addition of DMSO to a final concentration of 0.33%. Cells not exposed to DMSO were included as controls. Cells were incubated for a further hour prior to infection (or mock infection) with FCoV FIPV1146 or FCV F9 at MOI 0.01. Cell viability was assessed at 72 hpi and 48 hpi for FCoV and FCV respectively. Addition of resazurin, data acquisition, and data analysis were as previous described in Section 3.3.1.4.1. Each treatment was performed in triplicate and repeated in two independent experiments.

3.3.1.6. Determination of assay robustness

Although the primary aim of this project was to perform low throughput benchtop screening of a limited number of candidate chemicals, a secondary aim during the optimisation phase was to develop a "HTS ready" assay for future use. To this end, a series of experiments were conducted to determine the robustness and suitability for HTS of the optimised screening assays.

3.3.1.6.1. Feline coronavirus

CRFK cells were seeded at 5.0 x 10^3 cells.well^{-1} in 100 µl DMEM-10 in 96-well plates (µClear ®, Greiner Bio-One) using the centre 60 wells only. Wells on the perimeter of the plate contained 200 µl PBS. Plates were incubated at room temperature for 30 min and then at 37°C in 5% CO_2 in air for 5 h prior to the addition of 30 µl of DMEM (to simulate the addition of test compounds). Cells were infected (or mock infected) 1 h later with FCoV FIPV1146. For infection, plates were divided into four quadrants, with quadrants I and III the positive controls being mock infected with DMEM, and quadrants II and IV the negative controls infected with FCoV FIPV1146 in DMEM at MOI 0.01. Plates were incubated for a further 72 h at 37°C in 5% CO_2 in air prior to analysis. Addition of resazurin, data acquisition, and data analysis were as previous described in Section 3.3.1.3. Cell viability was calculated as described in Section 3.3.1.4.1. The experiment was performed in duplicate plates and repeated in two independent experiments to assess both intra-run and inter-run variation. The Z'-factor was calculated by the method of Zhang et al. (1999) according to the formula below:

$$Z' = 1 - \frac{(3\sigma_m + 3\sigma_i)}{|\mu_m - \mu_i|}$$

Where σ_m and σ_i represent the standard deviation of the mock infected control cells and the infected control cells respectively. μ_m and μ_i represent the mean of the mock infected and infected cells respectively. Thus the numerator in this equation takes into account the data variation while the denominator is a measure of the signal dynamic range.

3.3.1.6.2. Feline calicivirus

The determination of assay robustness for FCV was performed as described for FCoV in Section 3.3.1.6.1 except plates were seeded with 1.25 x 10^4 cells.well^{-1} and infected with FCV F9 at MOI 0.01 for a 48 h infection period. The experiment was performed in duplicate plates and repeated in two independent experiments.

3.3.1.7. Examination of the suitability of in-house prepared resazurin reagent

A range of commercially available resazurin reagents are available for *in vitro* use. In addition to resazurin these commercial reagents contain a poising agent to maintain the redox potential of the solution and enhance its stability (Sittampalam et al., 2013), and thus may offer advantages over the in-house prepared resazurin solution. To monitor the stability of the in-house produced resazurin, mapping of the optimal gain setting for control wells from sequential experiments was performed throughout this study to assess any systematic drift that may be associated with degradation of the stock solution.

The cost benefit of using the in-house reagent versus a commercial reagent was also determined. To this end the cost price of two commercial resazurin reagents, Alamar Blue (Life Technologies) and CellTitre Blue (Promega) were sourced from the manufacturer's websites. For the in-house reagent the cost price of resazurin powder, culture media for dilution, and 0.22 µm filters for sterilisation were sourced from the supplier (Sigma-Aldrich). To standardise the comparison between products the price per plate was calculated assuming all wells of a 96-well plate are used, a sample volume of 150 µl per well, and the manufacturers recommended protocol for reagent volume was followed.

3.3.2. Optimisation of a sulforhodamine B (SRB) assay

3.3.2.1. Fixation method

The SRB assay requires the fixation of cells to the well prior to staining. Poor fixation may result in loss of viable cells, and thus an underestimation of cell biomass, and hence an underestimation of antiviral effect or overestimation of the toxicity of a tested compound. A number of fixation methods using trichloroacetic acid (TCA) have been described in the

literature (Papazisis et al., 1997; Vichai and Kirtikara, 2006; Voigt, 2005), three of which were examined to determine the most effective protocol for our assay system.

CRFK cells were seeded in 96-well plates (µClear ®, Greiner Bio-One) at various densities, ranging from 1.25 x 10^3 to 6.0 x 10^4 cells.well^{-1} in in 200 µl DMEM-10, with eight replicates per density. One plate was set up per fixation method. Cells were incubated for 30 min at room temperature and then at 37°C in 5% CO_2 in air for 4 h prior to fixation. Cells were fixed by either (1) adding 50 µl cold 50% TCA to culture media (final in well TCA concentration of 10%), or by removing media by (2) decanting by inverting and flicking plate, or (3) aspirating media with multichannel pipette, followed by addition of 100 µl cold 10% TCA. For all plates, cells were fixed for 1 h at 4°C, rinsed 5 times with running tap water, and allowed to air dry. Plates were stained with 0.4% (w/v) SRB in 1% acetic acid for 30 min, rinsed 5 times in 1% acetic acid to remove unbound dye, and air dried. Once dry, SRB was solubilised by adding 150 µl 10 mM tris (pH 10) per well. Absorbance (OD_{510}) was measured after 30 min using a SpectraMax 250 microplate reader (Molecular Devices).

3.3.2.2. SRB concentration

Several SRB concentrations have been reported in the literature (Vichai and Kirtikara, 2006; Voigt, 2005). To assess the effect of SRB concentration three plates were set up and processed as detailed in Section 3.3.2.1 using the optimised decant method of fixation. Plates were stained using 0.4%, 0.2%, or 0.057% (w/v) SRB in 1% acetic acid for 30 min. Washing, drying, solubilisation, and data acquisition were as described in Section 3.3.2.1. Data represent Mean ± SD.

3.3.2.3. Sequential resazurin and SRB assays

To assess the effect of performing a resazurin viability assay prior to the SRB assay, duplicate plates were prepared with serial dilutions of CRFK cells as described in Section 3.3.2.1 with the exception that plating volume was reduced to 150 µl. Plates were incubated for 4 h to allow cells to attach after which 50 µl of a 1:10 dilution of 4 x stock resazurin in DMEM was added to the wells of the dual sequential treatment plate and 50 µl of DMEM added to the single treatment plate. Plates were incubated for a further 3 h at 37°C followed by 30 min at room temperature prior to fluorescence data acquisition as described in Section 3.3.1.3. Both plates were fixed using the optimised decant method. SRB staining, washing, drying, and solubilisation were performed as described in Section 3.3.2.2 using an SRB concentration of 0.2% (w/v). Absorbance (OD_{510}) was measured 30 min after solubilisation using a FLUOstar Omega microplate reader. Data represent Mean ± SD.

3.3.2.4. Determination of assay robustness

To determine the performance of the SRB-based assay, plates used to determine the robustness of the resazurin-based assay as described in Section 3.3.1.6.1 for FCoV and 3.3.1.6.2 for FCV were processed according to the optimised SRB protocol as detailed in Section 3.3.2.3.

3.4. RESULTS

3.4.1. Optimisation of resazurin assay

3.4.1.1. Cell distribution

Incubation of plates at 37°C immediately following seeding resulted in an uneven distribution of cells in the outer wells, with an increased cell density on the perimeter of the wells closest to the edge of the plate. This can be seen in Figure 3.3 on both the image of the entire plate (a), and more clearly on a closer image showing only the corner wells (b). In contrast, incubation for 30 min at room temperature immediately post seeding resulted in an even distribution of cells as shown in Figure 3.3 (c and d). For all subsequent experiments, cells were allowed to adhere for 30 min at room temperature prior to incubation to minimise variations in cell distribution across wells.

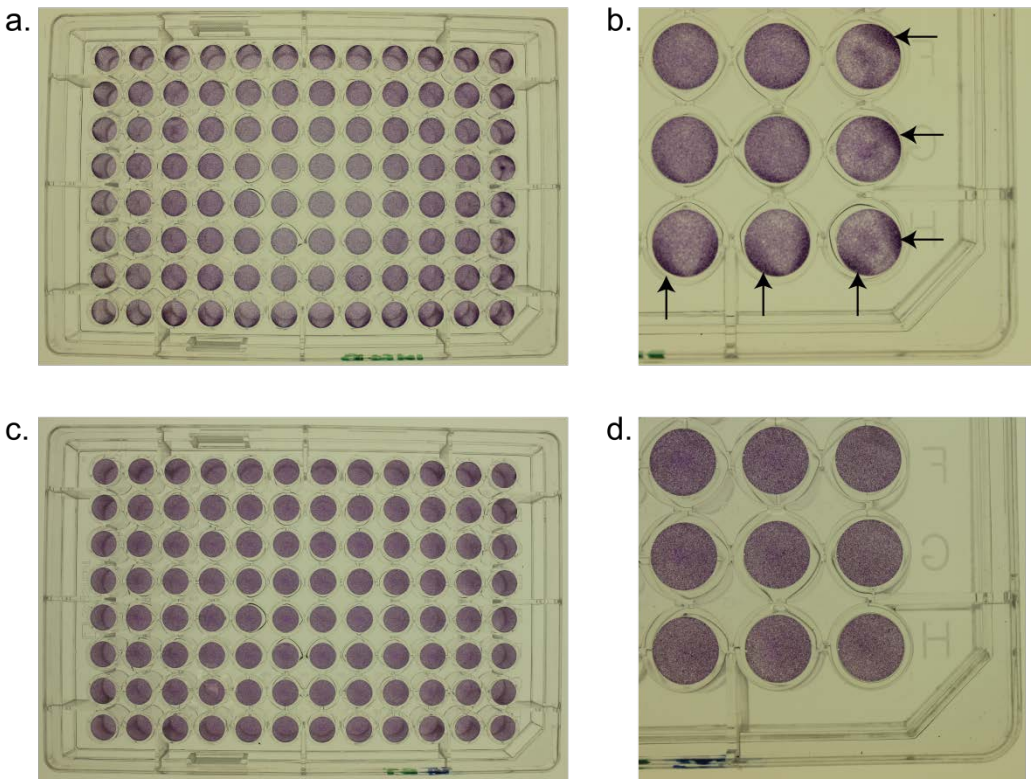

Figure 3.3: Effect of pre-incubation at room temperature on cell distribution. 6.0 x 10^4 cells.well^{-1} in 150 µl were plated in duplicate 96-well plates. One plate was placed immediately in the incubator at 37°C (panels a and b) and the other kept at room temperature for 30 min (panels c and d) prior to transferring to the incubator. Cells were fixed in 20% formalin in PBS 6 h post-seeding and stained with 1% crystal violet. Uneven distribution of cells in outer wells is evident on the plate placed in the incubator immediately post seeding. Arrows (panel b.) show areas of increased cell density located at the periphery of the edge wells closest to the edge of the plate. Images taken with a Canon EOS 600D digital camera.

3.4.1.2. Optimisation of resazurin incubation time

Resazurin incubation times of 2 to 24 h were examined using both fluorometric and colorimetric analysis. Using both analyses, signal linearity with cell number was greatest with incubation times < 4 h (R^2 > 0.98 for fluorescent > 0.99 for colorimetric) and dropped sharply at 12 and 24 h (R^2 = 0.93 and R^2 = 0.70 respectively for fluorometric and R^2 = 0.93 and R^2 = 0.71 for colorimetric readouts) (Figure 3.4). Both analyses provided similar results with simple linear regression of the mean RFU and mean OD values giving an R^2 value greater than 0.99 for all time points tested (Figure 3.5) except for the 2 h incubation, for which an R^2 = 0.98. As expected, the theoretical limit of detection, calculated as the cell number giving a signal equal to the zero cell (media only) signal plus three standard deviations decreased with increasing incubation times. Using fluorometric readout the limit of detection decreased from approximately 200 cells at 3 h to approximately 60 cells

following a 24 h incubation (Figure 3.6a). Colorimetric detection was less sensitive, with a limit of detection of approximately 3300 cells at 3 h reducing to approximately 500 cells at 24 h (Figure 3.6b). The increased sensitivity of the fluorescence readout compared to colorimetric is also demonstrated by the higher S/B ratio seen at all cell numbers (Figure 3.7). Based on these results a 3.5 h incubation period with fluorometric analysis was used for further studies.

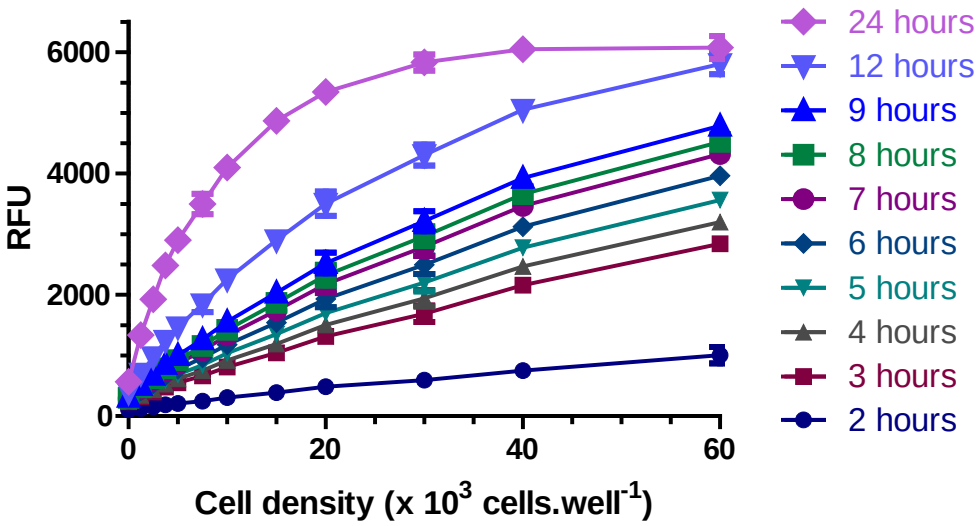

Figure 3.4: Effect of resazurin incubation time on signal linearity. Varying cell densities from 1.25 x 10^3 to 6.0 x 10^4 cells.well^{-1} were seeded in duplicate 96-well plates with eight replicates per density per plate. Cells were incubated at 37°C in 5% CO_2 for 4 h to allow adherence prior to the addition of resazurin. Signals were measured both fluorometrically and colorimetrically at the times indicated. Data shown is from fluorescence analysis. Data are Mean ± SD. RFU, relative fluorescence units.

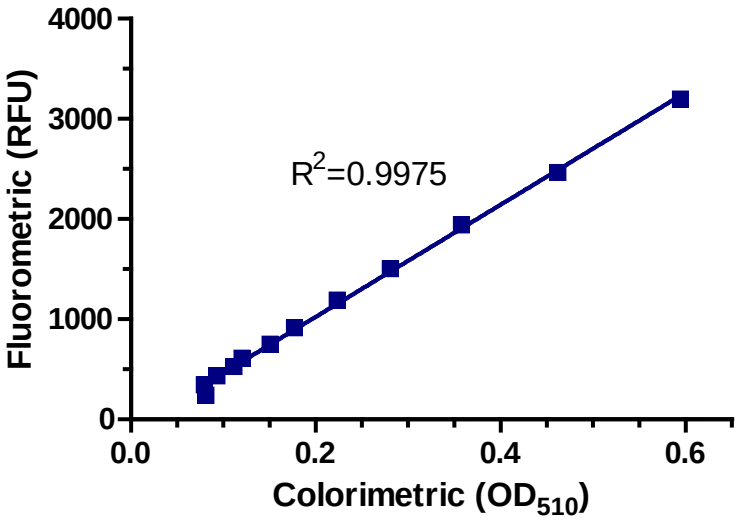

Figure 3.5: Correlation of fluorometric or colorimetric determination of resazurin signal. Varying cell densities from 1.25 x 10^3 to 6.0 x 10^4 cells.well^{-1} seeded in duplicate 96-well plates with eight replicates per density per plate. Cells were incubated at 37°C in 5% CO_2 for 4 h to allow adherence prior to the addition of resazurin. Signals were measured both fluorometrically and colorimetrically at various times post resazurin addition. Data shown are mean colorimetric and fluorometric values measured following a 3 h resazurin incubation time.

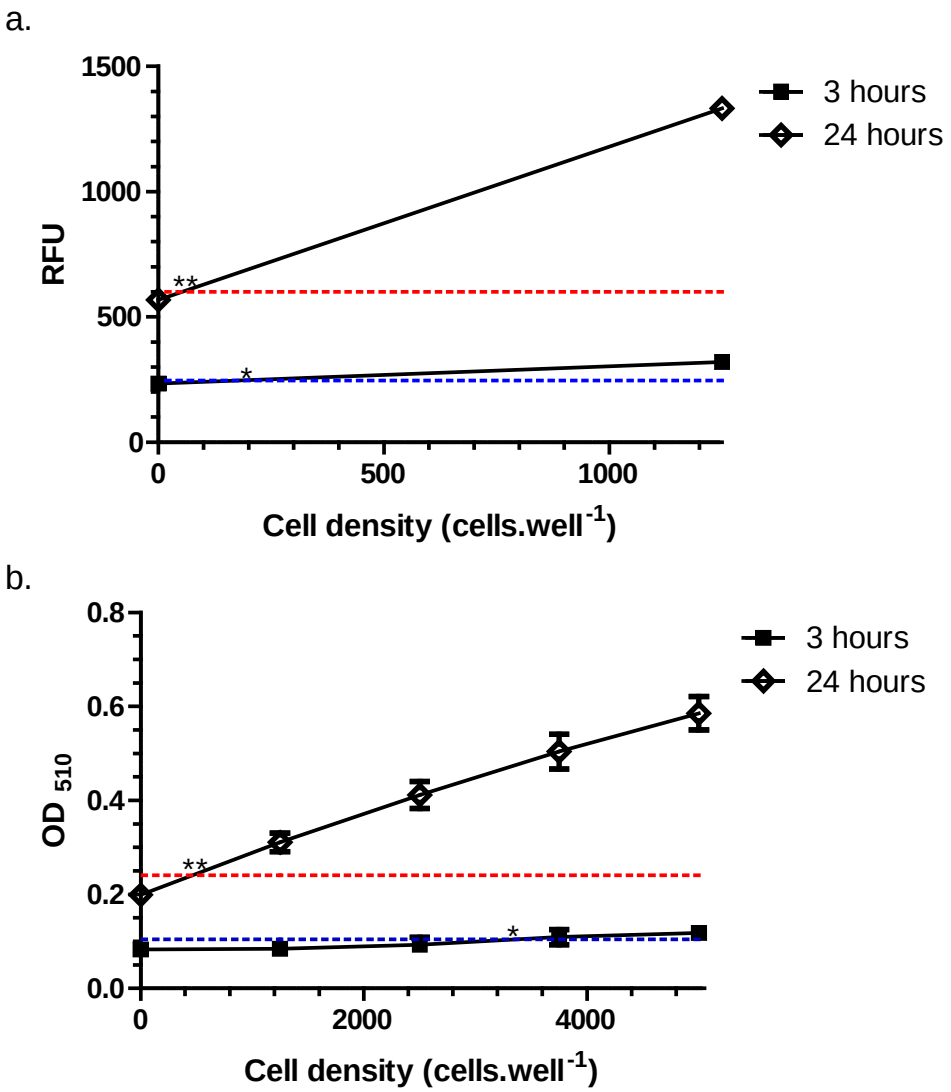

Figure 3.6: Effect of resazurin incubation time on the limit of detection using (a) fluorometric or (b) colorimetric readout. Varying cell densities from 1.25 x 10^3 to 6.0 x 10^4 cells.well^{-1} were seeded in duplicate 96-well plates with eight replicates per density per plate. Cells were incubated at 37°C in 5% CO_2 for 4 h to allow adherence prior to the addition of resazurin. Signals were measured both fluorometrically and colorimetrically at various times from 2 h to 24 h after the addition of resazurin. Theoretical limit of detection, defined by the zero cell number fluorescence intensity plus three standard deviations is shown for 3 h resazurin incubation (blue dashed line) and 24 h resazurin incubation (red dashed line). *, limit of detection at 3 h; **, limit of detection at 24 h. Data represent Mean ± SD.

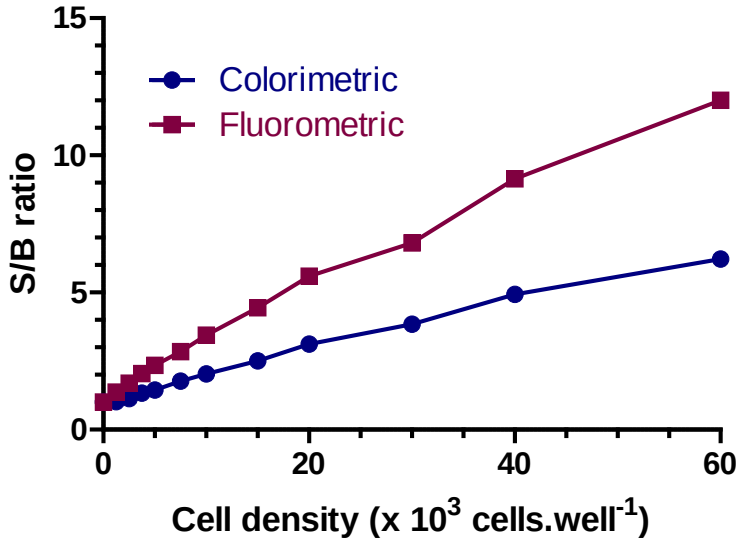

Figure 3.7: Comparison of signal-to-background (S/B) ratios using fluorometric and colorimetric analyses. Varying cell densities from 1.25 x 10^3 to 6.0 x 10^4 cells.well^{-1} were seeded in duplicate 96-well plates with eight replicates per density per plate. Cells were incubated at 37°C in 5% CO_2 for 4 h to allow adherence prior to the addition of resazurin. Signals were measured both fluorometrically and colorimetrically at various times from 2 to 24 h post addition of resazurin. S/B ratios were calculated from the mean signal (fluorescent or colorimetric) at a particular cell density divided by the mean signal (fluorescent or colorimetric) of wells containing media only. Data represent mean values following 3 h incubation with resazurin.

3.4.1.3. Optimisation of cell seeding density

The fluorescent signal from plates incubated for less than 30 h showed no evidence of cell growth plateauing (Figure 3.8). In contrast the signal from plates incubated for 54 h and 78 h began to plateau at an initial cell seeding density of greater than 1.5 x 10^3 cells.well^{-1} and 1.0 x 10^3 cells.well^{-1} respectively, suggesting cell overgrowth or nutrient depletion under these conditions. Morphological assessment of wells grown under these conditions showed confluent monolayers, with the higher density wells appearing hyperconfluent. Based on these results initial seeding densities of 2.5 x 10^4, 2 x 10^4, 1.25 x 10^4 and 5.0 x 10^3 cells.well^{-1} were used for experiments requiring infection periods of 24, 36, 48, and 72 h respectively.

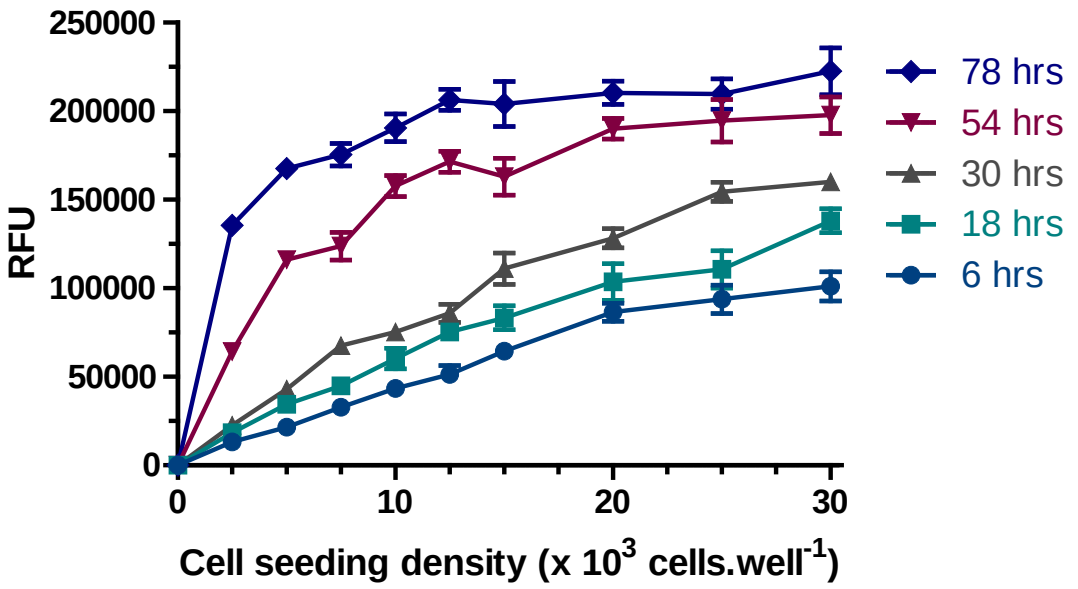

Figure 3.8: Optimisation of cell seeding density. CRFK cells were plated at different initial seeding densities from 2.5 x 10^3 to 3.0 x 10^4 cells.well^{-1} in 96-well plates and incubated for 6, 18, 30, 54, or 78 h, with resazurin added for the final 3.5 h. Fluorescent signal intensity was measured immediately following incubation. Data represent Mean ± SD.

3.4.1.4. Optimisation of infection conditions

Two general, but not unexpected trends were apparent from the infection condition optimisation data for both FCoV (Figure 3.9a) and FCV (Figure 3.9b). Firstly, the viability of infected cells decreased with a longer duration of infection and secondly, increased initial MOI was associated with lower cell viability. A clear difference was apparent in the onset and magnitude of CPE between FCoV and FCV in the CPE inhibition assay, with infection with FCV resulting in a more rapid and greater reduction in cell viability. These finding are consistent with morphological assessment of CPE induced by both viruses.

The optimal infection conditions for CPE inhibition assays for antiviral screening are those that result in a wide signal difference window with a low MOI. Infection at very low MOI resulted in increased signal variability as depicted by the larger error bars seen in Figure 3.9. Based on these results a 72 h infection time using MOI 0.01 for FCoV and a 48 h infection time with MOI 0.01 for FCV was chosen for further experiments.

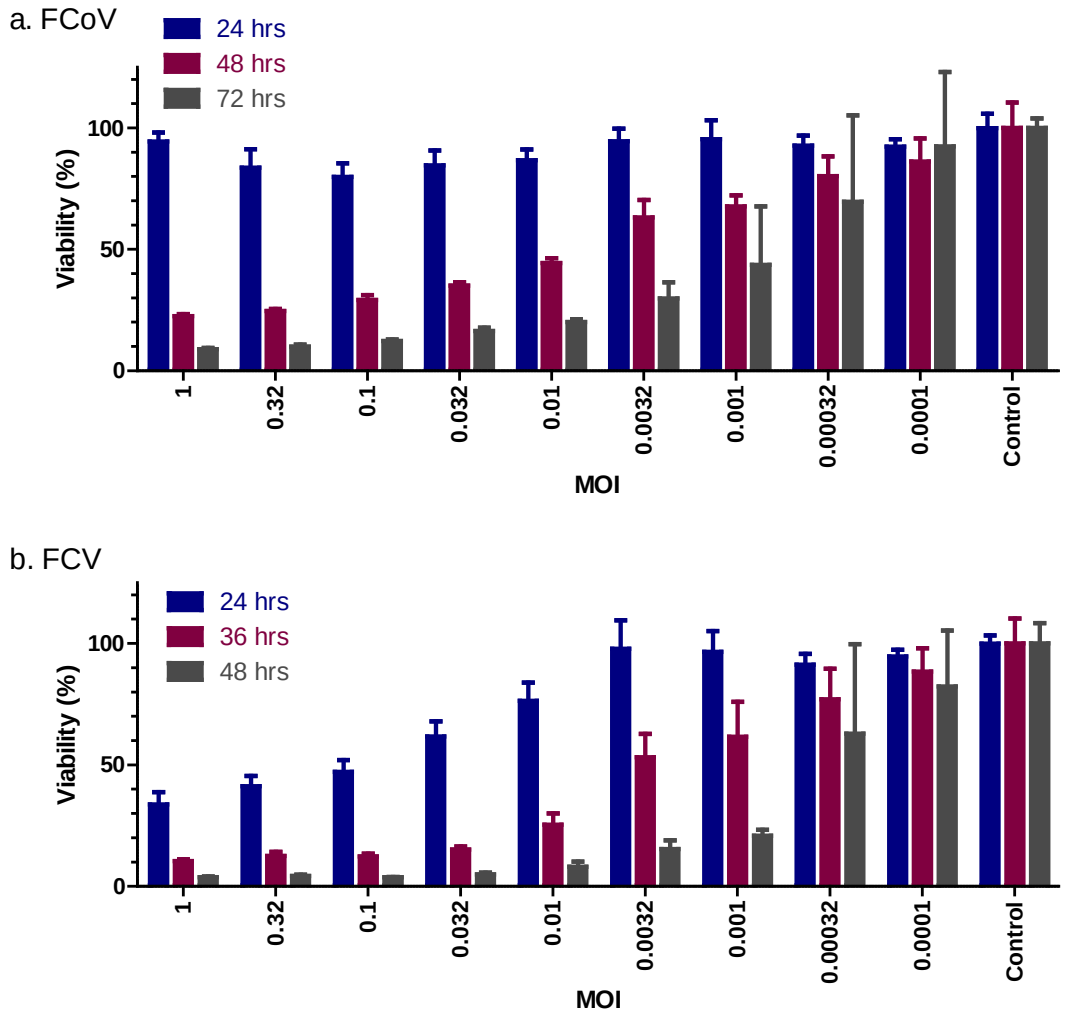

Figure 3.9: Optimisation of infection conditions for (a) FCoV and (b) FCV. CRFK cells were seeded in 96-well plates and incubated for 6 h at 37°C prior to infection with either FCoV FIPV1146 or FCV F9 at various MOIs from MOI 1 to MOI 1 x 10^{-4}, with 6 replicates per MOI, for a period of 24, 48, or 72 h (FCoV) or 24, 36, or 48 h (FCV). The initial cell seeding density for each plate varied depending on the required duration of infection, with 2.5 x 10^4 cells.well^{-1} in 100 µl of DMEM-10 used for 24 h infection period, while for 36 h, 48 h, and 72 h infection periods the density was reduced to 2 x 10^4, 1.25 x 10^4 and 5.0 x 10^3 cells.well^{-1}. Resazurin was added to the cells for the final 3.5 hours of incubation and signals were acquired fluorometrically (Ex:544 nm, Em:590 nm). Data represent Mean ± SD of a single experiment.

3.4.1.5. Determination of maximum DMSO concentration

The addition of DMSO to actively dividing CRFK cells resulted in a concentration-dependent decrease in cell viability at concentrations greater than 0.375% (v/v) as illustrated in Figure 3.10. Based on this 0.33% DMSO was set as the maximum DMSO concentration for this assay. This concentration was demonstrated to have no effect on virus replication for either

FCoV or FCV as determined by the resazurin-based CPE inhibition assay (data not presented).

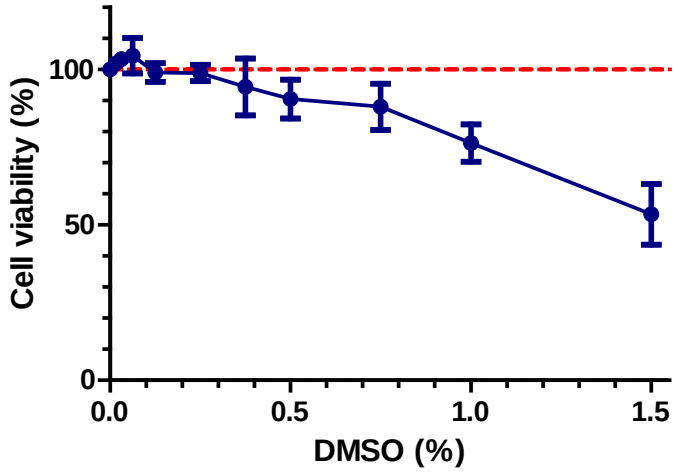

Figure 3.10: Effect of DMSO on cell viability. Cells were seeded at 5.0 x 10^3 cells.well^{-1} in 96-well plates and incubated at room temperature for 30 min and then at 37°C in for 5 h prior exposure to concentrations of DMSO from 1.5% to 0% (mock treated cells) for 72 h. Resazurin was added to the cells for the final 3.5 h of incubation and signals were acquired fluorometrically (Ex:544 nm, Em:590 nm). Data represent Mean ± SD of a single experiment.

3.4.1.6. Determination of assay robustness

Using the optimised assay conditions described above the resazurin-based CPE inhibition assays for both FCoV and FCV proved to be robust and suitable for screening purposes. Figure 3.11 shows data from a representative plate for (a) FCoV and (b) FCV. The calculated mean assay parameters are detailed in Table 3.1. Intra- and inter-run variation was within acceptable limits. The Z'-factor for FCoV was 0.71 and 0.64 for run 1 and 0.73 and 0.71 for run 2 while for FCV, the Z'-factor was 0.75 and 0.69 for run 1 and 0.87 and 0.71.

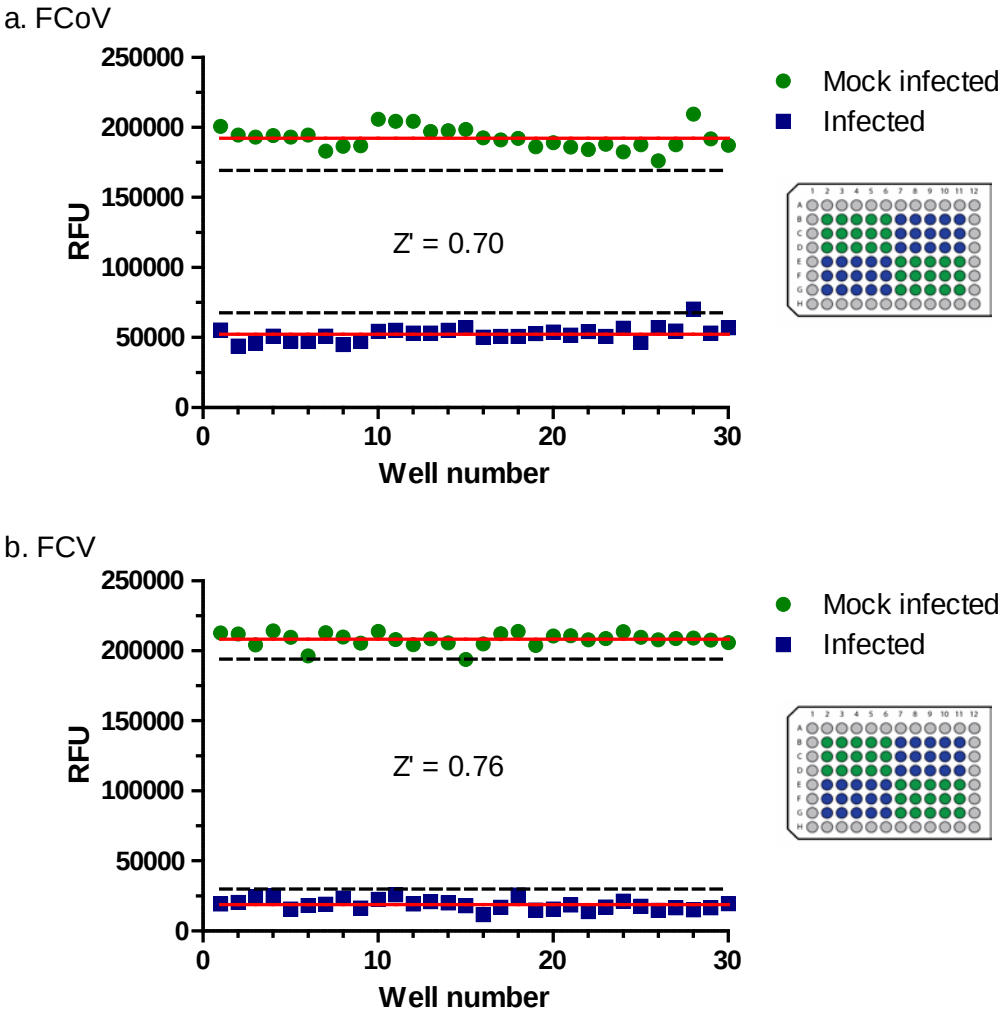

Figure 3.11: Representative plate data from Z'-factor assessment of resazurin-based CPE inhibition assay for (a) FCoV and (b) FCV. Duplicate plates for each virus were set up to assess intra-run variation and the experiment repeated to assess inter-run variation. Plates were setup and processed using the optimised resazurin-based assay parameters. Plates were divided into quadrants with quadrants I and III being mock infected (positive control) and quadrants II and IV infected (negative control). Red lines indicate mean values of positive and negative controls and dotted lines indicate three SD from these mean values. Z'-factor was calculated according to the method of Zhang et al. (1999). Z'-factor shown is the mean value from four plates. An assay with a Z'-factor > 0.5 is considered an excellent assay and suitable for HTS.

Table 3.1: Performance of the optimised resazurin-based assay. Results represent mean values of four plates. CV, coefficient of variation; S/B, signal to background ratio.

Parameter	FCoV assay	FCV assay
Z'-factor	0.70	0.76
CV – mock infected	4.69%	5.59%
CV – infected	9.59%	21.91%
S/B	3.66	11.75

3.4.1.7. Examination of the suitability of in-house prepared resazurin reagent

Storage of the 4 x stock resazurin solution at -20°C for 6 months was not associated with any obvious decrease in performance, with the automatic optimal gain settings, calculated based on the positive control wells on each individual plate, demonstrated not to drift in any systematic way during the course of these studies. Similarly, there was no significant difference in the optimal gain setting obtained using freshly prepared or stored stock resazurin solutions.

Comparison of the reagent cost per plate demonstrated that the in-house produced resazurin solution was significantly less expensive that the commercially available products, with a cost price of a few cents per plate compared to $15 or $28 per plate for the commercial reagents (Table 3.2).

Table 3.2: Cost comparison of some commercially available resazurin-based reagents versus in-house prepared resazurin. Prices listed were obtained from the manufacturer's website as at December 2013 and are reported in Australian dollars. For in-house resazurin the price includes the cost of culture media for dilution and 0.22 µm filters for sterilization. Price per plate is calculated assuming all wells of a 96-well plate are used, a sample volume of 150 µl per well, and the manufacturers recommended protocol for reagent volume is followed.

Product	Price of reagents	Cost per plate (AU $)
Alamar Blue (Life Technologies)	$271 for 25 ml	$15.66
CellTitre-Blue (Promega)	$196 for 20 ml	$28.24
In-house prepared resazurin solution (Sigma-Aldrich)	Resazurin = $44.50 for 1 g DMEM = $13.50 for 500 ml 500 ml 0.22µl filter = $16.67 per filter Total $195.33	$0.04

3.4.2. Optimisation of SRB assay

3.4.2.1. Fixation method

Results of the different fixation strategies are shown in Figure 3.12. All fixation methods showed good linear correlation between OD_{510} and cell number with R^2 values greater than 0.99. The mean coefficient of variation (CV) differed between the fixation methods, being the lowest for the decanting method, while the overlay method and the aspirate method had CV almost twice as large. Microscopic examination of the SRB stained plates prior to solubilisation showed large round pink stained structures that were present in significant numbers in wells fixed by overlaying TCA and not seen in wells fixed by alternative methods, providing a likely explanation for the increased CV with the overlay method. These structures were many times larger than single cells and microscopically they did not appear cellular in nature. Given that these inclusions were also present in media only control wells they likely represent aggregations of media components such as serum proteins, which become fixed to the plate. The presence of these inclusions results in an increased background with a correspondingly low S/B ratio in plates fixed with this method. The increased CV seen with the aspiration fixation method may be due to dislodging of cells during the aspiration procedure. Based on these results the decanting fixation method was chosen for further assays.

a. **Overlay**

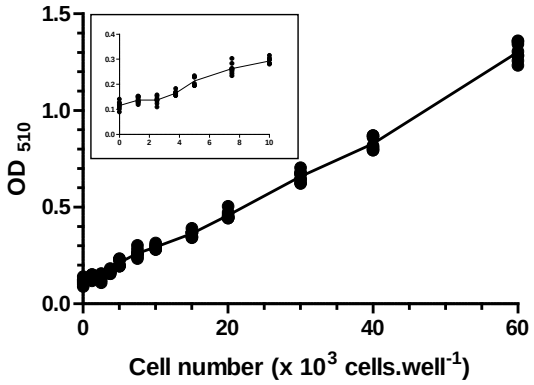

R^2	CV (mean)	S/B (max)
0.9910	6.83	11.31

b. **Decant**

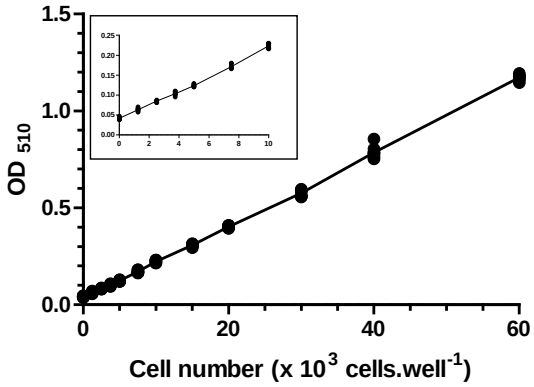

R^2	CV (mean)	S/B (max)
0.9982	3.51	27.83

c. **Aspirate**

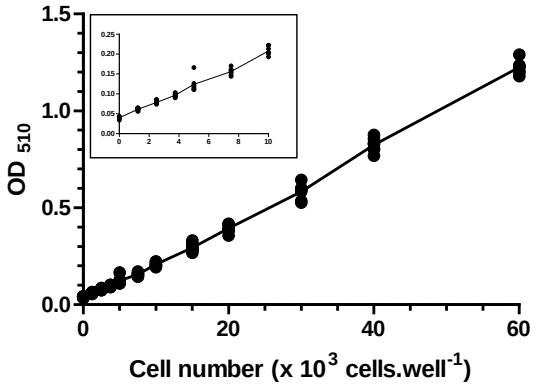

R^2	CV (mean)	S/B (max)
0.9948	6.35	30.41

Figure 3.12: Effect of fixation strategies on SRB assay performance. Three 96-well plates were seeded with CRFK cells at various densities, ranging from 1.25 x 10^3 to 6.0 x 10^4 cells.well^{-1}, with eight replicates per density. Eight media only control wells were included on each plate. Cells were incubated for 4 h to allow attachment and then fixed using one of three methods: (a) addition of 50% (w/v) TCA to culture media, or by adding 10% (w/v) TCA after (b) decanting or (c) aspirating culture media. Cells were fixed for 1 h at 4°C prior to SRB staining.

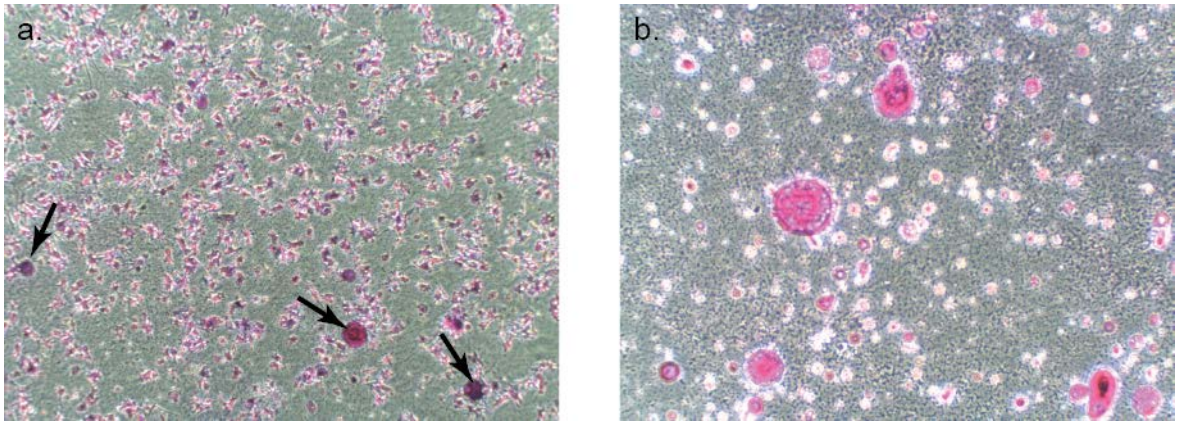

Figure 3.13: Effect of cell fixation method on SRB staining. Micrographs showing large SRB staining aggregates seen with the overlay fixation method. Panel (a) shows the several large aggregates (arrowheads) with a background of cells [40 x magnification]. Panel (b) shows these aggregates at a higher magnification from a well containing media only [100 x magnification]. Note the presence of both small and large inclusions.

3.4.2.2. SRB concentration

To examine the effect of SRB concentration on assay performance identical plates were stained with three different concentrations of SRB. There was a good linear correlation between cell number and signal, with $R^2 = 0.995$ for all tested concentrations as illustrated in Figure 3.14. There was a decrease in signal in plates stained with lower SRB concentrations and a corresponding decrease in S/B ratio, although the higher background OD seen in plates stained with 0.4% SRB in part negated this effect. In all cases the mean coefficient of variation was low. Based on the minimal improvement in signal seen at the highest tested concentration, and potential cost savings using lower concentrations, the intermediate SRB concentration of 0.2% (w/v) was selected for further experiments.

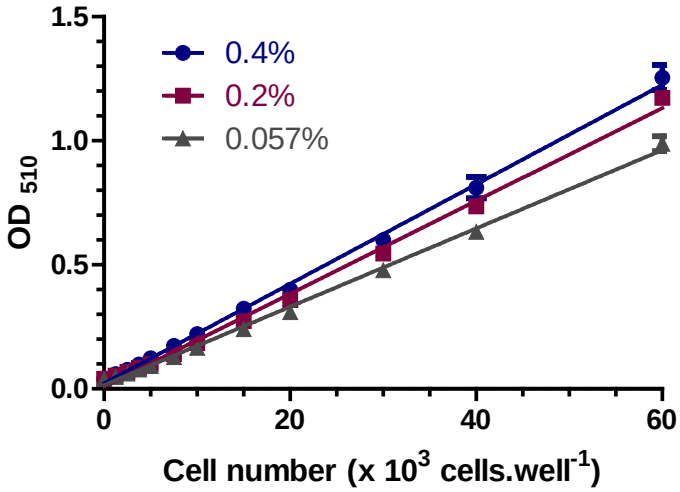

Figure 3.14: Effect of SRB concentration on assay performance. Three 96-well plates were seeded with CRFK cells were at various densities, ranging from 1.25 x 10^3 to 6.0 x 10^4 cells.well^{-1}, with eight replicates per density. After 4 h incubation culture media was decanted by inverting and flicking the plate and cells fixed with cold 10% (w/v) trichloroacetic acid for 1 h at 4°C. Cells were washed and allowed to dry prior to staining with SRB at a concentration of 0.4%, 0.2% or 0.057% in 1% acetic acid for 30 min. Cells were washed with 1% acetic acid to remove unbound dye and allowed to air dry. SRB was solubilised with 10 mM Tris (pH 10) and absorbance at 510 nm measured. Data represent Mean ± SD from a single experiment.

3.4.2.3. Sequential assays

Prior performance of a resazurin-based assay had little effect on the results of subsequent SRB assay performed on the same plate. Overall there was a slight decrease in signal from the dual assay plates compared to the single assay plate (Figure 3.15), however the R^2 value for both plates was 0.999, and the mean CV was similar (2.5% for dual plate versus 2.6% for single plate). Based on these results the use of sequential resazurin-based and SRB-based assays is a suitable approach for performing two-step dual-parameter viability assessment.

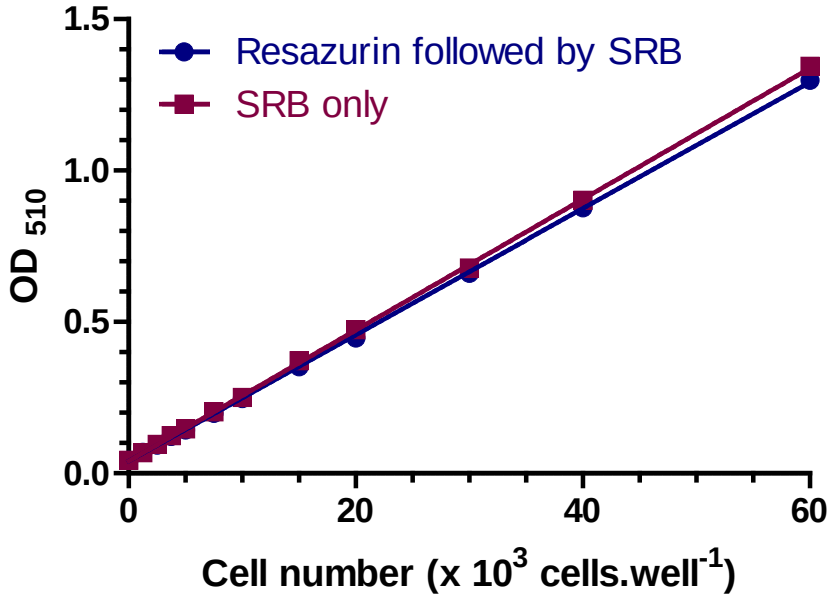

Figure 3.15: Effect of prior resazurin treatment on SRB assay. Two 96-well plates were seeded with CRFK cells at various densities, ranging from 1.25 x 10^3 to 6.0 x 10^4 cells.well^{-1}, with eight replicates per density. For the dual assay plate, resazurin in DMEM was added to wells 4 h after seeding, while for the single assay plate DMEM was added. Fluorescent readout (Ex:544 nm, Em: 590 nm) from the dual assay plate was acquired following a 3.5 hour exposure to resazurin, following which cell in both plates were fixed in 10% TCA and stained with 0.2% SRB. SRB was solubilised with 10mM Tris (pH 10) and OD_{510} measured. Data represent Mean ± SD from a single experiment.

3.4.2.4. Determination of assay robustness

Using the optimised assay conditions described above the SRB-based CPE inhibition assay for both FCoV and FCV proved to be a robust assay suitable for screening purposes. The calculated assay parameters and example data from representative plates are shown in Table 3.3 and Figure 3.16 respectively.

Table 3.3: Performance of the optimised SRB-based assay. Results represent mean values of four plates. CV, coefficient of variation; S/B, signal-to-background ratio.

Parameter	FCoV assay	FCV assay
Z'-factor	0.86	0.91
CV – mock infected	1.85%	2.05%
CV – infected	8.14%	13.84%
S/B	4.59	15.61

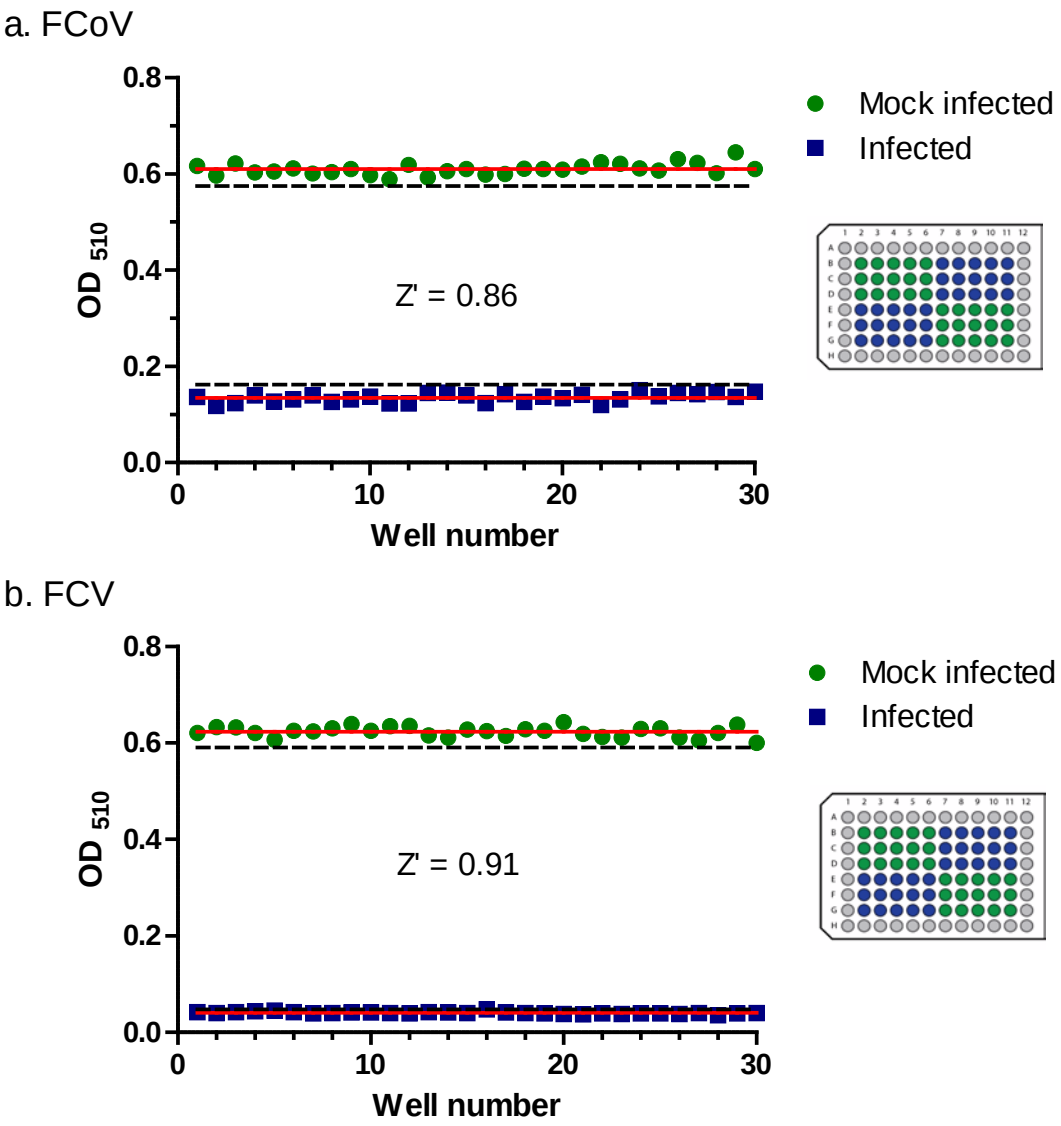

Figure 3.16: Representative plate data from Z'-factor assessment of SRB-based CPE inhibition assay for (a) FCoV and (b) FCV. Duplicate plates for each virus were set up to assess intra-run variation and the experiment repeated to assess inter-run variation. Plates were setup and processed using the optimised SRB-based assay parameters. Plates were divided into quadrants with quadrants I and III being mock infected (positive control) and quadrants II and IV infected (negative control) Red lines indicate mean values of positive and negative controls and dotted lines indicate three SD from these mean values. Z'-factor was calculated according to the method of Zhang et al. (1999). The Z'-factor shown represents the mean value from four individual plates. An assay with a Z'-factor > 0.5 is considered an excellent assay and suitable for HTS.

3.5. DISCUSSION

Here we report the development of resazurin- and SRB-based CPE inhibition assays for screening compounds for antiviral properties against two important feline pathogens, FCoV and FCV. For all assays, in particular cell-based assays with their inherent variability, optimisation of assay parameters is critical to provide reliable, robust, and repeatable data. In this study various assay conditions were successfully optimised in a step-wise manner through a series of isolating experiments for each important variable. A schematic of the final optimised resazurin-based assays for both FCoV and FCV are provided in Figure 3.17 and Figure 3.18 respectively, while details of the SRB-based assay are illustrated in Figure 3.19.

The initial stage of optimisation was directed at optimising the performance of the detection reagents, resazurin and SRB. For resazurin this involved determination of the ideal incubation time and method of detection, while for the SRB this involved optimising the cell fixation and staining protocol.

The optimal resazurin incubation time has been reported to vary for different cell lines and culture conditions (Nakayama et al., 1997). The optimal incubation time was that which maximised the linearity of signal with cell number, and signal to background ratio. In this case signal linearity was high for incubation times out to 4 h, and decreased thereafter. Signal to background ratios increased with longer incubation times, therefore to maximise both parameters a 3.5 h incubation period was chosen for further studies. Preliminary experiments demonstrated non-uniform fluorescent signal strength across the plate, with outer wells on the periphery of the plate having lower signals than identical wells in the centre. This uneven spatial distribution occurred even with short incubation periods suggesting excessive evaporation from outer wells was an unlikely cause (Irwin et al., 2008). As the fluorescent signal of resazurin has been shown to be temperature dependent (Anonymous), it was hypothesised that the non-uniform signals across the plate were due to temperature differentials across the plate arising from more rapid cooling of the outer wells compared to those in the centre on removal from the incubator prior to data acquisition. To address this, the final 30 min of incubation was performed at room temperature to allow well temperatures to equilibrate prior to reading, which eliminated the edge effect.

As expected, both colorimetric and fluorometric detection methods gave suitable results for the resazurin-based assay, with a strong linear correlation (R^2=0.998) demonstrated between the two analyses. There are several benefits of the fluorometric method however that make it the preferred option. Firstly the overlap between the absorbance spectra of resazurin and the reduced resorufin results in reduced assay sensitivity when measured colorimetrically (Czekanska, 2011). This was confirmed in the current study where the calculated theoretical

limit of detection was greater than 10-fold lower with fluorometric (200 cells.well^{-1}) compared to colorimetric detection (2300 cell.well^{-1}). Given the large signal differences between positive and negative controls for both FCoV and FCV assays, improved sensitivity at low cell numbers is not critical in the current 96-well plate format, however may become important if the assay were miniaturised to higher cell density plates with a correspondingly lower cell number per well. The second benefit of fluorometric over colorimetric readout is the former is relatively insensitive to slight variations in well media volume, while the OD values of colorimetric readout are directly proportional to path length, and hence well volume (Gribbon and Sewing, 2003).

The most critical feature of the SRB assay for optimisation was the method of fixation. Proper fixation of cells to the plastic substratum is essential to achieve accurate results with the SRB assay, as loosely or non-attached cells will be lost during the staining and multiple washing steps, resulting in an underestimation of the number of cells in a well. Several different fixation methods have been reported for this assay using TCA. In the original method of Skehan et al. (1990) concentrated TCA (50%) was overlaid on culture media, resulting in a final in well TCA concentration of 10%. Papazisis et al. (1997) reported an optimised procedure involving aspiration of the culture media before addition of 10% TCA. Both of these methods, as well as the method of decanting culture media prior to the addition of 10% TCA were assessed in this study. All tested fixation methods showed a strong linear correlation between the cell number and OD_{510}, with R^2 values greater than 0.99, however there were clear differences in the S/B ratio and the CV between the methods. In this study, although the optimised aspirate method gave the highest S/B ratio, the CV using this method was almost twice as high as the decant method. The increased CV in this study may reflect the fact that aspiration was performed manually with a multichannel pipette rather than an automated plate washer as described by Papazisis et al. (1997). For further studies the decant method was utilised based on its superior CV, high S/B ratio, and practical convenience.

The next stage of optimisation involved determining the cell culture and infection conditions of the assay. A multicycle assay strategy, involving infection at low MOI with a long incubation period, enables the detection of antiviral compounds acting at all stages of the replication cycle. The reported single cell cycle for FCoV is approximately 12 to 14 h (Dewerchin et al., 2005; Rottier et al., 2005), and for FCV is 10 to 12 h (Ossiboff et al., 2007), meaning 72 and 48 h incubation periods for FCoV and FCV respectively allow for multiple rounds of viral replication. Too low a MOI results in a narrow dynamic range with a resultant reduction in the Z'-factor for the assay. Further at very low MOIs there is increased signal variation in infected cells, most likely a reflection of variability in the small number of input

virions at these MOI. For this study MOI 0.01 was selected for both FCoV and FCV, with a 72 h incubation period for the former, and a 48 h incubation period for the latter

Determination of the DMSO sensitivity of a cell-based screening assay is important given its almost ubiquitous nature as a solvent in compound screening. Unlike biochemical based assays, which can tolerate high concentrations of DMSO, for cell-based assays it is recommended that DMSO concentration does not exceed 1% (Iversen et al., 2012), however DMSO has been documented to have a range of negative effects on cell function even when used at concentrations lower than this (Yu and Quinn, 1994). The deleterious effects of DMSO have been shown to vary with cell type (Bentrivedi et al., 1990; Da Violante et al., 2002) and culture conditions (Bentrivedi et al., 1990), highlighting the need to optimise DMSO concentrations under specific assay conditions. Under conditions identical to the final assay, DMSO was demonstrated to have a negative effect on cell viability as determined by the resazurin-based assay at concentrations greater than 0.375% (v/v), with a marked reduction in viability at concentrations greater than 0.75% (v/v). In addition to its effect on cells, DMSO has been shown to have a concentration-dependent effect on the replication of a number of different viruses, with low doses resulting in enhancement of viral replication, and high doses suppressive of replication (Scholtissek and Müller, 1988). DMSO at the maximum concentration used for screening in this study had no effect on FCoV or FCV replication as determined using the CPE inhibition assay.

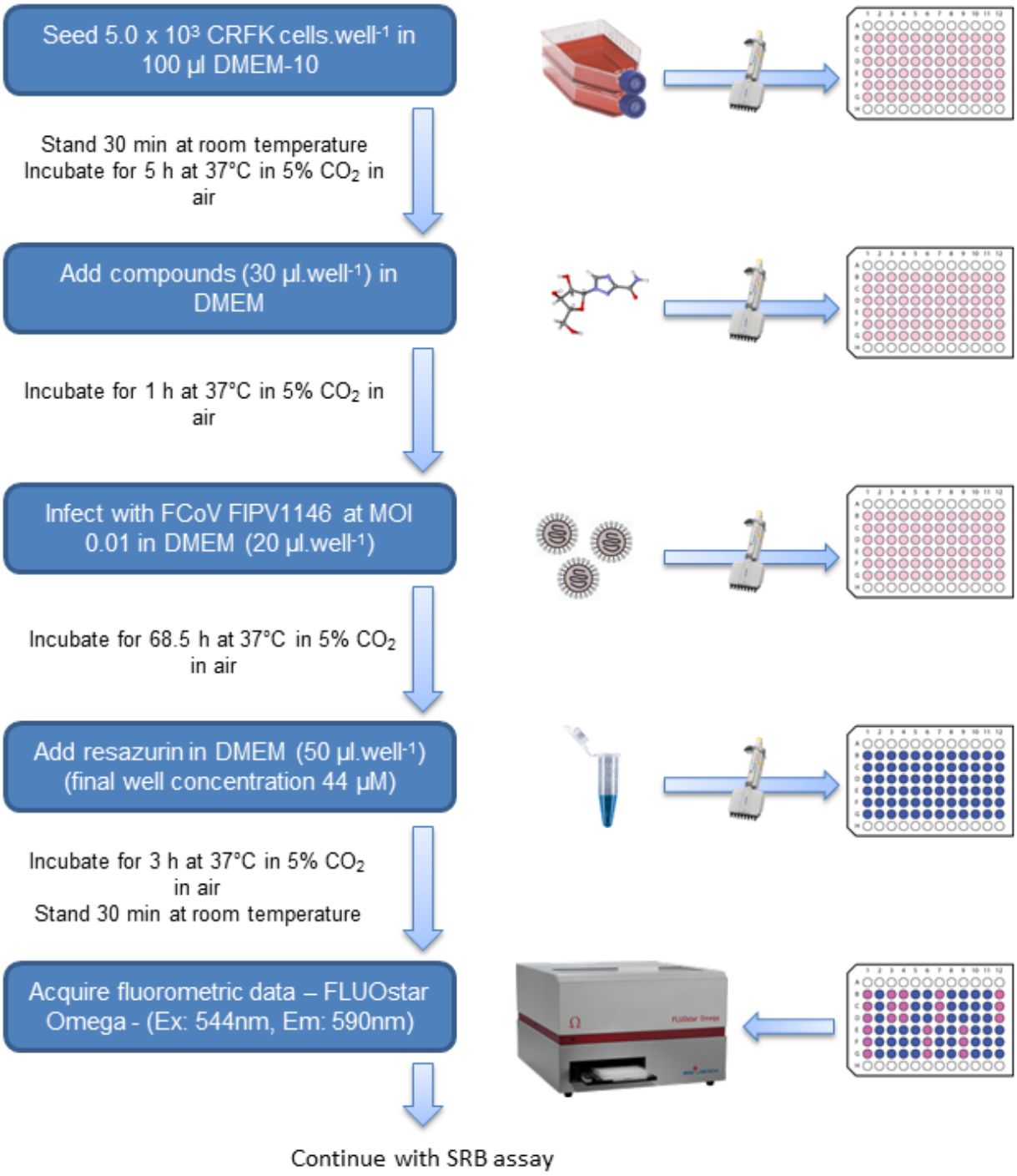

Figure 3.17: Schematic of optimised resazurin-based CPE inhibition assay for feline coronavirus**.**

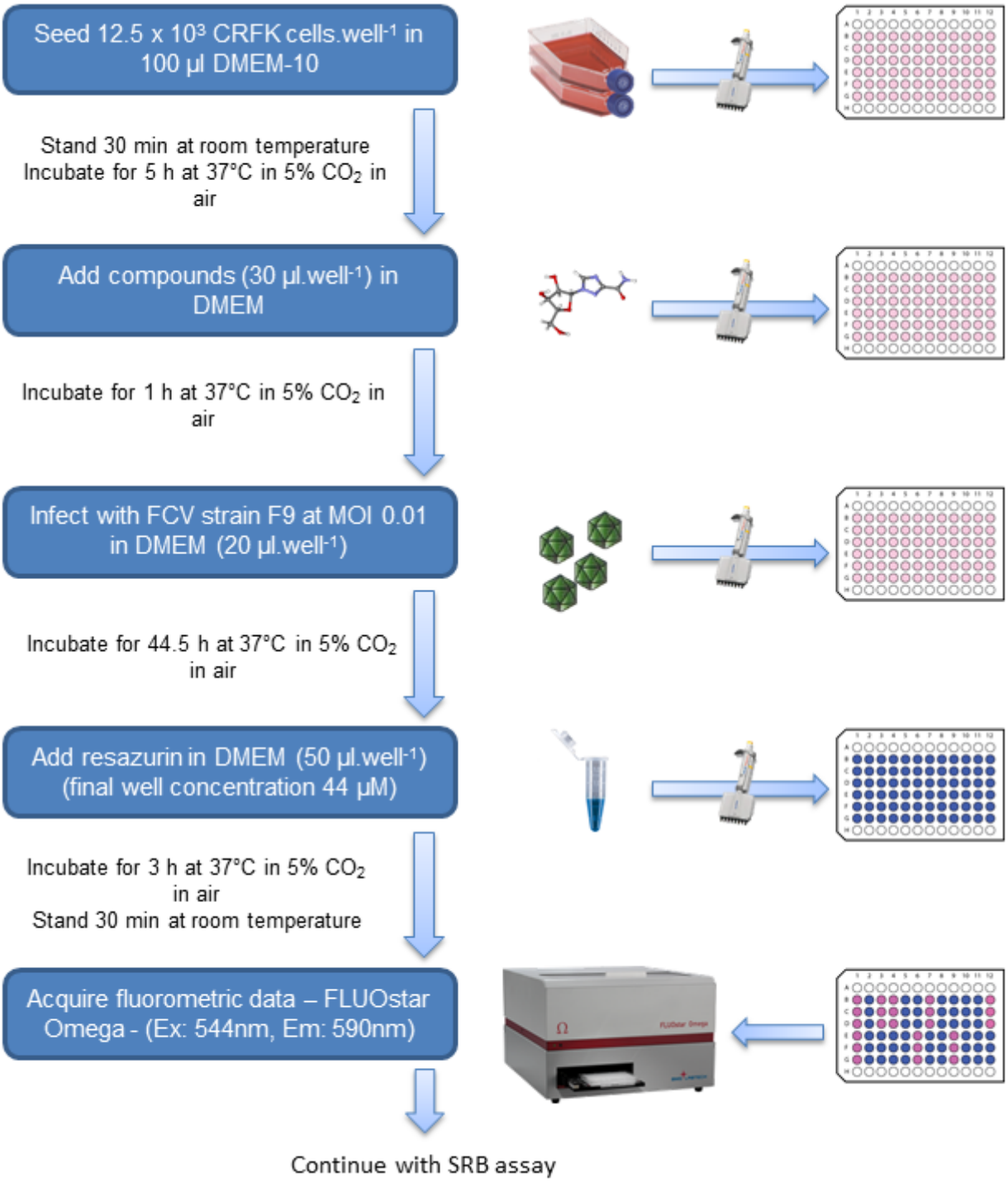

Figure 3.18: Schematic of optimised resazurin-based CPE inhibition assay for feline calicivirus**.**

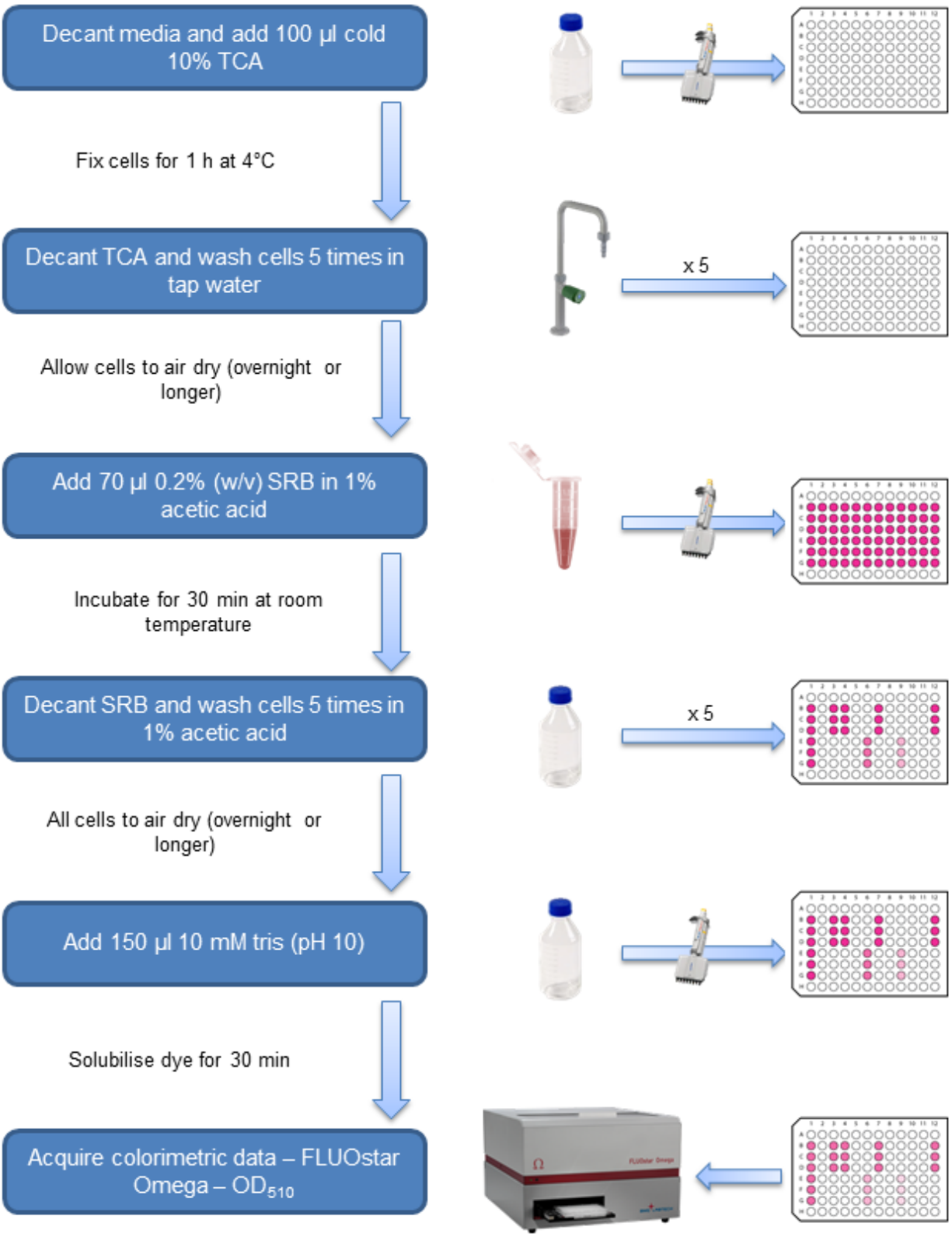

Figure 3.19: Schematic of the optimised SRB-based assay**.**

Although the primary goal of this study was to develop an assay suitable for low to medium throughput screening of a limited number of compounds, a secondary aim was to develop a "HTS ready" assay for future studies. One of the most commonly used measures of assay performance in HTS is the Z'-factor. The Z'-factor is a dimensionless number that can take any value less than or equal to one ($1 \geq Z' > -\infty$). According to Zhang et al. (1999) a perfect (idealised) assay has a Z' = 1, an excellent assay $1 > Z' \geq 0.5$, and a marginal assay $0.5 > Z' > 0$. At Z '= 0 the positive and negative control populations begin to overlap, and thus assays with Z' < 0 are considered unsuitable for screening. For HTS a Z' > 0.5 is recommended (An and Tolliday, 2010). The mean Z'-factor for the resazurin-based assays was 0.70 for FCoV and 0.76 for FCV. Based on these results these assays are suitable in their current form for adaptation to HTS. These values compare favourably to other reported assays used for HTS, including a HTS screen for SARS-CoV using a luminescent ATP based detection system which demonstrated a Z'-factor of 0.68 (Severson et al., 2007). The optimised SRB-based assay demonstrated higher Z'-factors than the resazurin-based assay, at 0.86 and 0.91 for FCoV and FCV respectively. Inter- and intra-day variation in Z'-factors were low, and in all cases Z'-factors were > 0.60 demonstrating the reliability and repeatability of both assays.

In addition to showing each assay performed well independently, this study demonstrated that the SRB-based assay could be performed sequentially with the resazurin-based assay, with no loss of sensitivity. Although both assays provide information on whole-well cell viability, the variables measured by the assays differ, and thus sequential use of these assays provides an opportunity for orthogonal testing on the same samples. Orthogonal testing is recommended in screening programs to rule out false positive results that can occur, for example, if a tested compound interferes with the readout of the primary assay (Iversen et al., 2012). For resazurin-based assays, such a result could occur with compounds displaying intrinsic fluorescence in the same wavelengths as resorufin, or for compounds with inherent reducing activity (Sittampalam et al., 2013).

Whilst there are several benefits of the SRB-based assay as described, including a higher Z' factor, higher S/B ratio, and the ability to fix plates and store indefinitely prior to staining and data acquisition, the resazurin-based assay was selected as the primary screening assay for further experiments based on practical considerations. The SRB-based assay, although technically simple to perform, does require multiple steps prior to data acquisition. In the absence of automation, the requirement for multiple manual handling steps increases the chance of operator error. In contrast, although the resazurin-based assay had a slightly

lower Z'-factor for each virus, the simple single-step protocol prior to assay readout offered considerable practical benefits and minimised the opportunity for human error.

A number of resazurin-based assays are commercially available. A comparison of the cost per plate of some commercially available reagents and the in-house produced resazurin solution demonstrated that the latter is considerably more economical. With a price of only a few cents per plate, the in-house prepared reagent is orders of magnitude cheaper than the commercially available reagents. A potential benefit of the commercially available reagents is the inclusion of a poising agent to maintain the redox potential of the solution and enhance its stability. When stored in single use aliquots at -20°C, no deterioration of the in-house prepared reagent was noted in this study. The in-house produced resazurin reagent therefore offers significant benefits, particularly for less well funded fields of research.

In conclusion, this study describes the successful development and optimisation of two alternative CPE inhibition assays suitable for screening compounds for antiviral activity against FCoV and FCV. Validation using control plates of positive and negative controls demonstrated minimal intra- and inter-day variability, with Z'-factors demonstrating suitability for HTS in the current format. Although the SRB-based assay provided slightly better performance, the resazurin-based assay was selected for subsequent screening studies based on benefits in terms of cost and convenience. The demonstration that the resazurin and SRB assays could be performed sequentially enables orthogonal testing to be performed on the same plate during initial screening, providing a convenient method to identify compounds which due to their inherent properties may interfere with the resazurin assay.

4

Identification and characterisation of small molecule inhibitors of feline coronavirus replication

4.1. ABSTRACT

The prognosis for cats with feline infectious peritonitis (FIP) remains poor despite clinical intervention. Current treatment options are directed primarily at modulating the host immune response and are, at best, palliative in nature. The use of direct acting antivirals effective against feline coronavirus, the causative agent of FIP, would address the underlying root cause of the pathology and, in combination with immunomodulatory therapy, likely provide significant therapeutic benefit. This chapter describes the *in vitro* screening and evaluation of a panel of nineteen candidate compounds for antiviral activity against FCoV. Three compounds, chloroquine, mefloquine, and hexamethylene amiloride demonstrated marked inhibition of virus induced CPE at low micromolar concentrations. Orthogonal assays confirmed inhibition of CPE was associated with significant reductions in viral replication. Selectivity indices calculated based on *in vitro* cytotoxicity screening and reductions in extracellular viral titre were 217, 24, and 20 for chloroquine, mefloquine, and hexamethylene amiloride respectively. Preliminary experiments performed to inform the possible antiviral mechanism of the compounds demonstrated all three acted at an early stage of viral replication. Taken together these results suggest that these compounds, or their derivatives, warrant further investigation for clinical use in cats with FIP.

4.2. INTRODUCTION

Infection with feline coronavirus (FCoV) is extremely common in domestic cats, with seroprevalence as high as 100% when cats are housed in situations of high population density (Pedersen, 1995). Fortunately, infection results in little, if any, morbidity in the majority of cats, however in a small proportion infection with mutated virulent FCoV can result in the development of FIP. Current treatment options for FIP are generally considered palliative, with a median life expectancy following diagnosis typically measured in days or

weeks. Although the pathology of FIP is immune mediated in nature, the triggering and perpetuating event is the increased replication of FCoV in cells of the monocyte lineage (Kipar et al., 2006a; Kipar et al., 2005; Kipar et al., 2006b; Regan et al., 2008a; Simons et al., 2005). It is likely therefore that an antiviral effective against FCoV would be beneficial in treating this disease.

Historically, treatment for FIP has primarily focused on immune modulating drugs. There are a limited number of reports in the literature of purportedly successful treatments for FIP using immunomodulatory therapy (Table 1.3), however despite the sometimes impressive results reported, these initial positive findings have not been borne out with subsequent clinical experience, or drugs have been shown to be ineffective when larger, and well controlled studies have been conducted (Fischer et al., 2011; Hartmann and Ritz, 2008; Ritz et al., 2007). The incongruity between initial reports and the subsequent studies is most likely due to methodological flaws in the former, particularly relating to inadequate criteria for diagnosing FIP.

Less has been reported regarding the use of direct acting antivirals against FCoV. A number of compounds have demonstrated an inhibitory effect on the virus *in vitro* (Barlough and Scott, 1990; Barlough and Shacklett, 1994; Hsieh et al., 2010; Keyaerts et al., 2007), however for most of these there is little or no published data regarding their clinical use in treating FIP. The broad spectrum antiviral ribavirin, which had demonstrated efficacy *in vitro* (Barlough and Scott, 1990; Weiss and Oostrom-Ram, 1989), provided limited clinical benefit and was associated with significant toxicity in cats with FIP (Weiss et al., 1993b). In the absence of an effective vaccine or treatment, further research is clearly needed to address the unmet need for effective and safe antiviral therapeutics for the treatment of FIP.

The initial stage in modern antiviral drug discovery often involves high throughput screening of vast chemical libraries, sometimes containing in excess of one million compounds. In many cases the screening is unfocused, with libraries containing an essentially random collection of potentially bioactive compounds. The expected hit rate during such screening is typically low, and given many reported hits are false positive results or have unsuitable pharmacokinetic or toxicity profiles, large numbers of compounds must be screened to identify suitable candidate compounds. These large scale unfocused screens are also expensive (An and Tolliday, 2009), an important consideration for the less well funded areas of antiviral research. One alternative approach is to utilise a more focused screening strategy, enriching the compound library by selecting and testing compounds considered likely to have an antiviral effect. Selection of compounds for screening based on an a prior knowledge of their pharmacodynamics and the viral lifecycle will likely increase the hit rate considerably, allowing a reduction in the number of compounds tested, and the associated

costs. These more focused screening panels may consist of compounds of a particular class known to be effective against the challenge virus, a panel of derivative compounds of a known effective antiviral, or compounds shown previously to be effective against closely related viruses. In the latter regard, FIP researchers can benefit significantly from the increased interest in the study of antiviral chemotherapeutics for coronaviruses triggered by the emergence and global spread of the highly pathogenic SARS-CoV in 2002/2003.

A number of direct acting antivirals were used to treat patients during the SARS pandemic, however the short duration of the outbreak limited information regarding their use. Ribavirin, the most commonly used antiviral drug, offered inconsistent results, although in some studies it appeared to confer benefits in reducing mortality and intensive care unit admissions, and improving symptoms (Momattin et al., 2013). These benefits were reduced with delays in initiating treatment and were frequently associated with significant adverse events (Momattin et al., 2013). The use of retroviral protease inhibitors lopinavir and ritonavir, with or without ribavirin, was also associated with a favourable clinical response (Momattin et al., 2013). Despite the end of the SARS pandemic, a significant research effort continued focusing on identifying compounds effective against this newly recognised pathogen. In the immediate aftermath of the pandemic, from May 2003 to November 2005, more than 190 of the 982 papers published on SARS-CoV were therapeutics related (Wu et al., 2006). A number of review articles have subsequently been published detailing compounds showing anti-coronavirus activity (De Clercq, 2006; Pyrc et al., 2007; Tong, 2009a, b; Wu et al., 2006).

Although the SARS pandemic ended a little over six months after it was declared, this outbreak highlighted that cross species transmission of coronaviruses remains an ever present threat. The recent emergence of a novel coronavirus in Saudi Arabia known as Middle East respiratory syndrome coronavirus (MERS-CoV) has again exemplified this risk of cross species transmission. With a reported case fatality rate of 43% [82 deaths from 189 laboratory confirmed cases] (ProMED, 2014) there clearly remains an urgent need for chemotherapeutics effective against coronaviruses (Chan et al., 2013).

In the current study we screened a panel of nineteen compounds with previously demonstrated antiviral activity against coronaviruses or other RNA viruses for antiviral activity against FCoV using the optimised resazurin-based CPE inhibition assay described in Chapter 3. Cytotoxicity of compounds was determined prior to screening using sequential resazurin- and SRB-based assays to determine the optimal minimally toxic test concentration and to enable calculation of selectivity indices. The antiviral effects of compounds identified during screening were confirmed with plaque reduction and virus yield reduction assays. Virucidal suspension assays and time of addition assays were performed to provide initial

information as to the stage of viral replication targeted and the potential antiviral mechanism of action.

4.3. MATERIALS AND METHODS

4.3.1. Test compounds

Details of the compounds tested in this study are shown in Table 4.1. Compounds were selected for inclusion based on their reported *in vitro* antiviral properties against coronaviruses or other RNA viruses (referenced in Table 4.1). Stock solutions were prepared by dissolving compounds in ultrapure water or DMSO (Sigma-Aldrich) to the concentrations listed. Compounds were sterile filtered with a 0.22 µm regenerated cellulose filter (Corning), aliquoted into sterile single use microtubes (Sarstedt), and stored at -80 °C until use. Compounds were used within six months of suspension.

Table 4.1: Compounds selected for antiviral screening. Superscripts indicate compound supplier: *, Sigma-Aldrich; †, Santa Cruz Biotechnology; ‡, Virbac.

Compound	Stock concentration	Antiviral effects reported against (not a complete list)
Chloroquine diphosphate*	100 mM in water	SARS-CoV (Keyaerts et al., 2004; Vincent et al., 2005), hepatitis C virus (HCV) (Mizui et al., 2010), human coronavirus OC43 (Keyaerts et al., 2009), human immunodeficiency virus (HIV) (Savarino et al., 2001)
Quercetin*	100 mM in DMSO	HCV (Bachmetov et al., 2012), porcine epidemic diarrhoea virus (Choi et al., 2009a), dengue virus (Zandi et al., 2011)
Curcumin†	100 mM in DMSO	Influenza A (Chen et al., 2010), SARS-CoV (Wen et al., 2007)
Rutin trihydrate†	100 mM in DMSO	Canine distemper virus (CDV) (Carvalho et al., 2013), parainfluenza virus 3 (Orhan et al., 2010)
Indomethacin†	100 mM in DMSO	SARS-CoV (Amici et al., 2006), HIV (Bourinbaiar and Lee-Huang, 1995)
Glycyrrhizic acid*	100 mM in DMSO	SARS-CoV (Cinatl et al., 2003). HIV (Fiore et al., 2008)
Hesperidin†	200 mM in DMSO	Human rotavirus (Bae et al., 2000), CDV (Carvalho et al., 2013)
Aurintricarboxylic acid*	100 mM in DMSO	SARS-CoV (He et al., 2004), influenza A (Hashem et al., 2009)
Hesperetin†	100 mM in DMSO	SARS-CoV (Lin et al., 2005), Sinbis virus (Paredes et al., 2003)
Mefloquine hydrochloride*	100 mM in DMSO	JC virus (Brickelmaier et al., 2009)

Table 4.1 cont.: Compounds selected for antiviral screening. Superscripts indicate compound supplier: *, Sigma-Aldrich; †, Santa Cruz Biotechnology; ‡, Virbac.

Compound	Stock concentration	Antiviral effects reported against (not a complete list)
Artesunate*	65 mM in DMSO	SARS-CoV (Li et al., 2005b)
Ribavirin*	31 mM in DMSO	FCoV (Weiss and Oostrom-Ram, 1989), FCV (Povey, 1978b)
Baicalin hydrate†	100 mM in DMSO	SARS-CoV (Chen et al., 2004)
Hexamethylene amiloride†	50 mM in DMSO	SARS-CoV (Wilson et al., 2006a), HCV (Premkumar et al., 2004)
Cinanserin†	25 mM in DMSO	SARS-CoV (Chen et al., 2005)
Artemisinin*	100 mM in DMSO	Bovine viral diarrhoea virus (Romero et al., 2006), HCV (Paeshuyse et al., 2006)
Niclosamide†	20 mM in DMSO	SARS-CoV (Wu et al., 2004), human rhinovirus (Jurgeit et al., 2012)
Lactoferrin*	10 $mg.ml^{-1}$ in DMEM	FCV (McCann et al., 2003), feline herpes virus (Beaumont et al., 2003)
Recombinant feline interferon ω‡	$10x10^6$ $units.ml^{-1}$ in water	FCoV (Mochizuki et al., 1994; Truyen et al., 2002)

4.3.2. Cytotoxicity screening of test compounds

Cytotoxicity screening was performed using a modification of the resazurin- and SRB-based CPE inhibition assays described in Chapter 3 (summarised in Figure 3.17 and Figure 3.19). Clear-bottomed black-walled 96-well plates (µClear ®, Greiner Bio-One) were set up as in Figure 4.1 with 5 x 10^3 cells.well^{-1} in 100 µl DMEM-10 (or 100 µl DMEM-10 for control wells containing no cells). Plates were held at room temperature for 30 min post-seeding then incubated then at 37°C in 5% CO_2 in air for 5 h prior to compound addition. Nine serial half-log or one-third log dilutions of test compounds were prepared in DMEM, and 50 µl.well^{-1} added in triplicate wells per concentration. Fluorometric controls were included to assess potential interference from compounds on assay performance. These controls identify compounds with intrinsic fluorescence in the same range as resazurin, or those with inherent reducing activity that could artefactually increase signals, resulting in an underestimation of cytotoxicity or an overestimation of antiviral effects. Fluorometric controls consisted of the highest tested concentration of compound in wells containing no cells. Sodium dodecyl sulfate (SDS) was included as a positive toxicity control at a concentration of 0.1% (w/v). Negative control (cell only), vehicle control (0.33% DMSO), and media only (no cell) controls were also included in triplicate on each plate. Cell viability was determined after 72 h exposure to the test compounds using sequential resazurin- and SRB-based assays as described in Chapter 3. Data were exported to Microsoft Excel and GraphPad Prism for analysis. Cell viability for the resazurin-based assay was calculated according to the following formula:

$$Cell\ viability\ (\%) = \frac{RFU_{Tx}}{RFU_{Control}} \times 100$$

Where RFU_{Tx} is the mean fluorescence intensity of treated cells and $RFU_{Control}$ is the mean fluorescence intensity in untreated cells. For the SRB-based assay, cell viability was calculated similarly, with OD_{510} values rather than RFU values used in calculations. Two independent experiments were performed and the results represent Mean ± SE. Test compound concentrations selected for subsequent antiviral screening were those resulting in viability of at least 80% or greater (≥ CC80) based on manual interpolation of graphs.

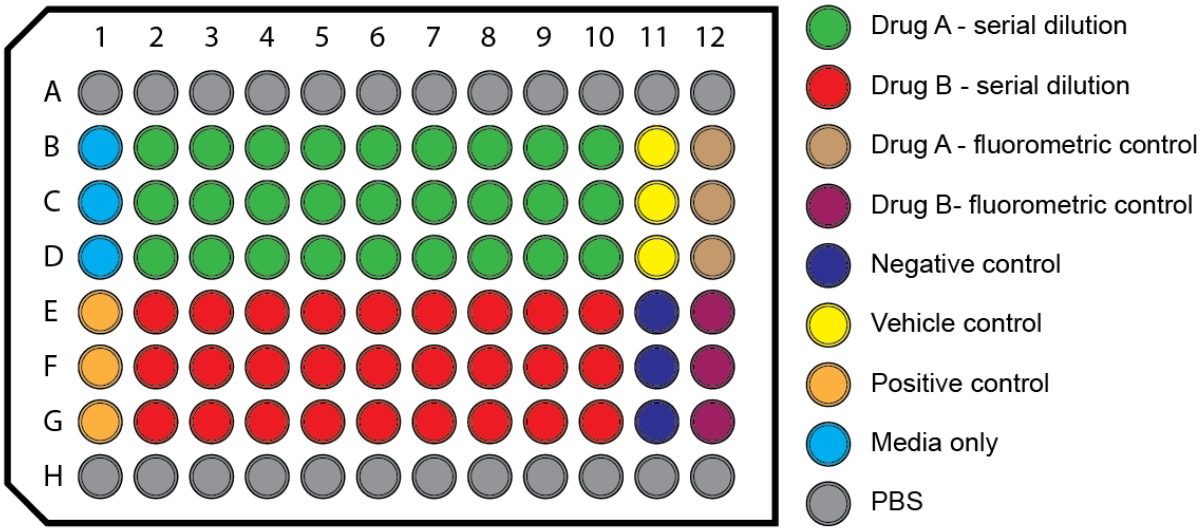

Figure 4.1: Plate layout for cytotoxicity testing. Cytotoxicity testing was performed on two compounds per plate.

4.3.3. Antiviral screening using CPE inhibition assay

Antiviral screening of compounds listed in Table 4.1 was performed using the optimised resazurin-based CPE inhibition assay described in Chapter 3 and summarised in Figure 3.17. Plate setup was as shown in Figure 4.2, with CPE inhibition and cytotoxicity screening performed on the same plate. Test compound concentration was as determined in Section 4.4.1. Data analysis was performed in Microsoft Excel and GraphPad Prism. The percentage inhibition of virus induced CPE was calculated by:

$$CPE\ inhibition\ (\%) = \frac{RFU_{Tx} - RFU_{V(+)}}{RFU_{V(-)} - RFU_{V(+)}} \times 100$$

Where RFU_{Tx} is the mean fluorescence intensity of treated infected cells; $RFU_{V(+)}$ is the mean fluorescence intensity in untreated infected cells; and $RFU_{V(-)}$ is the mean fluorescence intensity of untreated uninfected cells. Cell viability of the uninfected cells was determined as detailed in Section 4.4.1. Each treatment was performed in triplicate and repeated in three independent experiments. Results represent Mean ± SE. Compounds showing marked, moderate, or mild antiviral effects were defined as those showing 75-100%, 50-74%, and 25-49% inhibition of CPE respectively. Compounds demonstrating marked CPE inhibition were selected for further characterisation.

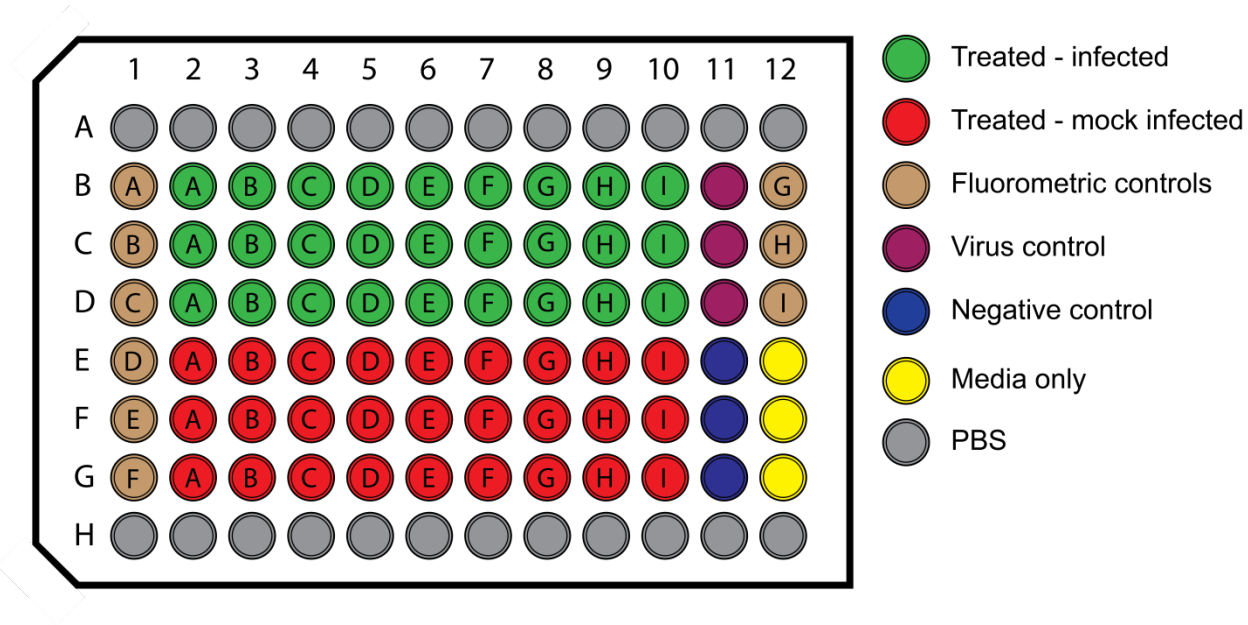

Figure 4.2: Plate setup for antiviral screening. Each compound was tested at a single concentration in triplicate (as indicated by letters A→ I) for both antiviral effect (Rows B,C, and D) and also cytotoxicity (Rows E, F, and G).

4.3.4. Titration of effective compounds and determination of selectivity index

Using the optimised FCoV CPE inhibition assay a concentration-response experiment was conducted with serial dilutions of identified candidate compounds (nine concentrations per compound). To enable calculation of the selectivity index, a repeat cytotoxicity screen was performed concurrently. The cytotoxicity screen was performed as per the CPE inhibition assay (Figure 3.17) except that cells were mock infected with 20 µl DMEM. Each treatment was performed in triplicate and repeated in three independent experiments. Data were exported to Microsoft Excel for calculation of cell viability and CPE inhibition according to the formulae in Sections 4.3.2 and 4.3.3 respectively. Data analysis were conducted in GraphPad Prism, with the 50% inhibitory concentration (IC50) and 50% cytotoxic concentration (CC50) values calculated using the inbuilt non-linear curve fitting functions following $\log_{10}$ transformation of compound concentrations. The selectivity index (SI) for each compound was calculated according to the following formula:

$$SI = \frac{CC50}{IC50}$$

4.3.5. Confirmatory assays

Plaque reduction and virus yield reduction assays were performed to confirm antiviral effects of candidate compounds identified using the CPE inhibition assay.

4.3.5.1. Virus yield reduction assay

Virus yield reduction assays were performed in 24-well plates (Sarstedt). Wells were seeded with 4.0 x 10^4 cells.well^{-1} in 400 µl DMEM-10. Plates were kept at room temperature for 30 min and then at 37°C in 5% CO_2 in air for 5 h prior to the addition test compounds. Compounds were diluted in DMEM to the required concentrations (five or six concentrations per compound) with 75 µl added to each well. Cells were incubated at 37°C in 5% CO_2 in air for an additional 1 h prior to infection with FCoV FIPV1146 at MOI 0.1 in 25 µl DMEM. Cells were incubated for a further 48h at 37°C in 5% CO_2. At 24 and 48 hpi cell monolayers were visually assessed for CPE using an Olympus CKX41 inverted phase-contrast microscope and culture media was collected and stored at -80°C for virus titration. Untreated infected cells, untreated uninfected cells, and treated uninfected cells were included as controls. This latter control was included to allow assessment of morphological changes to cells due to compound treatment. Titration of extracellular virus harvested at 24 and 48 hpi was performed using the TCID50 method described in Section 2.3.1.2.2. The relative viral titre was calculated for each treatment, with the titre of untreated control cells defined as 100%. Data were analysed in GraphPad Prism. Each treatment and time point was performed in triplicate and repeated in two independent experiments, with results representing Mean ± SE.

4.3.5.2. Plaque reduction assay

Plaque reduction assays were performed in 12-well plates (Corning) using a modification of the standard plaque assay for FCoV virus titration as described in Section 2.3.1.2.1. Cells seeded at a density of 6 x 10^4 cells.well^{-1} in 1 ml DMEM-10 were held at room temperature for 30 min prior to incubation at 37°C in 5% CO_2 in air for 60 h, by which time monolayers were approximately 90% confluent. Culture media was discarded and replaced with 400 µl DMEM-2 plus 75 µl of various concentrations of test compounds in DMEM (or 75 µl DMEM only for control wells) using five or six concentrations per compound. After exposure to the compound for 1 h, cells were infected with approximately 30 pfu.well^{-1} FCoV FIPV1146 in 25 µl DMEM. Virus was allowed to adsorb for 90 min with plates rocked every 15 min to ensure an even distribution of inoculum. Culture media was discarded after 90 min and cells overlaid with 1 ml CMC plaque assay overlay media containing the same concentration of compound as present prior to and during infection. Incubation, fixation, staining, and counting of plaques was as previously described in Section 2.3.1.2.1. The relative plaque number was calculated for each treatment, with the value of untreated control defined as 100%. Each treatment was performed in duplicate, and repeated in three independent experiments, with data representing Mean ± SE.

4.3.6. Virucidal suspension assay

A virucidal suspension assay was performed to assess virucidal effects of test compounds. The assay was performed as per the standard 12-well FCoV plaque assay described in Section 2.3.1.2.1 with the exception that virus was mixed and incubated with test compounds prior to infection. Stock FCoV FIPV1146, diluted in DMEM to 2 x 10^6 pfu.ml^{-1}, was mixed with an equal volume of test compound diluted in DMEM to 2 x the test concentration used during screening in Section 4.3.3. The control virus suspension was mixed with DMEM containing an equal concentration of DMSO as the test samples. Virus suspensions were incubated for 1 h at room temperature before serial dilution in DMEM to infect cells with approximately 25 pfu.well^{-1} in 100 µl. Following serial dilution of the virus, cells were exposed to test compounds at concentrations greater than 4 $\log_{10}$ lower than concentrations previously shown to have no antiviral effect. Virus was allowed to adhere for 90 min following which the viral inocula was discarded and cells overlaid with 1 ml CMC plaque assay overlay media. Incubation, fixation, staining, and counting of plaques was as previously described. The experiment was performed in triplicate and repeated in two independent experiments. Data represent Mean ± SE.

4.3.7. Time of addition assay

4.3.7.1. CPE inhibition

A modification of the resazurin-based CPE inhibition assay was performed to assess the effect of time of compound addition on the antiviral efficacy of identified compounds. The CPE inhibition assay was performed as detailed in Section 4.3.3 with the exception that test compounds were added at various time points before and after infection. The selected time points were 1 h prior to infection, concurrent with infection, and 1, 3, or 6 h post infection. Treatments were performed in triplicate and repeated in three independent experiments. Data represent Mean ± SE.

4.3.7.2. Immunofluorescence assay

To further elucidate the stage of viral replication affected by each compound the effect of time of addition on viral antigen expression was examined. Cells were seeded at a density of 5.0 x 10^3 cells.well^{-1} in 100 µl DMEM-10 in 96-well plates (µClear ®, Greiner Bio-One). A lower cell density was used for this experiment for ease of cell segmentation during post acquisition image analysis. After seeding plates were kept at room temperature for 30 min and then incubated at 37°C in 5% CO_2 in air for 5 h prior to the first time-point of compound addition. Compounds were added in 30 µl to duplicate wells at different time points prior to, concurrent with, or post infection as shown in Figure 4.3. Cells were infected with FCoV FIPV1146 at MOI 0.5 in 20 µl or mock infected with 20 µl DMEM for an infection period of 1

h. At 12 hpi (measured from the end of the infection period) cells were fixed, stained, and imaged as described in Section 2.5.3. The 12 h duration was selected based on the reported one step growth curve of FCoV (Dewerchin et al., 2005; Rottier et al., 2005). Image analysis was performed using CellProfiler with data exported to FCS Express Image Cytometry for analysis as described in Section 2.5.3.3.

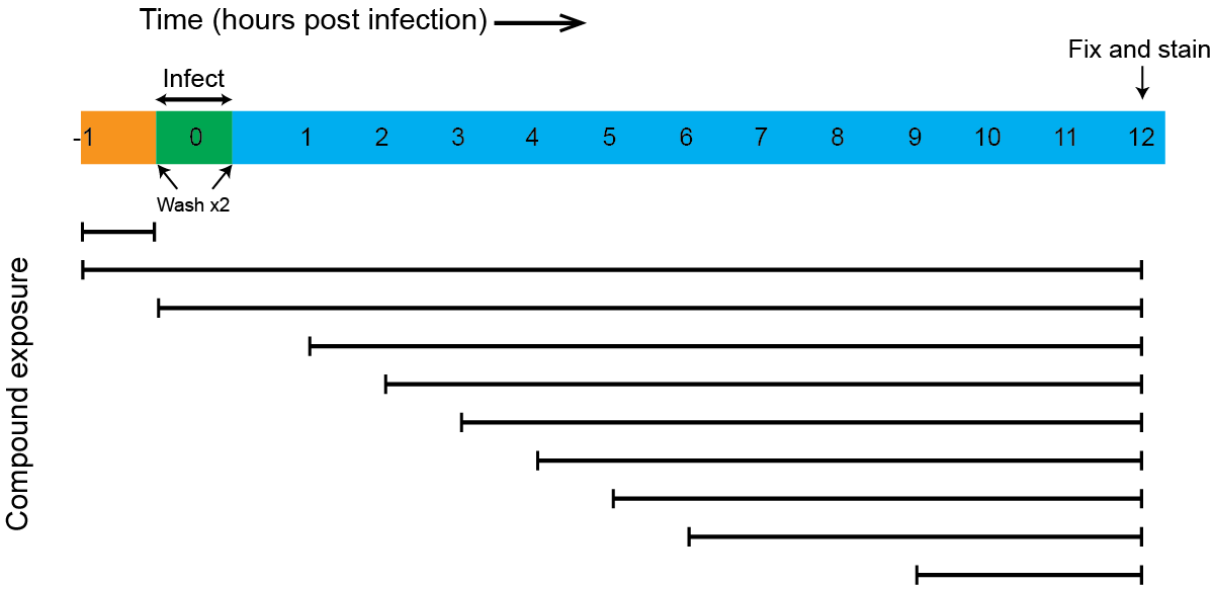

Figure 4.3: Schematic of compound exposure during time of addition studies. Individual compounds were added to duplicate wells at different time points prior to, concurrent with, or post infection. Individual bars represents the duration and timing of compound exposure for each treatment.

4.3.8. Strain variation

To assess efficacy against different FCoV strains, identified candidate compounds were tested against FCoV FECV1683 using the resazurin-based CPE inhibition assay. The assay was performed as previously described in Section 4.3.3, excepting that cells were infected with either FCoV FIPV1146 or FECV1683 at MOI 0.01. Each treatment was performed in triplicate and repeated in three independent experiments, with data representing Mean ± SE.

4.4. RESULTS

4.4.1. Cytotoxicity screening of test compounds

Cytotoxicity screening was performed to determine the concentration of test compounds to be used for antiviral screening. Dual resazurin- and SRB-based assays were performed for all compounds with the exception of lactoferrin and rFeINF- ω, which due to technical problems, were assessed using only the resazurin-based assay. Results of the screening are shown in Figure 4.4. In general there was good agreement between cell viability

calculated with the two different assays. There was no evidence of interference by the test compounds with the resazurin-based assay as fluorometric controls gave similar signals to media only controls. Concentrations resulting in cell viability greater than 80% (> CC80) were used for subsequent antiviral screening, and are indicated by the dotted lines on Figure 4.4.

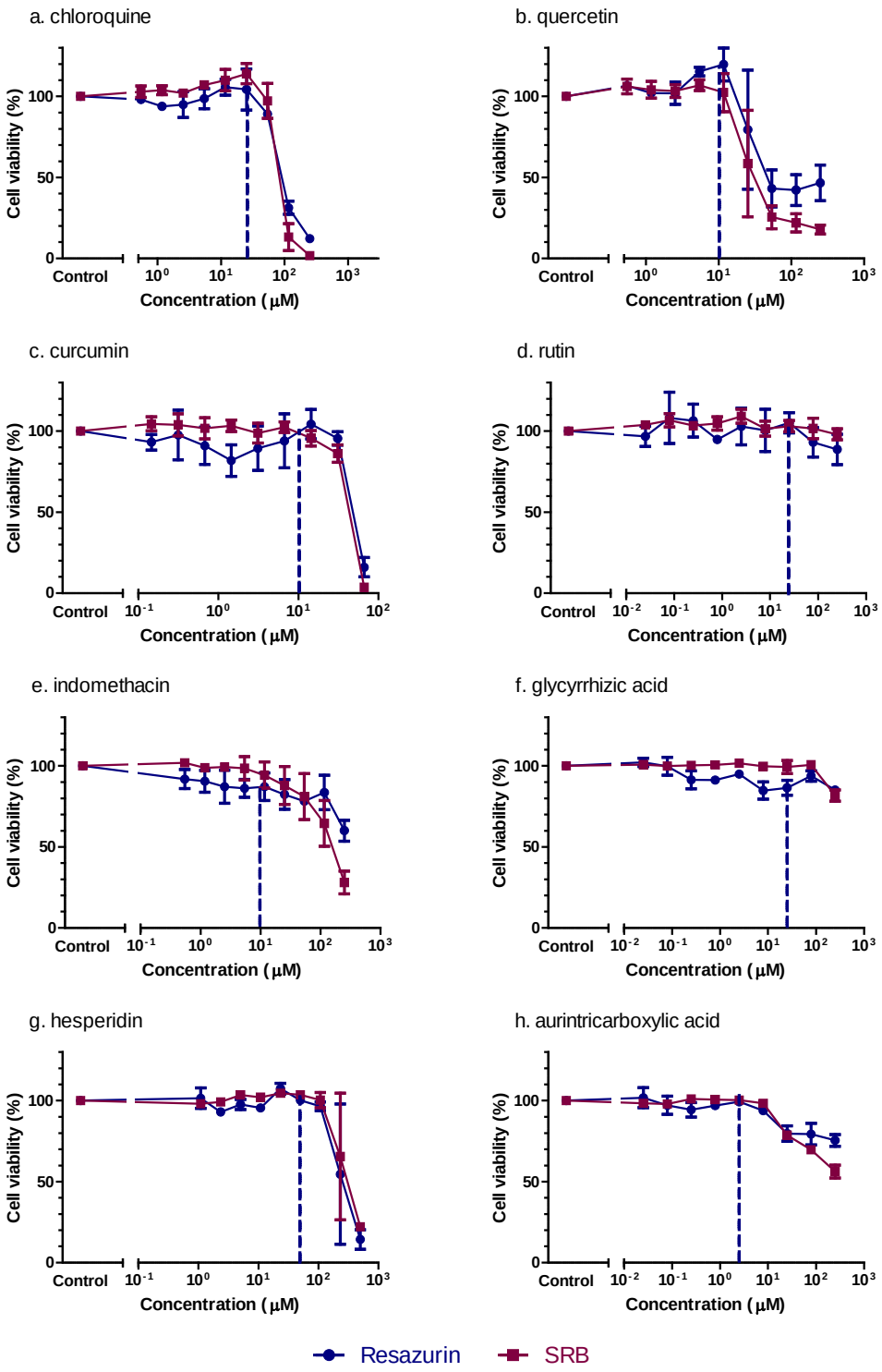

Figure 4.4: Results of cytotoxicity screening. Cells were treated with serial half-log or third-log concentrations of test compounds 5 h post seeding. Effects on cell viability were determined after a 72 h exposure period using sequential resazurin- and SRB-based assays. Each treatment was performed in triplicate and repeated in two independent experiments. Results represent Mean ± SE. Dotted lines indicate selected test concentration of compound used for subsequent antiviral screening.

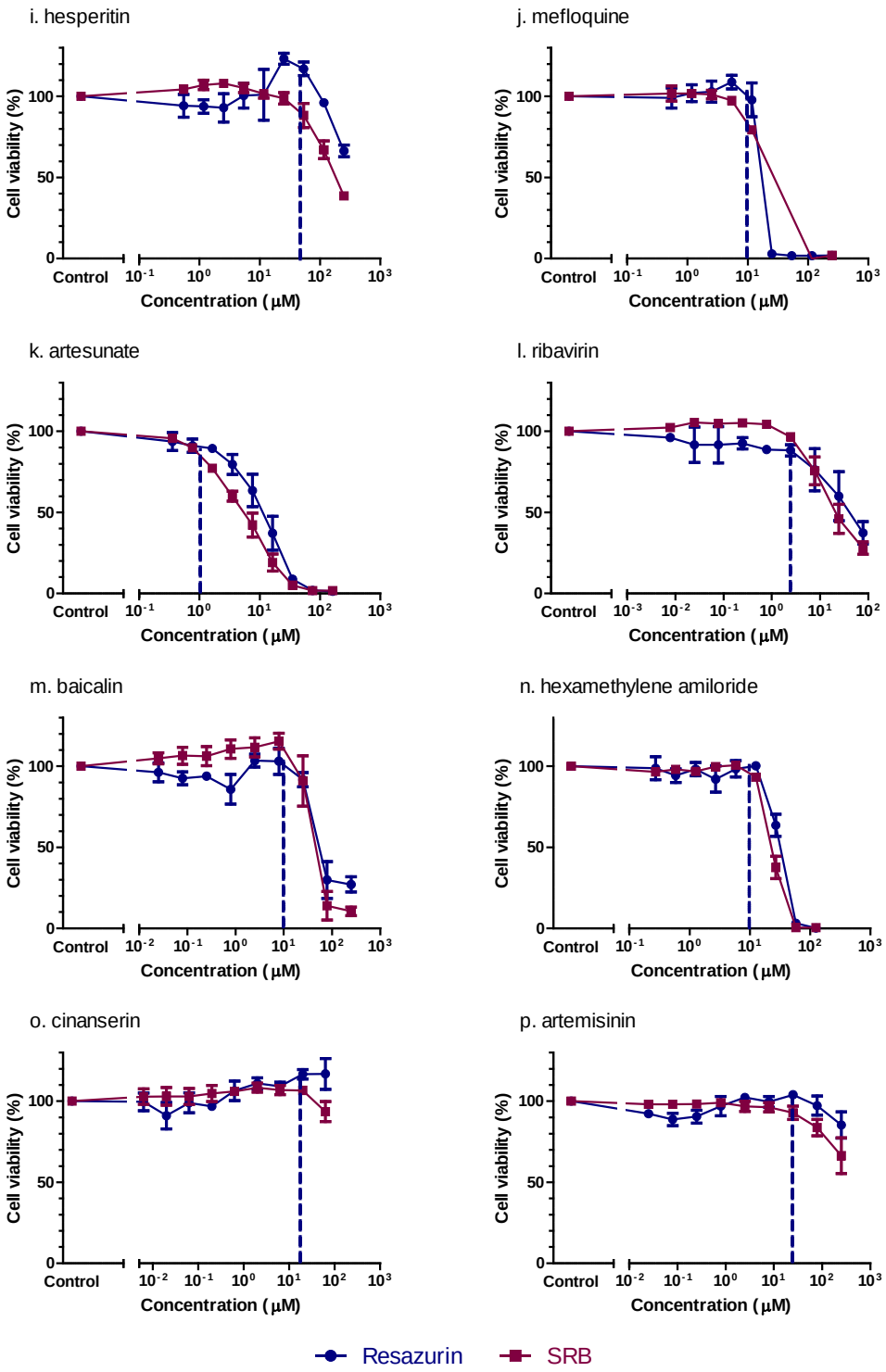

Figure 4.4 cont.: Results of cytotoxicity screening.

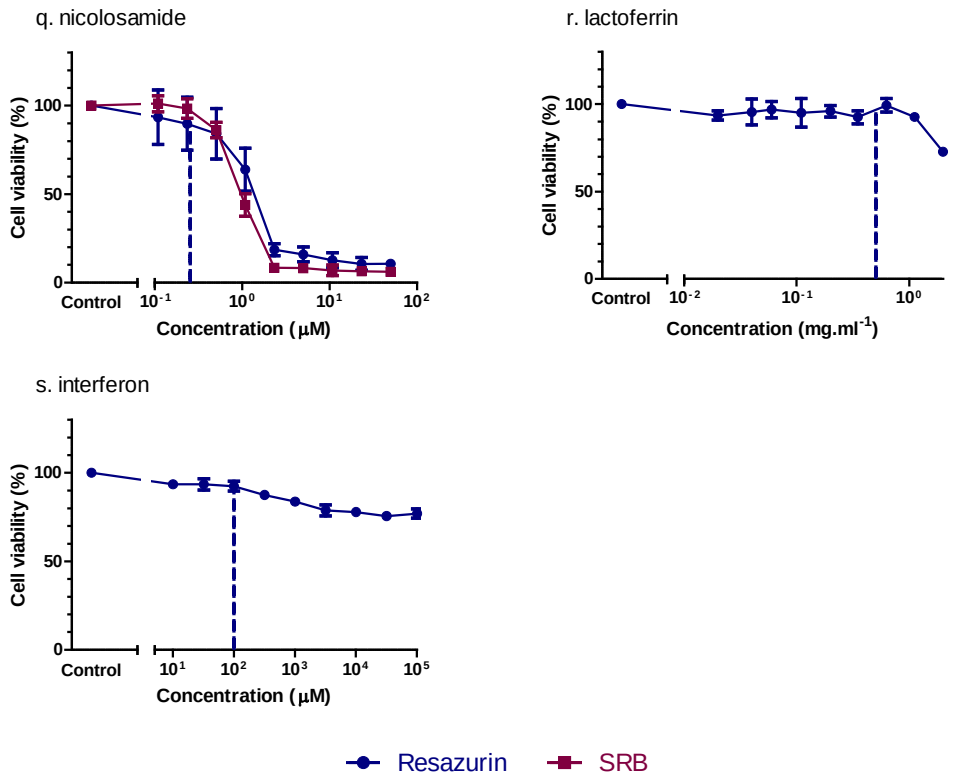

Figure 4.4 cont.: Results of cytotoxicity screening.

4.4.2. Antiviral screening using CPE inhibition assay

Based on the previously defined criteria, three of nineteen tested compounds showed marked inhibition of virus induced CPE and were selected for further characterisation. Pre-treatment with chloroquine at 25 µM, mefloquine at 10 µM, and hexamethylene amiloride at 10 µM resulted in 93.3%, 89.8%, and 77.6% inhibition of CPE respectively. A further two compounds, glycyrrhizic acid at 25 µM and cinanserin at 20 µM displayed a mild antiviral effect with a 26.7% and 34.0% reduction in CPE respectively. All other compounds demonstrated limited or no inhibitory effect on CPE. Included among these ineffective compounds was ribavirin, a broad spectrum antiviral compound that had previously shown *in vitro* (Barlough and Scott, 1990; Weiss and Oostrom-Ram, 1989), and to a limited extent *in vivo* efficacy against FCoV (Weiss et al., 1993b), as well as rFeINF-ω which had similarly shown previous *in vitro* efficacy against FCoV (Mochizuki et al., 1994; Truyen et al., 2002).

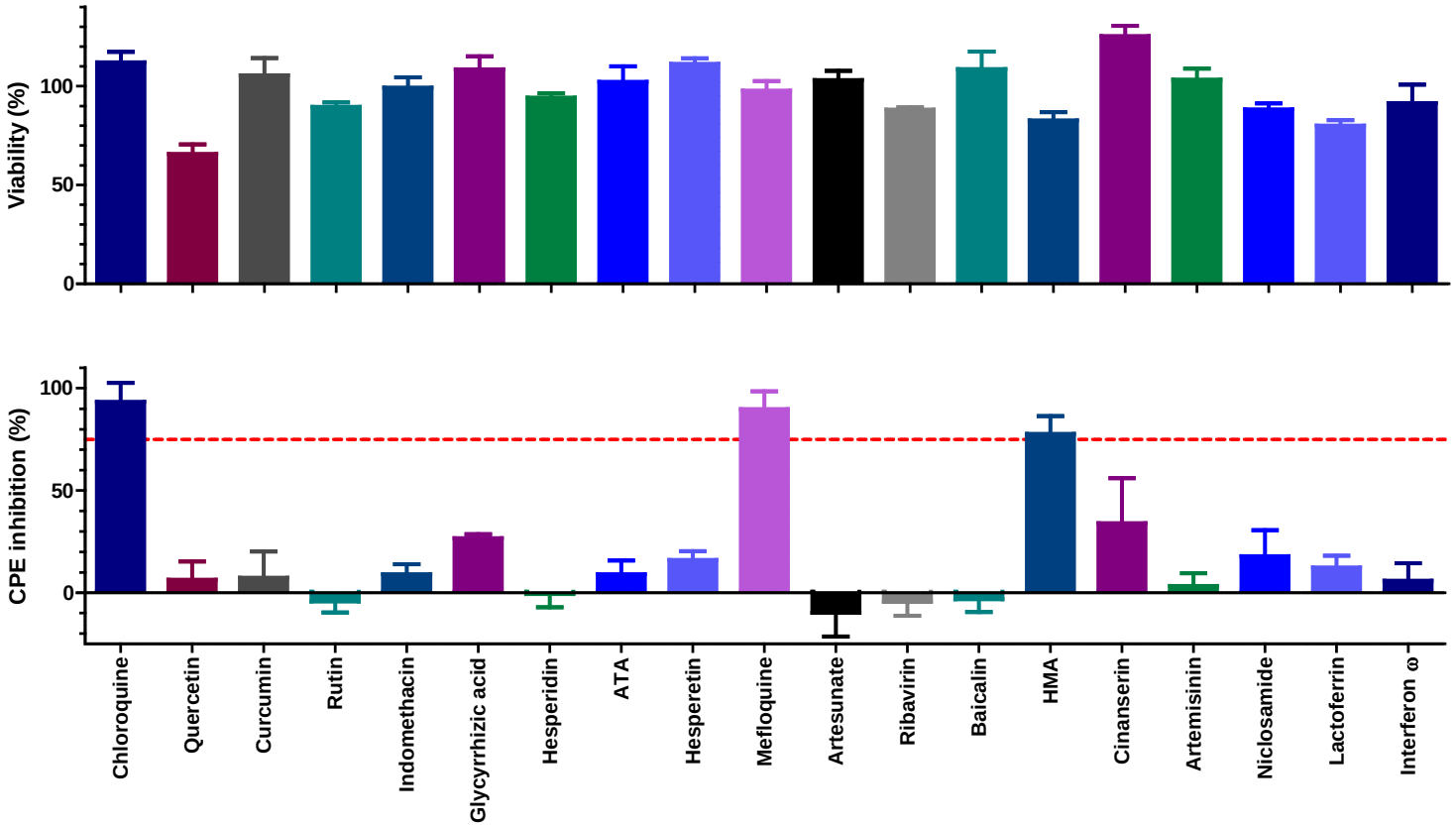

Figure 4.5: Results of FCoV antiviral screening experiment. Cells were pre-treated with compounds for 1 h prior to infection with FCoV FIPV1146 at MOI 0.01. Antiviral efficacy was determined 72 hpi using the resazurin-based CPE inhibition assay. A concurrent cytotoxicity screen was performed using the same protocol with the exception that cells were mock infected. Each treatment was performed in triplicate and repeated in three independent experiments. Results represent Mean ± SE. ATA, aurintricarboxylic acid; HMA, hexamethylene amiloride. Red dotted line = 75% inhibition.

4.4.3. Titration of candidate compounds

To confirm and further characterise the antiviral properties of candidate compounds identified during initial screening, a concentration-response study was conducted with chloroquine, mefloquine, and hexamethylene amiloride. A repeat cytotoxicity screen was concurrently performed for these compounds to allow calculation of selectivity indices. All compounds demonstrated a clear concentration-response effect over the tested range (Figure 4.6). Calculated IC50, CC50, and SI values for the compounds are shown in Table 4.2.

Table 4.2: IC50, CC50, and SI values for chloroquine, mefloquine, and hexamethylene amiloride as determined using the resazurin-based CPE inhibition assay. IC50 and CC50 values given with 95% confidence intervals.

Compound	IC50 (µM)	CC50 (µM)	SI
Chloroquine	16.63 (14.44-19.15)	82.31 (76.66-88.38)	4.95
Mefloquine	7.89 (7.50-8.31)	15.13 (13.69-18.05)	1.92
Hexamethylene amiloride	9.38 (8.99-9.79)	26.50 (25.42-27.63)	2.82

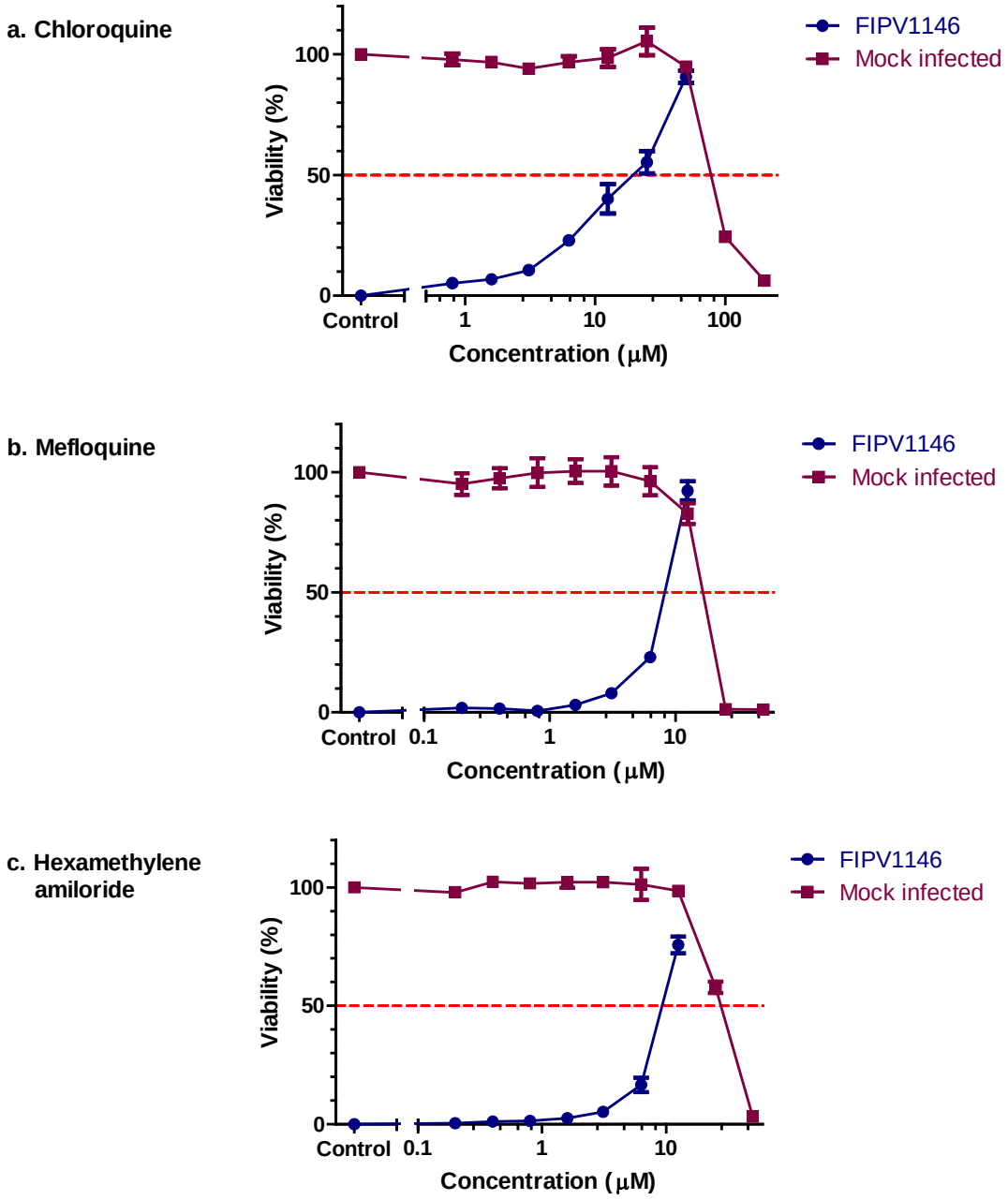

Figure 4.6: Results of antiviral titration for (a) chloroquine, (b) mefloquine, and (c) hexamethylene amiloride using resazurin-based CPE inhibition assay. Cells were pre-treated with serial dilutions of compounds for 1 h prior to infection with FCoV FIPV1146 at MOI 0.01. Antiviral efficacy was determined after a 72 hpi. A concurrent cytotoxicity screen was performed using the same protocol with the exception that cells were mock infected. Each treatment was performed in triplicate and repeated in three independent experiments. Results represent Mean ± SE.

4.4.4. Virus yield reduction assay

Virus yield reduction assays confirmed the CPE inhibition identified during screening was associated with a marked reduction in extracellular viral titre. Determination of extracellular virus titre was performed at 24 and 48 hpi with results shown in Figure 4.7. For chloroquine and mefloquine there was a considerable difference in the resulting concentration-response curves at 24 and 48 hpi, while for hexamethylene amiloride the shape of the curve was similar at both time points. Differences in concentration-response curves between the two time points is reflected in the IC50 values, with increased IC50 values for chloroquine and mefloquine at 48 hpi compared to 24 hpi, while for hexamethylene amiloride IC50 values were similar at both time points (Table 4.3).

Table 4.3: Calculated IC50 and SI values for chloroquine, mefloquine, and hexamethylene amiloride using the virus yield reduction assay. IC50 values given with 95% confidence intervals.

	24 hpi		48 hpi	
Compound	**IC50 (µM)**	**SI**	**IC50 (µM)**	**SI**
Chloroquine	0.38 (0.096-1.50)	217.60	28.87 (25.17-33.12)	2.85
Mefloquine	0.74 (0.32-1.73)	20.45	5.71 (4.43-7.36)	2.65
Hexamethylene amiloride	1.07 (0.66-1.73)	24.77	1.23 (0.71-2.14)	21.54

During the virus yield reduction assay cells were monitored for the development of CPE using phase contrast microscopy. It was noted that cells treated with chloroquine, mefloquine, or hexamethylene amiloride displayed characteristic morphological changes. These changes consisted of a large number of variably sized cytoplasmic (predominantly perinuclear) inclusions in addition to the presence, in some cells, of an increased number of cytoplasmic vacuoles (Figure 4.8). To investigate the nature of the inclusions staining with neutral red was performed. Neutral red is a vital dye that is known to accumulate in lysosomes. A separate experiment was conducted in which uninfected cells were treated with the candidate compounds at the previously calculated minimally toxic concentration (detailed in Section 4.4.1), or mock treated with DMSO, for 24 h prior to staining 33 $\mu g.ml^{-1}$ neutral red in DMEM for 2 h. Cells were washed in PBS and imaged with an inverted phase contrast microscope (Olympus CKX41). For all three compounds the cytoplasmic inclusions appeared red following neutral red staining suggesting the inclusions were likely dilated endosomes / lysosomes.

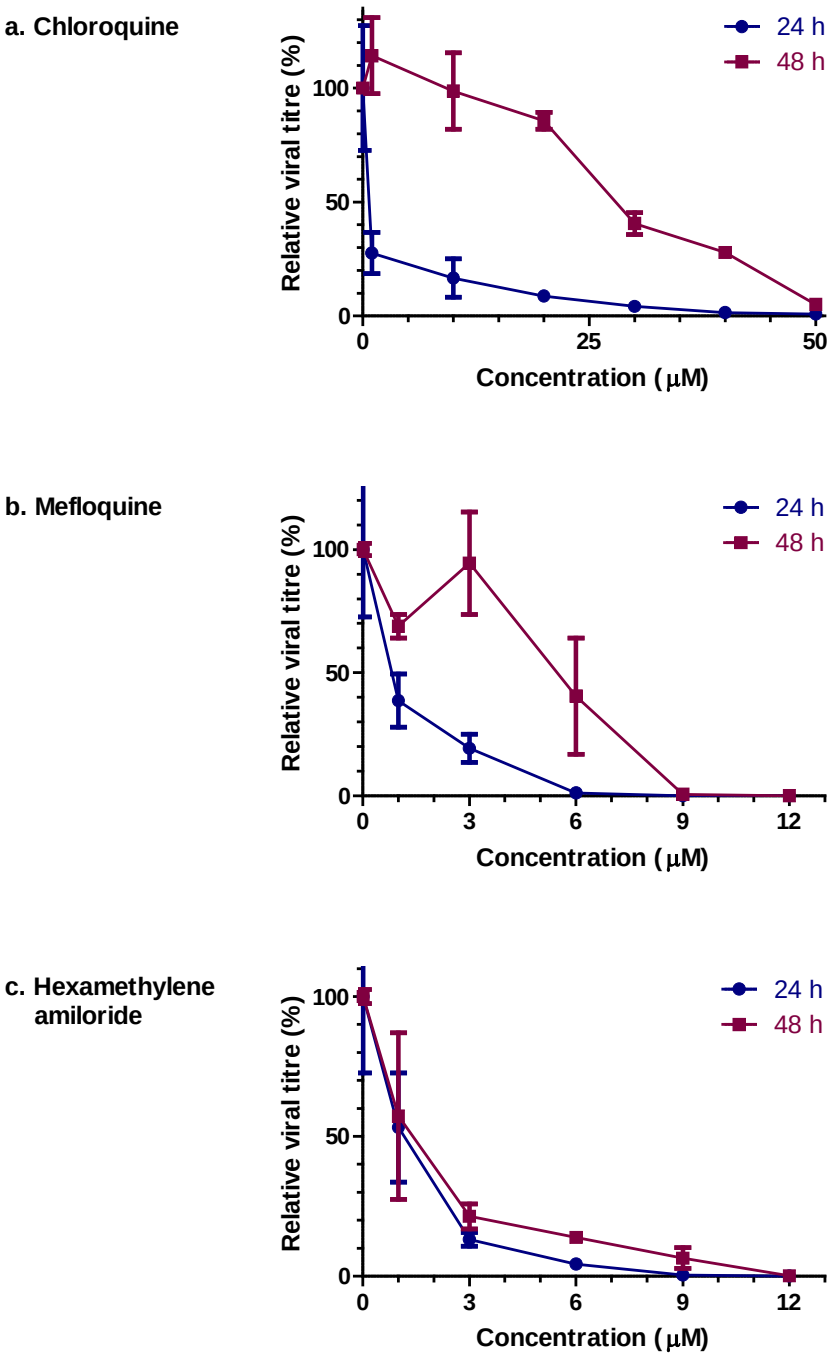

Figure 4.7: Results of virus yield reduction assay for chloroquine, mefloquine, and hexamethylene amiloride. Cells were pre-treated with various dilutions of compounds for 1 h prior to infection with FCoV FIPV1146 at MOI 0.1. Extracellular virus titres were calculated at 24 (blue circles) and 48 hpi (red squares) with a TCID50 end point assay. Titre of untreated control is defined as 100%. Each treatment was performed in triplicate and repeated in two independent experiments. Data represent Mean ± SE.

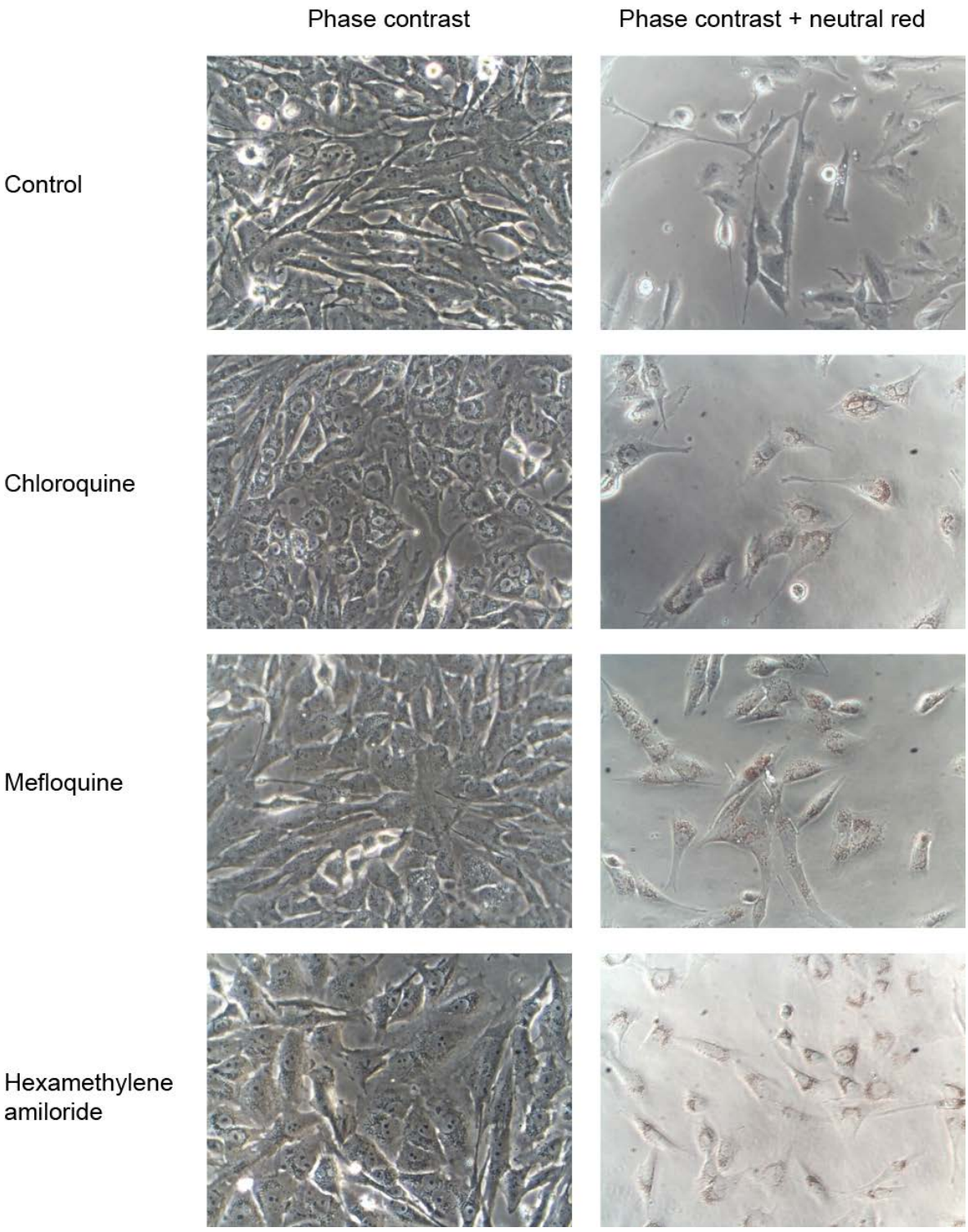

Figure 4.8: Representative micrographs of morphological changes induced by treatment with chloroquine, mefloquine, and hexamethylene amiloride. Treated cells showed increased numbers of variably sized cytoplasmic (predominantly perinuclear) inclusions which accumulated the vital dye neutral red. Images acquired at 200 x magnification.

4.4.5. Plaque reduction assay

Plaque reduction assays confirmed the findings of the CPE inhibition and virus yield reduction assays. Pre-treatment with chloroquine, mefloquine, or hexamethylene amiloride

resulted in a concentration-dependent decrease in plaque number, with high concentrations completely inhibiting macroscopic plaque formation. For all compounds plaque morphology was similar between treated and untreated wells however plaque size was smaller in treated versus untreated wells as shown in Figure 4.9. The calculated IC50 and SI values are shown in Table 4.4.

Table 4.4: IC50 and SI for chloroquine, mefloquine, and hexamethylene amiloride using plaque reduction assay. IC50 values given with 95% confidence intervals.

Compound	IC50 (μM)	SI
Chloroquine	2.58 (1.96-3.31)	31.90
Mefloquine	2.30 (1.98-2.68)	6.58
Hexamethylene amiloride	2.90 (2.49-3.37)	9.14

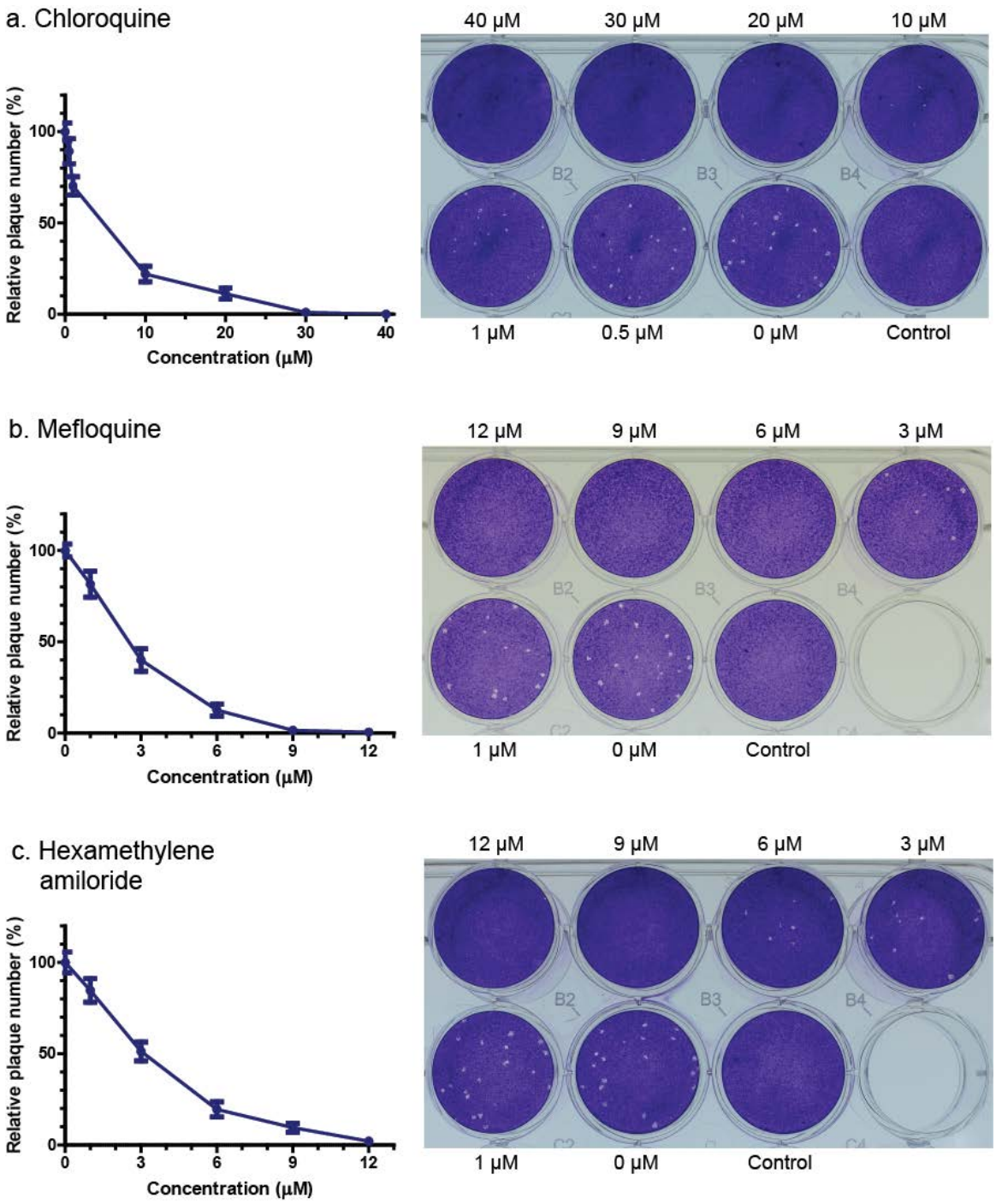

Figure 4.9: FCoV plaque reduction assays for chloroquine, mefloquine, and hexamethylene amiloride. Cells were pre-treated with various concentrations of compounds for 1 h prior to infection with approximately 30 pfu.well^{-1} FCoV FIPV1146. Virus was allowed to adsorb for 90 min and the cells overlaid with culture media containing 0.9% CMC and an equivalent concentration of test compounds. Cells were fixed and stained 48 hpi and plaques manually counted. Data expressed relative to plaque number of untreated control. Each treatment was performed in duplicate and repeated in three independent experiments. Data represents Mean ± SE.

4.4.6. Virucidal suspension assay

Virucidal properties of selected compounds were tested by incubating FCoV FIPV1146 with compounds for 1 h prior to titration of residual infectivity by plaque assay. Serial dilution of the virus-compound suspension prior to infection resulted in exposure of the test cells to the compounds at concentrations greater than 4 $\log_{10}$ lower than that previously demonstrated to have no effect. As shown in Figure 4.10, no virucidal effects were seen for chloroquine, mefloquine, or hexamethylene amiloride, with the infectivity of virus suspensions exposed to the compounds not significantly different from virus incubated with media alone.

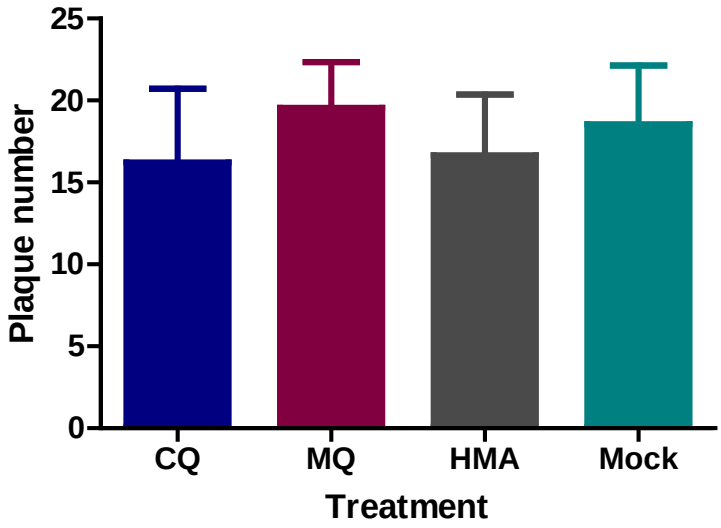

Figure 4.10: Virucidal suspension assay for chloroquine, mefloquine, and hexamethylene amiloride. FCoV FIPV1146 was exposed to chloroquine (CQ), mefloquine (MQ), or hexamethylene amiloride (HMA) for 1 h prior to titration of residual infectivity using the standard FCoV plaque assay. Each treatment was performed in triplicate and repeated in three independent experiments. Data represent Mean ± SE.

4.4.7. Effect of time of addition

The effect of time of addition on the antiviral activity of selected compounds was assessed using a modification of the resazurin-based CPE inhibition assay and through IFA of viral protein expression. Based on the CPE inhibition assay maximum antiviral effect was seen when compounds were added prior to or concurrent with infection, following which there was a time-dependent reduction in CPE inhibition (Figure 4.11). For all tested compounds CPE inhibition remained greater than 50% when compounds were added at the latest tested time point of 6 h post infection.

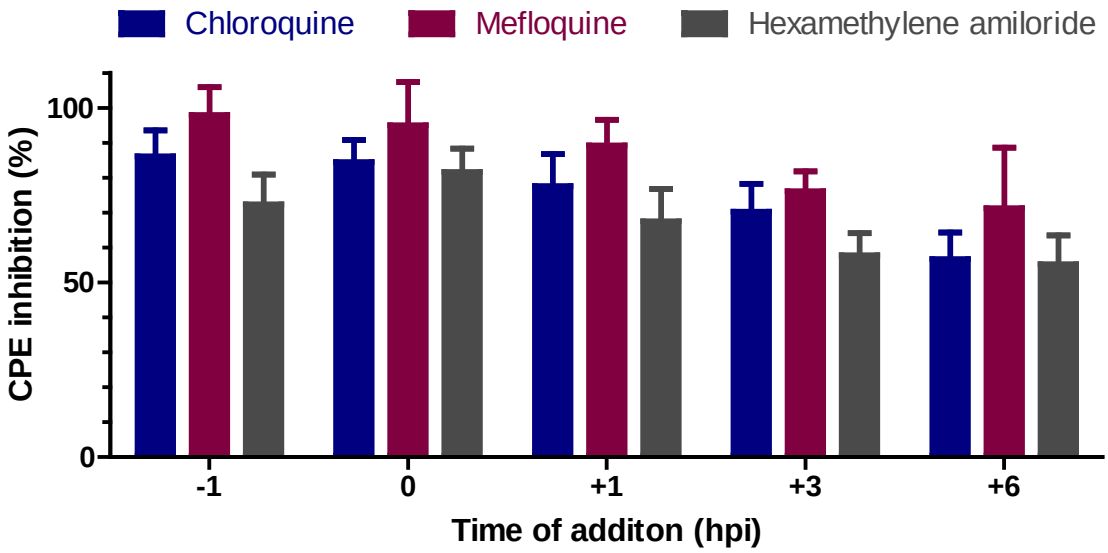

Figure 4.11: Effect of time of addition on CPE inhibition for chloroquine, mefloquine, and hexamethylene amiloride. Compounds were added 1 h prior to infection, concurrent with infection, and 1, 3, or 6 h post infection with FCoV FIPV1146 at MOI 0.01. CPE inhibition was determined after 72 hpi using the resazurin-based CPE inhibition assay. Each treatment was performed in triplicate and repeated in three independent experiments. Data represent Mean ± SE.

The CPE inhibition assay encompasses multiple rounds of viral replication. To further elucidate the stage of viral replication affected by test compounds a single replication cycle IFA-based assay was conducted, the results of which are shown in Figure 4.12. These results confirm that, based on viral antigen expression, all three compounds possess antiviral properties when added prior to, or at the time of infection. Furthermore all compounds displayed a time of addition dependent reduction in antiviral effect; however the extent and timing of this reduction varied.

The inhibitory effect of chloroquine was reduced, based on an increase in the percentage of FCoV antigen positive cells, when added at any time post infection. A similar result was seen for hexamethylene amiloride, although in this case a significant increase in the number of infected cells was not seen until compound addition was delayed until 1 hpi. In contrast, mefloquine remained effective when added up to 5 hpi suggesting it may act at a later stage of viral replication than chloroquine and hexamethylene amiloride.

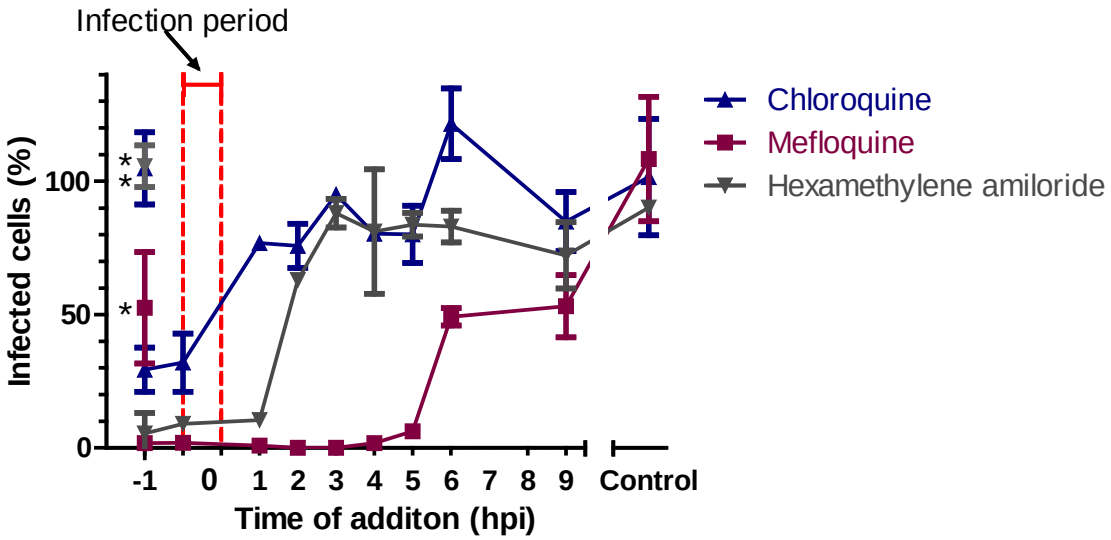

Figure 4.12: Effect of time of compound addition on viral antigen expression for chloroquine, mefloquine, and hexamethylene amiloride. Cells were treated pre-, concurrent with, or post-infection with chloroquine, mefloquine, or hexamethylene amiloride. Cells were infected with FCoV FIPV1146 at MOI 0.5. The infection period was 1 h, following which cells were washed and culture media replaced. Results represent Mean of duplicate wells ± SD. For ease of visualisation, samples treated with compounds only for the pre-infection period are not shown by connecting lines and are marked with an asterisks (*). For all other treatments the added compounds remained for the duration of the experiment.

4.4.8. Strain variation

The efficacy of the three identified candidate compounds was tested against FCoV FECV1683, a serotype II enteric biotype FCoV. Comparison of the virus control (no treatment) wells showed FCoV FIPV1146 infection resulted in more pronounced CPE over the 72 h infection period compared to FCoV FECV1683. As shown in Figure 4.13, pre-treatment with chloroquine, mefloquine, or hexamethylene amiloride provided a degree of protection against strain FCoV FECV1683. Pre-treatment with hexamethylene amiloride provided protection against virus induced CPE that was similar for the two strains, with a reduction in CPE of 89.5% and 86.0% for FCoV FIPV1146 and FECV1683 respectively. Both chloroquine and mefloquine however were more effective against FCoV FIPV1146 than FECV1683, with CPE inhibition for chloroquine of 76.9% for versus 63.8%, and for mefloquine 79.0% versus 67.5% for strains FIPV1146 and FECV1683 respectively.

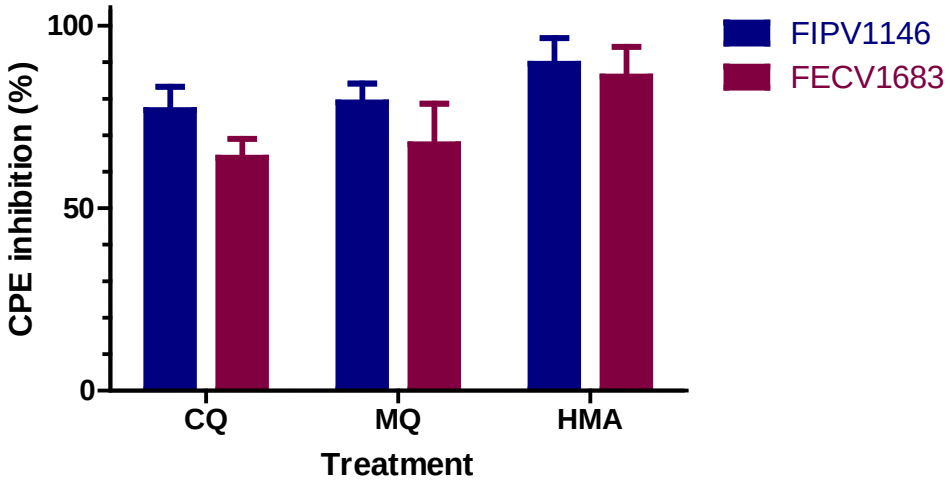

Figure 4.13: Efficacy of chloroquine, mefloquine, and hexamethylene amiloride against FCoV FIPV1146 and FECV1683. Cells were pre-treated with compounds for 1 h prior to infection at MOI 0.01. Antiviral efficacy was determined 72 hpi using the resazurin-based CPE inhibition assay. Each treatment was performed in triplicate and repeated in three independent experiments. Data represent Mean ± SE.

4.5. DISCUSSION

In this study we have reported the identification of three compounds demonstrating a marked inhibitory effect on FCoV replication *in vitro*. These compounds, chloroquine, mefloquine, and hexamethylene amiloride demonstrated significant reductions in virus induced CPE and viral titres at low micromolar concentrations when present during the early stages of viral replication. Given these *in vitro* findings, the *in vivo* use of these compounds for the treatment of FIP warrants further consideration and research.

In this study a directed antiviral screening approach was utilised, with compounds selected for inclusion based on previously demonstrated *in vitro* antiviral efficacy against other coronaviruses or, in a few cases, RNA viruses from other families. The screening strategy employed was to initially identify a suitable minimally-toxic test concentration for each compound based on cytotoxicity screening. This approach, practical in this case due to the relatively small number of tested compounds, has the benefit of minimising false negative results due to testing effective compounds at either cytotoxic concentrations or concentrations significantly below their therapeutic range. Pre-test cytotoxicity screening and the optimisation of individual test concentrations like this is impractical for modern high throughput screening methodologies that can test chemical libraries containing millions of compounds (Macarron et al., 2011). In these situations compounds are typically tested at a fixed concentration, commonly 10 µM. Of the compounds tested in this study, seven were

tested at concentrations less than 10 μM, six tested at 10 μM, and five tested at concentrations greater than 10 μM. Thus the optimum test concentration for two thirds of the compounds used in this study was different than that typically used in screening experiments confirming this as a useful approach. This enabled an accurate calculation of the optimal antiviral effect of all compounds to be determined during initial screening.

Extended duration cytotoxicity screening was performed on actively replicating cells in order to identify and exclude compounds that are both cytotoxic and/or cytostatic. Screening was performed using sequential resazurin- and SRB-based assays which provided the opportunity for orthogonal testing on the same samples. A multiparametric approach to cytotoxicity testing has been recommended to overcome some of the inherent limitations of individual assay formats, and may inform the mechanism of toxicity of tested compounds (Niles et al., 2009). In general there was good agreement between the cytotoxicity concentration-response curves generated using the two assays for all compounds tested. For several compounds (hesperidin, chloroquine) an increase in cell viability at sub-toxic concentrations was noted with the resazurin-based assay that was not reflected in the SRB-based assay. Concentration-response relationships like this, characterised by stimulation at low-concentrations and inhibition at high-concentrations, are known as hormetic responses (Calabrese, 2008), and may reflect a compensatory increase in cellular metabolism at sub-toxic concentrations.

The antiviral screening assay identified three compounds demonstrating marked inhibition of virus induced CPE: chloroquine, mefloquine, and hexamethylene amiloride, the molecular structures of which are shown in Figure 4.14. Two compounds, glycyrrhizic acid and cinanserin, demonstrated mild inhibition of CPE in the screening assay, and may warrant further investigation either in their native form, or as the basis for designing structural analogues, however these avenues were not pursued in this study. Interestingly, two compounds included in the screen, ribavirin (Barlough and Scott, 1990; Weiss and Oostrom-Ram, 1989) and rFeINF-ω (Mochizuki et al., 1994; Truyen et al., 2002), which had previously demonstrated *in vitro* efficacy against FCoV, failed to demonstrate significant inhibition of CPE in the current study. In both cases the lack of antiviral effect was most likely due to testing at concentrations below the therapeutic range for these compounds.

Additional testing of highly effective compounds identified during screening, using different assay formats and endpoints, confirmed their antiviral effects when used at low micromolar concentrations. The IC50 value, and corresponding selectivity index, for each compound varied with the assay method utilised. This is not unexpected given the assays measured different endpoints, and has been reported for other antiviral drugs such as the retroviral protease inhibitor saquinavir where the reported IC50 calculated based on production of viral

p24 antigen is approximately 30-fold lower than that based on production of mature virions (Buss and Cammack, 2001). Similarly, variation in assay conditions can result in the calculation of significantly different IC50 values, as demonstrated by Keyaerts et al. (2004) in a study on the efficacy of chloroquine against SARS-CoV. Using a PCR-based virus yield reduction assay, the concentration-response curve was shifted considerably to the right, with a corresponding increase in the IC50 value, when efficacy was determined 72 hpi compared to 24 hpi. A similar finding was noted in the current study, with differences in potency reported with the TCID50 based virus yield reduction assay performed at 24 and 48 hpi. For chloroquine and mefloquine there was a 76- and 7-fold reduction in the reported potency, respectively, between these time points. Interestingly, there was no significant difference in the potency of hexamethylene amiloride between the two time points which may suggest a prolonged duration of action for this compound.

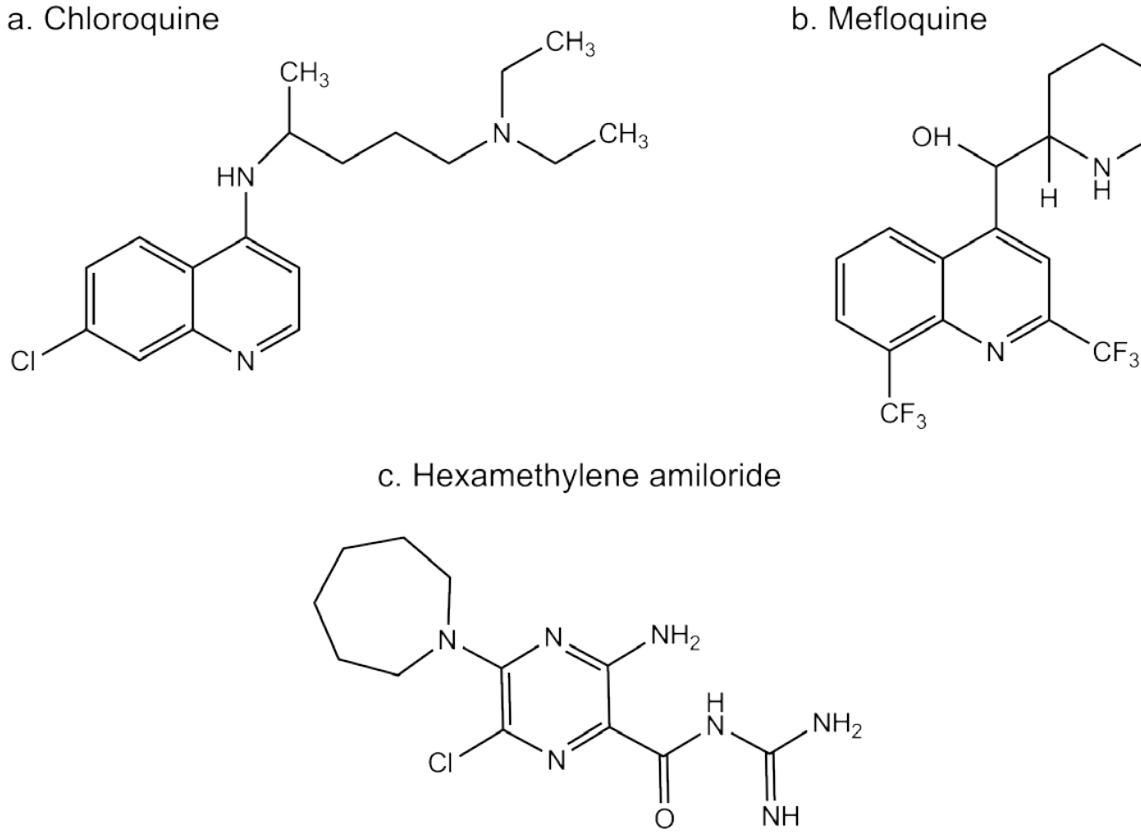

Figure 4.14: Chemical structures of effective compounds identified during primary antiviral screening: (a) chloroquine, (b) mefloquine, and (c) hexamethylene amiloride (Sigma-Aldrich).

It is interesting to note that all three compounds showing marked antiviral efficacy against FCoV in this study resulted in similar morphological changes in cells treated at sub-toxic concentrations. The presence of increased numbers of variably size cytoplasmic inclusions that accumulate the viral dye neutral red suggests the compounds resulted in perturbation of the normal endocytic pathway in CRFK cells. Alterations in the endocytic pathway have

previously been reported for chloroquine (Dean et al., 1984), mefloquine (Labro and Babin-Chevaye, 1988), and for amiloride and some of its derivatives (Dutta and Donaldson, 2012). These data suggests a common physiological effect on treated cells for all three candidate antivirals and possibly a shared mechanism of action. Viruses are known to usurp a variety of host endocytic pathways for cell entry and intracellular movement (Marsh and Helenius, 2006) and inhibition of these pathways may be a useful therapeutic approach. Although targeting a cellular pathway may be associated with an increased risk of toxicity, if that pathway is critical for viral replication this approach may have the benefit of slowing or limiting the development of resistance. This has been demonstrated for the compound niclosamide, which by neutralising endosomal pH, has been shown to be effective against a number of pH dependent viruses (Jurgeit et al., 2012). In a study by Jurgeit et al. (2012), serial passage of human rhinovirus, a picornavirus, through cells treated with various concentrations of niclosamide showed no evidence of escape mutants. In contrast, other anti-picornavirus compounds targeted at viral proteins, particularly structural proteins, rapidly select for drug resistance due to the high mutation rate of these RNA viruses (Thibaut et al., 2012).

Time of addition studies demonstrated all compounds were most effective when added prior to infection, suggesting a mechanism of action involving early stages of viral replication. The CPE inhibition based time of addition assay involved infection at low MOI with a 72 h infection period, allowing for multiple rounds of viral replication. As a result of this, even with the delayed addition of compounds, cells uninfected by the original inoculum are effectively pre-treated prior to challenge with progeny virions produced during the primary replication cycle. Using an IFA-based time of addition study involving a single replication cycle we were able to further clarify the effect of time of addition, and refine the possible stage of the viral life cycle targeted by each compound. Based on the IFA results chloroquine was effective only if present at the time of infection, while hexamethylene amiloride and mefloquine provided significant antiviral effects when compound addition was delayed for up to 1 and 5 hpi respectively. An IFA-based assay was selected to further investigate the effect of time of addition in this study, as the results of earlier CPE-based experiments suggested all compounds acted early in the replicative cycle. A limitation of this approach is that the anti-FCoV antibody (clone CCV2-2) used in this study targets viral nucleocapsid protein (Poncelet et al., 2008) and therefore compounds acting at times after the translation of N protein would appear ineffective using this single-cycle assay. Similarly, it is also possible that mefloquine may remain active when added more than five hours post infection. This seems unlikely given the results of the CPE-based time of addition assay, however the use of alternative assays involving quantification of extracellular viral titres could help to clarify this matter. For chloroquine and hexamethylene amiloride, pre-treatment and removal of the compound prior

to infection resulted in no inhibitory effect on viral replication, however under these same conditions mefloquine remained partly efficacious. This may be due to the strong binding or accumulation of mefloquine within CRFK cells resulting in a therapeutic concentration of the compound remaining despite multiple washing steps. Virucidal suspension assays showed no evidence of inactivation of virions by any of the compounds, confirming their effects were due to limiting viral replication. Taken together these data suggest that despite a likely common effect on components of endocytic pathway in CFRK cells, the nature and consequences of this effect and its result on viral replication may be different for each compound. Alternatively, different or additional antiviral mechanisms may account for the observed antiviral activity, and will be discussed in further detail for each compound.

4.5.1. Chloroquine

Chloroquine (Figure 4.14a.) is a 4-aminoquinoline used prophylactically and therapeutically as an antimalarial since 1946 (Jensen and Mehlhorn, 2009). In addition, chloroquine has long been known to possess anti-inflammatory and antiviral properties (Inglot, 1969; Shimizu et al., 1972). The antiviral effects of chloroquine are broad spectrum, with *in vitro* inhibition demonstrated against a range of diverse viruses including influenza A virus (Ooi et al., 2006), HIV (Savarino et al., 2001), HCV (Mizui et al., 2010), and a number of coronaviruses including SARS-CoV (Keyaerts et al., 2004), HCoV OC43 (Keyaerts et al., 2009), and FCoV (Takano et al., 2008a; Takano et al., 2013). Despite good *in vitro* efficacy, the results of *in vivo* studies on antiviral efficacy have in general been poor, and in some cases contradictory. Chloroquine showed no positive effect in ferret and mouse models of influenza A virus infection (Vigerust and McCullers, 2007) and was ineffective at preventing influenza infection in humans in a randomised, double-blind, placebo controlled trial (Paton et al., 2011). Similarly, antiviral efficacy was poor in animal models of Hendra and Nipah virus infection (Freiberg et al., 2010), and human studies of chikungunya virus (Lamballerie et al., 2008) and dengue virus infection (Tricou et al., 2010). Positive *in vivo* results of chloroquine as an antiviral agent have however been demonstrated in newborn mice infected with HCoV OC43 (Keyaerts et al., 2009) and, in a paper published following the conclusion of the experimental studies reported in this thesis, in cats infected with highly virulent FCoV FIPV1146, where chloroquine treatment was associated with minor improvements in clinical scores (Takano et al., 2013). Given the multiple physiological effects of chloroquine, a careful analysis of *in vivo* data is required to determine whether reported therapeutic benefits can be ascribed to its antiviral properties or to its immunomodulatory effects.

Several mechanisms have been proposed to account for the antiviral effects of chloroquine, including inhibition of glycosylation of viral proteins (Savarino et al., 2004) or cellular receptors for viral attachment (Vincent et al., 2005), inhibition of glycoprotein expression

(Dille and Johnson, 1982), or inhibition of endosome mediated viral entry (Savarino et al., 2003). Many of these mechanisms likely stem from the property of chloroquine, as a weak base, to accumulate within compartments of the endocytic pathway. The accumulation of lysosomotropic agents such as chloroquine within endocytic vesicles results in increased intravesicular pH (Ohkuma and Poole, 1978). Many viruses that enter via endocytosis require a low pH environment to trigger membrane fusion/penetration (Grove and Marsh, 2011). Although feline coronavirus is known to enter cells via receptor mediated endocytosis (Van Hamme et al., 2007), there is conflicting information regarding the pH dependency of cell entry. Takano et al. (2008a) reported concentration-dependent inhibition of FCoV type II (strain FIPV1146) in feline alveolar macrophages and monocytes by lysosomotropic agents (chloroquine and ammonium chloride) suggesting a pH dependent mechanism of entry. In contrast, Regan et al. (2008b) reported differential pH dependency for type II strains, with entry of FECV1683 highly pH dependent while strain FIPV1146 was only partially dependent on pH in the three continuous cell lines tested. This study also showed that the two strains differed in the use of cellular proteases during cell entry, with FCoV FECV1683 dependent on both cathepsin B and L in addition to an acidic environment, while FIPV1146 was dependent only on cathepsin B. This is interesting given the proposed antiviral mechanism of action of chloroquine against Hendra and Nipah viruses is through inhibition of cathepsin L (Porotto et al., 2009). Based on viral antigen expression we have demonstrated that treatment with chloroquine is associated with an inhibition of viral replication only when the compound is present at the earliest stages of viral replication. These results support the hypothesis that chloroquine acts during cell entry for FCoV FIPV1146, possibly through inhibition of endosomal pH, supporting the findings of Takano et al. (2008a). With these results it is important to differentiate effects at a single cell level from those in an animal when considering the potential therapeutic use of chloroquine. For a single cell chloroquine is effective as an antiviral only when present prior to infection, however this does not necessarily limit its *in vivo* efficacy to prophylactic use. In an infected animal at any time, only a proportion of susceptible cells are infected, thus the therapeutic use of chloroquine, even after the development of clinical signs, could still act to preventing further viral spread and infection. Clearance of already infected cells in this case would require a functional immune response, which given the lymphopaenia and immune dysregulation seen in FIP may potentially be difficult, and is another reason why combination therapy with antiviral and immunomodulatory drugs will provide the best chance for a successful therapeutic outcome in FIP.

In addition to its antiviral effects against FCoV, the anti-inflammatory properties of chloroquine may also provide therapeutic benefits in the treatment of FIP given that the disease is associated with significant immune dysregulation (Perlman and Dandekar, 2005).

Increased TNF-α appears to be central to the pathogenesis of FIP, with increased TNF-α produced by infected macrophages thought to be responsible for lymphocyte apoptosis and the resulting lymphoid depletion and lymphopaenia (Dean et al., 2003; Takano et al., 2007a). The anti-inflammatory properties of chloroquine arise in part due to antagonism of TNF-α, with reduction in both TNF-α production and a decrease in TNF-α receptor expression resulting in an impairment of TNF signalling (Savarino et al., 2003). A reduction in TNF-α production has been documented in chloroquine treated FCoV-infected feline monocytes and in cats with FIP (Takano et al., 2013). In both of these cases, reductions in TNF-α were associated with decreased virus replication as determined by extracellular viral titres and viral N gene expression respectively. From these studies it is unclear whether reductions in TNF-α are a direct result of the anti-inflammatory effect of chloroquine or secondary to its antiviral actions resulting in reduced viral replication and subsequent reduced TNF-α production from virus infected cells. Similarly, the apparent *in vivo* antiviral actions of chloroquine may stem from its antagonism of TNF-α resulting in less pronounced lymphopaenia, leading to enhanced immune control of viral replication. Further, as TNF-α has been shown to increase the expression of fAPN, a viral receptor for type II FCoV (Takano et al., 2007b), it is possible inhibition of TNF-α by chloroquine may have indirect antiviral effects via an alteration of fAPN expression. Chloroquine treatment of Vero cells has been shown to impair terminal glycosylation of ACE2, the cellular receptor for SARS-CoV, and it has been suggested that the antiviral effects of chloroquine against this virus may in part be due to a reduced affinity between the viral spike protein and the modified surface expressed ACE2 (Vincent et al., 2005). Alteration of APN glycosylation has been demonstrated to be an important determinant of cell tropism and viral entry for viruses in the genus *Alphacoronavirus* (Wentworth and Holmes, 2001), and thus it is possible that chloroquine induced alterations in fAPN glycosylation may play a role in the antiviral effect demonstrated against type II FCoV. Whilst fAPN has been demonstrated as the major receptor for type II FCoV in CRFK cells, in a study examining entry of type II FCoV into monocytes cells only 60% of bound virus co-localised with this receptor, suggesting the involvement of an alternative receptor on the primary target cells (Van Hamme et al., 2011). Thus if alterations in fAPN glycosylation were responsible for the anti-FCoV effect of chloroquine, it would be expected antiviral efficacy in monocytes would be lower than that in cell lines in which fAPN the sole receptor. Supporting this idea, the *in vitro* studies by Takano et al. (2013) demonstrated reduced antiviral potency of chloroquine in monocytes compared with Fcwf-4 cells, a cell line which type II FCoV entry is thought to be almost entirely due to binding fAPN (Hohdatsu et al., 1998). It should be noted if alterations in fAPN glycosylation were an important antiviral mechanism of chloroquine, the compound may be completely ineffective against the more prevalent type I FCoV, as fAPN is thought not to play a significant role in the entry of these viruses (Van Hamme et al., 2011).

In the current study we report the IC50 of chloroquine as 0.38 µM based on reduction in extracellular viral titre at 24 hpi and 16.63 µM based on CPE inhibition, similar in magnitude to inhibitory concentration reported for other coronaviruses. The IC50 concentration for SARS-CoV was reported as 8.8 µM based on CPE inhibition assay (Keyaerts et al., 2004), and against HCoV-OC43 of 0.306 µM based on reductions in viral genome copies (Keyaerts et al., 2009). To be an effective clinical antiviral, compound pharmacokinetics must allow an inhibitory concentration to be achieved at the site of infection and, in most cases, within target cells. As a human approved pharmaceutical there is significant data on the pharmacokinetics of chloroquine in multiple species, however there are no published pharmacokinetic studies of chloroquine in the cat, despite several reports of its use in this species. In studies to assess the toxic effect of chloroquine on the retina in a feline model, Gregory et al. (1970) reported using doses of 50 $mg.kg^{-1}$ (dose frequency not reported) for 2 years in cats without documenting any ill effects, while Kuhn et al. (1981) reported a dose of 25 $mg.kg^{-1}$ five days per week resulted in the death of six study cats after 33 to 39 weeks of treatment. In the latter study, a reduction of the daily dose to 20 $mg.kg^{-1}$ resulted in the survival of all remaining cats. Unfortunately, detailed monitoring of clinical, haematological, or biochemical parameters of treated cats was not reported in either of these studies, so it is possible, and perhaps likely given the known toxicological profile of chloroquine (Taylor and White, 2004), that although the reported doses were not lethal, they may have been associated with significant adverse effects in treated cats. In the recent small scale trial by Takano et al. (2013) a lower dose of 10 $mg.kg^{-1}$ was given subcutaneously every three days. Significant detail regarding the acceptability of this treatment or the nature of possible side effects was not provided, except to state without qualification that when "*the chloroquine concentration is increased a severe side effect may be induced*". If chloroquine toxicity in cats is similar to humans the above statement is not surprising as although chloroquine is generally a well-tolerated drug in humans it has a narrow therapeutic index, with lethal acute toxicosis reported with doses of only 30 $mg.kg^{-1}$, compared to the reported therapeutic dose of 25 $mg.kg^{-1}$ (total) divided over three days and the lower dose of 5 $mg.kg^{-1}$ once weekly used prophylactically (Taylor and White, 2004).

In the absence of feline pharmacokinetic studies, data from other species must be extrapolated to the feline patient, an exercise fraught with danger (Court, 2013). Peak plasma concentrations for chloroquine in humans following a single oral dose are reported to be approximately 1 µM (Mackenzie, 1983; Pussard and Verdier, 1994), which is higher than the IC50 value determined in this study based on extracellular viral titre at 24 hpi. In all species studied however, chloroquine has a large volume of distribution with extensive tissue accumulation (Moore et al., 2011). In rats and monkeys chloroquine has been shown to accumulate in leukocytes, and in *in vitro* studies with isolated human leucocytes drug

accumulation was highest in monocytes (French et al., 1987). Drug concentration in leukocytes may be two orders of magnitude greater than plasma concentration (Mackenzie, 1983) and thus therapeutic concentrations may be attained in the target cells of virulent biotype FCoVs at relatively low plasma concentrations, minimising the risk of dose-dependent adverse effects.

4.5.2. Mefloquine

Mefloquine (Figure 4.14b.) is a synthetic analogue of quinine, a naturally occurring antimalarial compound found in the bark of the cinchona tree. Initially synthesised during the Vietnam War as part of a large scale antimalarial development campaign conducted by the US Army, mefloquine became commercially available under the trade name Lariam in 1989 (Croft, 2007). It has since been used widely for malaria treatment and prophylaxis. In addition to its potent schizonticidal effects, *in vitro* antiviral effects of mefloquine have been reported against HIV (Owen et al., 2005) and against JC virus (Brickelmaier et al., 2009), a polyomavirus responsible for progressive multifocal leukoencephalopathy (PML) in immunosuppressed humans. No studies examining the effectiveness of mefloquine against coronaviruses have been reported. *In vivo* data on the use of mefloquine as an antiviral agent is limited. Adachi et al. (2012) described a single case report in which mefloquine and antiretroviral therapy resulted in resolution of clinical signs in an AIDS patient with PML, however a small multicentre controlled study failed to confirm this finding, with mefloquine demonstrating no antiviral activity against JC virus in PML patients, as determined by CSF viral loads, nor any positive effects on clinical or laboratory parameters in treated patients compared to controls (Clifford et al., 2013). The reason for the lack of *in vivo* antiviral effects in this study is not known, however the authors suggest it was not due to an inability to achieve therapeutic concentrations in target tissue, as brain mefloquine concentration determined in one patient post mortem was more than 20 times the *in vitro* IC50 reported by Brickelmaier et al. (2009). Nor is it likely that the *in vitro* effect was an artefact as a result of the use of non-representative cell lines or viruses, as antiviral efficacy was demonstrated in multiple cell types, including primary target cells against multiple viral strains.

The antiviral mechanism of action of mefloquine demonstrated *in vitro* is not known, nor is it clear whether the effects demonstrated against viruses with such different lifecycles (from two different Baltimore groups) is due to different mechanisms of action, or represents a single broad-spectrum effect. From an analysis of structure-activity relationships Brickelmaier et al. (2009) suggest that the antiviral activity of mefloquine may be due in part to its function as an adenosine mimetic based on it having a similar 3D conformation to several known adenosine analogues with demonstrated anti-JC virus activity. Adenosine analogues have previously shown no significant antiviral activity against SARS-CoV,

suggesting coronaviruses may not be susceptible to compounds acting via this mechanism (Barnard et al., 2004) Alternatively, as a lysosomotropic agent (Glaumann et al., 1992), the mechanism of inhibition may be though interference with normal endocytic pathways required for viral replication. In the current study the single cycle time of addition assay showed that mefloquine remained effective when added as late as 5 hpi suggesting, if antiviral effects arise through perturbation of endosomal function, the effect occurs after viral entry and uncoating. An effect post viral entry for JC virus was reported by Brickelmaier et al. (2009), as a delay in compound addition to of up to 24 h was not associated with decreased efficacy. Antivirals that act at post-entry steps may be more clinically useful, as they are effective against established infections in cells rather than just preventing new cells being infected, as occurs with agents acting only during virus entry.

There are no published pharmacokinetic data on the use of mefloquine in cats or any reports of its use in this species. In humans plasma concentrations of approximately 4 μM have been reported using prophylactic dosing regimens (Kollaritsch et al., 2000), while at the higher therapeutic doses plasma concentrations up to 23 μM may be achieved (Simpson et al., 1999). The compound is highly lipophilic with wide tissue distribution (Karbwang and White, 1990). Due to is long half-life, lipophilic nature, and its inhibition of P-glycoprotein 1 (Riffkin et al., 1996), mefloquine is known to concentrate within the brain parenchyma, with tissue concentrations of up to 50 μM reported (Jones et al., 1994; Pham et al., 1999). Mefloquine may therefore be particularly useful in the treatment of dry (non-effusive) FIP, where CNS lesions are common (Pedersen, 2009). Combined, these data show that in species for which the pharmacokinetics of mefloquine have been studied it is possible to obtain drug concentrations in blood approximating the *in vitro* IC50 of FCoV, and more importantly concentrations in excess of the IC50 in tissues.

4.5.3. Hexamethylene amiloride

Hexamethylene amiloride (HMA) [5-(N,N-hexamethylene amiloride)] (Figure 4.14c.) is a derivative of the potassium sparing diuretic amiloride, and like its parent compound, hexamethylene amiloride inhibits a variety of cellular sodium transport mechanisms (Kleyman and Cragoe, 1988). Amiloride and its derivatives have also demonstrated antiviral effects against a range of viruses from multiple viral families including canine parvovirus (Suikkanen et al., 2003), coxsackievirus B3 (Harrison et al., 2008), HIV (Ewart et al., 2004), FCV (Stuart and Brown, 2006), and a number of coronaviruses including SARS-COV, MHV, and HCoV-229E (Wilson et al., 2006a).

A variety of mechanisms have been suggested to account for the antiviral properties of amiloride and its derivatives, and it may be given the diverse range of viruses affected, that the nature of the antiviral effects are virus dependent. Antiviral effects against members of

the family *Picornaviridae* have been ascribed to inhibition of viral RNA replication by competitive inhibition of the viral RNA polymerase [coxsackievirus B3] (Gazina et al., 2011; Harrison et al., 2008), inhibition of viral release through an unknown mechanism [human rhinovirus 2] (Gazina et al., 2005), and via an indirect mutagenic effect [coxsackievirus B3] (Levi et al., 2010). Whilst this later effect is interesting, the susceptibility of coronaviruses to lethal mutagenesis is unclear given they appear relatively refractory to the effects of RNA mutagens, most likely through the actions of the virus encoded 3′-to-5′ exoribonuclease in maintaining replicative fidelity (Smith et al., 2013). An antiviral effect of amiloride derivatives due to interference with virus encoded ion channels, or viroporins, has been demonstrated for a number of viruses. In planar lipid bilayer studies amiloride derivatives have demonstrated antagonism of isolated HCV p7 (Premkumar et al., 2004), HIV Vpu (Ewart et al., 2004), and coronavirus E protein viroporins (Wilson et al., 2006a, b), and for the latter two this has been demonstrated to be associated with antiviral effects in cell culture. Conformation of the E protein as the target for antiviral effects in culture was demonstrated against the coronavirus MHV by showing the antiviral effect is abrogated against recombinant MHV with the E protein ORF deleted (Wilson et al., 2006a). While viroporin activity has not been demonstrated for the FCoV E protein, it has been shown to function as an ion channel for representative *Alpha*-, *Beta*-, and *Gammacoronaviruses* (Wang et al., 2011). The E protein is thought to be involved in virion assembly and release (Ye and Hogue, 2007), however the role of the ion channel, and the mechanism, if any, by which it mediates this is not clear. If the E protein viroporin plays a role in viral morphogenesis as hypothesised, the results of the current study do not support a mechanism of action of hexamethylene amiloride against FCoV involving antagonism of this ion channel, as inhibitory effects were seen only when the compound was present during the initial stages of infection, most likely during viral entry. Amiloride and it derivatives are inhibitors of macropinocytosis (Koivusalo et al., 2010), a documented route of entry for some viruses (Mercer and Helenius, 2009), and thus inhibition of this endocytic pathway may account for the observed antiviral effects, although utilisation of this pathway of entry has not been reported for coronaviruses.

Whilst amiloride is a relatively safe human approved pharmaceutical, there is very little information regarding the *in vivo* use of its more potent derivative hexamethylene amiloride. In a mouse tumour model doses of 20 $\mu g.g^{-1}$ intraperitoneally resulted in a peak plasma concentration of 8 μM (Luo and Tannock, 1994), which approximates the IC50 as determined by CPE inhibition assay, and is eight and three times greater than the IC50 values determined by virus yield reduction and plaque assays respectively. This paper does not provide any details of adverse effects related to hexamethylene amiloride treatment in mice except to state the maximum tolerable dose is approximately 30 $\mu g.g^{-1}$. The reported half-life

of hexamethylene amiloride in mice in this study was approximately 35 min, which if representative of the situation in cats could present a practical barrier to the therapeutic use of this compound given time of addition studies showed hexamethylene amiloride was only efficacious when present at an inhibitory concentration during the initial stages of the replicative cycle.

Limitations of the current study include a lack of *ex vivo* testing in primary feline cells and testing against only two FCoV isolates. FCoV FIPV1146 and FECV1683 used in this study are both type II viruses. A bias towards studies with type II FCoV is evident in the literature, despite the higher prevalence of type I strains worldwide (Benetka et al., 2004; Hohdatsu et al., 1992; Kummrow et al., 2005), due to the relative ease with which former can be grown in culture. At a genetic level the primary difference between type I and type II FCoV is within the spike protein, with the type II viruses thought to have arisen due to a recombination event with another alphacoronavirus, canine coronavirus. Using chimeric FCoVs, Tekes et al. (2010) demonstrated that the differences in the *in vitro* phenotype between type I and II FCoV is attributable solely to the spike protein. Differences in receptor usage have been demonstrated between type I and II FCoVs (Van Hamme et al., 2011) and there may be differences in virus entry steps further downstream (Regan and Whittaker, 2008; Takano et al., 2008a). As all three identified candidate compounds appear to act early in the replication cycle through an unidentified mechanism of action, it is possible that these reported antiviral effects may be unique to type II FCoV and may not extend to the more common type I viruses. In a similar vein it is possible that the mechanism of viral entry into CRFK cells as used in this study is different to that in feline monocytes, or that the latter possesses an alternate entry pathway. The presence of cell line dependent or alternative viral entry pathways is not without precedent (Aleksandrowicz et al., 2011). If this were the case for FCoV, the reported antiviral effects may not extend to provide therapeutic benefit in a clinical setting. To address some of these issues *ex vivo* testing in primary feline monocytes/macrophages against a diverse range of FCoV isolates should be conducted.

In conclusion this study has identified three compounds demonstrating marked *in vitro* inhibition of FCoV in an immortalised cell line at low micromolar concentrations. These preliminary studies open the way for further investigation and potential optimisation of these compounds as antiviral agents. Two of the effective compounds, chloroquine and mefloquine, are commercially available pharmaceuticals with an extensive body of supporting literature regarding their pharmacokinetics and safety in non-feline species. Considerably less is known about the *in vivo* effects hexamethylene amiloride; however there are reports of its application in mice. Given the current poor prognosis and dire lack of effective antivirals for FCoV, in light of the presented results, consideration should be given to a small scale clinical trial of these compounds in cats with FIP. Such a study was

published for chloroquine during the writing of this thesis and demonstrated a positive, but limited effect of treatment following experimental infection with highly virulent FCoV FIPV1146.

5

In vitro inhibition of feline coronavirus using RNA interference

Some of the content of this chapter has been published in McDonagh, P., Sheehy, P.A., and Norris, J. *In vitro* inhibition of feline coronavirus by small interfering RNA. (2011) *Veterinary Microbiology* 150 (3-4) 220-229. A copy of this paper is included as Appendix 3. This chapter includes additional results from subsequent experiments.

5.1. ABSTRACT

Infection with virulent biotypes of feline coronavirus (FCoV) can result in the development of feline infectious peritonitis (FIP), a typically fatal immune mediated disease for which there is currently no effective antiviral treatment. In this study we report on the *in vitro* efficacy of synthetic siRNA mediated RNA interference (RNAi) against a highly virulent FCoV strain in an immortalised cell line. A panel of eight siRNAs targeting four regions of the FCoV genome were screened for antiviral effects using qRT-PCR of viral messenger and genomic RNA, extracellular virus titres, and direct IFA for viral protein expression. All siRNAs demonstrated an inhibitory effect *in vitro*, with the two most effective, siRNAs L2 (targeting the leader sequence in the 5' UTR) and N1 (targeting the nucleocapsid ORF), resulting in greater than 95% reduction in viral titre. Further characterisation of these two siRNAs showed they remained effective when used at low concentrations, in cells challenged with high viral loads, and when used in combination. Serial passage of virus through siRNA treated cells highlighted one of the major challenges of RNAi-based antivirals, with a rapid acquisition of resistance due to mutations in the target site demonstrated when cells were treated with a single or a combination of two siRNAs. Treatment with three siRNAs was however able to prevent viral escape over the course of five passages. Finally, a comparison of the efficacy of canonical versus Dicer-substrate siRNAs for targets L2 and N1 showed equivalent or better potency for the latter depending on the target site. Combined, these data provide important preliminary information to inform the potential therapeutic application of antiviral RNAi against feline coronavirus.

5.2. INTRODUCTION

In 2006 Professors Andrew Fire and Craig Mello were awarded the Nobel Prize in Physiology or Medicine for "*discovering a fundamental mechanism for controlling the flow of genetic information*" (Nobelprize.org, 2006). Less than 10 years prior, the seminal work of Fire and Mello, building upon observations in plants (Napoli et al., 1990), fungi (Romano and Macino, 1992), and nematodes (Guo and Kemphues, 1995), demonstrated potent sequence specific suppression of gene expression following the introduction of double-stranded RNA (dsRNA) homologous to target genes (Fire et al., 1998). This method of gene regulation, termed RNA interference, has subsequently been shown to be a highly evolutionarily conserved mechanism, present in almost all eukaryotes (Cerutti and Casas-Mollano, 2006), and thought to have evolved initially as an immune defence against viruses and transposons (Shabalina and Koonin, 2008). In plants, insects, and worms RNAi remains an important defence mechanism, however its role in innate immunity in vertebrates remains unclear (Li et al., 2013; Maillard et al., 2013; Parameswaran et al., 2010; Sidahmed and Wilkie, 2010; Umbach and Cullen, 2009). The triggering substrate of RNAi, double stranded RNA, is formed during the replication of viruses from diverse viral families (Weber et al., 2006). In organisms where RNAi functions as an antiviral defence, this long dsRNA is cleaved by the enzyme Dicer into small interfering RNAs (siRNAs), ≈ 21 nt RNA duplexes with a characteristic 2 nt 3' overhangs, which are subsequently incorporated into the RNA induced silencing complex (RISC) to direct the sequence specific cleavage of viral messenger or genomic RNA. In mammalian cells the introduction of long dsRNA, either artificially or during viral replication, primarily triggers an interferon response, resulting in a cascade of cellular events and a general shutdown in host cell protein synthesis (Jacobs and Langland, 1996). Elbashir and colleagues (2001a) demonstrated that the RNAi pathway could be harnessed in mammalian cells via the direct introduction of exogenous siRNAs without triggering an interferon response, a finding that made available important tools for basic biological research and opened up exciting avenues for therapeutic intervention.

Following its discovery, the potential of siRNA mediated RNAi as an antiviral therapeutic was quickly realised. Efficacy has been demonstrated *in vitro* against numerous pathogens from diverse viral families including human respiratory syncytial virus [*Paramyxoviridae*] (Bitko and Barik, 2001), HIV [*Retroviridae*] (Martinez et al., 2002), influenza A virus [*Orthomyxoviridae*] (Ge et al., 2003), feline herpesvirus [*Herpesviridae*] (Wilkes and Kania, 2009), Ebola virus [*Filoviridae*] (Geisbert et al., 2006), poliovirus [*Picornaviridae*] (Gitlin et al., 2002), and SARS-CoV [*Coronaviridae*] (Wu et al., 2005a). *In vivo* efficacy has also been demonstrated against a number of these, including against influenza A virus (Tompkins et al., 2004), Ebola virus (Geisbert et al., 2006), and HIV (Kumar et al., 2008).

The efficacy of RNAi against different coronaviruses has been studied *in vitro* and *in vivo*, spurred by the emergence of SARS-CoV in 2002. Using synthetic siRNAs targeted at the replicase gene, the first report of antiviral RNAi against SARS-CoV was published in November 2003 (He et al., 2003), only eight months after the identification of the new virus in patients with SARS (Drosten et al., 2003). This rapid development, facilitated by advances in molecular biology techniques that enabled researchers to completely sequence the almost 30 kb genome of the newly identified pathogen within a month of its isolation (Marra et al., 2003), highlights a major benefit of RNAi-based therapeutics in combatting emerging diseases. Subsequent studies have shown effective inhibition of SARS-CoV *in vitro* through targeting sequences encoding structural proteins (He et al., 2009), non-structural proteins (He et al., 2006), and accessory proteins (Akerstrom et al., 2007), in addition to the UTRs located at both the 5' (Li et al., 2005c) and 3' (Wu et al., 2005a) end of the genome. Successful RNAi-based inhibition has also been demonstrated *in vitro* against other coronaviruses including human coronavirus NL63 (Pyrc et al., 2006), porcine transmissible gastroenteritis virus (TGEV) (He et al., 2012; Zhou et al., 2007), and avian infectious bronchitis virus (Meng et al., 2007). There are limited reports of the *in vivo* use of RNAi against coronaviruses. The effectiveness of both prophylactic and therapeutic antiviral RNAi against SARS-CoV was demonstrated in a primate model, with treatment resulting in a reduction in viral load and associated tissue pathology (Li et al., 2005a). In mini-pigs, prophylactic treatment with anti-TGEV shRNA expressing plasmids demonstrated positive effects in clinical, pathological, and virological parameters following viral challenge (Zhou et al., 2010). Thus, although there are significant challenges to the clinical use of antiviral RNAi, these *in vitro* and *in vivo* studies against coronaviruses suggest this may be useful approach for FCoV.

As discussed in Chapter 1, feline coronavirus is an important pathogen of domestic cats for which there are currently no effective antiviral treatments. In this study we investigated the potential of RNAi-based therapeutics as an antiviral approach for FCoV by screening a panel of eight siRNAs targeting four different regions of the FCoV genome for antiviral effects *in vitro*. The most effective siRNAs were further characterised by examining the effect of multiplicity of infection and siRNA concentration on their efficacy. Given one of the major challenges of antiviral chemotherapy is the development of resistance, studies were conducted to determine the efficacy of combinatorial siRNA therapy and its ability to delay or prevent the emergence of resistance. Finally, we examined the effectiveness of a siRNA structural variant, Dicer-substrate siRNA, that has been reported to result in increased efficacy when compared to canonical siRNAs (Kim et al., 2005). The efficacy of canonical and Dicer-substrate siRNAs, in terms of potency and duration of inhibition, was assessed for two different FCoV targets.

5.3. MATERIALS AND METHODS

5.3.1. siRNA design

siRNAs were designed to target conserved regions of the leader sequence of the 5' UTR, and the replicase, membrane, and nucleocapsid ORFs. To identify conserved regions full- and partial-length FCoV sequences were retrieved from GenBank (accessed April 2009) and aligned using Geneious software (Version 4.6 Biomatters Ltd, Auckland, NZ) using the proprietary Geneious alignment tool with default settings. Details of the sequences are shown in Appendix 2. Prospective siRNAs targeting the visually identified conserved regions were designed using Block-iT™ RNAi designer (Invitrogen) using the consensus sequence of FCoV FIPV1146 (Accession number DQ010921). Criteria for final siRNA selection were (1) high Block-iT™ RNAi designer ranking, (2) maximum sequence homology to other reported type I and type II FCoV strains, and (3) minimum homology to known feline sequences based on a BLAST search. Using these selection criteria the two highest ranking siRNAs targeting each region were selected. A siRNA (NSC-GFP) was selected targeting green fluorescent protein mRNA to act as a non-silencing control (Tschuch et al., 2008). The 5' end of the sense strand of NSC-GFP was conjugated to fluorescein isothiocyanate (FITC) to enable transfection efficacy to be monitored with fluorescence microscopy. siRNA sequences are shown in Table 5.1 and Figure 5.1. Deprotected and desalted custom siRNAs were purchased from Sigma-Aldrich in the lyophilised form. siRNAs were resuspended in nuclease-free water (Amresco) at 20 μM and stored in single use aliquots at -20°C.

Figure 5.1: Schematic of FCoV genome based on reported sequence of FCoV FIPV1146 (Accession number DQ010921). The location of siRNAs targeting the leader sequence (L1, L2) and the replicase (R1, R2), membrane (M1, M2), and the nucleocapsid (N1, N2) ORFs are shown. E, envelope; M, membrane; N, nucleocapsid; RFS, ribosomal frameshift element; 3ab and 7abc, accessory genes; TRS, transcription regulatory sequence.

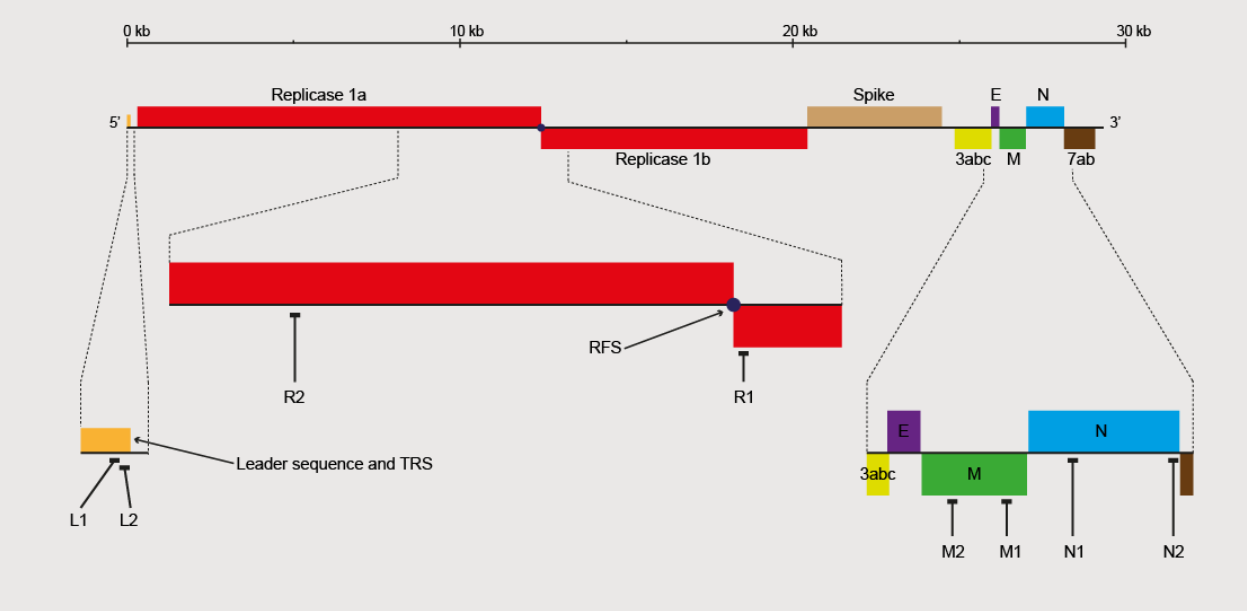

Table 5.1: Sequence of siRNAs targeting FCoV and their position in FCoV FIPV1146 genome (Accession number DQ010921). Sequence of non-silencing control siRNA (NSC-GFP) targeting GFP is also shown (Tschuch et al., 2008).

siRNA	Sequence	Position in genome
Leader1 (L1)		
Sense	5'-GCUAGAUUUGUCUUCGGACdTdT-3'	64-82
Antisense	5'-GUCCGAAGACAAAUCUAGCdTdT-3'	
Leader2 (L2)		
Sense	5'-GGACACCAACUCGAACUAAdTdT-3'	79-97
Antisense	5'-UUAGUUCGAGUUGGUGUCCdTdT-3'	
Replicase1 (R1)		
Sense	5'-GCACGUAAGGAUCUUACAAdTdT-3'	12479-12497
Antisense	5'-UUGUAAGAUCCUUACGUGCdTdT-3'	
Replicase2 (R2)		
Sense	5'-GCUGAUUACCGCAUGGCUUdTdT-3'	8673-8691
Antisense	5'-AAGCCAUGCGGUAAUCAGCdTdT-3'	
Membrane1 (M1)		
Sense	5'-CCUAGUAGAACCAUCGUUUdTdT-3'	26611-26629
Antisense	5'-AAACGAUGGUUCUACUAGGdTdT-3'	
Membrane2 (M2)		
Sense	5'-GCUGGCUCGUUUAUGGCAUdTdT-3'	26210-26228
Antisense	5'-AUGCCAUAAACGAGCCAGCdTdT-3'	
Nucleocapsid1 (N1)		
Sense	5'-GGAGUCUUCUGGGUUGCAAdTdT-3'	27112-27130
Antisense	5'-UUGCAACCCAGAAGACUCCdTdT-3'	
Nucleocapsid2 (N2)		
Sense	5'-GGCAUACACAGAUGUGUUUdTdT-3'	27885-27837
Antisense	5'-AAACACAUCUGUGUAUGCCdTdT-3'	
Non-silencing control (NSC-GFP)		
Sense	5'-[FITC] CAAGCUGACCCUGAAGUUCdTdT-3'	
Antisense	5'-GAACUUCAGGGUCAGCUUGdTdT-3'	

5.3.2. Screening of siRNAs

An initial screening experiment was conducted to identify siRNAs with an inhibitory effect on FCoV replication. Cells were forward transfected (or mock transfected) in 12-well plates (Corning) using 100 nM siRNA as described in Section 2.4.1. At the end of the transfection period cells were infected with FIPV1146 at a MOI of 0.2 for 60 min following which the viral inoculum was replaced with fresh DMEM-10. As controls, untreated cells (infected and mock infected), cells treated with transfection reagents without siRNAs (Lipo), and cells transfected with an irrelevant non-silencing control siRNA (NSC-GFP) were included. Cells were incubated at 37°C in 5% CO_2 in air. At 24 hpi efficacy was determined by qRT-PCR of intracellular viral RNA (detecting viral genomic and membrane (M) and nucleocapsid (N) mRNA) (Section 2.4.2), TCID50 infectivity assay of extracellular virus (Section 2.3.1.2.2), and direct IFA staining for viral antigen in cells grown on glass coverslips (Section 2.5.2). Additional wells were monitored for virus induced CPE out to 50 hpi using an Olympus CKX41 inverted phase contrast microscope with attached Moticam 2300 digital camera (Motic, Causeway Bay, Hong Kong). All treatments were performed in triplicate and repeated in three independent experiments. Relative viral titres and copy numbers were calculated by dividing individual treatment values by the mean of the untreated samples. Data represent Mean ± SE.

5.3.3. Titration of effective siRNAs

To assess the effect of siRNA concentration on viral replication a concentration-response study was conducted using highly effective anti-FCoV siRNAs (defined as those showing > 80% reduction in viral genome copies and extracellular virus titre) identified in the screening study. Transfection and infection conditions were identical to those of the screening experiment (Section 5.3.2) with the exception that siRNA concentration was varied from 200 nM to 5 nM. Efficacy was determined by TCID50 assay of extracellular virus as previously described (Section 2.3.1.2.2). All treatments were performed in triplicate and repeated in three independent experiments. Data represent Mean ± SE.

5.3.4. Effect of multiplicity of infection on siRNA efficacy

To assess efficacy of RNAi against high viral challenge, cells treated with highly effective siRNAs were challenged with FIPV1146 at increasing MOIs. Transfection and infection conditions were identical to those of the screening experiment (Section 5.3.2) with the exception that cells were challenged using a MOI of 0.2, 2, or 20. Preliminary experiments showed that infection of CRFK cells with FIPV1146 at high MOI was associated with significant cytopathic effect and cell loss by 24 hpi. To allow assessment of intracellular viral loads, cells were harvested at 18 hpi, prior to the development of significant CPE. Efficacy was determined at this time by measuring extracellular virus titres and intracellular viral

genome copies (Section 2.3.1.2.2 and 2.4.2 respectively). All treatments were performed in triplicate and repeated in three independent experiments. Data represent Mean ± SE.

5.3.5. Combinatorial siRNA treatment

To assess the efficacy of combination treatment CRFK cells were reverse transfected in 96-well plates (µClear ®, Greiner Bio-One) using single or a combination of multiple effective anti-FCoV siRNAs as described in Section 2.4.1. The total concentration of siRNA per treatment was held constant at 30 nM, meaning for treatment involving two, three, or four siRNAs the concentration or each siRNA was 15 nM, 10 nM, and 7.5 nM respectively. Following transfection, cells were infected with FIPV1146 at MOI 0.2 and incubated at 37°C in 5% CO_2 in air. At 36 hpi efficacy was assessed via titration of extracellular virus using the TCID50 protocol (Section 2.3.1.2.2) and by *in situ* IFA staining for viral antigen (Section 2.5.3). Image acquisition and analysis was as previously described in Section 2.5.3.2 and 2.5.3.3.

5.3.6. Viral escape from siRNA mediated inhibition

5.3.6.1. Serial passage of virus through siRNA treated cells

To investigate the ability of FCoV to evolve resistance to RNAi mediated inhibition an experiment was conducted in which virus was serially passaged in the presence of one or a combination of effective anti-FCoV siRNAs. CRFK cells were reverse transfected in 24-well plates (Sarstedt), as described Section 2.4.1, using one, or a combination two or three siRNAs, with four wells per treatment. Cells transfected with a NSC siRNA and untreated cells were included as controls. The total siRNA concentration per treatment was kept fixed at 30 nM irrespective of the number of different siRNAs used per treatment. For the first passage infection (P1) cells were infected with original stock virus (P0) at MOI 1 and wells were monitored every 8 h (beginning 24 hpi) for the development of CPE. When three or more wells of a particular treatment showed greater than 80% CPE, the culture media from all four wells was harvested, pooled, and stored at -80°C. For subsequent passages (P2 to P5) cells were transfected as described above and infected with 50 µl of culture media from identically treated cells of the previous passage which had been clarified by centrifugation at 1000 x g for 3 min. At the conclusion of the experiment all serially passaged viruses were titrated using the standard FCoV plaque assay (Section 2.3.1.2.1), and consensus sequencing performed as described in Section 2.4.3.

5.3.6.2. Phenotypic assessment of FCoV serially passaged in siRNA treated cells

An experiment was conducted to determine if mutations identified in viruses serially passaged in siRNA treated cells conferred a resistant phenotype. Cells were transfected or mock transfected in 96-well plates (µClear ®, Greiner Bio-One) (Section 2.4.1) using single

or multiple siRNAs, with a total siRNA concentration per treatment of 30 nM. At the end of the transfection period cells were infected at MOI 0.2. For each siRNA treatment (or control) duplicate wells were infected with P0 (original stock virus) and P1 to P5 viruses from identically treated cells. Additionally P1 to P5 viruses from cells treated with a single siRNA (either siRNA L2 or N1) were also tested in duplicate in cells transfected with the other single siRNA to which the virus had not previously been exposed. Untreated and uninfected control wells were included on each plate. Cells were fixed and stained for viral antigen expression 40 hpi (Section 2.5.3.1). Image acquisition and analysis was performed as previously described in Sections 2.5.3.2 and 2.5.3.3.

5.3.7. Comparison of Dicer-substrate versus canonical siRNAs

The canonical siRNA structure described by Elbashir et al. (2001b) consists of a 19 bp RNA duplex with 2 nt 3' overhangs. A range of structural variants of this classical siRNA have been described, many of which are purported to offer benefits in terms of increasing potency and duration of action, and decreasing off-target effects and non-specific immune stimulation (Chang et al., 2007; Kim et al., 2005; Rose et al., 2005; Salomon et al., 2010). In this study we compared the performance of one of these structural variants, Dicer-substrate siRNA (DsiRNA), against canonical siRNAs targeted against the same motif. DsiRNAs, based on highly effective anti-FCoV siRNAs and the non-silencing control siRNA, were designed according to the design rules outlined by Amarzguioui et al. (2006). DsiRNA sequences shown in Table 5.2. Custom synthesised DsiRNAs and a transfection control DsiRNA duplex conjugated to TYE™ 563 were purchased from Integrated DNA Technologies (IDT, Coralville, IA, USA) in the lyophilised form and resuspended to 5 µM in nuclease-free duplex buffer (IDT) containing 100mM potassium acetate and 30mM HEPES. Resuspended DsiRNAs were stored at -20°C in single use aliquots until required.

Table 5.2: Dicer-substrate siRNA sequences used in this thesis. RNA bases are uppercase, DNA bases are lower case. Previously tested siRNA sequences are shown shaded in grey (the central 19mer duplex). Dicer-substrate siRNAs designed based on the reported sequence of FCoV FIPV1146 (Accession number DQ010921).

DsiRNA	Sequence	
Leader (DsiRNA-L2)		
Sense	5′ GGACACCAACUCGAACUAAACGAaa	3′
Antisense	3′ AGCCUGUGGUUGAGCUUGAUUUGCUUU	5′
Nucleocapsid (DsiRNA-N1)		
Sense	5′ GGAGUCUUCUGGGUUGCAAGGGAtg	3′
Antisense	3′ UACCUCAGAAGACCCAACGUUCCCUAC	5′
NSC-GFP (DsiRNA-NSC)		
Sense	5′ CAAGCUGACCCUGAAGUUCAUCUgc	3′
Antisense	3′ CCGUUCGACUGGGACUUCAAGUAGACG	5′

A concentration-response experiment was performed to compare the antiviral effect of canonical and Dicer-substrate siRNAs. Cells were reverse transfected in 96-well plates (Sarstedt) with half-log dilutions from 10 nM to 0.1 nM of single siRNA or DsiRNA as described in Section 2.4.1. The potency of combination treatment was also compared by transfecting cells with 5 nM, 1.5 nM, or 0.5 nM combinations of two canonical or Dicer-substrate siRNAs. Cells transfected with NSC siRNA and DsiRNA, in addition to untreated cells, were included as controls. At the conclusion of the transfection period cells were infected (or mock infected) with FCoV FIPV1146 at MOI 0.2. Culture media was harvested at 40 hpi for titration of extracellular virus by TCID50 endpoint assay (Section 2.3.1.2.2). Relative viral titre was calculated for each treatment, with the no treatment control titre defined as 100%. Each treatment was performed in triplicate and repeated in three independent experiments. Data represent Mean ± SE.

A further experiment was conducted to assess the duration of antiviral action of canonical versus Dicer-substrate siRNAs against FCoV FIPV1146 using single and combination treatment. Cells were reverse transfected in 96-well plates (Sarstedt) with single or dual combination siRNAs or DsiRNAs with a total concentration of 5 nM as described in Section 2.4.1. At the conclusion of the transfection period cells were infected with FCoV FIPV1146 at MOI 0.5 and incubated at 37°C in 5% CO_2 in air. Culture media was harvested at 20, 40, 60, and 80 hpi for titration of extracellular virus by TCID50 endpoint assay (Section 2.3.1.2.2). Each treatment was performed in triplicate and repeated in two independent experiments. Data represent Mean ± SE.

5.4. RESULTS

5.4.1. siRNA design

At the time of siRNA design (April 2009) there were five full-length genome sequences of FCoV available on GenBank (Appendix 2), however two of these were independently derived full length sequences of FCoV FIPV1146. Additionally, there were two full-length membrane ORF and three full-length nucleocapsid ORF sequences available for analysis. Alignment of these sequences revealed a number of short regions in the targeted ORFs displaying minimal sequence variation against which siRNAs could be designed. For each targeted region (the 5' UTR and the replicase, membrane, and nucleocapsid ORFs) two siRNAs were selected for screening. The details of these are shown in Table 5.1 Subsequent to the siRNA design stage a considerable number of full-length FCoV sequences have been published. Alignment of all full-length sequences available as of July 2013 confirms that the originally identified regions are well conserved and that the designed siRNAs display a high degree of homology to published type I and type II strains (Table 5.3).

Table 5.3: Degree of conservation of FCoV siRNA target sites. Reported sequences were accessed in April 2009 (full and partial sequences) and July 2013 (full length sequences only) from GenBank. Results show the number of sequences with different degrees of target site homology. Accession numbers shown in Appendix 2.

Target region	Target	Degree of conservation (accessed April 2009): Matching nucleotides – number of sequences	Degree of conservation (accessed July 2013): Matching nucleotides – number of sequences
5' UTR	L1	19/19 – 5	19/19 – 31 18/19 – 2 17/19 – 2 1 - 1 insertion
	L2	19/19 – 5	19/19 – 34 18/19 – 1
Replicase ORF	R1	19/19 – 5	19/19 – 33 18/19 – 1 17/19 – 1
	R2	19/19 – 5	19/19 – 29 18/19 – 1 17/19 – 2 16/19 – 3
Membrane ORF	M1	19/19 – 6 18/19 – 1	19/19 – 27 18/19 – 8
	M2	19/19 – 6 17/19 – 1	19/19 – 28 18/19 – 5 17/19 – 2
Nucleocapsid ORF	N1	19/19 – 6 18/19 – 2	19/19 – 26 18/19 – 9
	N2	19/19 – 8	19/19 – 24 18/19 – 9 17/19 – 2

5.4.2. Effect of siRNAs on FCoV replication

All anti-FCoV siRNA duplexes tested in the initial screening experiment demonstrated an inhibitory effect on FCoV replication as determined by qRT-PCR of viral genomic and messenger RNA and extracellular viral titre; however the magnitude of the inhibition varied greatly between the different siRNAs. Reduction of viral genomic RNA in siRNA treated cells ranged from 23.1% to 90.7% (Figure 5.2a). Similar results were seen with viral mRNA, with membrane mRNA knockdown ranging from 27.7% to 92.3% (Figure 5.2b) and nucleocapsid mRNA knockdown ranging from 23.1% to 93.8% (Figure 5.2c). Reduction in extracellular viral titres paralleled the PCR data, ranging from 59.6% to 97.0% (Figure 5.2d), confirming viral gene knockdown is associated with a significant reduction in the production of progeny virions. In contrast treatment with the non-silencing control siRNA or mock transfection with Lipofectamine 2000 alone had no significant effect on viral replication confirming the

sequence specificity of siRNA mediated viral inhibition. The results of direct IFA further confirm these findings. A qualitative assessment of viral protein expression showed that treatment with FCoV specific siRNAs was associated with a reduction in the number of antigen positive cells, a finding most obvious for the highly efficacious siRNAs L2 and N1. Representative micrographs are shown in Figure 5.3. Additionally, phase contrast microscopy showed that virus specific siRNAs provided some protection from virus induced CPE, in the case of siRNAs L2 and N1 out to 50 hpi (Figure 5.3). Based on these data, siRNAs L2 and N1 were identified as being highly efficacious in showing greater than 80% inhibition in both extracellular viral titre and intracellular viral copy number, and were selected for further studies.

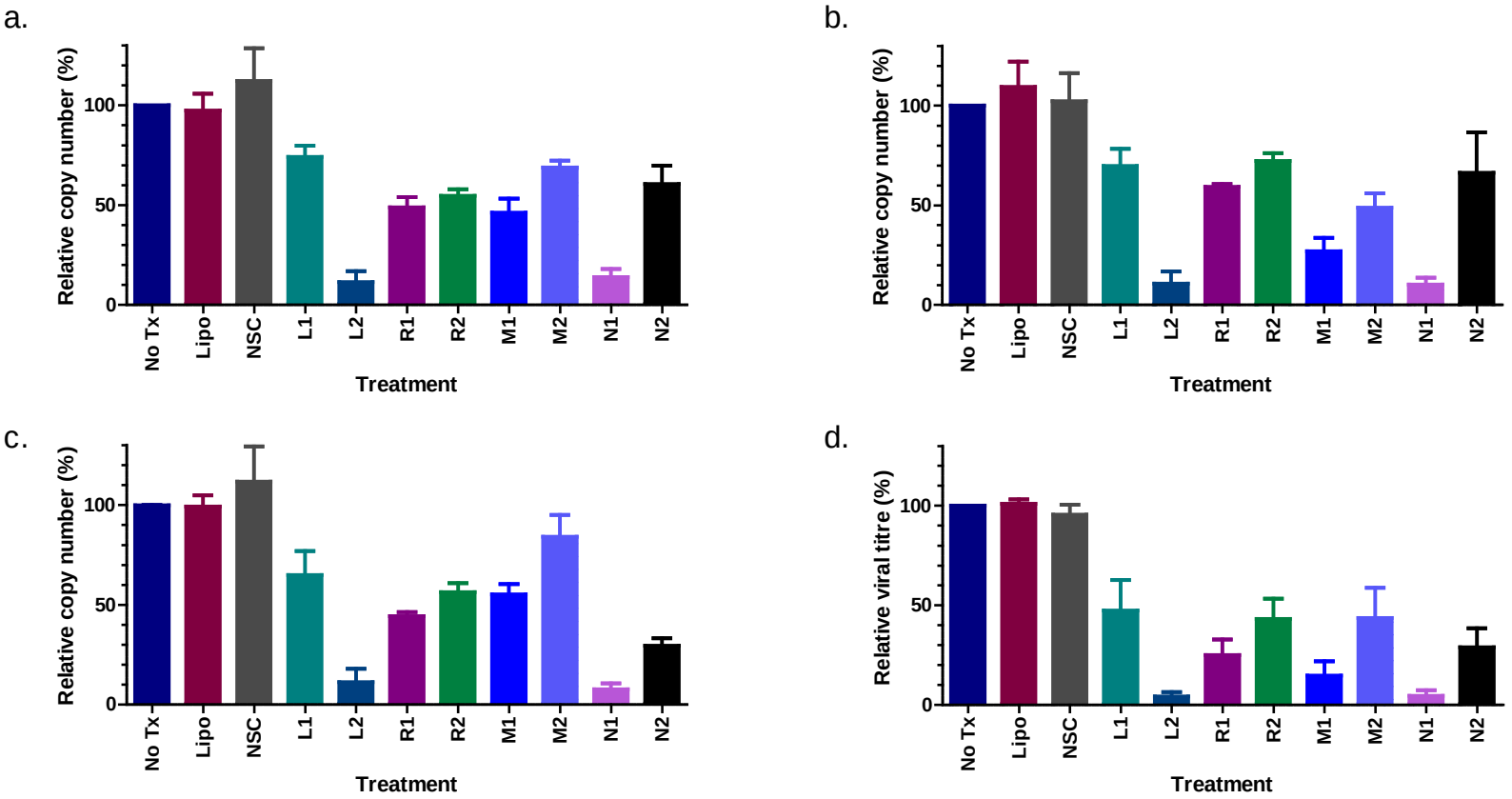

Figure 5.2: Results of FCoV siRNA screening experiment. Cells were transfected (or mock transfected) with 100 nM siRNA prior to infection with FIPV1146 at MOI 0.2. At 24 hpi intracellular (a) FCoV genome, (b) FCoV membrane mRNA, and (c) FCoV nucleocapsid mRNA copy number were determined by qRT-PCR and extracellular viral titres (d) were determined by TCID50 assay. Value of the untreated control sample is defined as 100%. Data expressed as Mean ± SE from three independent experiments. No Tx, no treatment control; Lipo, Lipofectamine only control; NSC, non-silencing control.

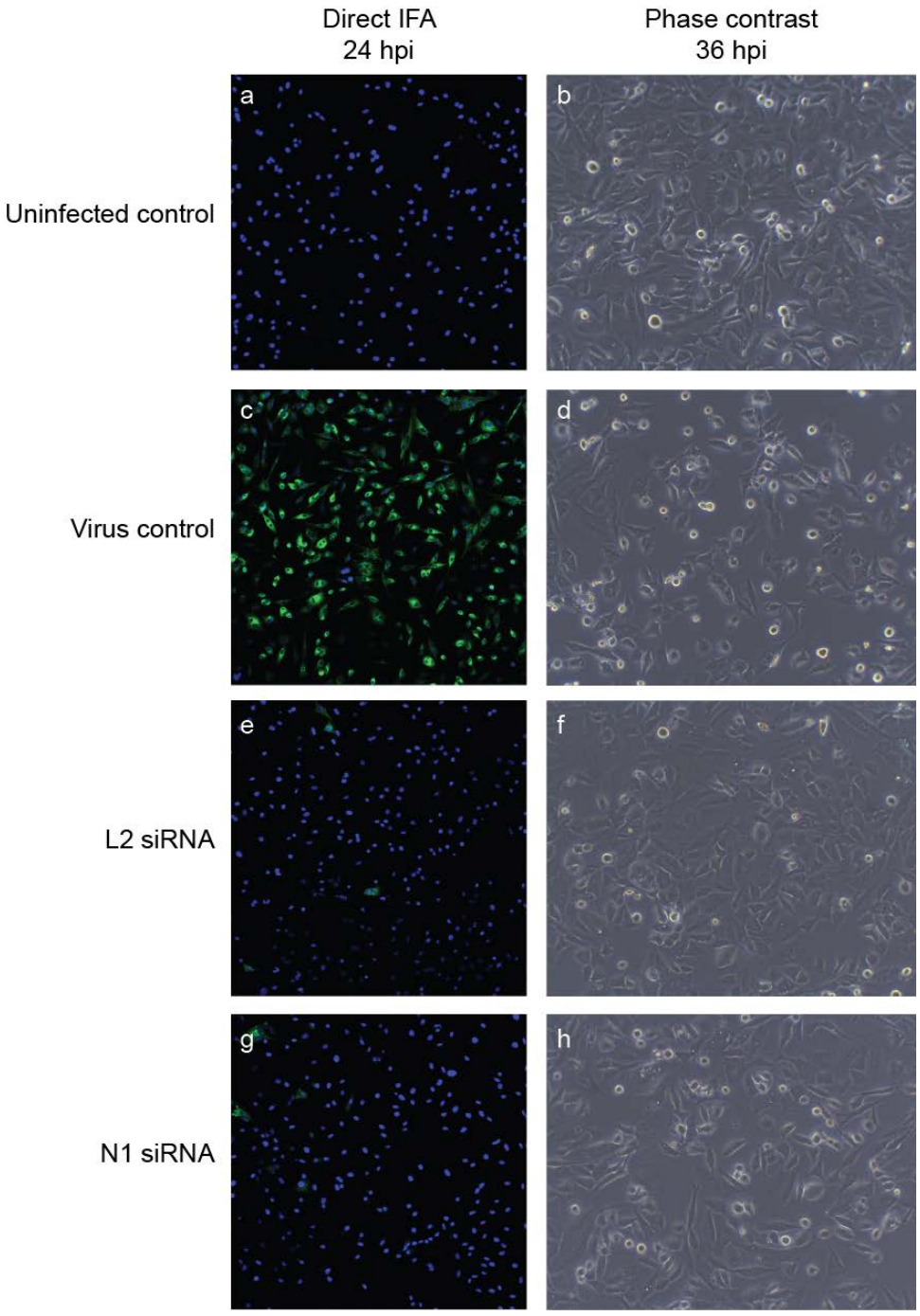

Figure 5.3: Viral antigen expression and cytopathic effect micrographs from FCoV siRNA screening experiment. Cells were transfected (or mock transfected) with 100 nM siRNA prior to infection with FCoV FIPV1146 at MOI 0.2. Representative direct IFA and phase contrast micrographs showing results from healthy uninfected and untreated samples (uninfected control), infected cells with no prior siRNA treatment (virus control), and samples treated with siRNAs L2 or N1 prior to infection. Virus infected cells demonstrate diffuse and punctate green (FITC) cytoplasmic staining in IFA micrographs. Cell nuclei counterstained with DAPI appear blue. Direct IFA = 100 x , Phase contrast = 200 x.

5.4.3. Effect of siRNA concentration on FCoV replication

Titration of siRNAs L2 and N1 from 200 nM to 5 nM demonstrated a clear concentration-response relationship with significant inhibition even at the lowest tested concentration (Figure 5.4). Reductions in extracellular virus titres at 200 nM were 93.2% and 96.4% for L2 and N1 respectively, decreasing to 80.6% and 83.1% at 5 nM concentration.

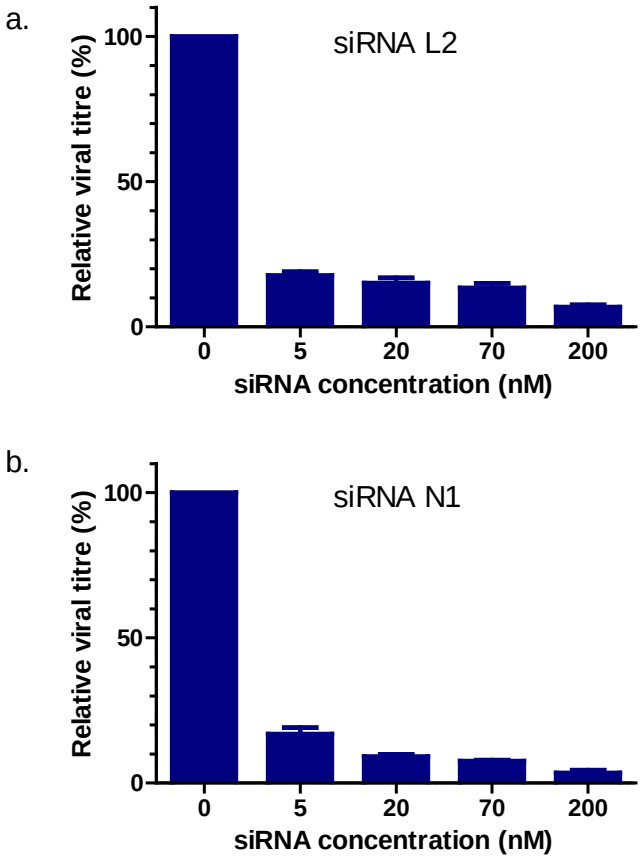

Figure 5.4: Concentration-dependent inhibition of FCoV replication by siRNA L2 and N1. Cells were transfected (or mock transfected) with (a) siRNA L2 or (b) siRNA N1 at concentrations from 200 nM to 5 nM prior to infection with FCoV FIPV1146 at MOI 0.2. The value of the untreated control sample (concentration 0 nM) is defined as 100%. Each treatment was performed in triplicate and repeated in three independent experiments. Data are expressed as Mean ± SE.

5.4.4. Effect of the magnitude of viral challenge on siRNA efficacy

Given the high viral loads seen in cats with FIP, we sought to determine if anti-FCoV siRNAs remained effective at inhibiting viral replication in the face of a high viral challenge. Both tested siRNAs remained efficacious at all tested MOI, demonstrating greater than 75% reduction in extracellular viral titre (Figure 5.5). qRT-PCR results showed less pronounced

inhibition at higher MOI when compared to viral titres. This difference was most marked for siRNA N1 which demonstrated a reduction in viral genome copy number of only 31.3% at MOI 20 as compared to 85.2% reduction in extracellular viral titre.

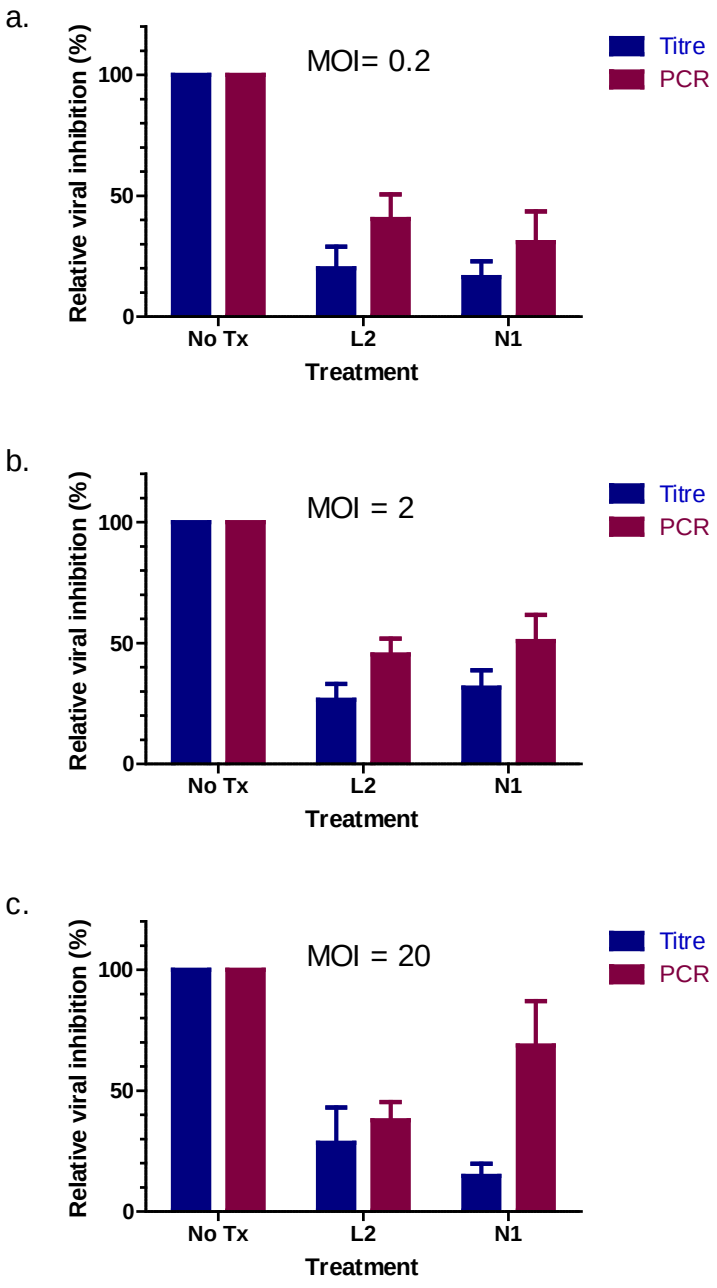

Figure 5.5: Efficacy of FCoV siRNAs in cells challenged with different MOI. Cells were transfected (or mock transfected) with 100 nM siRNA prior to infection with FCoV FIPV1146 at MOI (a) 0.2, (b) 2, or (c) 20. Extracellular viral titres and intracellular viral genomic RNA were measured 18 hpi. The value of the untreated control sample is defined as 100%. Each treatment was performed in triplicate and repeated in three independent experiments. Data are expressed as Mean ± SE. No Tx, no treatment control.

5.4.5. Effect of combination treatment on siRNA efficacy

Based on extracellular viral titre and intracellular viral antigen expression, pre-treatment with multiple siRNAs was highly effective at inhibiting viral replication, with no evidence of antagonistic effects noted at the concentrations tested. Interestingly, although the cell culture and infection conditions were different, the reduction in relative viral titre using the reverse transfection protocol was significantly greater than that previously seen in forward transfected cells, particularly for siRNAs M1 and N2. Pre-treatment with single siRNAs at 30 nM using reverse transfection resulted in a reduction of extracellular viral titres of 99.7%, 99.6%, 93.9%, and 91.4% for siRNAs L2, N1, M1, and N2 respectively (Figure 5.6a). Pre-treatment with a combination of two, three, or four siRNA, at a total concentration of 30 nM, resulted in a reduction in viral titre of greater than 99.5% for all tested combinations.

Analysis of viral antigen expression supported these findings. Combination treatment with multiple siRNAs was highly effective, resulting in a greater reduction in the percentage of infected cells compared to treatment with a single siRNA (Figure 5.6b). Interestingly, the percentage of infected cells following single treatment with siRNAs M1 or N2 (92.5% and 66.1% respectively) was significantly higher than would be expected given the degree of inhibition of extracellular virus (93.9% and 91.4% reduction respectively). This large difference was not apparent for cells treated singly with siRNAs L2 and N1, or cells treated with siRNA combinations, where significant inhibition of extracellular viral titre was associated with a similarly large reduction in the percentage of infected cells.

a.

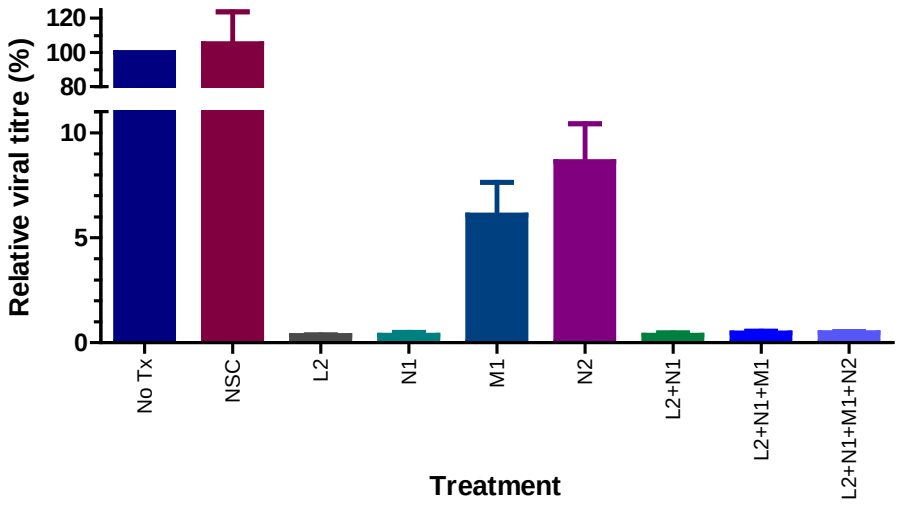

b.

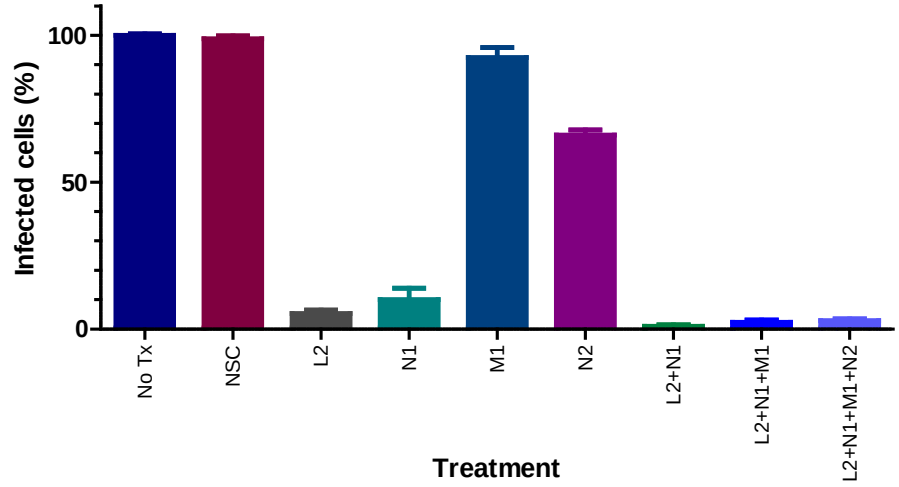

Figure 5.6: Efficacy of combination siRNA treatment against FCoV. Cells were reverse transfected with 30 nM of single or multiple siRNAs prior to infection with FCoV FIPV1146 at MOI 0.2. Efficacy was determined 36 hpi by (a) TCID50 titration of extracellular virus and (b) assessment of intracellular viral antigen expression by IFA. Value of untreated control samples is defined as 100%. Each treatment was performed in triplicate and repeated in three independent experiments. Data represent Mean ± SE. No Tx, no treatment control; NSC, non-silencing control.

5.4.6. Viral escape from siRNA mediated inhibition

Serial passage of FCoV FIPV1146 through cells treated with one or multiple anti-FCoV siRNAs was associated with the development of a number of single nucleotide polymorphisms within the sequenced siRNA target sites. For virus passaged through cells treated with a single siRNA, mutations were identified at P1 (for siRNA L2) and P2 (for siRNA N1), while for virus passaged through dual and triple siRNA treated cells, mutations were

identified first at P2 and P4 respectively. No mutations were detected in the siRNA L2 or siRNA N1 target sites when virus was serially passaged through untreated cells or cells treated with a NSC siRNA [Figure 5.7 (e and f)].

As shown in Figure 5.7 (a, c, and d), mutations were identified at two separate locations within the L2 target site. The first of these was a C-to-U transition at position ten (in virus passaged through cells treated with siRNA L2 alone and with siRNA combination L2+N1+M1) and the second, a C-to-A transition at position six (in virus passaged through cells treated with siRNA combination L2+N1). As siRNA L2 targets the leader sequence in the 5' UTR there are no associated amino acid changes as a result of these mutations. The L2 target site is however located within the putative leader-TRS hairpin, thought to be an important *cis*-acting element (Dye and Siddell, 2005), as well as incorporating several nucleotides of the proximal end of the TRS.

For the N1 target site [Figure 5.7(b, c, and d)], mutations were also identified at two locations. At position nine two polymorphisms were noted: a C-to-A transition (in virus passaged through cells treated with siRNA N1 alone) and a C-to-G transition (in virus passaged through cells treated with siRNA combinations L2+N1 and L2+N1+M1). The second mutation was a G-to-C transition at position seventeen. This mutation was seen only in virus passaged through cells treated with siRNA combination L2+N1+M1. All of the nucleotide substitutions within the N1 target site were associated with amino acid changes. Although position nine of the target site corresponds to the wobble position of the codon for phenylalanine in the original sequence, both identified polymorphisms at this location resulted in an amino acid change to leucine. Position seventeen corresponds to the middle base of the codon for alanine in the original sequence, and the G-to-C transition results in an amino acid substitution to valine.

Based on the inhibition of viral antigen expression, the identified mutations resulted in the acquisition of a fully or partially resistant phenotype (Figure 5.8). When treated with a single siRNA the acquisition of a mutation at the target site was associated with an almost complete loss of inhibition. For siRNA N1, although the C-to-A transition was not noted until P2, a highly resistant phenotype was apparent from P1. Analysis of the P1 electropherogram at this site shows a small adenine peak in addition to cytosine suggesting a subpopulation of the P1 viruses had undergone this mutation during the first passage. Given the 40 h infection period used in this study encompasses multiple replication cycles, the presence of even a low-prevalence resistant sub-population would likely result in the appearance of a highly resistant phenotype in this study. The development of resistance to siRNA mediated inhibition was demonstrated to be sequence dependent rather than mechanism dependent

as viruses with mutations in the L2 target site remained susceptible to RNAi mediated inhibition by siRNA N1 and vice versa (data not shown).

Mutations were not apparent until P2 for virus passaged through dual combination siRNA treated cells. A partially resistant phenotype was noted at P1 with relative viral antigen expression increasing from 3.3% at P0 to 27.7% at P1. By P2 mutations were present in both L2 and N1 target sites, with an accompanying increase in relative viral antigen expression to 91.1%. Interestingly relative viral antigen expression for P3 and P4 dual treated viruses remained at approximately 90% despite the presence of the apparently fixed mutations in both target sites, with complete resistance not seen until P5.

Virus passaged through triple combination siRNA treated cells remained susceptible to RNAi mediated inhibition for all five passages, although low level resistance was apparent from P1. Despite this early appearance of low level resistance, mutations were not identified in the L2 or N1 target regions until P4. At P4, a C-to-U transition was identified at position ten of the L2 target and a possible C-to-G transition was identified at position nine of the N1 target, although the electropherogram at this latter site showed two almost equal peaks. At P5 the mutation in the L2 target site remained and position nine of the N1 target had reverted to a C, although a small G peak was evident suggesting a subpopulation of viruses retained this mutation. A second novel mutation in the N1 target, a C-to-U transition at position seventeen, was identified at P5. None of the mutations present from P4 onwards appeared to confer a significant increase in resistance compared to earlier passages.

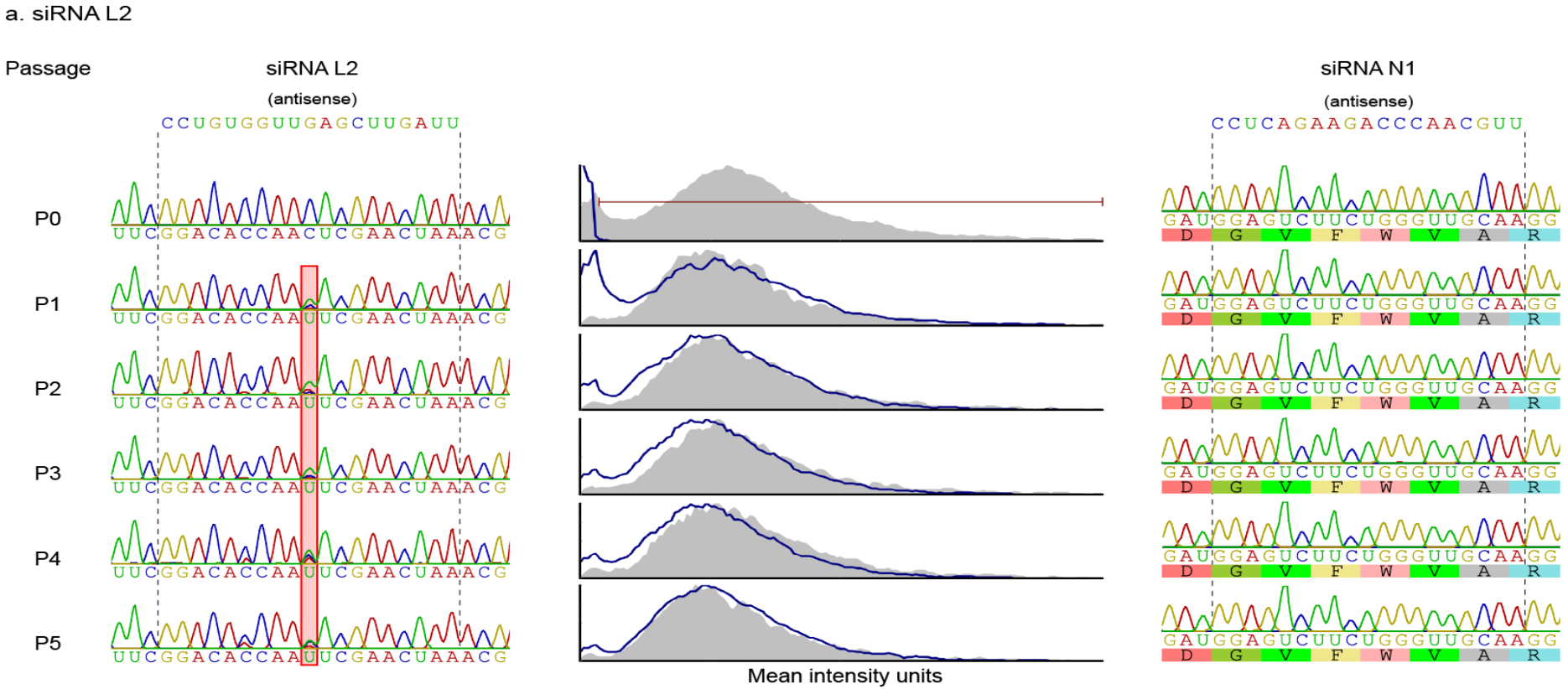

Figure 5.7: Viral escape from siRNA mediated inhibition. FCoV FIPV1146 was serially passaged five times through siRNA treated (or mock treated) cells. Consensus sequencing was performed for the target sites for siRNAs L2 and N1 of original stock virus (P0) and each passage (P1 to P5). Red rectangles on electropherograms highlight nucleotide substitutions compared to P0 sequence. Viruses were tested for a resistant phenotype by infecting cells pre-treated (or mock treated) in the same manner at MOI 0.2 with serially passaged viruses. At 40 hpi *in situ* IFA staining was performed and viral antigen expression quantified. Histograms show normalised mean cell intensity for each passage with the solid blue line representing siRNA treated cells and the filled grey histogram untreated control cells. Marker on P0 histogram shows gate for antigen positive cells.

b. siRNA N1

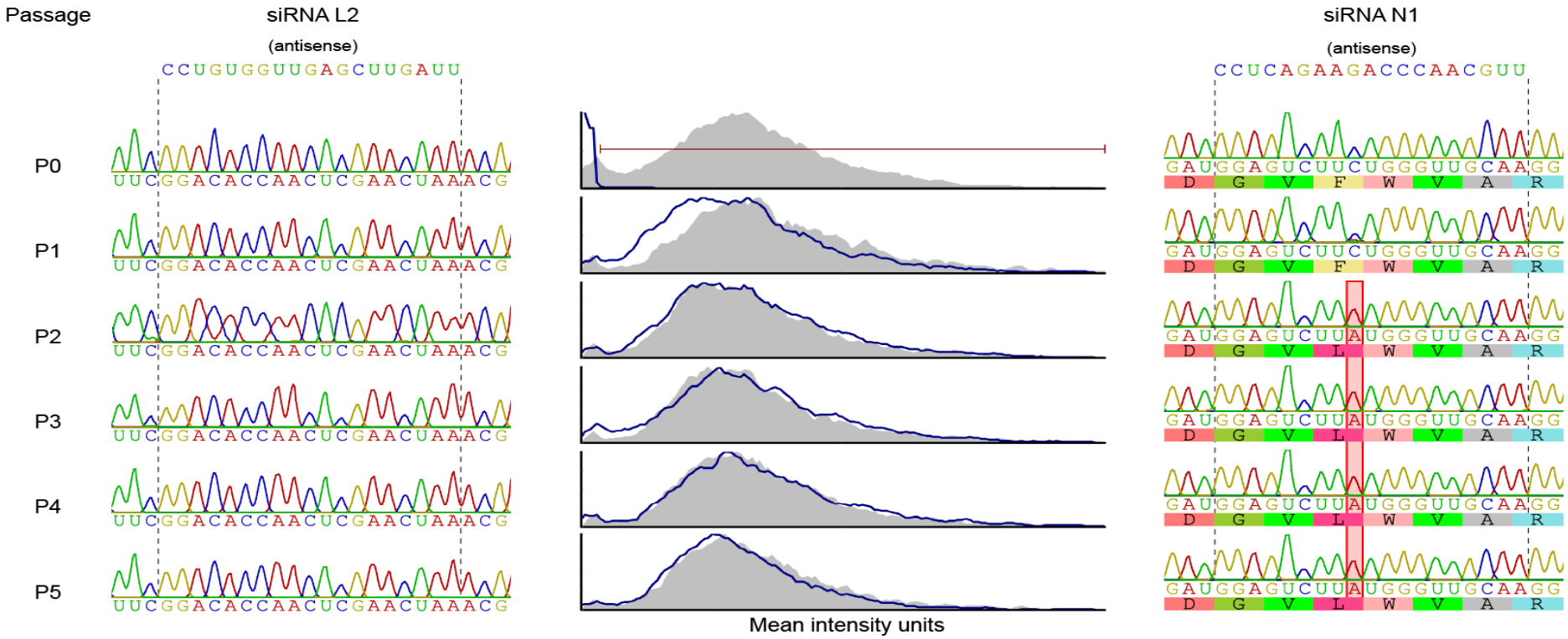

Figure 5.7 cont.: Viral escape from siRNA mediated inhibition.

c. Dual combination siRNA L2 + N1

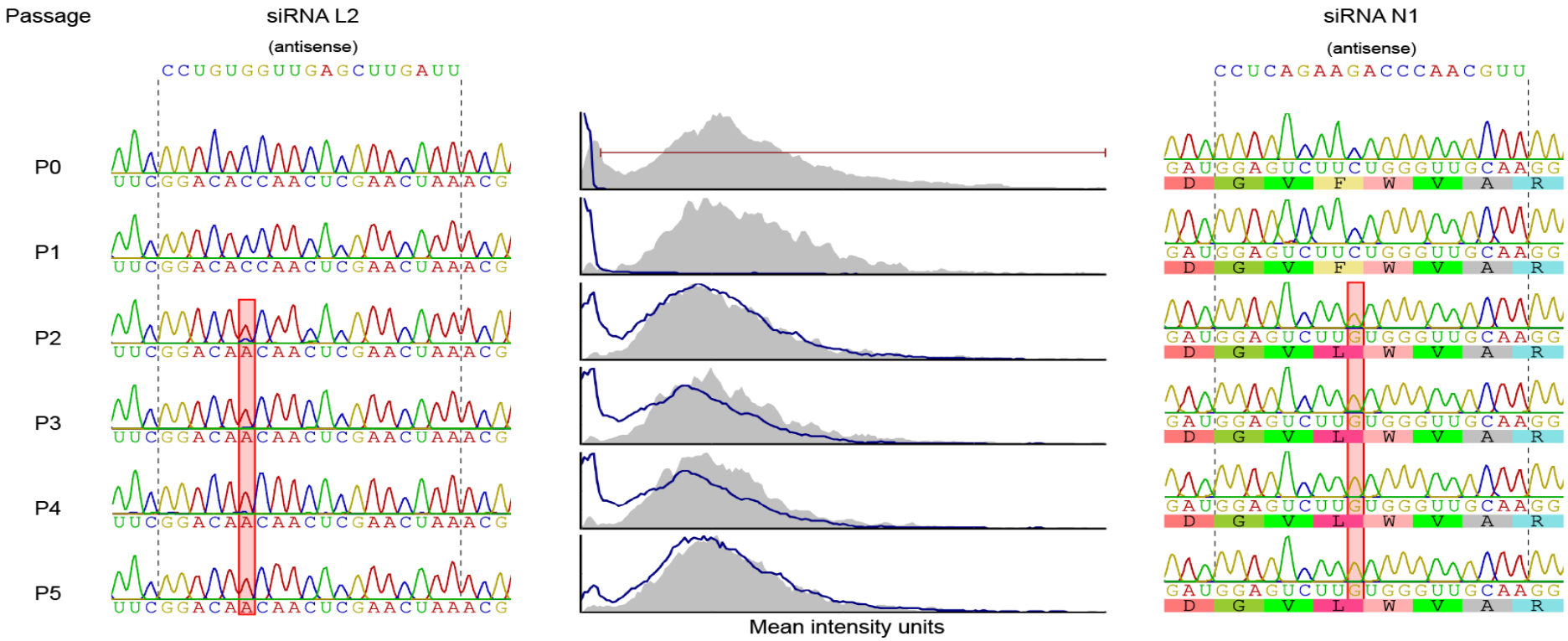

Figure 5.7 cont.: Viral escape from siRNA mediated inhibition.

d. Triple combination siRNA L2+N1+M1

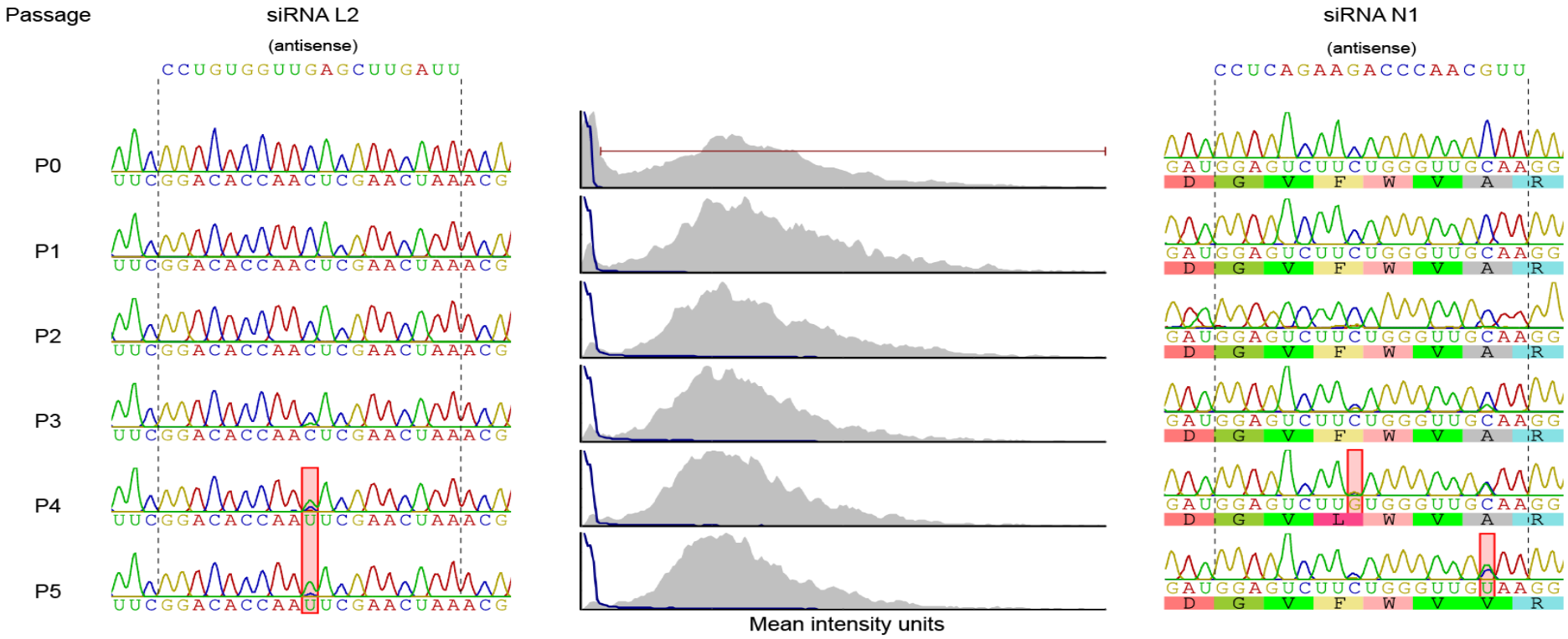

Figure 5.7 cont.: Viral escape from siRNA mediated inhibition.

e. siRNA NSC-GFP

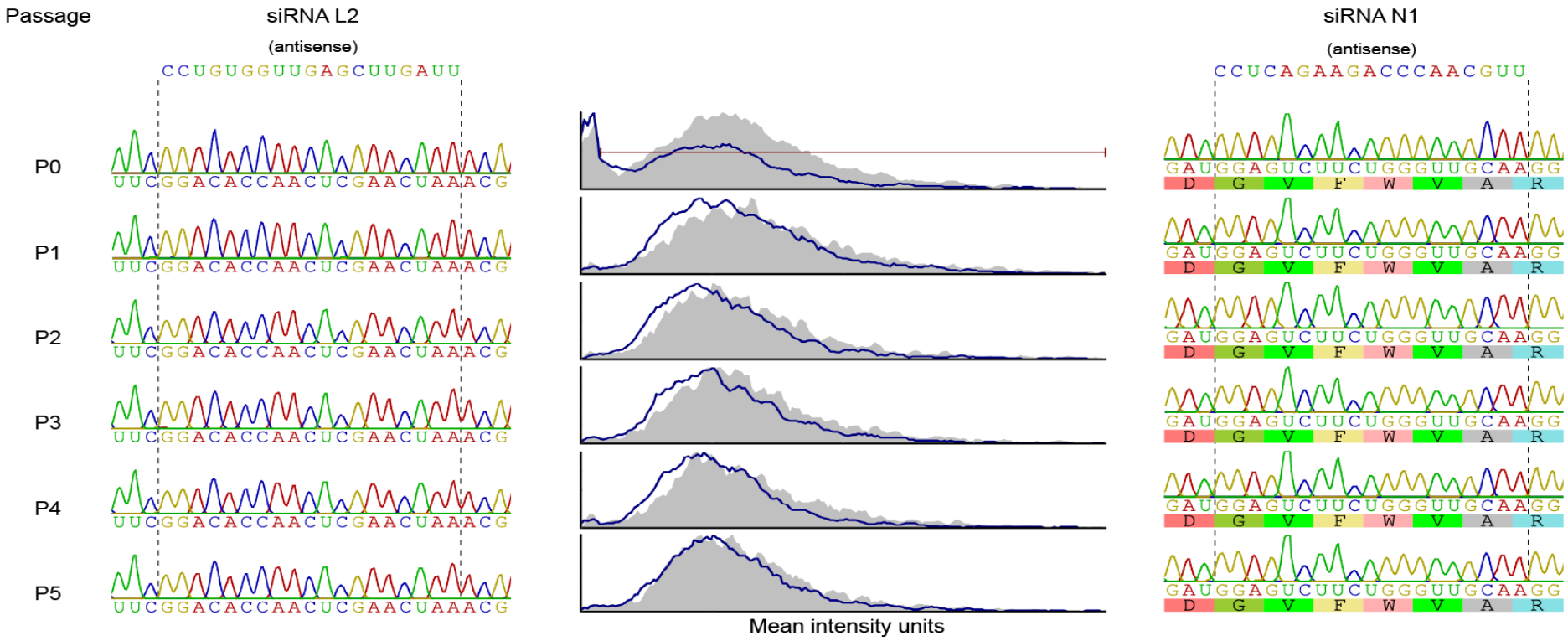

Figure 5.7 cont.: Viral escape from siRNA mediated inhibition.

f. No treatment

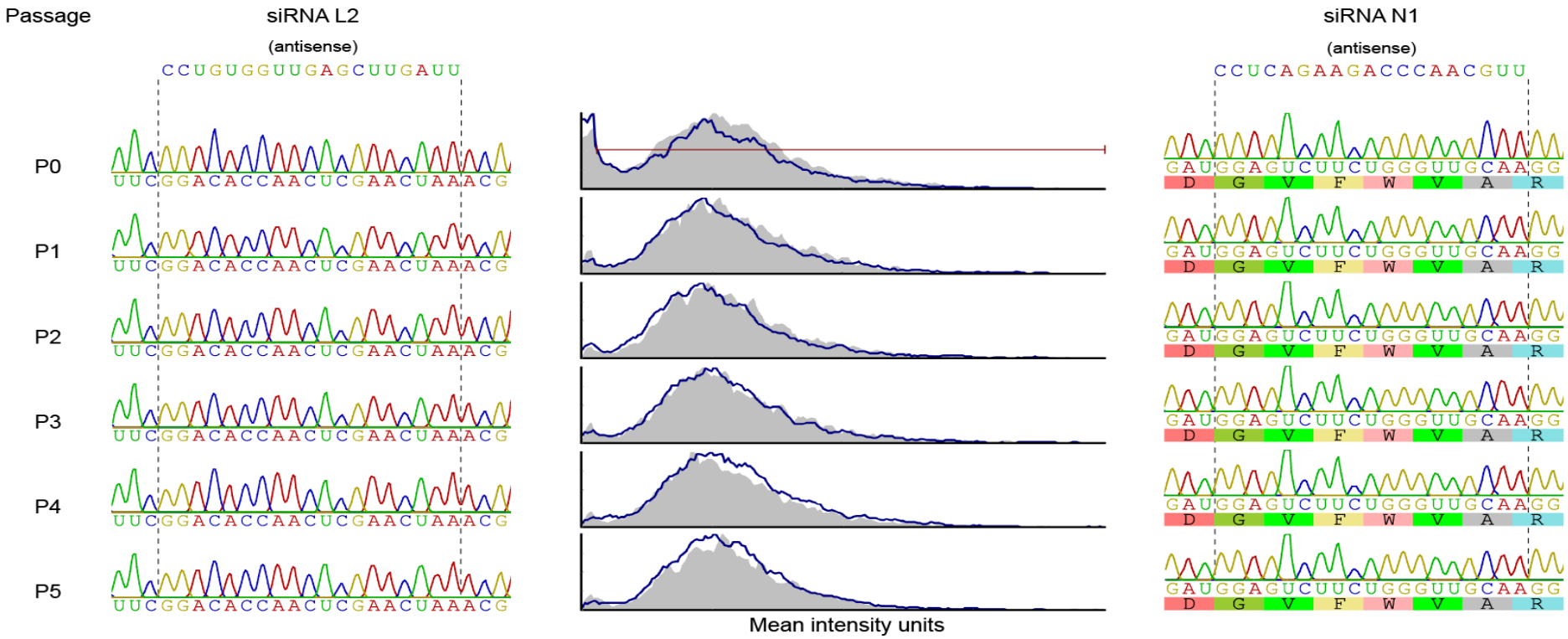

Figure 5.7 cont.: Viral escape from siRNA mediated inhibition.

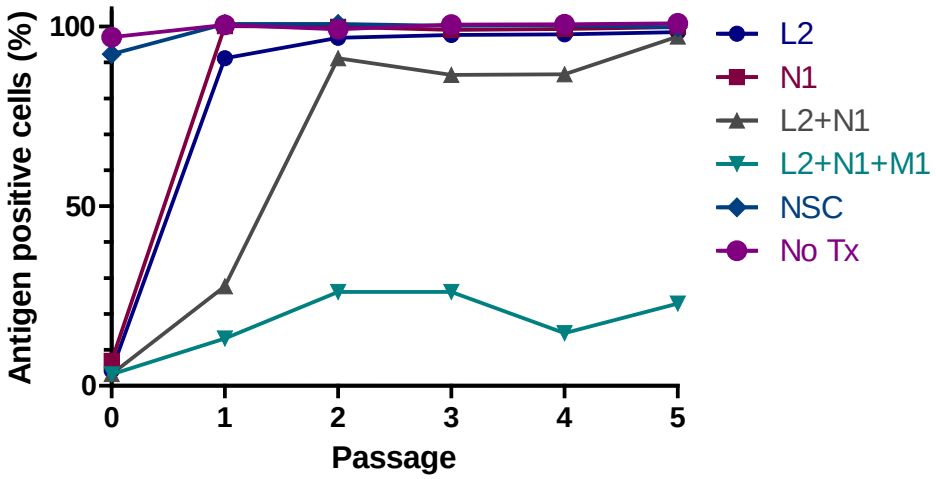

Figure 5.8: Effect of target site mutations on the inhibitory effect of antiviral siRNAs against FCoV FIPV1146. FCoV FIPV1146 was serially passaged five times through cells pre-treated with one or a combination of siRNAs previously shown to have antiviral effects, through cells pre-treated with a NSC siRNA, or through untreated cells. Virus from each passage and treatment was subsequently tested for the development of resistance by infecting cells pre-treated in the same manner at MOI 0.2 with serially passaged virus. Viral antigen expression was determined 40 hpi. The percentage of infected cells was calculated with the value of the no treatment control defined as 100%. Results represent Mean of duplicate wells. No Tx, no treatment; NSC, non-silencing control.

5.4.7. Comparison of Dicer-substrate siRNAs and canonical siRNAs

The efficacy of two different exogenous RNAi triggers, canonical and Dicer-substrate siRNAs targeting the same region, were examined via a concentration-response study, the results of which showed the relative potency of these RNAi triggers was dependent on the target. For the L2 target site DsiRNA was more potent than siRNA, with IC50 values of 0.31 and 1.18 nM respectively (Figure 5.9; Table 5.4). For target N1 the IC50 values for DsiRNA and siRNA were similar at 2.00 and 1.76 nM respectively. Dual combination DsiRNAs were considerably more potent than dual combination siRNAs, with an almost 10-fold reduction in IC50 value (0.28 nM compared to 2.65 nM).

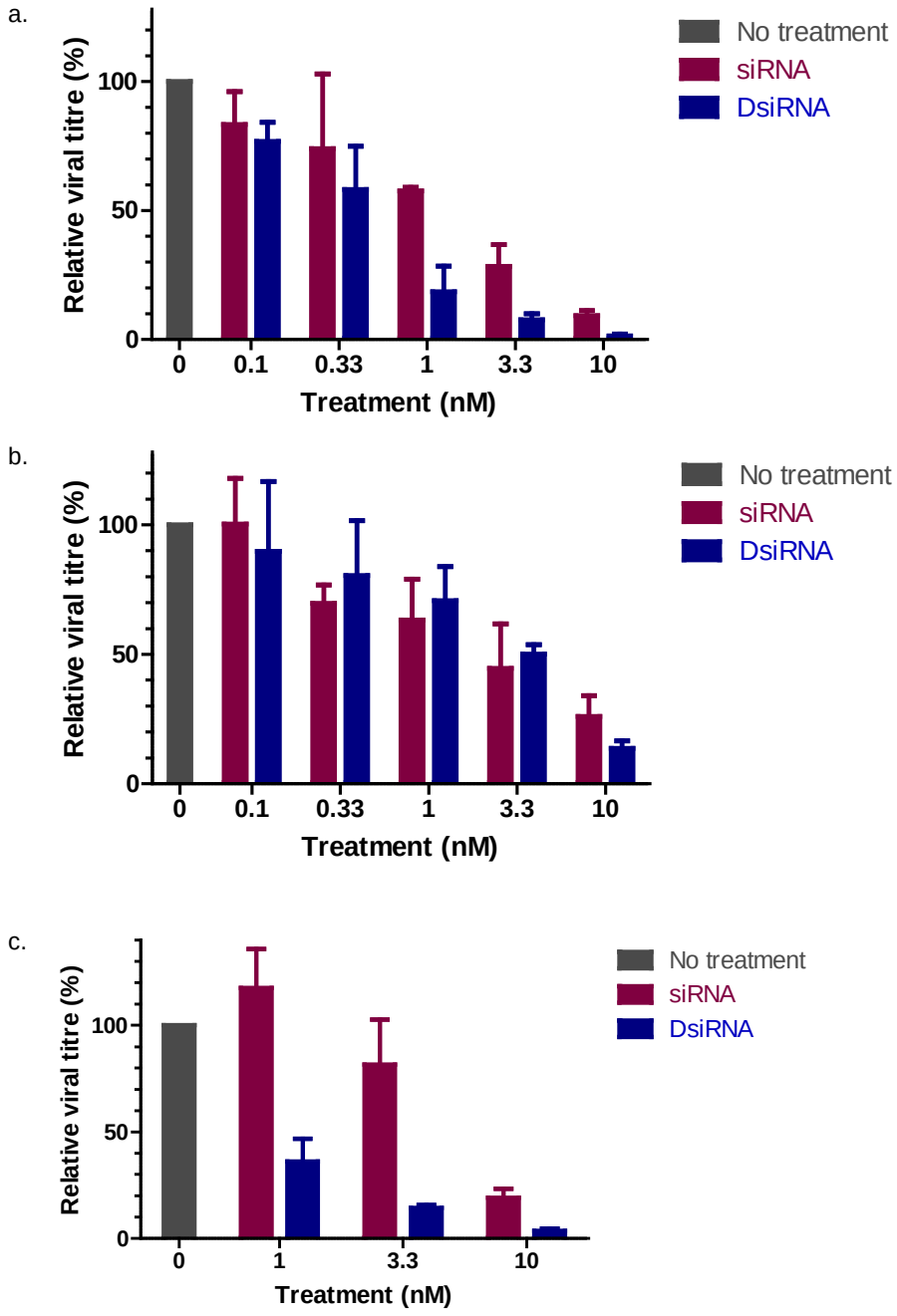

Figure 5.9: Comparison of antiviral efficacy of siRNAs and DsiRNAs targeting L2 and N1. Cells were reverse transfected (or mock transfected) with single siRNAs or DsiRNAs (a) L2 or (b) N1 at half-log concentrations from 10 nM to 1 nM or dual combination siRNAs or DsiRNAs targeting (c) L2 + N1 at concentrations of 5 nM to 1 nM. Cells were infected with FCoV FIPV1146 at MOI 0.2. Extracellular viral titres were determined 40 hpi. Value of the untreated control sample (concentration 0 nM) is defined as 100%. Each treatment was performed in triplicate and repeated in three independent experiments. Data are expressed as Mean ± SE.

Table 5.4: IC50 values (with 95% confidence intervals) for single and dual combination treatment with siRNAs and DsiRNAs targeting L2 and N1.

	siRNA	**DsiRNA**
Target	**IC50 (nM)**	**IC50 (nM)**
L2	1.18 (0.49-2.55)	0.31 (0.22-0.43)
N1	1.76 (0.96-3.25)	2.00 (1.07-3.87)
L2+N1	2.65 (1.54-4.57)	0.28 (0.13-0.63)

To assess the effect of the structural form of the triggering molecule on the duration of the antiviral response, extracellular viral titres were determined at four time points post infection in cells pre-treated with 5 nM canonical or Dicer-substrate siRNA. Based on the shape of the time-response curves generated, the duration of antiviral response was similar between siRNAs and DsiRNAs designed against the same target (Figure 5.10) and overall the duration of antiviral response appeared related to siRNA potency. For target L2, pre-treatment with DsiRNA resulted in almost complete inhibition of viral replication out to 40 hpi, followed by a rapid rise in extracellular viral titre, to reach a maximum titre approximately equal to that of untreated cells at 60 hpi. Pre-treatment with siRNA L2 resulted in a similar response, although in this case the degree of inhibition at 40 hpi was lower than that seen with DsiRNA pre-treatment. By comparison extracellular viral titres of untreated cells, and cells pre-treated with NSC siRNAs and DsiRNAs (data not shown), were similar, rising rapidly at 20 hpi and peaking at 40 hpi, before declining. A similar picture was seen for cells pre-treated with dual combination siRNA or DsiRNA against L2 and N1, although in this case the magnitude of the peak viral titre of treated cells was lower than in untreated cells (or NSC siRNA/DsiRNA treated cells). Molecules targeted at N1, which had previously been demonstrated to be less potent that those against L2, demonstrated a shorter duration of action, with peak viral titre occurring at 40 hpi.

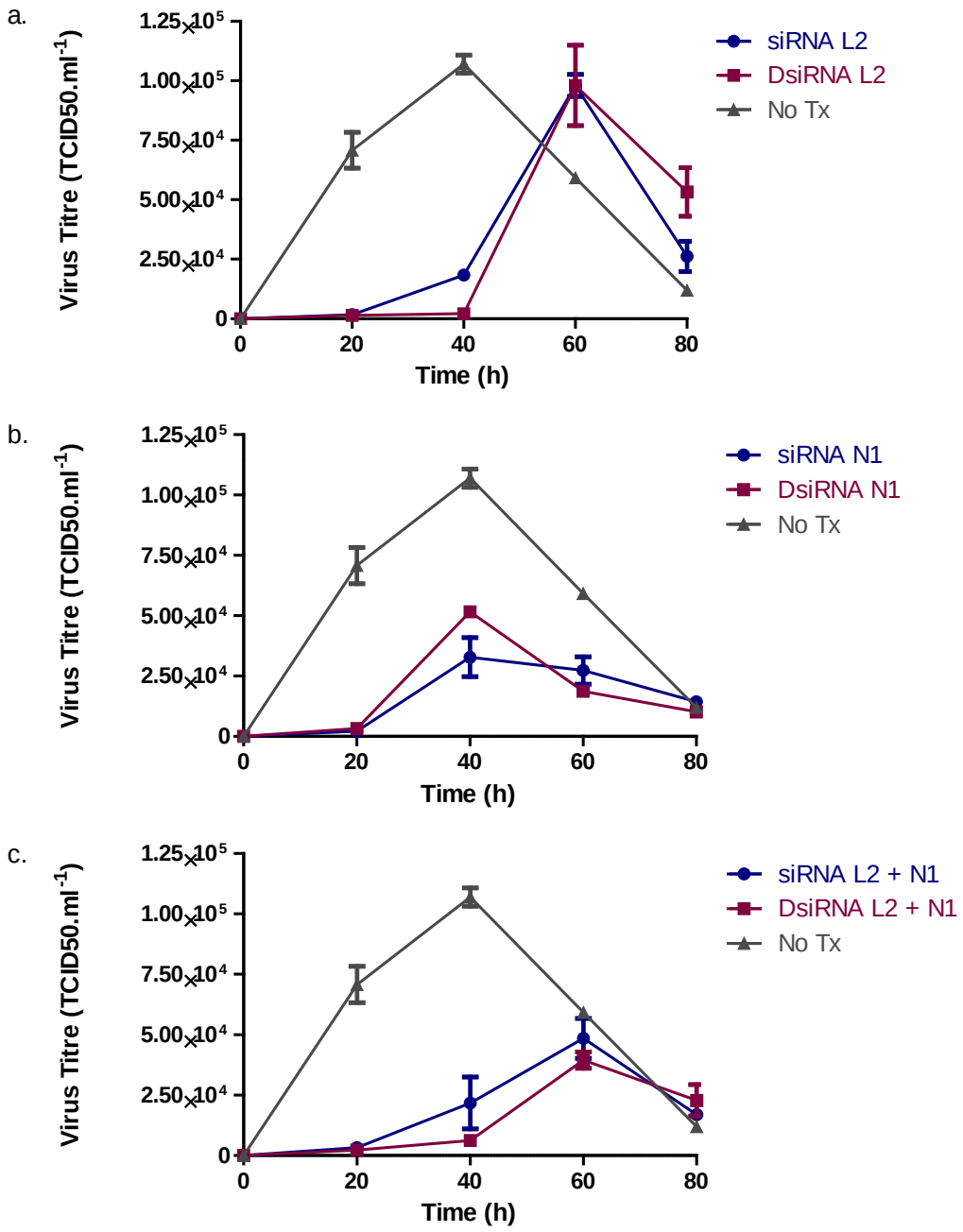

Figure 5.10: Duration of antiviral activity of canonical and Dicer-substrate siRNAs. Cells were reverse transfected with 5 nM single or dual combination siRNAs or DsiRNAs prior to infection with FCoV FIPV1146 at MOI 0.5. Culture media was harvested at 20, 40, 60, and 80 hpi for titration of extracellular virus titre. Each treatment and time-point was performed in triplicate and data represent Mean ± SE of duplicate experiments.

5.5. DISCUSSION

The current study has demonstrated the effectiveness of synthetic siRNA mediated inhibition of FCoV replication in an immortalised cell line. Further characterisation of the antiviral effects of these highly active compounds demonstrated they possess several characteristics that are likely essential for a useful therapeutic, including good efficacy at low nanomolar concentrations, when challenged with high viral loads, and when used in combination. In regards to the latter, combination therapy with three siRNAs targeting different regions of the viral genome was able to prevent viral escape, thus overcoming one of the greatest challenges of RNAi-based antiviral therapy. Taken together, these results provide in-principle proof of the effectiveness of specific siRNA mediated RNAi in substantially inhibiting FCoV replication *in vitro*, leading the way for an extension into *in vivo* use as a potential therapeutic agent for the deadly disease FIP, for which there is currently no effective treatment.

The selection of appropriate targets is a critical first step in using RNAi as an antiviral therapeutic. As a Baltimore group IV virus, the lifecycle of FCoV theoretically enables the simultaneous degradation of both viral genomic and messenger RNA via RNAi. Additionally, the unique discontinuous transcription mechanism of coronaviruses, resulting in a nested set of subgenomic mRNAs (Masters, 2006), enables targeting of multiple viral mRNA species as well as viral genomic RNA with a single siRNA. A common leader sequence, which plays a critical role in coronavirus gene expression, is present on the 5' end of each viral mRNA (Masters, 2006) and provides an additional highly conserved target present on all viral RNA species. In the current study a panel of eight siRNAs targeting four different regions of the FCoV genome were designed and tested. siRNAs were designed to target structural genes (M1, M2, N1, N2), non-structural genes (R1, R2), and the 5' UTR (L1, L2). The effectiveness of RNAi-based therapeutics targeting these regions has previously been demonstrated using an *in vitro* SARS-CoV model (He et al., 2003; He et al., 2006; Li et al., 2005c).

The design of successful siRNAs targeting viral sequences poses additional challenges compared to designing siRNAs to knock down cellular genes. This challenge arises due to the high mutation rates and short replicative cycles of viruses, a consequence of which is that within an infected animal, and also amongst viruses circulating within the broader population, there exists a significant degree of genetic heterogeneity. The term quasispecies is often used to refer to this phenomenon whereby genetic variation results in a population of related viruses that are closely distributed around a consensus sequence. The viral mutation rate, and hence the magnitude of the challenge, vary amongst different viruses. In general mutation rates are higher for RNA viruses than DNA viruses (Sanjuán et al., 2010) and there is an inverse correlation between mutation rates and genome length (Bradwell et al., 2013).

The higher mutation rate in RNA viruses is generally considered to be due to the poor fidelity of the virally encoded RNA dependent RNA polymerase and, in most cases by the lack of any proof reading or error correction machinery (Lauring et al., 2013). Unique among RNA viruses, it has been shown that coronaviruses encode a proofreading exoribonuclease that is essential for maintaining replication fidelity (Denison et al., 2011; Minskaia et al., 2006), however even with this, mutation rates are thought to be similar to that of other RNA viruses (Sanjuán et al., 2010).

To be clinically useful an antiviral therapeutic must be efficacious against all, or at least the majority of field isolates. This is a considerable challenge particularly against viruses as genetically variable as coronaviruses, given that just a single nucleotide mismatch between an siRNA and its target site can render it ineffective (Du et al., 2005). Targeting conserved regions of the viral genome is one way to maximise coverage of field isolates (Naito et al., 2006). Such a strategy may also help to limit the development of escape mutants during treatment as highly conserved regions are more likely to be structurally or functionally constrained. During the siRNA design phase only a limited number of FCoV sequences were available. Conserved regions of the genome were identified for targeting using simple alignment and visual assessment. Based on the data available at the time, five of the eight siRNAs displayed 100% homology to all reported FCoV sequences. For two of the remaining siRNAs, a single nucleotide mismatch was seen in a single sequence, and for the final siRNA two mismatches in the target site were seen, again for a single sequence. Since the time of siRNA design a considerable number of FCoV sequences have become available. Analysis of siRNA target sites in the 35 full-length sequences available at the time of writing, confirmed that the target sites were highly conserved, with the percentage of strains showing complete target site homology ranging from 97% (siRNA L2) to 69% (siRNA N2). These results highlight the success of the simple approach utilised in this study for identifying suitable targets, however it is possible a more advanced approach for identifying appropriate siRNA targets in highly divergent viruses, such as that applied by Naito et al. (2006) or Lee et al. (2009), may identify additional, or better siRNA targets.

For initial screening, the effectiveness of siRNAs was assessed at the genetic level, measuring viral genomic and messenger RNA, and downstream, by a qualitative assessment of viral protein synthesis and quantification of the production of progeny virions. All of the siRNAs tested demonstrated an inhibitory effect on FCoV replication; however the magnitude of inhibition varied significantly. The highly effective siRNAs L2 and N1 were able to reduce extracellular virus titres by more than 95%, while less effective siRNAs such as L1 resulted in a reduction of approximately 60%. Such variability in potency between different siRNAs has been frequently encountered in RNAi studies, even when they target closely associated regions (Holen et al., 2002). This was demonstrated in the current study where the

extracellular virus titre for siRNA L2 was more than 10-fold lower than for siRNA L1, despite the two targeting contiguous regions of the genome.

Key to successful RNAi mediated gene knockdown, is the delivery of the triggering duplex into the cytoplasm. For chemically synthesised siRNAs in cell culture this is most commonly performed using a forward transfection protocol in which transfection complexes are added to pre-seeded cells. An alternative protocol, referred to as reverse transfection, involves simultaneously transfecting and plating cells, and is used frequently for high throughput screening of RNAi libraries (Echeverri and Perrimon, 2006). For the initial screening experiments a standard (forward) transfection protocol was used, however in some later studies performed, due to miniaturisation into a 96-well plate format, a reverse transfection protocol was utilised. Based on these studies a direct comparison of antiviral efficacy between transfection methods is not possible, as other assay parameters, including siRNA concentration, MOI, and duration of infection varied between experiments. Despite this, the level viral inhibition seen in later experiments using reverse transfection, based on a reduction in relative and absolute viral titres, was greater than would be expected based on the results from the screening experiment for all siRNAs tested using both methods. These results suggest that reverse transfection is more efficient in delivering siRNAs in CRFK cells, in agreement with the findings of Reid et al. (2009). Whilst the delivery of siRNAs to cells growing in culture is far removed from the practicalities of *in vivo* treatment, these results highlight the critical dependence of optimised siRNA delivery for therapeutic use to maximise antiviral efficacy.

For each siRNA treatment, the magnitude of inhibition determined by measurement of extracellular virus titre was greater than the inhibition seen in viral genome copy number. Although these two assays are looking at different endpoints, the consistent discrepancy may be in part explained by the fact that the qRT-PCR for viral genome is able to detect cleaved, and therefore non-infectious viral genomes, that have not yet been degraded, and thus likely underestimates the potency of the siRNAs. Viral mRNA was also assayed by qRT-PCR. For siRNAs targeting structural genes, the knockdown of the respective mRNA was greater than the knockdown of viral genome. This finding may be due to the viral genome being at least partially protected from the effects of these siRNAs, perhaps due to their association with viral proteins. A critical step in virus assembly is genome encapsidation by the nucleocapsid protein to form a helical nucleocapsid (Masters, 2006). The tight genome – nucleocapsid protein interaction may serve to partially protect progeny genomes from RNAi mediated degradation through steric hindrance of RISC access to the target site, as has been suggested for other viruses (Bitko and Barik, 2001; Hu et al., 2002). Differences in RNA secondary structure between the smaller viral mRNA and the full length genomic copies may also limit target site accessibility (Shao et al., 2007). Alternatively, the difference may be

attributed to the smaller mRNAs being degraded more rapidly following RISC mediated cleavage than the larger full length genome copies.

In this study we demonstrated that siRNAs L2 and N1 inhibit FCoV replication in a concentration-dependent manner. Importantly, both of these highly effective siRNA were still able to significantly inhibit FCoV replication at the lowest tested concentration. From a potential therapeutic point of view, efficacy at low concentrations is important as off-target effects associated with RNAi are in part concentration dependent (Behlke, 2006), and thus may be minimised by using low concentrations of highly potent siRNA.

In the screening and titration experiments cells were infected at a relatively low MOI (0.2). To assess the usefulness of the siRNAs in a therapeutic setting siRNAs L2 and N1 were tested at higher MOIs: 0.2, 2, and 20. The development of FIP is associated with high viral loads, and it was considered that the higher MOI would more accurately mimic the findings in a natural infection (Kipar et al., 2006a). Both siRNAs remained effective, showing greater than 75% inhibition of extracellular virus compared to the control samples even when challenged with a 100-fold increase in virus. As with the earlier experiments the reduction demonstrated in viral genome copies was less than the reduction in extracellular virus production. Again, a likely explanation is that qRT-PCR detects non-infectious cleaved genomic RNA prior to its degradation. This hypothesis would explain the significantly increased N1 qRT-PCR results compared with L2 results, as the target site and the location of the PCR primers in the former are separated by over 25 kb.

The development of antiviral resistance was proposed by Herrmann and Herrmann (1977) as a defining feature of a compound demonstrating specific antiviral effects, highlighting that the development of resistance to antiviral drugs during treatment is almost inevitable (Pillay and Zambon, 1998). This problem is particularly acute for nucleic acid based therapeutics that rely on Watson-Crick base pairing between the molecule and target for specificity. In contrast to small molecule antivirals, where the acquisition of resistance is often associated with conformational changes to viral proteins, and which may be associated with negative phenotypic effects, for RNAi-based antiviral therapeutics, resistance may be acquired by a single synonymous mutation in the target site, with no fitness cost to the virus. The acquisition of resistance has been shown to occur *in vitro* following short duration exposure to highly effective siRNAs for RNA viruses such as poliovirus (Gitlin et al., 2002; Gitlin et al., 2005), HIV (Boden et al., 2003; Das et al., 2004), and HBV (Wu et al., 2005b). In the current study we have similarly shown a rapid emergence of resistance following siRNA treatment, particularly in the case of monotherapy, where a resistant population was identified following a single passage in cells treated with siRNA L2 or N1, although in the latter case, based on sequencing, the resistant population was a minority.

Strategies for preventing or delaying the development of resistance include targeting siRNAs to conserved regions of the viral genome, targeting siRNA against cellular factors involved in viral replication or other factors that have the potential to effect viral fitness, or combination therapy with multiple siRNAs (or siRNAs and direct acting antivirals). Targeting conserved regions of the viral genome, in addition to increasing the likelihood of providing broad spectrum effects against circulating strains, may delay the development of resistance as such sites may be structurally or functionally constrained. It must be considered however that in many cases such constraints are at the protein level and that due to redundancy in the genetic code, synonymous mutations at the target site may occur with no effect on the structure of the encoded protein and therefore no fitness cost to the virus. Targeting *cis*-acting RNA elements may be a more appropriate target, as constraints for these sites may arise due to the primary or secondary structure of the RNA (Liu et al., 2009a), however high degrees of secondary structure may limit the access of RISC to such target sites. Dye and Siddell (2005) reported a number of putative *cis*-acting elements within the 5' and 3' UTRs of FCoV. One of these, the leader-TRS hairpin located within the 5' UTR was targeted by siRNAs L1 and L2 in the current study. Although the target site of L2 is highly conserved among published FCoV sequences, and it is entirely located within what is purported to be an important *cis*-acting element, antiviral resistance developed within a single passage when siRNA L2 was used as monotherapy in the current study, highlighting that additional methods are required to minimise the development of resistance.

Targeting siRNAs against cellular genes essential for viral replication is an alternative strategy for minimising the risk of resistance developing during treatment. Whilst viral escape is possible when targeting cellular cofactors, the evolutionary leap required is considerable, particularly when compared to the single nucleotide substitution required for viral mutational escape using traditional RNAi targeted at viral sequences (Leonard and Schaffer, 2005a). This approach has been successful *in vitro* against a number of viruses including HIV (Anderson et al., 2003; Eekels et al., 2011), HCV (Korf et al., 2005), and influenza A virus (Sun et al., 2010). *In vivo* success with this strategy has been shown for HIV, where siRNA mediated knockdown of CCR5, a co-receptor used for viral entry, was shown to protect humanised mice from HIV challenge (Kim et al., 2009). Targeting cellular cofactors significantly increases the risk of adverse events related to treatment, as cellular cofactors co-opted during viral replication may be essential for normal cell function. Identification of a suitable cellular target for knockdown is a critical first step for this approach. Further elucidation of the details of FCoV replication, in particular the cellular receptors/co-receptors may be informative in this regard. Recently published data by Harun et al. (2013) on the transcriptional profile of FCoV infected cells may also provide information

on novel cellular targets, as has occurred for other viruses using a similar approach (DeFilippis et al., 2003).

Treatment with a combination of siRNAs may be effective in delaying or preventing the emergence of resistant viruses, in the same manner that highly active antiretroviral therapy (HAART) using small molecule antivirals is used in HIV infected patients. HARRT, currently the recommended gold standard treatment, involves concurrent treatment with a combination of three or more small molecule antivirals, which when applied can significantly hinder the emergence of resistant viruses and is associated with reductions in morbidity and mortality (Shafer and Vuitton, 1999). Such combination therapy may act to minimise the development of resistance in a probabilistic sense due to the requirement for multiple simultaneous mutations to occur, or may act by causing a more rapid and pronounced reduction in the viral replication rate, resulting in an attendant reduction in the formation of mutant, and potentially resistant viruses (Hodge and Field, 2010). Regardless of the mechanism involved, experimental data, including that presented in the current work, confirms that combinatorial therapy with siRNAs can significantly delay the emergence of resistance (Gitlin et al., 2005; ter Brake et al., 2008; ter Brake et al., 2004; Wilson and Richardson, 2005).

The number of antivirals required to successfully inhibit the development of resistance is dependent upon factors related to the nature of the compounds, and the ease with which resistance can develop (the so called genetic barrier), in addition to the biological properties of viral replication, including the viral mutation and replication rates. Unfortunately for siRNA based antivirals the genetic barrier is low, with resistance easily developing with just a single synonymous nucleotide mismatch, meaning multiple siRNAs targeting independent sites would be needed. Whilst theoretically each additional antiviral added to a treatment regimen will further reduce the likelihood of resistance occurring during treatment, this must be balanced against the potential for increased toxicity or antagonistic effects that can arise with combination therapy. For RNAi-based therapeutics, each additional siRNA will compete for access to the RISC machinery, and thus combination therapy with multiple siRNAs may result in highly potent siRNAs being diluted by the presence of less potent molecules (Bitko et al., 2005; Castanotto et al., 2007). Similarly, competition for incorporation into RISC between siRNAs and endogenous microRNAs may increase the risk of off-target effects. Mathematical modelling can be performed to optimise combination therapy by estimating the probability of acquiring resistance using different numbers of antiviral compounds. Using a model for HIV that incorporated specific mechanistic features of RNAi-based inhibition, in addition to details regarding the biology of HIV replication *in vivo*, Leonard and Schaffer (2005b) showed that a combination of four siRNAs targeting independent regions of the genome would be sufficient to prevent the emergence of escape variants *in vivo*. These results are similar to those obtained using models for small molecule antivirals, where the

probability of acquiring resistance to a triple drug combination therapy (based on the probability of generating all possible 3-base mutations) during the course of an influenza A virus infection was in the order of 1×10^{-7} while for HIV, a slightly lower probability of approximately 1×10^{-8} (per day) was reported (Hoopes et al., 2011). The results of the current study support these theoretical calculations, in that it would appear for FCoV, that combination therapy with siRNAs targeting at least three independent regions would be required to minimise the development of resistance.

An interesting extension of the combinatorial therapy approach to minimising the emergence of resistance during treatment is to use a combination containing a highly effective siRNA in addition to number of siRNAs designed to recognise and inhibit the most likely escape sequences for that targeted region, a so-called second generation of siRNAs (Schopman et al., 2010). For this approach to be practical requires only a limited number of possible viral escape routes. Targeting highly conserved regions will maximise the probability of this occurring as mutations in these sites are more likely have deleterious effects on viral fitness leading to replication incompetent progeny. In the current study, despite targeting conserved regions, selection pressure due to siRNA treatment resulted in the generation of two unique mutations for L2 and three unique mutations for N1. Further large scale screening for escape sequences would be required to determine whether the mutations identified in the current small scale study represent the most likely route of viral escape, and also whether such an approach is practical for these targets based on the overall number of escape sequences possible. Recent studies using this approach with HIV have shown that although viral escape via mutations targeted by the second generation of siRNAs are inhibited, selection pressure results in the development of resistance via alternate routes (Schopman et al., 2010).

Whilst the previous discussion has focused on combinatorial therapy using multiple siRNAs, combination therapy with small molecule inhibitors and siRNAs has been reported to provide similar benefits (Vigne et al., 2009). In this regard combination therapy with effective siRNAs and one or more of the small molecule inhibitors identified in Chapter 4 may be a useful approach, however given that all are known to have an effect on aspects of the endocytic pathway, their use may affect the uptake and processing of exogenous nucleic acids (Khalil et al., 2006). Interestingly, chloroquine has been shown to increase the efficacy of RNAi and the uptake of siRNAs *in vitro* when using cell penetrating peptides for delivery (Veldhoen et al., 2006), and thus it may possible to achieve synergistic effects *in vivo* via this novel mechanism of enhancing cellular delivery. Conversely, antagonistic effects may be seen if a co-administered small molecule inhibitor results in reduced cytoplasmic entry of siRNAs.

The structure of the double-stranded RNA molecule responsible for mediating RNAi is a 21 nucleotide duplex hybridised to result in two nucleotide overhangs at the 3' end of each strand, often referred to as the "19 + 2" structure (Elbashir et al., 2001a). Chemically synthesised siRNAs are traditionally designed to mimic this structure, with a central 19 nucleotide duplex complementary to the target sequence, and with the overhangs commonly deoxythymidines. In the search for improved efficacy and reduced off-target effects, a range of non-classical siRNA structural variants have been investigated, some of which appear to offer advantages over the canonical "19 + 2" structure (Chang et al., 2007; Kim et al., 2005; Rose et al., 2005; Salomon et al., 2010). One of these, a 27 nt duplex referred to as a Dicer-substrate siRNA, was shown by Kim et al. (2005) to be 10 to 100 times more potent than its sequence matched canonical siRNA, without inducing interferon or protein kinase R. In addition to improved potency, DsiRNAs were reported to have an enhanced duration of action. Further refinement of the originally blunt-ended 27-mer duplex resulted in the DsiRNA structure used in the current study: a 25 nucleotide sense strand in which the two 3' terminal nucleotides are replaced with DNA, and a 27 nt antisense strand hybridised to give a blunt ended sense 3' terminus and 2 nt overhang at the sense 5' terminus (Amarzguioui et al., 2006; Amarzguioui and Rossi, 2008; Rose et al., 2005). Asymmetry and the incorporation of DNA bases into the DsiRNA structure results in the preferential incorporation of the antisense strand into RISC, improved complex formation with proteins known to be important for RNAi, as well as minimising the activation of the innate immune response (Amarzguioui et al., 2006; Snead et al., 2013). Not all published data however supports the contention that Dicer-substrate siRNAs offer any advantage over the canonical siRNAs on which they are based. Foster et al. (2012) compared the performance of DsiRNA and siRNA against a range of targets and found no class effect, with both canonical and Dicer-substrate siRNAs comparable in terms of potency and duration of activity, both *in vitro* and *in vivo* in this study. Dicer-substrate siRNA were also reported to be less tolerant of chemical modifications and more immunostimulatory, however in regards to antiviral therapy, the latter may actually be a desirable feature (Stewart et al., 2011).

In the current study the relative efficacy of canonical and Dicer-substrate siRNAs varied with target site. For monotherapy against target L2, and combination treatment for L2 and N1, DsiRNA were more potent, while there was little difference between siRNA and DsiRNA for monotherapy targeted at N1. Increased potency was greatest for combination therapy, with the IC50 of dual combination DsiRNA almost 10-fold lower than that for dual siRNA therapy. The duration of action appeared related to the potency of the molecule, with increased potency resulting in increased duration of activity. Previous studies investigating the duration of activity of canonical versus Dicer-substrate siRNAs have targeted cellular genes. In these cases the cessation of silencing is thought related to a reduction of intracellular siRNA due to

the activity of ribonucleases or through a dilution effect caused by cell division (Takahashi et al., 2012). In the current study the apparent cessation of antiviral effect may also be due to the emergence of resistant isolates or through a simple overwhelming of the RNAi machinery, as cells are exposed to progressively higher MOI as viral replication proceeds. Both of these hypotheses fit with the experimental data showing that prolonged duration of activity correlated with increased potency.

A potential limitation of this study is the lack of testing against a diverse range of FCoV isolates. The virus used in the current study was a type II FCoV. The prevalence of type II FCoV varies worldwide, however in all reported studies infection with type I viruses is more common (Pedersen, 2009). It is unlikely that the higher prevalence of type I infections would invalidate any therapeutic application of the siRNAs tested in this study, as the primary difference between type I and II FCoVs is the spike protein, a region not targeted by any of the tested siRNAs. Furthermore, siRNAs were selected in part based on homology to reported FCoV strains, including both type I and type II FCoVs, and subsequent alignment of siRNA targets against the most recently published sequences confirmed a high degree of conservation among both types.

In conclusion, whilst significant challenges remain to be overcome in the translation from *in vitro* to *in vivo* use of RNAi therapeutics, the preliminary information from the current study suggest that siRNA or DsiRNA mediated RNAi may be a useful therapeutic option for FIP. It is however unlikely that antiviral siRNA therapeutics, or any antiviral therapeutic for that matter, will be effective as a monotherapy in treating FIP. While increased viral replication is a triggering and perpetuating event in the disease pathogenesis, the characteristic pathological lesions of widespread serositis, vasculitis, and pyogranuloma formation, and the attendant clinical signs are immunopathological in nature. Thus effective treatment of FIP will likely require immunomodulatory therapy in addition to antiviral therapy. The results of this current study demonstrate that siRNA mediated RNAi may be an appropriate choice in fulfilling the latter requirement. Although not investigated in the current work, an RNAi-based approach directed at modulating the host immune response may offer a more targeted approach in addressing the former.

6

Identification and characterisation of a small molecule inhibitor of feline calicivirus

6.1. ABSTRACT

Feline calicivirus (FCV) is an important viral pathogen of domestic cats causing clinical signs ranging from mild or inapparent oral ulceration or upper respiratory tract disease through to a severe virulent, and often fatal systemic disease. Additionally, FCV is implicated in the pathogenesis of feline chronic gingivostomatitis syndrome, an intractable condition resulting in high morbidity and a significant reduction in quality of life. Current therapeutic options are limited, with no direct acting antivirals available for the treatment of FCV. To begin to address this shortfall, this chapter describes the *in vitro* screening of a panel of nineteen candidate compounds for antiviral activity against FCV strain F9. Of the compounds tested, only mefloquine, a potent schizonticidal drug used for the prevention and treatment of malaria, demonstrated a marked inhibitory effect, with an IC50 value of 6.94 µM based on CPE inhibition and a selectivity index of 3.18. Orthogonal assays confirmed inhibition of CPE was associated with a significant reduction in viral replication, with IC50 values as low as 0.79 µM based on reductions in extracellular viral titre. Mefloquine exhibited a strong inhibitory effect against a panel of seven recent FCV isolates from Australia, with calculated IC50 values for the field isolates approximately 50% lower than against the reference strain FCV F9. *In vitro* combination therapy with recombinant feline interferon-ω, a biological response modifier currently registered for the treatment of FCV, demonstrated additive effects with a concurrent reduction in the IC50 of mefloquine. These results are the first report of antiviral effects of mefloquine against a calicivirus and support further *in vitro* and *in vivo* evaluation of this compound as an antiviral therapeutic for FCV.

6.2. INTRODUCTION

A number of viruses in the family *Caliciviridae* are of medical and veterinary importance. Worldwide, human norovirus (genus *Norovirus*) is the major viral cause of gastroenteritis

(Wilhelmi et al., 2003). In veterinary medicine, rabbit haemorrhagic disease virus (genus *Lagovirus*) emerged in China in the mid-1980s as a highly virulent pathogen of lagomorphs. This virus, which typically results in a rapidly fatal systemic disease in susceptible rabbits, has subsequently spread worldwide, both through natural movements and, in the case of Australia and New Zealand, through intentional release as a biological control agent against the wild rabbit population (Abrantes et al., 2012). In domestic cats, feline calicivirus (FCV) (genus *Vesivirus*) is a common and important pathogen (Radford et al., 2007). Infection with FCV typically results in upper respiratory tract signs (often referred to as "cat flu") or ulcerative oral lesions. The majority of presentations are mild, although in young kittens disease may be more severe, and in some cases fatal. Less frequent disease manifestations associated with FCV include a lameness syndrome, pneumonia, and more recently the recognition of FCV-associated virulent systemic disease (FCV-VSD), a condition associated with high morbidity and mortality, even in previously vaccinated adult cats (Hurley and Sykes, 2003; Pedersen et al., 2000; Radford et al., 2007). FCV is also suspected in the pathogenesis of feline chronic gingivostomatitis syndrome (FCGS), a condition involving chronic inflammation of the oropharyngeal mucosa; however its role as a primary or perpetuating factor in this condition is unresolved (Lyon, 2005).

Both inactivated and modified live FCV vaccines are available to help control calicivirus-related disease in cats. Whilst generally effective at reducing the severity and duration of clinical signs, they do not prevent infection or shedding (Radford et al., 2007). Furthermore, due to the high level of antigenic variability amongst FCV isolates there are some concerns regarding the level of cross protection afforded by some the older vaccines (Radford et al., 2006). Of particular concern regarding vaccine efficacy is the observation that many cats with virulent systemic disease had been vaccinated (Hurley and Sykes, 2003). Whether lack of protection against VSD strains in vaccinated cats is due to antigenic variability and resulting poor cross neutralisation, or is due to other altered biological properties of the virulent strains remains unresolved, however regardless of the cause it is clear that therapeutic options are clearly needed for this rare, but devastating condition. Similarly, an effective and safe antiviral therapeutic for the more severe cases of oro-respiratory disease and chronic infections would be a significant advance for feline medicine.

There are currently no direct acting antiviral drugs registered for the treatment of FCV, although the immune modulating drug rFeINF-ω, which likely has indirect antiviral properties, has a registered indication for the treatment of FCV. Efficacy of both human and feline interferons has been demonstrated *in vitro* against FCV (Fulton and Burge, 1985; Mochizuki et al., 1994; Taira et al., 2005; Truyen et al., 2002) and it has been reported that the use of rFeINF-ω has a positive therapeutic effect in FCV infected cats in experimental and field efficacy trials (Ninomiya et al. 1991, Uchino et al. 1991, cited in Ohe et al. (2008)).

Treatment with rFeINF-ω was also associated with an improvement in clinical signs in cats with refractory FCGS in a double-blinded placebo-controlled study, however no attempt was made to monitor FCV shedding, and thus it is unclear whether the improvement was due to the antiviral or immunomodulatory properties of interferon (Hennet et al., 2011). The small molecule antiviral ribavirin markedly inhibits FCV *in vitro* (Povey, 1978b), however the drug was demonstrated to be ineffective in an experimental challenge where treatment had no effect on the course of disease or shedding, and was associated with significant toxicity (Povey, 1978a). Bovine lactoferrin has demonstrated antiviral effects against FCV in cell culture (McCann et al., 2003), and in a single case report in which the resolution of clinical signs of FCGS and the cessation of FCV shedding was attributed by the authors to bovine lactoferrin despite additional concurrent therapies (Addie et al., 2003a). Recently, feline calicivirus specific antiviral phosphorodiamidate morpholino oligomers (PMO) were tested in naturally occurring outbreaks of FCV-VSD (Smith et al., 2008). The oligonucleotide antivirals were highly efficacious, with treatment resulting in improved survival, reduction in shedding, and a more rapid clinical recovery.

The aim of this study was to screen a panel of compounds for antiviral activity against FCV using the optimised resazurin-based CPE inhibition assay described in Chapter 3. The compounds tested in this study had demonstrated antiviral effects, in many cases broad spectrum effects, against a number of RNA viruses. The antiviral effects of compounds identified during screening were confirmed with plaque reduction and virus yield reduction assays. Effective compounds were tested against a panel of recent FCV field isolates from Australia to confirm their effectiveness against more clinically relevant viruses. Effective compounds were also tested in combination with rFeINF, currently the only licenced treatment for FCV in Australia.

6.3. MATERIALS AND METHODS

6.3.1. Antiviral screening using CPE inhibition assay

Antiviral screening was performed with a resazurin-based CPE inhibition assay using the optimised assay parameters for FCV detailed in Chapter 3 (summarised in Figure 3.18). Test compounds and screening concentrations were as described in Sections 4.3.1 and 4.4.1 respectively, and plate layout was as shown in Figure 4.2. Each treatment was performed in triplicate and results represent Mean ± SE of three independent experiments. Compounds showing marked, moderate, or mild antiviral effects were defined as those showing 75-100%, 50-74%, and 25-49% inhibition of CPE respectively. Compounds demonstrating marked CPE inhibition were classified as candidate compounds and were selected for further characterisation.

6.3.2. Titration of candidate compounds and determination of selectivity index

Using the optimised FCV CPE inhibition assay (Figure 3.18), a concentration-response experiment was conducted with serial dilutions of candidate compounds identified during screening. To enable calculation of the selectivity index a repeat cytotoxicity screen was performed concurrently. The cytotoxicity screen was performed as per the CPE inhibition assay with the exception that cells were mock infected with DMEM. Each treatment was performed in triplicate and repeated in three independent experiments, with results presented as Mean ± SE. IC50, CC50, and SI values were calculated as described in Section 4.3.4.

6.3.3. Confirmatory assays

6.3.3.1. Virus yield reduction assay

Virus yield reduction assays were performed in 24-well plates (Sarstedt) seeded with 6.0 x 10^4 cells.ml^{-1} in 400 µl DMEM-10. Plates were incubated at room temperature for 30 min and then 37°C in 5% CO_2 in air for 6 h prior to the addition of 75 µl test compound diluted to the appropriate concentration in DMEM. Five concentrations of test compound were assessed. After 1 h of compound exposure, cells were infected with FCV F9 at MOI of 0.05 in 25 µl DMEM. At 12 and 24 hpi cellular morphology was assessed for CPE using an inverted phase contrast microscope (CKX41, Olympus) and supernatant was harvested and stored at -80°C prior to titration of extracellular virus (Section 2.3.2.3.2). The relative viral titre was calculated for each treatment with the value of untreated control defined as 100%. Each treatment and time point was performed in triplicate and repeated in two independent experiments. Results represent Mean ± SE.

6.3.3.2. Plaque reduction assay

Plaque reduction assays were performed in 6-well plates (Sarstedt) using a modification of the standard plaque assay for FCV titration (Section 2.3.2.3.1). Cells seeded at 1.2 x 10^4 cells.well^{-1} in 2 ml DMEM-10 were incubated for 60 h until approximately 90% confluent. Culture media was discarded and replaced with 700 µl DMEM-2 plus 75 µl of five different dilutions of test compounds in DMEM (or 75 µl DMEM for control wells). After exposure to the compound for 1 h cells were infected with approximately 60 pfu.well^{-1} FCV F9 in 25 µl DMEM. Virus was allowed to adsorb for 90 min with plates rocked every 15 min to ensure an even distribution of inoculum. After 90 min culture media was discarded and cells overlaid with 2 ml 0.9% CMC plaque assay overlay media containing the same concentration of compound as present prior to, and during infection. Incubation, fixation, staining, and counting of plaques was as previously described in Section 2.3.2.3.1. The relative plaque number was calculated for each treatment with the value of untreated control defined as

100%. Each treatment was performed in duplicate, and the results represent Mean ± SE of three independent experiments.

6.3.4. Antiviral efficacy against field isolates of FCV

Given the known genetic variability of FCV and the unknown passage history of the tested FCV F9 strain we sought to determine whether compounds identified as effective against FCV F9 were also efficacious against currently circulating field isolates. Using the optimised FCV CPE inhibition assay (Figure 3.18) cells were pre-treated with identified candidate compounds for 1 h prior to infection with FCV isolates 83E, 131M, 178N, IW1E, IW10, IW16, IW25, or F9. Details of these viruses have been previously reported in Table 2.1. Untreated cells were also infected with the different isolates as virus controls and uninfected and untreated cells included as positive controls. Each treatment was performed in triplicate wells for each virus, and repeated in three independent experiments. Percentage inhibition of virus induced CPE was calculated using the following formula:

$$CPE\ inhibition\ (\%) = \frac{RFU_{Tx} - RFU_{V(+)}}{RFU_{V(-)} - RFU_{V(+)}} \times 100$$

Where RFU_{Tx} is the mean fluorescence intensity of treated cells infected with a specific FCV isolate; $RFU_{V(+)}$ is the mean fluorescence intensity in untreated cells infected with the same isolate; and $RFU_{V(-)}$ is the average fluorescence intensity of untreated uninfected cells. Data expressed as Mean ± SE.

To further investigate the antiviral efficacy against different isolates a concentration-response study was conducted using field isolates 178N and IW1E. The concentration-response experiment was conducted as detailed in Section 6.3.2 with the exception that cells were infected with field isolates. Each treatment was performed in triplicate and results represent Mean ± SE of three independent experiments. Calculation of IC50, CC50, and SI values was performed as described in Section 4.3.4.

6.3.5. Combination treatment with mefloquine and rFeINF-ω

Recombinant feline interferon omega is currently registered for the treatment of feline calicivirus infections. Using the optimised FCV CPE inhibition assay (Figure 3.18) cells were pre-treated with varying combinations of rFeINF-ω and mefloquine at concentrations from 0 to 1000 units.ml^{-1} and 0 to 12 µM respectively prior to infection with FCV F9 at MOI 0.01. Each treatment was performed in triplicate and repeated in three independent experiments with data presented as Mean ± SE. IC50 values were calculated as described in Section 4.3.4.

6.4. RESULTS

6.4.1. Antiviral screening using CPE inhibition assay

Mefloquine, at a concentration of 10 μM, was the only compound of the nineteen tested that demonstrated marked inhibition (88.6%) of virus induced CPE (Figure 6.1). All other compounds demonstrated a limited, or no inhibitory effect on CPE. Included among these are four compounds – ribavirin, lactoferrin, chloroquine, and rFeINF-ω – that had previously demonstrated *in vitro* efficacy against FCV (Kreutz and Seal, 1995; McCann et al., 2003; Povey, 1978b; Truyen et al., 2002).

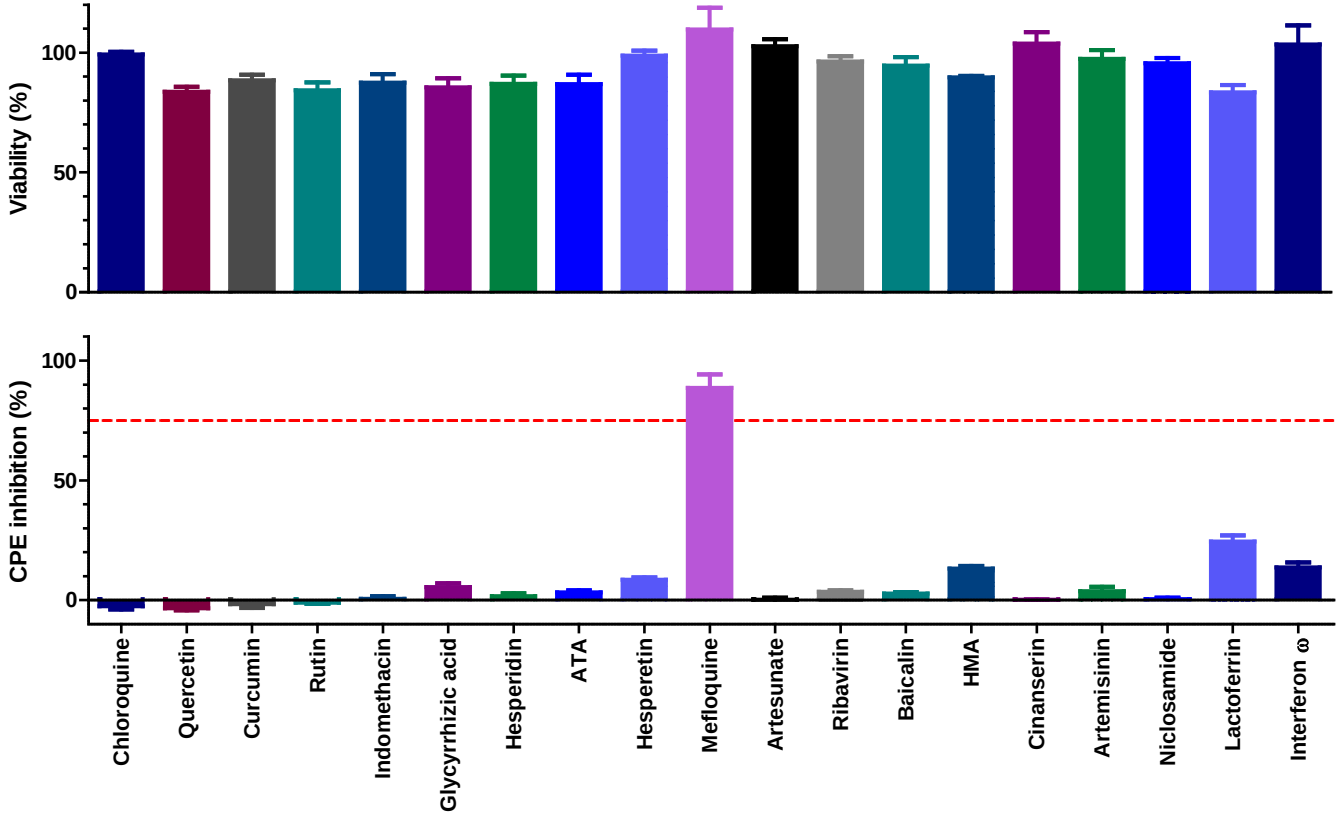

Figure 6.1: Results of FCV antiviral screening experiment. Cells were pre-treated with various compounds for 1 h prior to infection with FCV F9 at MOI 0.01. Antiviral efficacy was determined 48 hpi using the resazurin-based CPE inhibition assay. A concurrent cytotoxicity screen was performed using the same protocol with the exception that cells were mock infected. Each treatment was performed in triplicate and repeated in three independent experiments. Results represent Mean ± SE. ATA, aurintricarboxylic acid; HMA, hexamethylene amiloride. Red dotted line = 75% inhibition of CPE.

6.4.2. Titration of candidate compounds and determination of selectivity index

To confirm and further characterise the antiviral properties of compounds identified during initial screening, a concentration-response study was conducted with mefloquine. A repeat cytotoxicity screen was also performed to allow calculation of the selectivity index under identical conditions. The inhibition of CPE demonstrated a clear concentration-response relationship, with almost complete inhibition at the highest tested concentrations reducing to zero inhibition at lowest tested concentration (Figure 6.2). Calculated IC50, CC50, and SI values are shown in Figure 6.2.

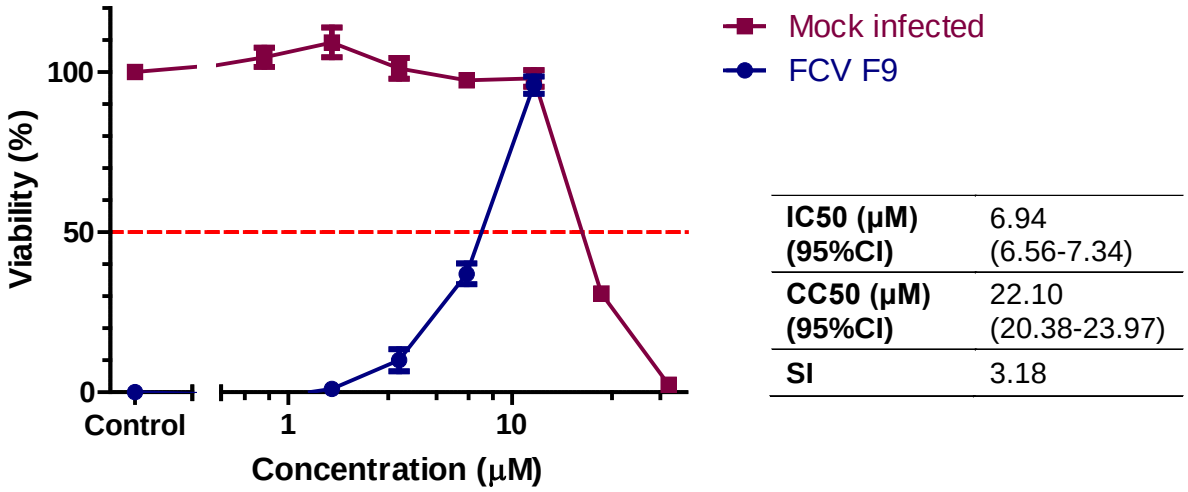

IC50 (µM) (95%CI)	6.94 (6.56-7.34)
CC50 (µM) (95%CI)	22.10 (20.38-23.97)
SI	3.18

Figure 6.2: Titration of mefloquine against FCV using the resazurin-based CPE inhibition assay. Cells were pre-treated with serial dilutions of mefloquine for 1 h prior to infection with FCV F9 at MOI 0.01. Antiviral efficacy was determined 48 hpi using the resazurin-based CPE inhibition assay. A concurrent cytotoxicity screen was performed using the same protocol with the exception that cells were mock infected. Each treatment was performed in triplicate and repeated in three independent experiments. Results represent Mean ± SE. Calculated IC50, CC50, and SI values are shown in the accompanying table.

6.4.3. Confirmatory assays

6.4.3.1. Virus yield reduction assay

Virus yield reduction assays confirmed that CPE inhibition identified using the resazurin-based screening assay was associated with a marked reduction in extracellular viral titre. Extracellular viral titres at 12 and 24 hpi demonstrated a concentration-response relationship (Figure 6.3). At high concentrations reductions in viral titre at 24 hpi was greater than 3 $\log_{10}$, while at 12 hpi this reduction was reduced to between 1-2 $\log_{10}$. Calculated IC50 and SI values for at 12 and 24 hpi are shown in Figure 6.3.

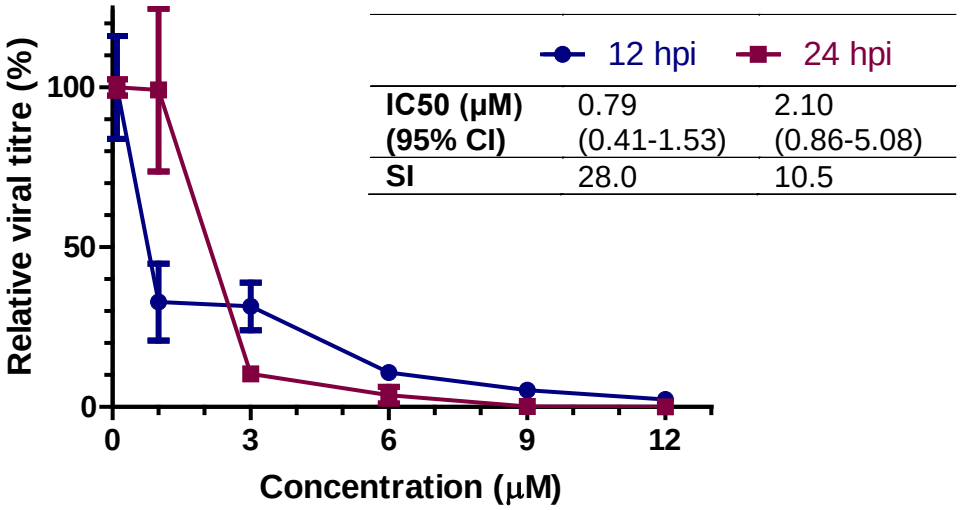

	12 hpi	24 hpi
IC50 (μM) (95% CI)	0.79 (0.41-1.53)	2.10 (0.86-5.08)
SI	28.0	10.5

Figure 6.3: Virus yield reduction assay for mefloquine against FCV. Cells were pre-treated with various dilutions of mefloquine for 1 h prior to infection with FCV F9 at MOI 0.05. Extracellular virus titre was calculated at 12 (blue circles) and 24 hpi (red squares) with a TCID50 end point assay. Titre of untreated control is defined as 100%. Each treatment was performed in triplicate and repeated in two independent experiments. Data represent Mean ± SE. Calculated IC50 and SI values for each time point are shown in the accompanying table.

6.4.3.2. Plaque reduction assay

Plaque reduction assays confirmed the findings of the resazurin-based CPE inhibition assay. Pre-treatment with mefloquine resulted in a concentration-dependent reduction in plaque number (Figure 6.4). Plaque size and morphology varied considerably in both treated and untreated cells, however in general plaque size was smaller and plaque morphology more consistent in wells treated with higher concentrations of mefloquine. Calculated IC50 and SI values are shown in Figure 6.4.

a.

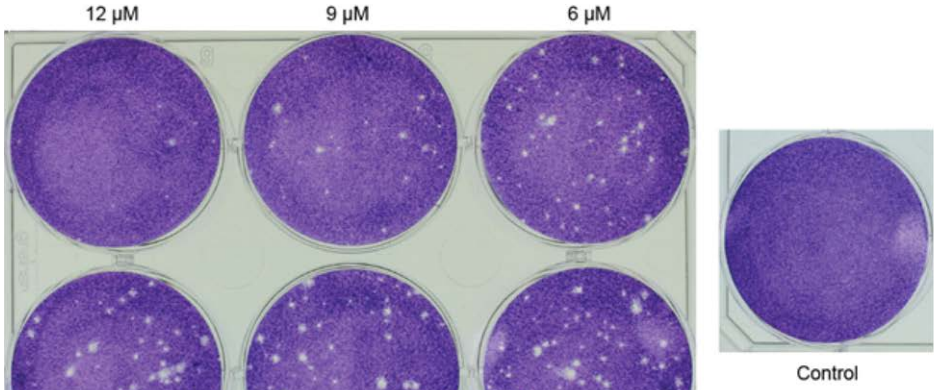

b.

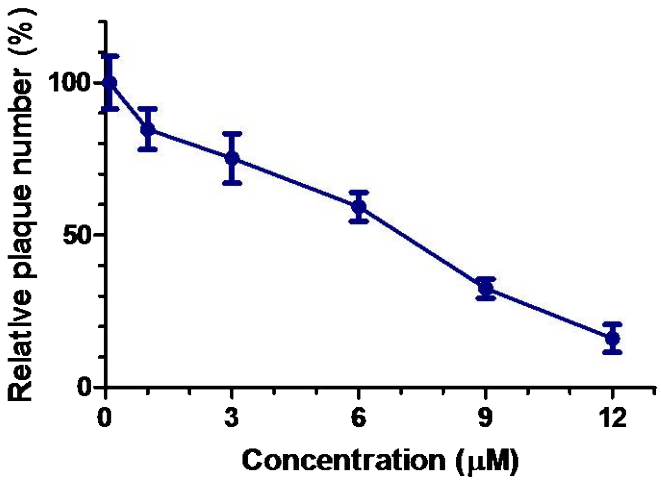

IC50 (µM)	6.03
(95% CI)	(5.43-6.70)
CC50 (µM)	22.10
(95% CI)	(20.38-23.97)
SI	3.67

Figure 6.4: Plaque reduction assay for mefloquine against FCV. Cells were pre-treated with various concentration mefloquine for 1 h prior to infection with approximately 60 pfu.well^{-1} FCV F9. Virus was allowed to adsorb for 90 min and the cells overlaid with culture media containing 0.9% CMC and an equivalent concentration of test compound. Cells were fixed and stained 36 hpi. Each treatment was performed in duplicate and repeated in three independent experiments. Panel (a) shows a representative plate demonstrating in the concentration-dependent inhibition of plaque formation and the variation in plaque size/morphology. Panel (b) shows relative plaque number for mefloquine treated wells compared to untreated control wells. Results represent Mean ± SE. Plaque number of untreated wells defined as 100%. Calculated IC50 and SI values are shown in the accompanying table.

6.4.4. Antiviral efficacy against field isolates

To assess the potential usefulness of mefloquine in a clinical setting an experiment was conducted to determine its antiviral efficacy against a panel of recent field isolates. Mefloquine demonstrated greater than 90% inhibition of virus induced CPE against all tested isolates at a concentration of 12.5 µM (Figure 6.5).

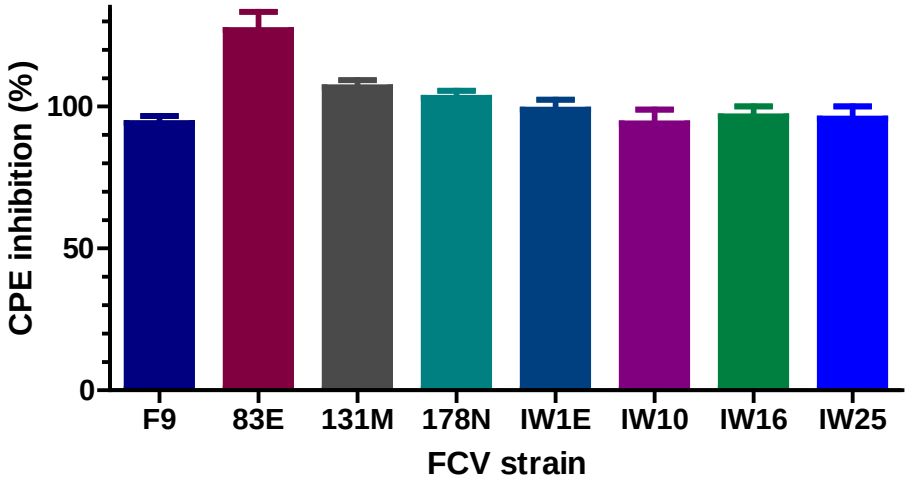

Figure 6.5: Antiviral efficacy of mefloquine against recent Australian field isolates of FCV. Cells were pre-treated with 12.5 µM mefloquine for 1 h prior to infection at MOI 0.01. Antiviral efficacy was determined 48 hpi using the resazurin-based CPE inhibition assay. Each treatment was performed in triplicate and repeated in three independent experiments. Results represent Mean ± SE.

To assess any quantitative difference in the efficacy of mefloquine against different field isolates a concentration-response experiment was conducted using two field isolates, IW1E and 178N. Mefloquine demonstrated concentration-dependent inhibition of both isolates, with similar shaped dose-response curves and IC50 values (Figure 6.6). Calculated IC50 and SI values for these isolates, in addition to the previously calculated values for FCV F9 are shown in Figure 6.6. These data confirm that mefloquine was more potent against field isolates than the reference strain, with IC50 values for the field isolates less than half of that for FCV F9.

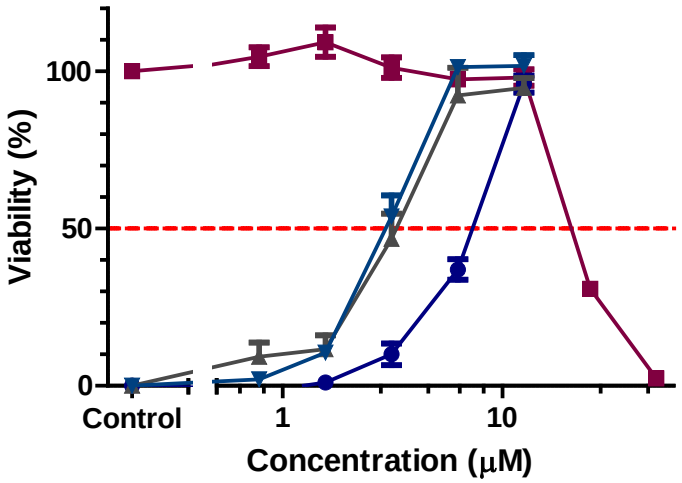

	F9	178N	IW1E	Mock infected
IC50 (μM) (95%CI)	6.94 (6.56-7.34)	3.16 (2.72-3.68)	2.94 (2.75-3.14)	
SI	3.18	6.68	7.52	

Figure 6.6: Antiviral titration of mefloquine against Australian field isolates of FCV. Cells were pre-treated with serial dilutions of mefloquine for 1 h prior to infection with FCV isolate 178N or IW1E at MOI 0.01. Antiviral efficacy was determined 48 hpi using the resazurin-based CPE inhibition assay. Each treatment was performed in triplicate and repeated in three independent experiments. Results represent Mean ± SE. Results of previous titration of mefloquine against FCV F9 and cytotoxicity screening reported in Section 6.4.2 are included for comparison.

6.4.5. Combination treatment with mefloquine and rFeINF-ω

As shown in Figure 6.7, rFeINF-ω exerted concentration-dependent additive antiviral effects *in vitro* when combined with mefloquine. Increasing the rFeINF-ω concentration from 0 to 500 units.ml^{-1} resulted in a shift of the concentration-response curve to the left with a corresponding decrease in the calculated IC50 value. The additive effect of rFeINF-ω on the antiviral efficacy of mefloquine appeared to peak at 500 units.ml^{-1} as increasing the concentration above this was not associated with a reduction in the IC50 value.

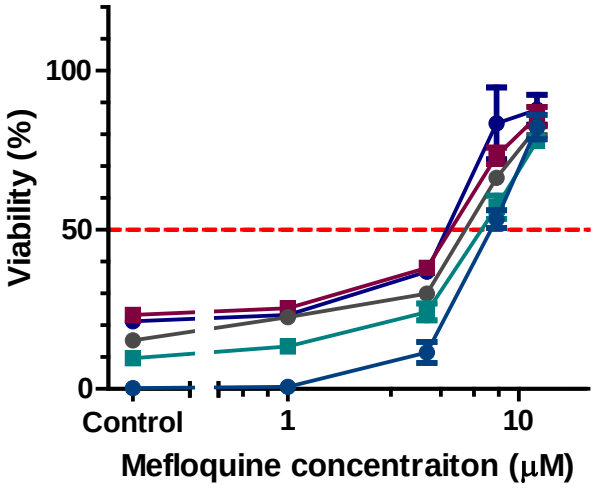

	rFeINF-ω (units.ml^{-1})				
	1000	500	100	10	0
IC50 (μM)	3.96	3.92	5.19	6.75	7.61
(95% CI)	(2.62-5.99)	(2.62-5.88)	(3.89-6.91)	(5.84-7.79)	(7.23-8.02)

Figure 6.7: Effect of combination treatment with mefloquine and rFeINF-ω against FCV F9. Cells were pre-treated with varying combinations of rFeINF-ω and mefloquine prior to infection with FCV F9 at MOI 0.01. Antiviral efficacy was determined 48 hpi using the resazurin-based CPE inhibition assay. Each treatment was performed in triplicate and repeated in three independent experiments. Results represent Mean ± SE. IC50 values for mefloquine were calculated for each rFeINF-ω concentration.

6.5. DISCUSSION

In this study we have demonstrated a marked inhibitory effect of mefloquine on the replication and associated cytopathic effects of FCV in cell culture. Initial screening and confirmatory assays were performed with the culture adapted vaccine strain F9; however subsequent testing against a panel of seven currently circulating Australian field isolates demonstrated the antiviral efficacy remained excellent against potentially more relevant viruses, with concentration-response studies confirming that mefloquine is a more potent inhibitor of field isolates than the vaccine strain. Combination treatment with rFeINF-ω resulted in additive effects with a reduction in the IC50 value for mefloquine. These data provide important preliminary information into the use of mefloquine as an antiviral therapeutic for the treatment of FCV-associated diseases.

In this study the panel of nineteen compounds previously screened for inhibitory effects against FCoV (Table 4.1) were tested for antiviral efficacy against FCV. Given the essentially infinite nature of the small molecule chemical space, as well as practical and

financial considerations relating to testing large numbers of compounds, a rational approach to compound selection was used to define this panel to increase the likelihood of identifying effective molecules. Criteria for selection were based on previously documented antiviral efficacy against RNA viruses, with the panel including several compounds that had previously demonstrated *in vitro* antiviral effects against FCV. Unlike compound selection for FCoV, which has benefited from many years of successful research into antiviral therapy for human coronaviruses (particularly SARS-CoV), the field of calicivirus antiviral research is extremely limited, and did not provide a similar large pool of potential candidates. Therefore the finding that only a single compound from this panel, mefloquine, demonstrated marked inhibition of virus induced CPE during the screening study, compared to the three highly effective compounds identified for FCoV in Chapter 4, is not surprising given the compound panel tested was enriched for potentially effective anti-FCoV antivirals.

The marked inhibitory effect of mefloquine demonstrated in the CPE inhibition assay was confirmed with orthogonal testing using virus yield reduction and plaque reduction assays. As was shown for FCoV in Chapter 4, the IC50 value calculated using the virus yield reduction assay was significantly lower than that calculated with the CPE inhibition assay. Although the virus yield reduction assay therefore appears more sensitive, its use in screening, particularly involving large numbers of compounds, is limited due to practical difficulties of performing the assay on a large scale.

Initial screening and the orthogonal confirmatory assays were performed with FCV F9, a well characterised strain originally isolated in 1958 (Glenn et al., 1999). FCV F9 was chosen for screening purposes due to its well characterised *in vitro* growth properties, however it is unclear whether FCV F9 used in the current study is representative of currently circulating viruses, due to natural viral evolution of circulating field viruses over the last half century (including evolution in the face of vaccination with F9 based vaccines), and perhaps more importantly, in light of the unknown passage history of our particular F9 strain. Cell culture adaptation, as can occur with high passage levels, may significantly alter the biological properties of a virus. It is therefore possible that results obtained against FCV F9 may not be representative of efficacy against circulating strains, particularly given the known genetic heterogeneity of FCV (Coyne et al., 2012) . To overcome this limitation and to ascertain the likely spectrum of coverage and potency against field isolates, additional antiviral screening was performed against a panel of seven recent FCV isolates from Australia. Such a study provides important information as it is well recognised that antiviral efficacy can vary against different circulating strains. Variation can arise rapidly due to viral evolution in response to selection pressures imposed by the use of an antiviral drug in a population, however variation in sensitivity may also pre-exist in a treatment naive population. This was demonstrated, for example, in a study by Ferraris et al. (2005) which showed significant

variability in the sensitivity of influenza A viruses to the neuraminidase inhibitors zanamivir and oseltamivir, even in viruses isolated prior to the widespread use of these drugs. In contrast, in the current study all tested FCV isolates were susceptible to the inhibitory effects of mefloquine based on the CPE inhibition assay. A concentration-response study demonstrated a greater than two-fold increase in potency against the field isolates compared to the reference virus FCV F9. Although further studies are required to determine whether this is a general feature of field isolates, or whether unique to the two tested isolates, it does highlight that consideration must be given to the viral strain used for screening.

Combination antiviral therapy offers several potential theoretical benefits over monotherapy including a more rapid and complete inhibition of replication, a reduction in the likelihood of viral escape, and may also potentially allow a reduction in the dose of individual drugs, and thereby minimise adverse effects. Combination therapy is not without risk however, and therefore combination therapy should be tested to investigate the potential for antagonism between the agents and overlapping toxicities. The use of combination antiviral therapy is common practice in significant human viral infections such as HIV and HCV (Feld and Hoofnagle, 2005; Shafer and Vuitton, 1999). For HCV, combination therapy of ribavirin, a direct acting antiviral, and interferon has for a long time been the standard of care, and has demonstrated good clinical success (Feld and Hoofnagle, 2005). As rFeINF-ω is an approved therapeutic in cats we sought to investigate its use in combination with mefloquine. Interferon monotherapy has previously demonstrated small antiviral effects against FCV *in vitro* with Mochizuki et al. (1994) reporting a reduction in extracellular viral titre of 0.2 $\log_{10}$ when CRFK cells were pre-treated for 24 h with 100 units.ml^{-1} rFeINF-ω, while Truyen et al. (2002) demonstrated a 0.1 $\log_{10}$ reduction in titre when cells were treated with 5 x 10^4 units.ml^{-1} at 1 hpi. *In vivo* efficacy has also been reported in experimental and field studies of FCV (Ninomiya et al. 1991, Uchino et al. 1991, cited in Ohe et al. (2008)). At the concentration used in the current study however, monotherapy with rFeINF-ω provided limited protection from CPE. Combination therapy with rFeINF-ω and mefloquine demonstrated additive effects, with increasing concentrations of interferon resulting in a reduction in the IC50 of mefloquine. This combination may prove a useful therapeutic option for FCV infections, particularly if it allows a reduction in the dose of mefloquine.

The results of this study further expand the known antiviral spectrum of mefloquine. Efficacy against HIV and JC virus has been previously reported (Brickelmaier et al., 2009; Owen et al., 2005) and from the previous work in this thesis (Chapter 4) we demonstrated efficacy against FCoV. The mechanism of action of mefloquine against this diverse group of viruses is not known, nor is it clear whether antiviral efficacy against these viruses is due to a common broad spectrum mechanism of action. Investigations into the likely mechanism of action of mefloquine against FCV were not conducted in the current study. Given the

documented effects of mefloquine on endocytosis, and the morphological changes suggestive of alterations in these pathways in CRFK cells previously reported in Section 4.4.4, it is tempting to speculate that the antiviral effects against FCV may arise through perturbation of these pathways. Cellular entry of FCV occurs via receptor mediated endocytosis following binding to the cellular receptor fJAM-A (Stuart and Brown, 2006). Treatment with known inhibitors of different steps of viral entry, including inhibitors of endocytosis, revealed FCV entry involves clathrin coated pits and that endosome acidification was required for infection, in agreement with a previous report by Kreutz and Seal (1995) that showed that chloroquine inhibited viral replication. As previously mentioned, under the assay conditions of the current study chloroquine provided no protection against virus induced CPE, suggesting that if viral inhibition was arising though the lysosomotropic effects of mefloquine (Glaumann et al., 1992), this effect is considerably more potent for mefloquine than for chloroquine. Alternatively, a mechanism unrelated to its accumulation in lysosomes, such as an action as an adenosine analogue as hypothesised for JC virus (Brickelmaier et al., 2009), may account for the observed antiviral effects.

As considered in Section 4.5.2, although mefloquine is a human approved pharmaceutical with a significant body of literature regarding its pharmacokinetics and safety, its use in cats has not been reported. It is well recognised that due to deficiencies in a number of drug metabolism pathways, the pharmacokinetics of certain drugs in cats can be quite different to those of other species, a fact which should be borne in mind when extrapolating human pharmacokinetic data to this species (Court, 2013). The IC50 value calculated for the field isolates, based on inhibition of CPE, was approximately 3 µM which is lower than plasma concentrations of mefloquine reported in human studies (4 to 23 µM depending on dosing regimens) (Kollaritsch et al., 2000; Simpson et al., 1999). Thus, extrapolating from the available data, it would appear that it may be possible to achieve *in vivo* concentrations of mefloquine within the therapeutic range.

In addition to the marked inhibitory effect of mefloquine, three additional compounds, lactoferrin, rFeINF-ω, and hexamethylene amiloride demonstrated small reductions in CPE (24.4%, 13.6% and 13.2% respectively) during screening. The antiviral effect of these compounds as monotherapies was not further investigated in this study.

The *in vitro* efficacy of lactoferrin against FCV was previously reported by McCann et al. (2003), with a reduction in virus induced CPE reported when cells were exposed to concentrations of 1 $mg.ml^{-1}$ for 1 h concurrent with infection. A restricted window of exposure was used in this study as the authors reported concentrations as low as 0.1 $mg.ml^{-1}$ resulted in significant cytotoxicity when cells were exposed for the entire 24 h duration of the experiment. In contrast, under the conditions of our screening assay, that is continuous

exposure for 48 h, significant cytotoxicity was not evident at concentrations below 0.5 $mg.ml^{-1}$. Using this concentration however resulted in limited efficacy in our assay system. The therapeutic benefit of topical lactoferrin for FCGS associated with FCV has been reported in a single case report, where topical treatment (200 mg sprinkled directly onto oral lesions), in addition to thalidomide given orally, was associated with a resolution of clinical signs and cessation of FCV shedding (Addie et al., 2003a). Lactoferrin had previously been shown to have positive effects on clinical signs in FIV-positive and FIV-negative cats with intractable stomatitis, however the calicivirus status of these cats was unknown (Sato et al., 1996). In both of these reports it is possible that the therapeutic benefit derived from lactoferrin was due to its immunomodulatory properties (Conneely, 2001; Weinberg, 2003), with the cessation of calicivirus shedding in the report by Addie et al. (2003a) possibly attributable to an enhanced immune response due to lactoferrin rather than specific anti-calicivirus effects. Regardless of the cause, the results from the current study, in addition to the possibility that significantly higher concentrations of lactoferrin can be achieved with topical therapy without any apparent ill effects, do not exclude a potential therapeutic role for lactoferrin in treating FCV-positive FCGS.

Similar to lactoferrin, topical use of interferon has been proposed as a treatment for FCGS. In a study by Hennet et al. (2011) daily oromucosal treatment with 1×10^5 units rFeINF-ω has been shown to improve clinical lesions and reduce pain scores, however its effect on calicivirus shedding was not studied, and again the clinical improvement seen may have been due immunomodulatory rather than antiviral effects. Despite the limited antiviral efficacy of rFeINF-ω demonstrated in the current study, given that high local concentrations are attainable with topical therapy, and the pleiotropic effects of interferons, rFeINF-ω may be a useful therapeutic option for FCGS associated with FCV.

Amiloride, and its more potent derivative 5-(N-Ethyl-N-isopropyl) amiloride have also demonstrated inhibitory effects on FCV (Stuart and Brown, 2006), however in this study hexamethylene amiloride did not provide any protection against CPE. As discussed previously, this may be due to the different assay conditions or testing at sub-therapeutic concentrations, or it may be due to differential antiviral effects of amiloride derivatives as has been previously described (Wilson et al., 2006b).

The lack of effect of two of the other tested compounds is worth mentioning. In studies to elucidate the mechanism of FCV entry, chloroquine has previously been shown to inhibit viral replication based on reduction in extracellular viral titres and viral protein expression when present at the time of infection (Kreutz and Seal, 1995; Stuart and Brown, 2006). In the study by Kreutz and Seal (1995) pre-treatment with 25 μM chloroquine, the same concentration used in the current screening assay, resulted in a 50% reduction in

extracellular virus titres determined 8 hpi. It is not therefore surprising that chloroquine demonstrated no protective effect against CPE in the screening assay, given that the CPE inhibition assays appear less sensitive to small antiviral effects and that the infection period of the current study was six times longer than that previously tested. Finally, ribavirin demonstrated no inhibitory on FCV, contrary to previous reports (Povey, 1978b), however similar to the lack of efficacy reported against FCoV in Chapter 4, this was most likely due to screening at a sub-therapeutic concentration.

In conclusion this study has identified mefloquine as a potent inhibitor of FCV *in vitro* when present at low micromolar concentrations. This represents the first report of the antiviral activity of mefloquine against a calicivirus. Testing against a panel of recent Australian FCV isolates demonstrated the antiviral effects of mefloquine against the reference strain FCV F9 extend to more clinically relevant isolates, and there was no evidence of antagonism when used concurrently with rFeINF-ω. Based on these results further investigation is warranted into the therapeutic use of mefloquine for treating the more serious manifestations of FCV infection. Consideration should also be given to investigating the effectiveness of mefloquine against other members of the family *Caliciviridae*.

7

In vitro inhibition of feline calicivirus using RNA interference

7.1. ABSTRACT

Feline calicivirus is a common infection of domestic cats. In most cases infections are mild and self-limiting; however the recent identification of a severe systemic form of the disease, associated with a high mortality rate, has highlighted the lack of effective treatments for feline calicivirus related diseases. In this study, a panel of eight siRNAs were designed targeting four conserved regions of the feline calicivirus genome. siRNAs were screened for *in vitro* antiviral efficacy against FCV F9 by determination of extracellular virus titres and morphological assessment of protection from cytopathic effect. Three of the tested siRNA (FCV3.7, FCV4.1, and FCV4.2) demonstrated a marked antiviral effect with a greater than 99% reduction in extracellular viral titre. Titration of these effective siRNAs demonstrated a clear concentration-response relationship, with IC50 values of approximately 1 nM, and combination treatment with multiple siRNAs demonstrated additive or synergistic effects. To assess the likely usefulness of the compounds in a clinical setting, siRNAs were screened against a panel of six recent Australian FCV isolates. The siRNAs shown to be effective against the reference strain FCV F9 were broadly active against the majority of the isolates tested, although some variability was noted. Taken together these results suggest that an RNAi-based approach may be a useful therapeutic option for treating severe FCV-associated disease in cats.

7.2. INTRODUCTION

Feline calicivirus is a highly prevalent pathogen in domestic cats. As a Baltimore group IV virus, replication of feline calicivirus is dependent upon a virally encoded RNA dependent RNA polymerase (RdRp). Due to the poor replicative fidelity of this enzyme, FCV is a genetically diverse virus. One consequence of this genetic variation is the existence of viral biotypes that differ in the nature and the severity of the disease they induce. Many FCV infections are mild and self-limiting, or result in no overt signs of disease, however more severe, and sometimes fatal manifestations do occur. The most notable of these, referred to

as FCV-associated virulent systemic disease (FCV-VSD), was first reported in 2000 in the United States (Pedersen et al., 2000), although descriptions of sporadic cases of severe multisystemic calicivirus disease pre-date this report (Ellis, 1981; Love and Baker, 1972). The role of FCV in the pathogenesis of VSD is unquestioned given the condition can be experimentally recreated with viruses isolated from infected cats (Pedersen et al., 2000). Subsequent to the initial report, FCV-VSD outbreaks have now been seen in many countries with mortality rates in excess of 50% reported (Hurley et al., 2004; Pedersen et al., 2000; Radford and Gaskell, 2011; Reynolds et al., 2009; Schorr-Evans et al., 2003; Schulz et al., 2011). The current generation of calicivirus vaccines appears to offer minimal protection against FCV-VSD (Coyne et al., 2006b; Reynolds et al., 2009; Schulz et al., 2011). A newer inactivated vaccine containing a VSD-FCV isolate from the original outbreak has been developed, and its use in a dual strain preparation been shown to result in broader cross neutralisation against non-VSD and VSD-associated FCV isolates and protection against homologous challenge (Huang et al., 2010). Given that hypervirulent FCV strains associated with each VSD outbreak are thought to have arisen independently from a unique local circulating isolate (Coyne et al., 2006b; Schulz et al., 2011), it is questionable whether this vaccine, or any other, will provide protection against all VSD isolates, highlighting the need for a safe and efficacious feline calicivirus antiviral. Currently, treatment for cats with VSD, or for that matter any FCV-associated disease, is symptomatic, with no direct acting antiviral drugs commercially available. A novel oligonucleotide based approach using phosphorodiamidate morpholino oligomers (PMOs) was investigated in a series of field outbreaks of VSD-FCV (Smith et al., 2008). Using a PMO targeting the 5' UTR of FCV, a highly conserved region of the genome, 47 of 59 treated cats survived, in comparison to only 3 of 31 of the untreated controls. These data illustrate the benefits of timely administration of effective antivirals in treating severe calicivirus disease.

Another serious disease manifestation that may be associated with chronic feline calicivirus infection is feline chronic gingivostomatitis syndrome (FCGS). In contrast to VSD, the link between FCV and FCGS is less clear. Numerous studies have shown a higher prevalence of chronic FCV infections in cats with FCGS than matched controls (Dowers et al., 2010; Knowles et al., 1989; Thompson et al., 1984) however, whilst acute gingivitis/stomatitis has been reported following experimental infection with FCV isolates, it has not been possible to recreate FCGS-like chronic disease experimentally (Knowles et al., 1991; Reubel et al., 1992). A role for FCV, either as primary cause or perpetuating factor, in the aetiopathogenesis of FCGS is supported by immunophenotyping of lesions suggesting a viral aetiology based on a preponderance of $CD8^+$ over $CD4^+$ lymphocytes (Harley et al., 2011). Considering the likely link between FCV and FCGS, it is possible that an effective FCV antiviral could provide a useful therapeutic option for this difficult to treat condition. Further,

an effective antiviral may also help to unravel the role of FCV in the pathogenesis of this condition.

As discussed in Chapter 5, harnessing the RNAi pathway as a therapeutic antiviral approach has garnered significant interest since the first description of the mechanism by Fire et al. (1998). The efficacy of this approach has been demonstrated against numerous viruses, including the caliciviruses Tulane virus (Fan et al., 2013), RHDV (Ghareeb, 2008), and FCV (Rohayem et al., 2010; Taharaguchi et al., 2012). In this chapter we investigate the effectiveness of synthetic siRNA mediated RNAi in inhibiting FCV *in vitro*. The results presented herewith provide important information regarding the potential therapeutic application of RNAi for treating FCV-associated diseases.

7.3. MATERIALS AND METHODS

7.3.1. siRNA design

FCV specific siRNAs were designed as reported for FCoV (Section 5.3.1). Briefly, full-length FCV genome sequences were extracted from GenBank and aligned using the Geneious alignment function of Geneious bioinformatics software (v5.3.6). Details of sequences are shown in Appendix 2. Conserved regions were visually identified and prospective siRNAs targeting these regions designed using Block-iT RNAi designer. Criteria for final siRNA selection were (1) high Block-iT RNAi designer ranking, (2) maximum sequence homology to other reported FCV strains, and (3) minimum homology to known feline sequences based on a BLAST search. Deprotected and desalted custom siRNAs were purchased from Sigma-Aldrich in the lyophilised form. siRNAs were resuspended in nuclease-free water (Amresco) and stored in single use aliquots at -20°C.

7.3.2. Screening of siRNAs for anti-FCV activity

An initial screening experiment was conducted to identify siRNAs with an inhibitory effect on FCV replication. siRNAs were reverse transfected (or mock transfected) in 96-well plates (Sarstedt) using 100 nM siRNA and 10000 cells.well^{-1} (Section 2.4.1). Following the transfection period the culture media was replaced with fresh DMEM-10 and cells were infected with FCV F9 at MOI 0.05 in 50 µl DMEM. Cells were incubated at 37°C in 5% CO_2 in air. Cells were monitored for virus induced CPE using an Olympus CKX41 inverted phase contrast microscope at various magnifications and images were acquired using a Moticam 2300 digital camera (Motic). Culture media was harvested at 24 hpi and stored at -80°C prior to titration of extracellular virus (Section 2.3.2.3.2). Each treatment was performed in triplicate and repeated in three independent experiments. The relative viral titre was

calculated for each treatment with the titre of untreated control cells defined as 100%. Data represents Mean ± SE.

7.3.3. Efficacy of anti-FCV siRNAs against field isolates of FCV

siRNA efficacy against different field isolates of FCV was assessed using a modification of the resazurin-based CPE inhibition assay (Chapter 3, summarised in Figure 3.18). Cells were reverse transfected with 100 nM siRNA as described in Section 2.4.1 in 96-well plates (µClear ®, Greiner Bio-One). At the conclusion of the transfection period the culture media was replaced with 100 µl DMEM-10 and the cells infected at a MOI of 0.05 with different FCV field isolates or FCV F9. Details of the field isolates have been previously described (Table 2.1). Untreated infected cells (for each isolate) and untreated mock infected cells were included as controls. Plates were incubated at 37°C in 5% CO_2 in air for a further 20.5 h prior to the addition of 50 µl of a 1:10 dilution of 4 x stock resazurin in DMEM (final in well resazurin concentration of 44 µM). Plates were returned to the incubator for 3 h and read at 24 hpi using a FLUOstar Omega microplate reader after allowing the culture media to equilibrate to room temperature for 30 min. The percentage inhibition for each siRNA was calculated according to the following formula:

$$CPE\ inhibition\ (\%) = \frac{RFU_{Tx} - RFU_{V(+)}}{RFU_{V(-)} - RFU_{V(+)}} \times 100$$

Where RFU_{Tx} is the mean fluorescence intensity of cells treated and infected with a particular FCV isolate; $RFU_{V(+)}$ is the mean fluorescence intensity in untreated cells infected with the same FCV isolate; and $RFU_{V(-)}$ is the average fluorescence intensity of untreated uninfected cells. Each treatment was performed in triplicate and repeated in two independent experiments. Data expressed as Mean ± SE.

7.3.4. Titration of effective anti-FCV siRNAs

A concentration-response experiment was performed using siRNAs identified as highly effective in the screening assay (defined as > 80% reduction in extracellular viral titre). Experimental conditions were identical to those of Section 7.3.2 with the exception that siRNA concentration was varied from 100 nM to 1 nM in half-log dilutions. Each treatment was performed in triplicate and repeated in three independent experiments. The relative viral titre was calculated for each treatment with the titre of untreated control cells defined as 100%. Data expressed as Mean ± SE.

7.3.5. Combination treatment

To assess the efficacy of combination treatment CRFK cells were reverse transfected in 96-well plates (Sarstedt) using single or a combination of multiple anti-FCV siRNAs as described

in Section 2.4.1. The total concentration of siRNA per treatment was held constant at 10 nM, meaning for those treatments involving two or three siRNAs the concentration per siRNA was 5 nM and 3.33 nM respectively. Following transfection, cells were infected with FCV F9 at MOI 0.05 and incubated at 37°C in 5% CO_2 in air. Cells were examined for CPE and cell culture media harvested and stored at -80°C for titration of extracellular virus at 24 hpi. Each treatment was performed in triplicate and repeated in two independent experiments. The relative viral titre was calculated for each treatment with the titre of untreated control cells defined as 100%. Data expressed as Mean ± SE.

7.4. RESULTS

7.4.1. siRNA design

At the time of siRNA design there were 14 full length FCV sequences (Appendix 2) available on GenBank. Alignment of these sequences revealed four short regions displaying minimal sequence variation. Details of the identified regions are shown in Table 7.1.

Table 7.1: Details of conserved regions in FCV genome. Position given relative to FCV F9 (Accession number M86379.1).

Region	**Size (nt)**	**Position***	**Region encompassed**	**Degree of conservation** (Matching nucleotides – number of sequences)
1	45	1-45	5' UTR and proximal ORF1	45/45 for 14 sequences
2	29	2420-2448	ORF1 (p30 non-structural protein)	29/29 for 12 sequences 28/29 for 2 sequences
3	58	5288-5345	3' end ORF 1, short UTR, and 5' end ORF2	58/58 for 11 sequences 57/58 for 2 sequences 55/58 for 1 sequence
4	25	7555-7579	ORF3	25/25 for 12 sequences 24/25 for 2 sequences

Two siRNAs were designed targeting each identified region (Figure 7.1 and Table 7.2). Due to the short length of the targeted regions there was considerable overlap between the two siRNAs used to target each of regions 1, 2, and 4. With the exception of siRNAs targeting region 2, selected siRNAs displayed 100% homology with the published FCV F9 sequence. siRNAs FCV2.1 and FCV2.3 contained a single nucleotide mismatch (G→A) compared to FCV F9 at position 13 and 9 respectively of the sense strand (Table 7.2). The degree of

conservation for each siRNA, at both the time of design and the time of writing, is shown in Table 7.3.

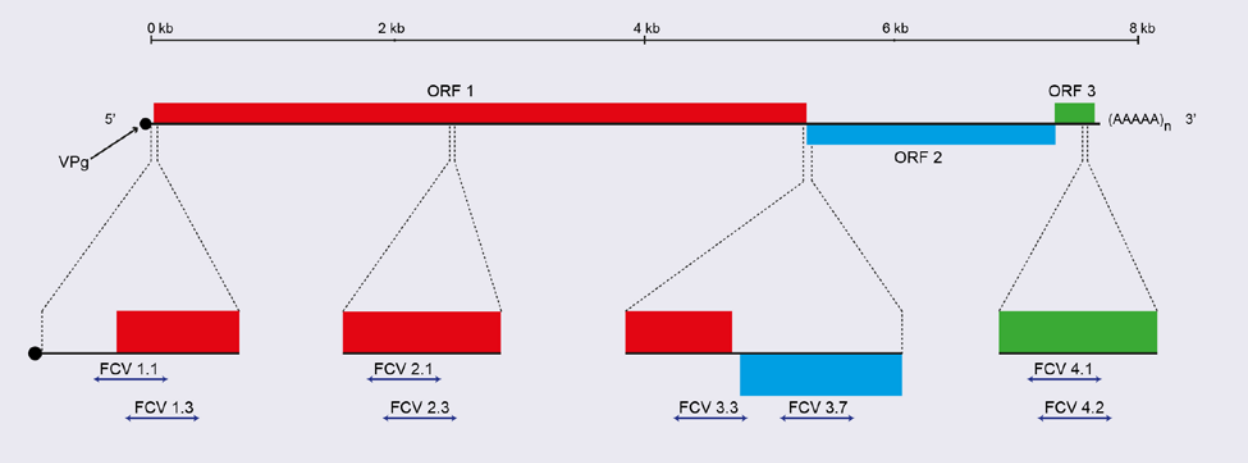

Figure 7.1: Schematic of FCV genome based on reported sequence of FCV F9 (Accession number M86379.1). The location of siRNAs targeting each of the four identified conserved regions are shown with double ended arrows.

Table 7.2: Sequence of FCV specific siRNAs and their location within the FCV F9 genome (Accession number M86379.1). Adenine (A) marked with asterisk in siRNA FCV2.1 and 2.3 is a guanine (G) in FCV F9. Sequence for the non-silencing control siRNA used in these studies is shown in Table 5.1.

siRNA	Sequence	Position in genome
FCV 1.1		
Sense	5'-UGAGACAAUGUCUCAAACUdTdT-3'	13-31
Antisense	5'-AGUUUGAGACAUUGUCUCAdTdT-3'	
FCV 1.3		
Sense	5'-UGUCUCAAACUCUGAGCUUdTdT-3'	21-39
Antisense	5'-AAGCUCAGAGUUUGAGACAdTdT-3'	
FCV 2.1		
Sense	5'-ACCCGCCAAUCAA*CAUGUGdTdT-3'	2425-2443
Antisense	5'-CACAUGUUGAUUGGCGGGUdTdT-3'	
FCV 2.3		
Sense	5'-GCCAAUCAA*CAUGUGGUAAdTdT-3'	2429-2447
Antisense	5'-UUACCACAUGUUGAUUGGCdTdT-3'	
FCV 3.3		
Sense	5'-GUGUUCGAAGUUUGAGCAUdTdT-3'	5297-5313
Antisense	5'-AUGCUCAAACUUCGAACACdTdT-3'	
FCV 3.7		
Sense	5'-CCUGCGCUAACGUGCUUAAdTdT-3'	5324-5342
Antisense	5'-UUAAGCACGUUAGCGCAGGdTdT-3'	
FCV 4.1		
Sense	5'-GGUUGACCCUUACUCAUACdTdT-3'	7556-7574
Antisense	5'-GUAUGAGUAAGGGUCAACCdTdT-3'	
FCV 4.2		
Sense	5'-GACCCUUACUCAUACACAAdTdT-3'	7560-7578
Antisense	5'-UUGUGUAUGAGUAAGGGUCdTdT-3'	

Table 7.3: Degree of conservation of FCV siRNA target sites. Reported sequences were accessed in July 2011 and February 2014 from GenBank. Data shows the number of published sequences showing different degrees of target site homology.

Target region	Target	Degree of conservation (accessed Jul 2011): Matching nucleotides – number of sequences	Degree of conservation (accessed Feb 2014): Matching nucleotides – number of sequences
5' UTR and proximal ORF1	FCV1.1	19/19 – 14	19/19 – 28
	FCV1.3	19/19 –14	19/19 – 28
ORF1 (p30 non-structural protein)	FCV2.1	19/19 – 12 18/19 – 2	19/19 – 26 18/19 – 2
	FCV2.3	19/19 – 12 18/19 – 2	19/19 – 26 18/19 – 2
3' end ORF 1, short UTR, and 5' end ORF2	FCV3.3	19/19 – 13 16/19 – 1	19/19 – 27 16/19 – 1
	FCV3.7	19/19 – 13 18/19 – 1	19/19 – 27 18/19 – 1
ORF3	FCV4.1	19/19 – 12 18/19 – 2	19/19 – 25 18/19 – 3
	FCV4.2	19/19 – 13 18/19 – 1	19/19 – 26 18/19 – 2

7.4.2. Effect of siRNAs on FCV replication

Based on extracellular viral titres, three of the tested siRNAs, FCV3.7, FCV4.1, and FCV4.2 had a marked inhibitory effect on FCV replication in cell culture (Figure 7.2). For these highly efficacious siRNAs the extracellular viral titres were reduced greater than 99%, from a mean titre of 1.7×10^7 TCID50.ml^{-1} in untreated wells to 3.93×10^4 TCID50.ml^{-1} (FCV3.7), 1.13×10^5 TCID50.ml^{-1} (FCV4.1), and 4.00×10^4 TCID50.ml^{-1} (FCV4.2) in wells pre-treated with 100 nM siRNA. siRNAs FCV2.1 and FCV2.3 also demonstrated a mild inhibitory effect with a reduction in extracellular viral titre of 71.5% and 40.4% respectively.

Phase contrast microscopy confirmed that cell monolayers pre-treated with siRNAs FCV3.7, FCV4.1, or FCV4.2 were largely protected from CPE, with only occasional scattered small areas of rounded up cells (Figure 7.3). In contrast untreated infected wells, and wells pre-

treated with other siRNAs displayed complete destruction of the cell monolayer with rounding up and detachment of cells. This included monolayers pre-treated with siRNAs FCV2.1 and FCV2.3, which despite demonstrating some inhibition of viral replication based on extracellular viral titres, showed marked CPE and were morphologically indistinguishable from untreated infected wells.

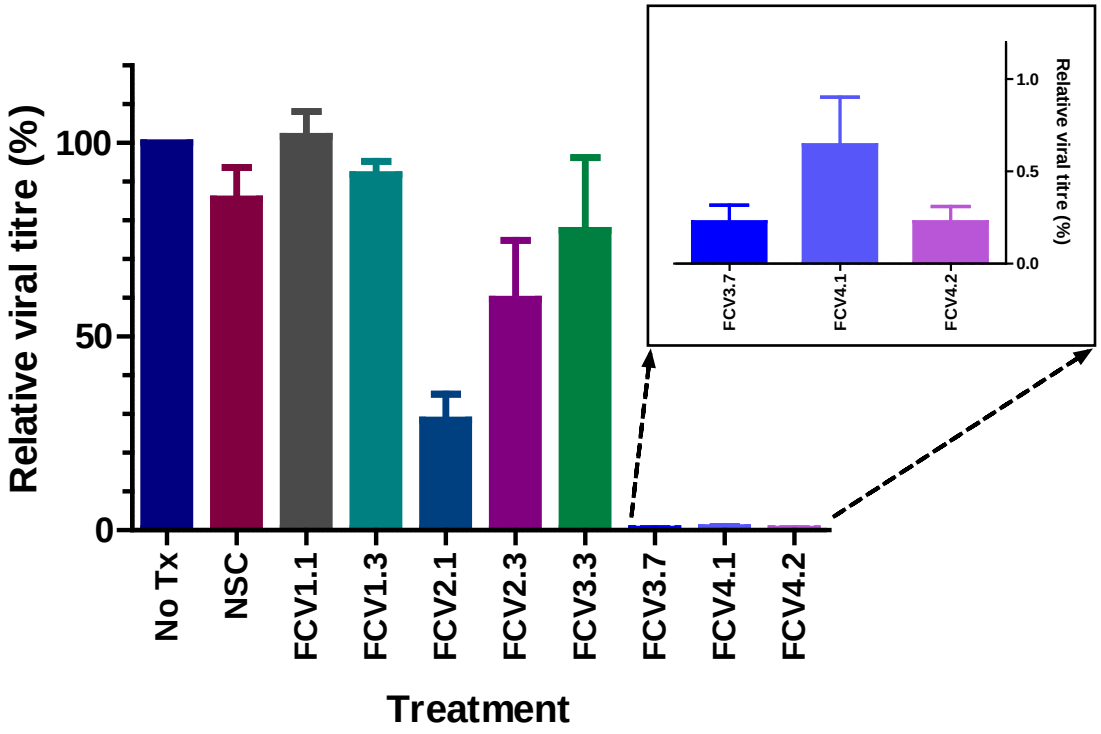

Figure 7.2: Results of FCV siRNA screening experiment. Cells were transfected with 100 nM siRNA (or mock transfected) prior to infection with FCV F9 at MOI 0.05. Extracellular viral titres were determined by TCID50 infectivity assay. Value of the untreated control sample (No Tx) is defined as 100%. Each treatment was performed in triplicate. Values are expressed as Mean ± SE from three independent experiments. No Tx, untreated control cells; NSC, non-silencing control siRNA**.**

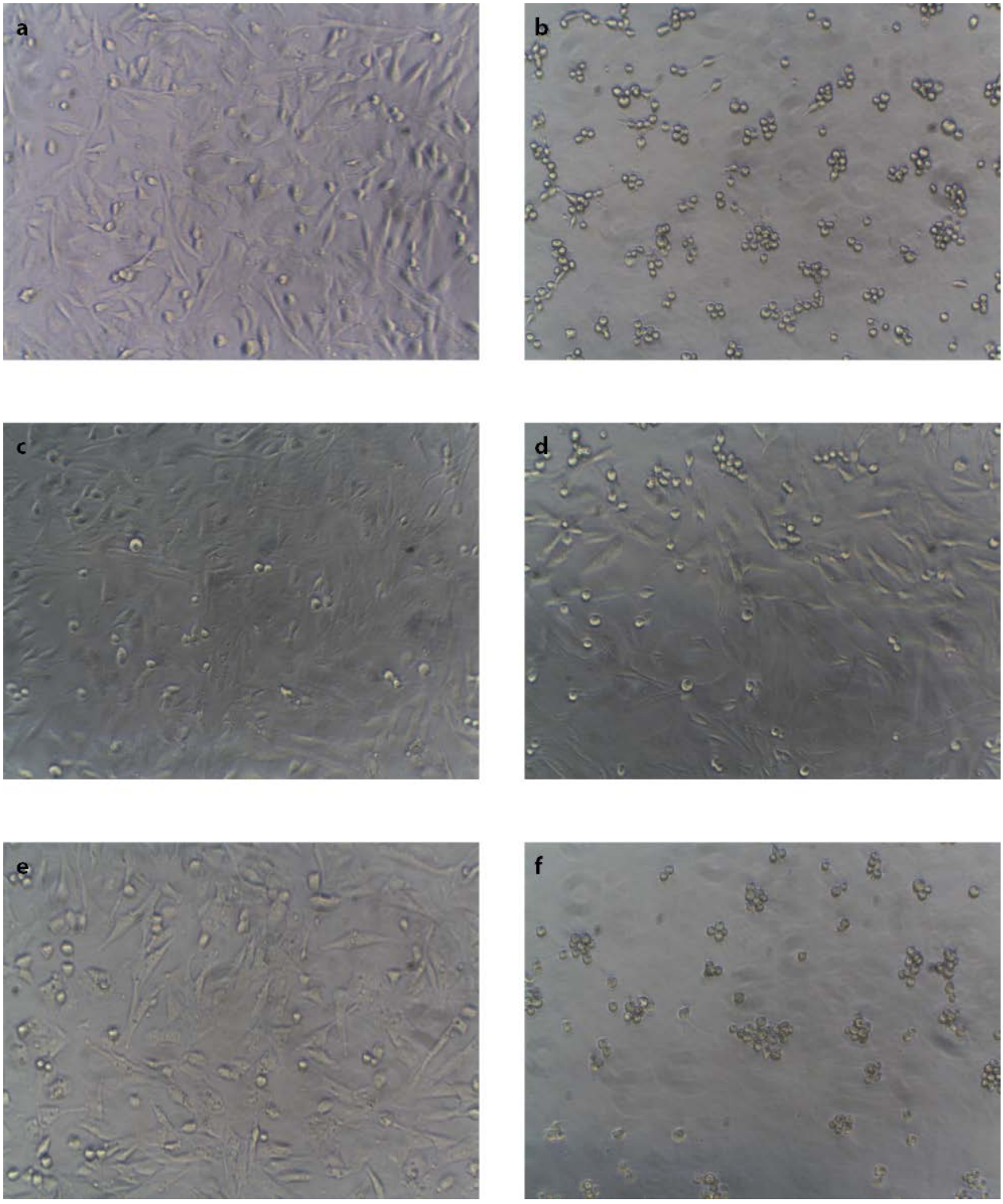

Figure 7.3: Representative phase contrast micrographs showing the effect of siRNAs on virus induced CPE. Cells were transfected with 100 nM siRNA (or mock transfected) prior to infection with FCV F9 at MOI 0.05. (a) untreated and uninfected control cells (b) untreated and infected control cells, and infected cells pre-treated with (c) FCV3.7, (d) FCV4.1, (e) FCV4.2, and (f) FCV2.1. Images taken at 100 x magnification.

7.4.3. Efficacy of anti-FCV siRNAs against field isolates of FCV

The eight candidate siRNAs were tested at a fixed concentration against six different FCV field isolates (IW1E, IW10, IW16, IW25, 131M, and 178N) in addition to the vaccine strain F9. The field isolates were taken from cats with diverse clinical manifestations and from two geographically distinct regions, and thus represent an unbiased, albeit small, sample of circulating viruses (Table 2.1).

Using the CPE inhibition assay, the efficacy of the siRNAs against various field isolates was broadly reflective of the results obtained against the reference strain FCV F9 as determined by titration of extracellular virus titres and detailed in Section 7.4.2. The three previously identified effective siRNAs displayed a range of efficacy against the field isolates tested. siRNA FCV3.7 was highly efficacious against all isolates with cell viability greater than 70% for all tested strains (Figure 7.4). siRNAs FCV4.1 and FCV4.2 were more variable in their inhibitory effect, although both resulted in greater than 50% inhibition in five or three of six tested isolates, respectively. Of particular interest is isolate IW10 which appeared partially resistant to the antiviral effects of siRNA FCV4.1 and completely resistant to FCV4.2. That a single strain displayed resistance to both siRNA FCV4.1 and 4.2 is not surprising given their overlapping target sites are shifted by only four nucleotides. Also of interest were the results obtained with siRNAs FCV2.1 and FCV2.3 against field isolates. Based on the published sequence of FCV F9 there was a single nucleotide mismatch (G→A) in the sense strand of FCV2.1 and FCV2.3. For FCV2.3 there was some inhibition of CPE for all field strains tested, with cell viability ranging from 13.7% (IW1E) to 35.6% (131M) compared with no effect on F9, which is in agreement with the morphological assessment for this siRNA in the screening study. For FCV2.1 significant CPE inhibition was only demonstrated against a single field isolate (131M) with a cell viability of 27.6%.

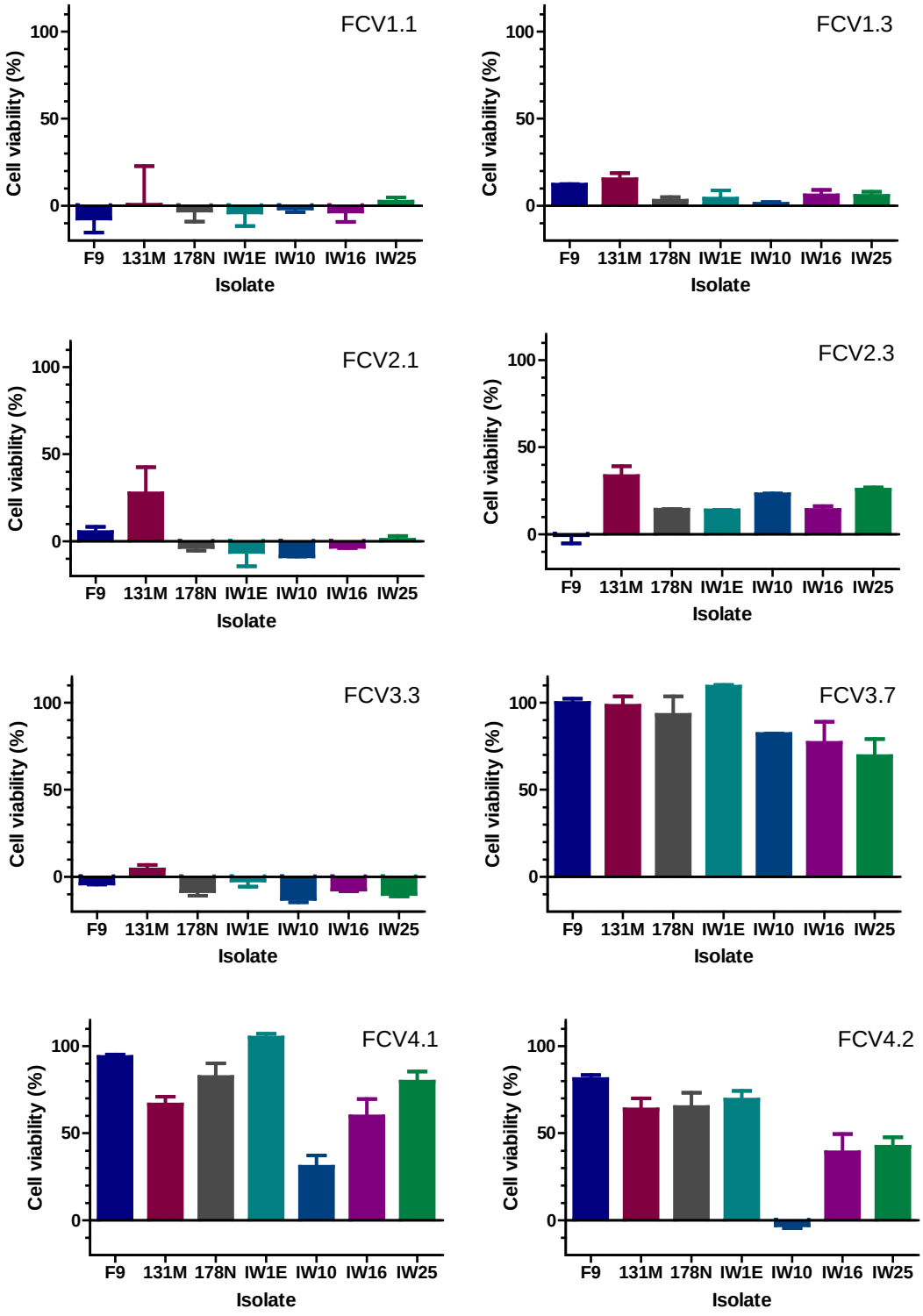

Figure 7.4: Efficacy of siRNAs on field isolates of FCV. Cells were pre-treated with 100 nM siRNA prior to infection with FCV isolates at MOI 0.05. Cell viability was determined 24 hpi using a resazurin-based CPE inhibition assay. Each treatment was performed in triplicate and data represent Mean ± SE from duplicate experiments.

7.4.4. Titration of effective siRNAs

Titration of siRNAs from 100 nM to 1 nM demonstrated a clear concentration-response relationship for the three effective siRNAs identified in the screening experiment. Reductions in extracellular viral titres at 100 nM were 99.0%, 99.0%, and 99.7% for siRNAs FCV3.7, FCV4.1 and FCV4.2 respectively, decreasing to 64.7%, 56.8%, and 46.3% at 1 nM, as shown in Figure 7.5.

7.4.5. Combination treatment

Treatment with two or three siRNAs demonstrated additive or synergistic interactions, with no evidence of antagonistic effects noted at the concentrations tested (Figure 7.6). Treatment with single siRNAs at 10 nM resulted in 97.5%, 96.9%, and 98.1% inhibition for siRNAs FCV3.7, FCV4.1, and FCV4.2 respectively. Dual treatment with two siRNAs at 5 nM (10 nM total) resulted in inhibition of 99.0% (FCV3.7 and 4.1), 98.7% (FCV3.7 and 4.2), and 97.6% (FCV4.1 and 4.2). Combination treatment with three siRNAs (FCV3.7, 4.1, and 4.2) at 3.33 nM (10 nM total) resulted in inhibition of 98.7%. Morphological assessment of pre-treated cells confirmed the reduction in extracellular viral titre was associated with significant protection from virus induced CPE.

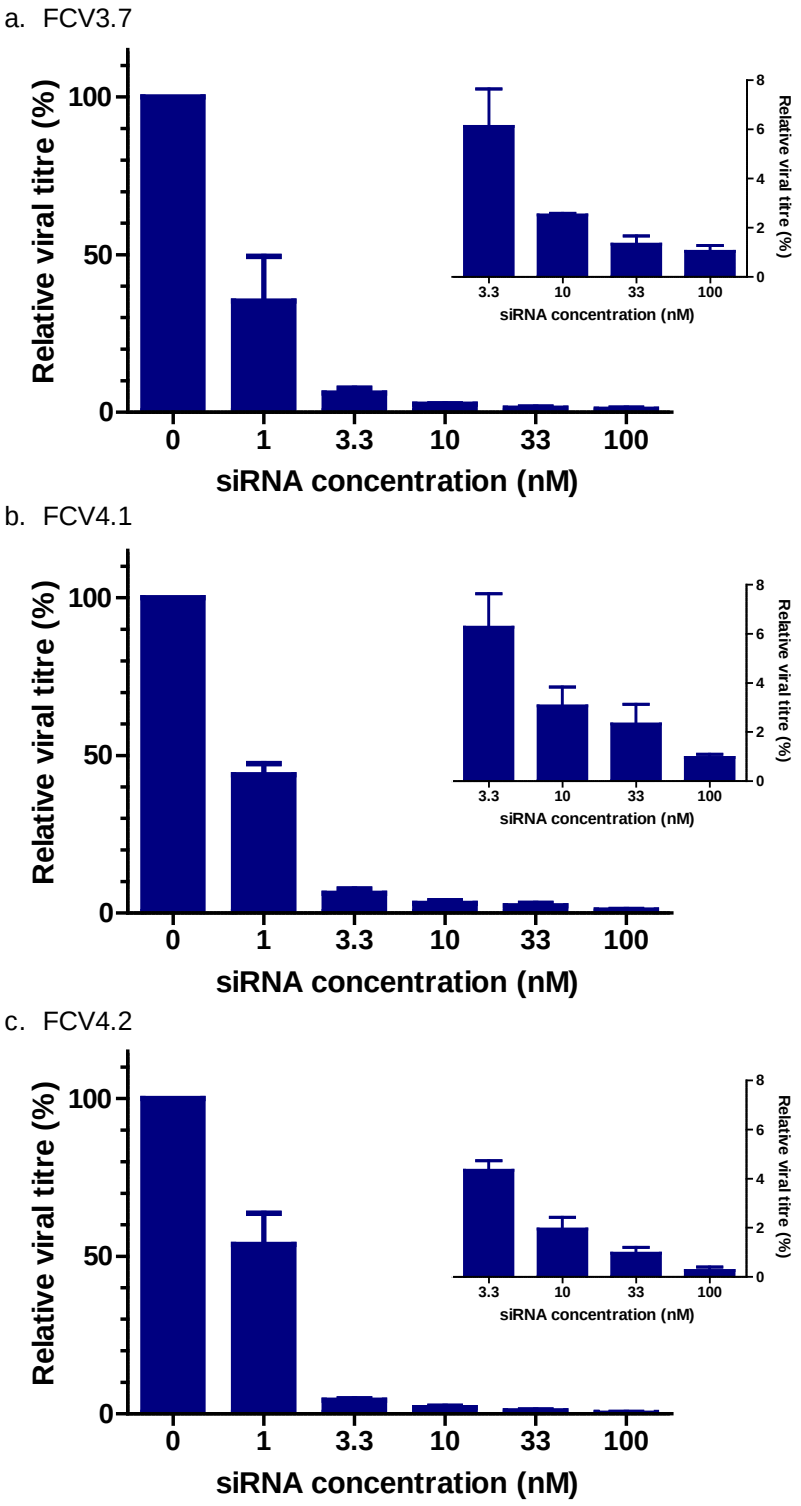

Figure 7.5: Concentration-dependent inhibition of FCV replication by siRNAs (a) FCV3.7, (b) FCV4.1, and (c) FCV4.2. Cells were reverse transfected with siRNAs at concentrations from 100 nM to 1 nM in half-log dilutions prior to infection with FCV F9 at MOI 0.05. Value of the untreated control sample (concentration 0 nM) is defined as 100%. Values are expressed as Mean ±SE from three independent experiments.

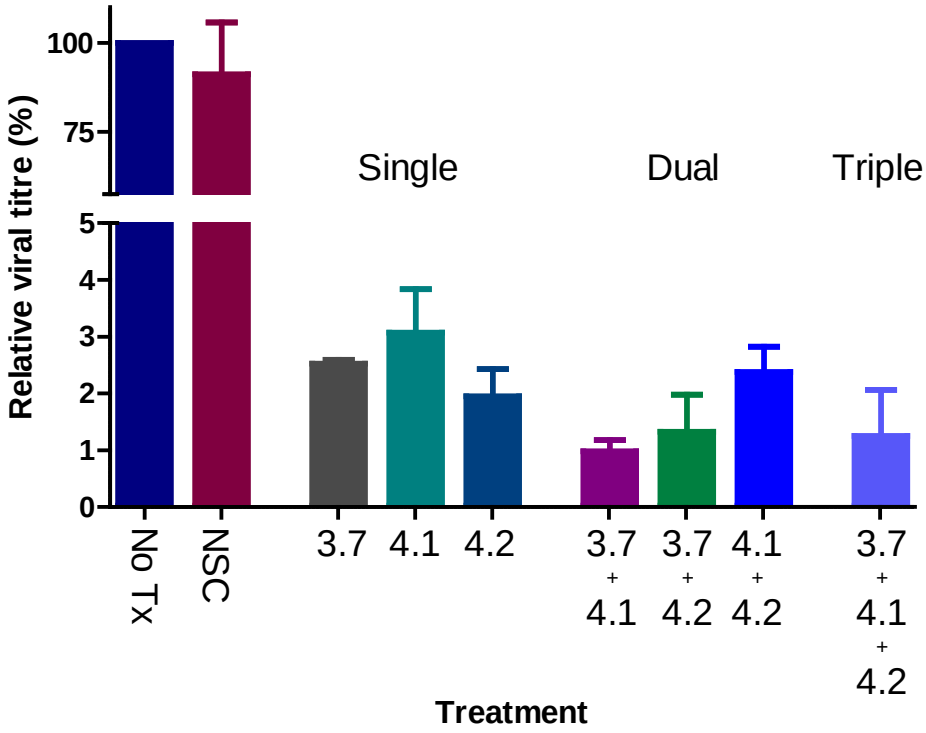

Figure 7.6: Effect of combination siRNA treatment on FCV replication. Cells were pre-treated with 10 nM of a single siRNA or a combination of two or three siRNAs (total concentration 10 nM) prior to infection with FCV F9 MOI 0.05. Extracellular virus was quantified with a TCID50 infectivity assay 24 hpi. The value of the untreated control well (No Tx) is defined as 100%. Each treatment was performed in triplicate and repeated in three independent experiments. Data are expressed as Mean ± SE. No Tx, no treatment; NSC, non-silencing control.

7.5. DISCUSSION

In this study we have demonstrated the effectiveness of siRNA mediated RNAi against FCV in cell culture. Screening of the initial panel of eight siRNAs identified three molecules showing marked inhibition of viral replication based on extracellular virus titres and a reduction in virus induced CPE. This protective effect was shown to be concentration-dependent, with IC50 values, calculated based on reductions in extracellular viral titres, in the low nanomolar range for all three effective siRNAs. Importantly, the performance of these siRNAs against range of field isolates demonstrated efficacy that was broadly representative of the performance against the reference strain. These results suggest that an RNAi-based therapy may be a valid approach for the treatment of serious FCV-related disease.

The selection of appropriate targets for RNAi-based antivirals is critical for success, as previously discussed for FCoV (Chapter 5). For RNA viruses, such as FCV, that are known to exist as a quasispecies (Radford et al., 1998) this is a greater challenge, as the development of a useful therapeutic is dependent upon targeting a region that is well conserved across isolates. One of the benefits of an RNAi-based approach, given the short region of nucleic acid targeted, is the large number of potential targets, even in viruses with short genomes (Leonard and Schaffer, 2005a). That said, restricting potential target sites to those showing only limited genetic diversity does significantly reduce the number of potential targets, particularly for a small genetically diverse virus such as FCV. The design approach used in the current study was to first identify conserved regions based on visual assessment following alignment. Using this method four regions spanning a total of 157 nt, or approximately 2% of the genome was identified as being highly conserved, and considered appropriate for targeting.

Initial screening, performed against FCV F9, demonstrated a significant variation in efficacy between siRNAs. siRNA FCV3.7, FCV4.1, and FCV4.2 were identified as being highly effective, with a reduction in viral titre of greater than 99% and an associated reduction in virus induced CPE. In comparison, targeting the highly conserved 5' end of the genome was completely ineffective in the current study, in contrast to a previous report by Rohayem et al. (2010). The two overlapping siRNAs targeting this region were located further upstream than the target site reported to be effective by Rohayem et al. (2010), although there was an 11 nt overlap between siRNA FCV1.3 and the previously reported effective site. The reason for the poor performance of siRNAs targeting this region in the current study is not known. The 5' UTR is extremely well conserved, not only at the species, but also at the genus level. Thus, whilst possible, it is unlikely that the particular FCV isolates used in the current study harboured mutations that rendered ineffective the two 5' UTR targeted siRNAs. Inaccessibility of the target site to RISC due to local secondary structure or genome association with viral proteins may limit siRNA efficacy. The 5' end of the calicivirus genome is covalently bound to the VPg protein which is essential for the initiation of translation (Goodfellow et al., 2005). It is possible that VPg, with or without bound cellular initiation factors, may act to sterically hinder the access of RISC to target sites immediately downstream. Alternatively, secondary RNA structure may interfere with access to the target site. The 5' UTR and the proximal end of ORF1 of caliciviruses are suspected to contain a number of structural elements (Simmonds et al., 2008) which may prevent RISC access.

The results obtained with siRNAs FCV2.1 and FCV2.3 are interesting in that, based on published sequence data for FCV F9, both siRNAs contained a single mismatched nucleotide at position 7 and 11 of the antisense strand respectively. Despite the mismatch pre-treatment with both siRNA resulted in a reduction in extracellular viral titre of 71.5% and

40.4% for siRNAs FCV2.1 and FCV2.3 respectively. It is reported that target complementarity within the seed region, corresponding to nucleotides 2 to 8 of the antisense strand, is most important for target binding as this region contributes the majority of the target-binding energy (Haley and Zamore, 2004). It is interesting therefore that siRNA FCV2.1 was more effective than siRNA FCV2.3 despite the former containing a mutation in the seed region, and may indicate a degree of tolerance for mismatches in this region.

Concentration-response and combination therapy studies demonstrated siRNAs FCV3.7, FCV4.1, and FCV4.2 to be highly potent, with no evidence of antagonistic effects when used in combination. These results are important when considering the therapeutic application of RNAi. Host toxicity is a significant challenge for traditional small molecule antiviral therapeutics. As obligate intracellular parasites, viruses harness numerous normal cell processes during replication, and therefore small molecule compounds affecting viral replication may be inherently toxic to the host cell. Theoretically at least, RNAi provides the opportunity to specifically target only viral genomic or messenger RNA, however it is now recognised that significant off-target effects can occur due to only limited sequence complementarity between siRNAs and cellular transcripts (Jackson et al., 2006b). These off-target effects are concentration-dependent, and can therefore be minimised, although not eliminated, through the use of highly potent siRNAs. Combination therapy may also act to further reduce the occurrence of off-target effects if the siRNAs act in a synergistic or additive manner. In this case equivalent or enhanced potency may be achieved using a lower concentration of each individual siRNA, which will reduce the occurrence of sequence dependent off-target effects. In a clinical setting combination therapy, perhaps with the small molecule compounds discussed in Chapter 6 may help to delay the emergence of resistant isolates (Hodge and Field, 2010). In Chapter 5 we showed that a minimum of three siRNA were required to prevent the emergence of resistance in FCoV over five passages. Using modelling for RNAi-based inhibition of HIV, Leonard and Schaffer (2005b) reported that four siRNAs would likely be sufficient to prevent the emergence of resistance *in vivo*. The primary method by which combination antiviral therapy can delay the emergence of resistance is through raising the so-called “genetic barrier” to resistance. Combination therapy with siRNAs FCV4.1 and 4.2 may not provide such a benefit, as due to the considerable overlap of their target sites (15 nt) it is possible that a single mutation in this shared region may simultaneously render both siRNAs ineffective. Despite this overlap, a benefit of this combination may be seen in terms of reducing off-target effects, as the critical seed region of these siRNAs is more than 50% different.

Importantly, for the clinical application of RNAi, the effective siRNAs in this study were shown to be broadly protective against currently circulating field isolates. In common with many RNA viruses, FCV is genetically diverse, a fact highlighted by the limited amount of

conserved regions identified during siRNA design. Highly diverse viruses pose a particular problem for a nucleic acid based therapy like RNAi that requires Watson-Crick base pairing for target recognition and antiviral action, as sequence variation of as little as one nucleotide may render a siRNA inactive (Boden et al., 2003; Gitlin et al., 2005). To be clinically useful an antiviral therapeutic must provide protection against a significant number of circulating isolates. In this regard there is a risk using only a reference virus such as FCV F9 for screening, as this virus, which was isolated more than half a century ago, and which has likely undergone numerous passages in cell culture since that time, may not be representative of the field viruses against which efficacy is sought. Whilst published sequence data can be used to identify the likelihood of an siRNA providing broad spectrum coverage, based on sequence conservation at the target site, it is possible that mutations outside of this site may influence efficacy (Westerhout et al., 2005), and thus such *in silico* assessment may not provide the entire picture.

There are several additional features of interest to arise from the screening of all siRNAs against the panel of field isolates. Firstly, the efficacy of siRNAs targeting ORF3, siRNAs FCV4.1 and FCV4.2, was quite variable against field isolates, with isolate IW10 appearing partially resistant to siRNA FCV4.1 and completely resistant to siRNA FCV4.2. Based on prior sequence analysis the target sites in ORF3 were highly conserved, with greater than 90% of published sequences demonstrating 100% homology at the target sites. The finding that one of six field isolates was resistant to the siRNAs directed at this site, most likely through harbouring a pre-existing mutation, suggests that this region may not be as conserved as initially thought.

Secondly the efficacy of siRNA FCV2.3 appears to be greater against field isolates than FCV F9. This is not surprising as although it was identified during siRNA design that the region targeted by this siRNA within ORF1 was highly conserved, there was a single nucleotide mismatch for FCV F9. Based on CPE inhibition, the efficacy of siRNA FCV2.3 was not as great as that for the highly potent siRNAs, and therefore this siRNA may not be suitable for monotherapy. Given the limited number of conserved regions available for targeting, it may however be useful for combination therapy to raise the genetic barrier to delay the development of resistance.

The current study is not the first to report the efficacy of siRNA-based RNAi for feline calicivirus. In a review paper discussing antiviral strategies for caliciviruses, Rohayem et al. (2010) briefly reported on the preliminary testing of two siRNAs against FCV, targeting the 5' ends of ORF1 and ORF2. This latter siRNA was identical to FCV3.7 used in the current study. Whilst limited details of the experimental parameters are provided, the authors report both siRNAs were effective *in vitro* when used prophylactically against FCV strain

Dresden/2006/GE, with an EC50 value of 0.44 μM reported for the siRNA targeting ORF1. A patent application by the same author, for a novel siRNA design displaying increased thermodynamic stability at the 3' end of the guide strand, also references RNAi-based experiments against FCV targeting the ORF1 (Rohayem, 2010). In this patent application, as with the published work, only limited detail is provided regarding the transfection and infection conditions. Given the paucity of information regarding experimental details provided it is difficult to make meaningful comparisons between the results reported by Rohayem and the current study.

The second report of RNAi against FCV was published during the conduct of the experiments described in this chapter (Taharaguchi et al., 2012). In this study siRNAs targeting ORF1, in the region encoding the 76 kDa ProPol protein (siRNA-pol), and the 5' end of OFR2, in the so called leader of the capsid region (siRNA-LC) were assessed for *in vitro* efficacy against FCV (Taharaguchi et al., 2012). The siRNAs were designed based on the partial sequence of FCV-B, an isolate from Japan taken from a cat displaying neurological signs (Sato et al., 2002). In the study by Taharaguchi et al. (2012) siRNA-LC was reported to be ineffective at inhibiting viral replication using FCV-B as the challenge virus. The target site of FCV-LC begins 2 nt downstream from that of siRNA FCV3.7 used in the current study, which was shown to be highly effective against FCV F9, in addition to a panel of recent field isolates. Although this lack of efficacy for siRNA-LC may represent a genuine difference in performance between itself and FCV3.7, it may also reflect differences in the assay conditions chosen, as efficacy was determined by a morphological assessment of CPE 48 hpi compared to the 24 h infection period in the current study. The siRNA targeting the proteinase-polymerase region of ORF1 was reported to be effective against FCV-B based on morphological assessment of CPE, and subsequent determination of extracellular viral titre and intracellular viral RNA. This siRNA was however shown to be completely ineffective when tested against three additional isolates. This result highlights a limitation of the approach used by Taharaguchi et al. (2012) in basing siRNA design on a single sequence. Alignment of the target sequence reported for siRNA-pol with full-length FCV sequences (Appendix 2) revealed that no published isolate shared 100% homology with siRNA-pol, with most sequences revealing multiple nucleotide mismatches. Thus although this previous work demonstrated in principle that RNAi could be a useful approach for calicivirus, targeting the siRNA at a variable region of the genome means that the therapeutic utility of the tested siRNA is extremely limited**.**

Translation of the *in vitro* results of the current study to a clinical setting requires an appropriate delivery system. In this regard it is important to consider the different FCV disease manifestations for which siRNA therapy may be appropriate. Given the likely high cost associated with a nucleic acid based therapy, in addition to the mild and self-limiting

nature of many infections, such treatment is unlikely to be used, and nor is it needed, for the majority of infected cats. For more severe disease manifestations however, such as virulent systemic disease, pneumonia, or FCGS, the application of this therapy may be warranted. Due to the pathogenesis of disease in each of these cases, the optimal delivery method to obtain therapeutic concentrations at the required target site will vary.

Delivery is considered the greatest challenge facing the therapeutic application of RNAi. The major issues to be resolved are threefold: improving biological stability, maximising cytoplasmic delivery, and maximising uptake by the appropriate cell type. These challenges are relevant to all delivery methods, topical, local, or systemic, however the magnitude of the challenge varies for each. Given the extraordinary potential of RNAi-based therapeutics in treating a range of infectious and non-infectious diseases, optimisation of delivery methods to meet these challenges is an active area of research (Gao and Huang, 2013; Shim and Kwon, 2010). Systemic delivery is potentially the most challenging, and would be required for FCV-VSD due to the more widespread viral replication of hypervirulent strains (Pesavento et al., 2008). Successful systemic delivery for antiviral applications has been reported for highly virulent Ebola virus using a non-human primate model (Geisbert et al., 2010), demonstrating the feasibility of the method for treating FCV-VSD despite the considerable challenges**.**

For treating FCV-associated pneumonia, siRNA delivery to the site of infection, the lower airways and lung parenchyma, is possible via either systemic or local delivery. In general local delivery offers a number of advantages over systemic delivery, such as a reduction in the dose required, the potential for higher bioavailability, and reduced systemic adverse effects (Shim and Kwon, 2010; Whitehead et al., 2009). Local delivery to the lungs does however present its own unique challenges. As the most common route of infection, the respiratory tract has evolved a series of overlapping mechanical, physiological, and innate immune barriers to prevent the deposition of, or to remove foreign particles (Lam et al., 2012). Despite these barriers successful pulmonary delivery of both modified and naked siRNA has been demonstrated in animal studies, and local administration has been shown to be effective in animal models of SAR-CoV (Li et al., 2005a), parainfluenza virus (Bitko et al., 2005), and human respiratory syncytial virus (RSV) infections (Bitko et al., 2005; Zhang et al., 2005). Successful human studies have also been conducted for RSV using an unmodified intranasally administered anti-RSV siRNA (DeVincenzo et al., 2010). In these studies the most common method of administration for pulmonary delivery has been via the intranasal route; however delivery via inhalation, through nebulisation or the use of inhalers, may result in enhanced delivery (Lam et al., 2012). Given the reported success with local delivery, even when using unmodified naked siRNAs, an siRNA-based approach for FCV-associated pneumonia warrants consideration.

Local mucosal delivery of siRNAs to inflamed tissue in FCGS may represent the least challenging delivery option from a technical point of view, although practically speaking the mercurial nature of cats, their lightning fast reflexes, and their frequent intolerance of oral manipulation may pose a challenge. Topical mucosal application of antiviral siRNAs has been studied in the context of sexually transmitted infections (Katakowski and Palliser, 2010). Successful antiviral effects have been demonstrated in mouse models of herpes simplex virus 2 infection using a commercially available lipid-based transfection reagent (Palliser et al., 2006), however care must be taken with this delivery approach for antiviral applications as high doses of lipid reagent have been reported to facilitate viral infection, possibly through enhancing fusion of the viral envelope with the cell membrane or by inducing mild inflammation (Wu et al., 2009). A number of alternative delivery methods have been reported for topical administration, including conjugation to cholesterol, chemical modification to improve stability, and encapsulation in biodegradable polymer nanoparticles (Katakowski and Palliser, 2011). Specific studies with these, or any other technique, on the delivery of siRNAs to the oropharyngeal mucosa have not been reported. *In vitro* stability studies have demonstrated naked siRNAs are rapidly degraded in saliva, with an associated loss of function (Hickerson et al., 2008), and thus structural modifications or encapsulation would be required to maximise efficacy. The presence of saliva and mucous overlying the oropharyngeal tissues may also present a barrier to the cellular uptake of siRNAs. The concurrent use of mucolytics, such as N-acetylcysteine, or muscarinic antagonists such as atropine, may be useful to reduce saliva and mucous secretion, and thereby increase the interaction between siRNAs and target cells to facilitate cellular uptake. Again, despite these challenges, given the excellent *in vitro* efficacy demonstrated in the current study, investigation of delivery options for topical siRNA therapy should be considered for the treatment of FCV-positive FCGS**.**

The current study has focused on an RNAi-based approach, however an alternative nucleic acid based antiviral therapy, namely phosphorodiamidate morpholino oligomers (PMO), has already demonstrated excellent efficacy in field conditions against VSD-FCV (Smith et al., 2008). Whilst both siRNAs and PMOs bind specifically to RNA via Watson-Crick base-pairing, gene silencing occurs through different mechanisms. For siRNA inhibition occurs through association with RISC and cleavage of target sequences. PMOs, a third-generation antisense oligonucleotide, bind to RNA and sterically hinder translation or RNA processing. Due to their modified backbone they do not interact with, or function via, an RNase H mechanism (Summerton, 1999) (see Figure 1.1). For PMOs that function via blocking translation (as opposed to inhibiting splicing), effective target sites are effectively limited to those located between the 5' cap and approximately 25 nt downstream of the initiation codon (Summerton, 1999). This requirement limits the available number of target sites for

inhibition, particularly in the case of viruses with small genomes, such as FCV, that have only a small number of ORFs. A previous study with two different vesiviruses demonstrated that only PMOs targeted against ORF1 resulted in viral inhibition, with PMOs targeted at ORF2 and ORF3 showing no-effect or, in the case of the later, resulting in a significant increase in viral titre (Stein et al., 2001). This limitation may have consequences for antiviral applications as combination therapy may be required to delay the almost inevitable emergence of resistance when using monotherapy, however as the indications for FCV antivirals are primarily for acute infections, the importance of this may be limited. Further, although combination PMO therapy may not be possible, concurrent treatment with a small molecule inhibitor, potentially mefloquine as described in Chapter 6, or siRNAs as described herein, could be used to help delay the emergence of resistance.

FCV is a very common infection in domestic cats, however only a relatively small percentage of cases result in severe disease. It is this subset of infections, including FCV-VSD, calicivirus pneumonia, severe refractory oral ulceration, and possibly FCGS, where the lack of a calicivirus antiviral is conspicuous. In the current study we demonstrated the successful inhibition of FCV using synthetic siRNAs. Although this is not the first report of successful inhibition of FCV with RNAi, the current work does address some of the critical basic questions regarding possible therapeutic application of this technology. The effective siRNAs in this study were demonstrated to be highly potent and were efficacious against a panel of currently circulating field isolates, in contrast to a previous report. The successful translation of these *in vitro* results into a clinical setting will likely provide a useful tool in the treatment of severe FCV-associated diseases.

8

Conclusions and future directions

Viral disease is a significant cause of morbidity and mortality in domestic cats. Fortunately, for several of the important pathogens, safe and effective vaccines are available. Whilst the aphorism "*prevention is better than cure*" certainly holds true, there remain viruses, such as feline coronavirus (FCoV), the causative agent of FIP, for which the quest for an effective vaccine remains elusive. In the case of feline calicivirus (FCV), although vaccines provide good immunity in the majority of cases and can reduce the severity of clinical signs post challenge, current vaccines appear to provide little protection against recently emerged hypervirulent strains associated with VSD (Coyne et al., 2006b; Reynolds et al., 2009; Schulz et al., 2011). Current treatment options for FIP and severe FCV-associated disease are essentially supportive rather than specific, with no direct acting antiviral agents currently in use. The overarching aim of the work presented within this thesis was to begin to address this shortfall by investigating new antiviral strategies for FCoV and FCV. The studies contained herein provide vital preliminary information regarding the *in vitro* effectiveness of a number of compounds against these pathogens. It is hoped that the successful clinical application of the principles established within these studies may provide feline practitioners with viable treatment options for diseases caused by these two common and problematic viruses.

8.1. ANTIVIRAL DRUG DISCOVERY

In this study two strategies were utilised to identify inhibitory compounds. The first involved screening a panel of small molecule compounds which had previously demonstrated inhibitory effects against other, in most cases related, viruses. Enriching the test panel for compounds in this way increases the likelihood of identifying an effective compound. Furthermore, as a number of the small molecules tested are human approved pharmaceuticals, or have significant *in vivo* toxicology and safety data, this approach maximises the likelihood that effective compounds will be suitable for therapeutic use. Unfortunately, safety in humans, or other species does not necessarily equate to safety in cats, due to well-recognised differences in feline drug metabolism, particularly in relation to several conjugation pathways (Court, 2013). This process of finding new indications for

existing drugs, commonly referred to as drug repurposing, is a growing area of human pharmaceutical research, owing to considerable savings in time and resources compared to *de novo* drug development. (Muthyala, 2012). Given the relatively poorly funded world of companion animal veterinary research, this approach has considerable merit. Drug repurposing also offers the benefit of a more rapid translation into clinical use, an important feature when considering severe diseases which currently have no effective therapies, and will also likely provide a more affordable and accessible treatment option than a new molecular entity.

The second approach was based on harnessing the cellular mechanism of RNAi through the use of chemically synthesised siRNAs. In contrast to the empirical approach of the small molecule screen, which requires no *a priori* knowledge of the molecular target or mechanism of action of a compound, the RNAi-based approach could be considered a simplified rational approach to drug development, given that siRNAs are designed specifically to target unique viral sequences. This antiviral approach has been demonstrated effective *in vitro* against a diverse range of pathogens of medical and veterinary importance (Ge et al., 2003; Martinez et al., 2002; Wilkes and Kania, 2010), however challenges relating to *in vivo* delivery has limited the therapeutic application of this technology.

The translation of the *in vitro* results for siRNAs presented in Chapters 5 and 7 will be dependent on the development of effective and affordable delivery options. In contrast effective small molecule inhibitors identified in Chapters 4 and 6 may be suitable for immediate use. This is highlighted by the recent small scale study reported on the *in vivo* efficacy of chloroquine, a compound identified in Chapter 4 as effective against FCoV, in treating FIP (Takano et al., 2013).

8.2. SMALL MOLECULE INHIBITORS OF FCOV AND FCV

In Chapter 3 we described the development and optimisation of low to medium throughput resazurin- and sulforhodamine B (SRB)-based CPE inhibition assays for screening compounds for antiviral effects against FCoV and FCV. Both assay formats proved robust, with Z'-factors, a commonly used measure of assay performance, indicating an "excellent assay" according to the criteria of Zhang et al. (1999). Whilst the SRB-based assay gave a superior Z'-factor, the resazurin-based assay was selected for compound screening due to practical advantages relating to assay simplicity and cost. In regards to the latter, the in-house prepared resazurin reagent, with a cost price of only a few cents per plate, provides an economical choice, particularly if screening large numbers of compounds.

Using this assay, three compounds – chloroquine, mefloquine, and hexamethylene amiloride – were identified during screening as possessing marked antiviral effects against FCoV

(Chapter 4), whilst for FCV (Chapter 6) only mefloquine displayed marked inhibitory effects during screening. The lower hit rate for FCV compared to FCoV was not surprising as the panel of compounds screened was biased towards molecules with previously demonstrated efficacy against coronaviruses. These effective compounds demonstrated concentration-dependent inhibition that was confirmed with orthogonal testing, with IC50 values in the low micromolar range. Whilst the demonstration of *in vitro* efficacy is important, it in no way guarantees that an identified compound will be therapeutically useful. Attrition of candidate compounds during drug development frequently occurs due to poor pharmacokinetic or safety profiles (Hughes et al., 2011; van de Waterbeemd and Gifford, 2003). The pharmacokinetics and safety profile of chloroquine and mefloquine, as human approved pharmaceuticals, have been extensively studied in humans and other species, including in the case of chloroquine some limited work on toxicity in cats. Based on these data, and the calculated IC50 values, it would appear, if the pharmacokinetics in cats is similar to other species, that therapeutic concentrations of these compounds may be attainable with doses used in humans, although as previously mentioned peculiarities of feline drug metabolism must always be considered. In contrast to chloroquine and mefloquine there is considerably less reported regarding the *in vivo* use of hexamethylene amiloride, and thus the potential usefulness of this compound is more difficult to assess.

For FCoV, investigations were conducted to determine the stage of infection and possible mechanism of action of the three identified compounds. Interestingly, treatment of uninfected CRFK cells with all three compounds resulted in similar morphological changes that were not seen in mock treated cells. These changes, consisting of an increased number of cytoplasmic inclusions that accumulated the vital dye neutral red, suggest the compounds result in a perturbation of the normal endocytic pathways. Despite what appears to be a common physiological effect, a common antiviral mechanism of action for all three compounds against FCoV is unlikely based on the finding that mefloquine, unlike chloroquine and hexamethylene amiloride, remained effective when added after the period of viral attachment and entry. Whilst compounds effective only prior to cell entry are able to limit the spread of infection within an animal, they will have no effect on cells once infected. In these cases a functional innate or adaptive immune response would be required to stop viral replication and mediate viral clearance. With the documented immune dysregulation that occurs in FIP (Perlman and Dandekar, 2005), and the endemicity of FCoV within feline populations, the use of an antiviral effective after cell infection (such as mefloquine is likely to be) is preferable. Similar studies were not conducted for FCV, however given that mefloquine was effective against two unrelated viruses, it would be interesting to determine whether a single common mechanism of action was responsible for these broad spectrum effects.

A limitation of the current study is that antiviral effects were tested only in a single cell type. The use of an immortalised cell line, in this case the well characterised Crandell Rees feline kidney cell line, is important for reproducibility during screening assays. It is possible however that such a cell line may not provide a physiologically relevant target if viral replication in these cells is different than that in the natural target cells of the virus *in vivo*. In light of the apparent broad spectrum antiviral effect of mefloquine, studies with alternate cell types could be used to demonstrate the documented antiviral effect is not a laboratory artefact due to some unique property of reference cell line chosen.

To be clinically useful, an antiviral therapeutic must be effective against a broad a range of circulating field isolates. In this study mefloquine was demonstrated to be effective against a panel of recent field isolates of FCV. Testing of different FCoV isolates in addition to the reference strain FIPV1146, was limited to another type II FCoV, strain FECV1683. Given that two of the compounds demonstrating antiviral effects against FCoV appear to act during viral entry, and that there appear to be differences in cell entry between type I and type II FCoV, testing efficacy against the more common type I viruses would be indicated.

8.3. RNAI FOR INHIBITING FCOV AND FCV

Chapters 5 and 7 described the investigation of siRNA mediated RNAi as an antiviral strategy against FCoV and FCV respectively. These studies demonstrated some of the significant benefits of this antiviral approach, however the results also highlighted some of the challenges to its therapeutic application.

Appropriate selection of siRNAs is critical for antiviral RNAi. To maximise the potential for siRNA target recognition against diverse field isolates and to minimise the potential for viral escape during treatment, conserved regions of the viral genome were targeted. The number and size of conserved regions for FCoV was greater than for FCV, a fact that reflects the larger genome size and complexity of the former. Although four independent conserved sites were identified in FCV, the target motifs of the two siRNAs designed for some of these regions overlapped considerably. In a therapeutic setting this limited number of independent conserved motifs may have implications given that combinatorial therapy with multiple independent siRNAs is one of the primary strategies to delay the emergence of viral resistance.

Overall the results of these studies demonstrate that appropriately designed siRNAs can have a potent inhibitory effect on the replication of FCoV and FCV at low nanomolar concentrations in cell culture. For FCV, siRNAs were tested against a panel of recent field isolates, with the antiviral effects demonstrated against these relevant viruses broadly reflective of those seen against the reference strain FCV F9. For FCoV, only efficacy against

the reference strain FIPV1146 was assessed, however a bioinformatics approach using published sequences suggests that the designed siRNAs would be effective against the majority of field isolates.

A significant challenge for RNAi-based antivirals is the emergence of resistance during treatment. The exquisite sequence specificity of the mechanism, coupled to the high mutation rate and rapid replicative cycles of RNA viruses, has been shown, for a number of different viruses, to result in the rapid emergence of resistance (Boden et al., 2003; Gitlin et al., 2005). In the current study, despite targeting highly conserved regions of the FCoV genome, viral escape occurred within a single passage when siRNAs were used as monotherapy. Combination therapy with multiple siRNAs showed no evidence of antagonistic effects (for both FCoV and FCV), and in the case of FCoV was shown to delay the emergence of resistance. In this regard one of the strengths of the RNAi-based approach, that is the relative ease and rapidity with which multiple independent antiviral molecules can be designed for combinatorial therapy, was able to overcome the challenge of antiviral resistance inherent in this approach.

A number of different structural siRNA variants have been described, many of which are purported to offer benefits over canonical siRNAs regarding potency, off-target effects, and duration of action. We investigated one of these, the Dicer-substrate siRNA, and compared it to canonical siRNAs targeting the same motifs in the FCoV genome. The results of our study showed that both canonical and Dicer-substrate siRNAs were effective, with superior performance, in terms potency and duration of action, for DsiRNA demonstrated for one target, and approximately equivalent performance demonstrated for the other target tested. It would appear from these results, and other recently published data (Foster et al., 2012), that the differences between canonical and Dicer-substrate siRNAs are target dependent, and that therefore the most appropriate structural form should be empirically determined in each case.

8.4. POTENTIAL FURTHER RESEARCH

Whilst the results of the current study provide important information regarding potential antiviral therapies for FCoV and FCV, there is significant scope for further investigations into the identified antivirals, both *in vitro* and *in vivo*, which are described below.

8.4.1. In vitro studies

8.4.1.1. Confirmation of antiviral efficacy in different cell types and against different viral isolates

As previously discussed a limitation of the current work is that all antiviral testing was performed in CRFK cells, and in the case of FCoV, with culture adapted viruses that may not be representative of those encountered in the field. It is important to address these issues to determine whether the compounds identified are likely to be of therapeutic use. In this regard *ex vivo* testing in relevant target cells would confirm whether the observed antiviral effects are cell line dependent. This is more critical for the small molecule inhibitors than for siRNAs, as in the case of the latter there is unlikely to be significant mechanistic differences between different cell types. Differences in transfection efficacy between cell lines may impact the apparent antiviral efficacy; however the therapeutic relevance of this would be difficult to interpret as the complexity of *in vivo* siRNA delivery is far removed from the culture dish. For small molecule inhibitors however the effect of the cell line on efficacy may be more dramatic as features of the viral replication cycle, for example the cellular receptors used for entry, may vary between cell types.

For FCoV, further studies investigating the antiviral efficacy against different field isolates is warranted, however such studies are hampered by difficulties in propagating the more common type I FCoV in cell culture. The immortalised cell line Fcwf-4 or primary monocytes and macrophages can support the growth of these viruses and would be a suitable choice for additional testing (Pedersen, 2009). Desmarets et al. (2013) recently reported on the development of immortalised cell lines derived from feline ileocytes and colonocytes that support the replication of both type I and type II enteric FCoV biotypes. Whilst enteric biotypes are in themselves essentially avirulent, based on our current understanding of the pathogenesis of FIP, infection and continued replication of these viruses, may lead to FIP following the acquisition of specific mutations. In a purely probabilistic sense, the likelihood of a mutation arising, and therefore the risk of FIP, is related to the magnitude and duration of viral replication. An antiviral that can limit or eliminate replication of enteric biotypes may therefore reduce the incidence of FIP. At this time this approach is likely to be prohibitively expensive for RNAi-based therapeutics, but it may be suitable for the small molecule compounds identified. Studies on the efficacy of the identified compounds using these cell lines and field isolates may be the first step in the development of a novel prophylactic strategy for controlling FIP.

For FCV, additional testing against VSD isolates may be warranted as all the isolates tested in the current study were from cases of classical oro-respiratory disease or FCGS. This is particularly important given that neither the mechanism of action of mefloquine nor the

biological basis for the expanded tissue tropism and hypervirulent nature of VSD isolates is currently understood. This additional testing is not as critical for anti-FCV siRNAs as an analysis of the target site motifs from published sequences demonstrated a high degree of conservation for both VSD and non-VSD isolates however testing may still be beneficial as other aspects of the molecular biology of the hypervirulent strains may impact on the efficacy of RNAi mediated inhibition.

8.4.1.2. Determining the mechanism of action of candidate small molecule inhibitors of FCoV and FCV

Determining the mechanism of action of the small molecule antivirals identified in these studies may be beneficial in informing their clinical application. This knowledge may also allow for the identification or development of alternate antiviral agents that may act via a similar mechanism. Time of addition experiments, as performed in the current study for FCoV, can help to determine the stage of the viral replication cycle at which a compound acts and is often the first step to determining a mechanism of action. It would be interesting to compare the results of similar studies performed for mefloquine on FCV to determine whether the antiviral effects displayed against two unrelated viruses occur due to a common mechanism of action. Beyond the relatively simple time of addition assays to determine the stage of infection targeted, further assays would be required to define the mechanism by which the compounds acted. Studies on plaque purified resistant isolates generated following *in vitro* exposure to the compound may be beneficial in this regard.

8.4.1.3. Effect of combination therapy

The development of resistance is considered an almost inevitable consequence of antiviral treatment. The current work demonstrated resistance developed rapidly for FCoV when siRNA monotherapy or dual combination therapy was used, however it was delayed considerably with a combination of three siRNAs targeting independent sites. It is possible, but would appear unlikely based on these results and published literature, that viral escape from siRNA mediated inhibition would be any less likely with the target sites chosen for FCV. For FCV, although three siRNAs were shown to be highly efficacious, the target site for two of these, siRNA FCV4.1 and FCV4.2, overlapped considerably meaning a single nucleotide mutation could render both ineffective. Thus combination therapy with the three effective anti-FCV siRNAs in this study, in reality could be considered to only target two independent sites. Given the rapidity with which resistance can develop with even with dual combination therapy, alternative strategies should be investigated to minimise this risk. In this regard additional siRNAs could be tested targeting the identified conserved regions, however the limited size of these regions and the fact that siRNAs targeting these areas have already been demonstrated to be of limited efficacy, suggest that this approach may not be

successful. Thus combination therapy with other, non-siRNA based antivirals, may be appropriate. Combination treatment with an siRNA and interferon-α was demonstrated to have synergistic effects in culture against SARS-CoV (He et al., 2009), and thus investigations into combination therapy with rFeINF-ω would be a logical next step, for both FCoV and FCV. Investigation into combination therapy with the small molecule inhibitors identified in the current study may also provide a useful, and cost effective, therapeutic option against both viruses.

8.4.1.4. Chemical and structural modifications of siRNAs

A variety of chemical and structural modifications have been suggested to improve the performance of siRNAs in terms of enhanced efficacy, reduced off target effects and non-specific immune stimulation, reduced susceptibility to nuclease degradation, and improved pharmacokinetics and cell delivery (Behlke, 2008). Chemical modifications affecting the phosphate backbone, the ribose moiety, and nucelobase have all been reported (reviewed by Bramsen et al. (2012)). Chemical modification, such as the use of locked nucleic acids (Elmen et al., 2005; Fluiter et al., 2009), of the effective siRNAs described in this thesis may improve their *in vivo* biological properties, making them more likely to be successfully translated into clinical use. As chemical modifications can have a negative impact on efficacy it is important that efficacy is verified *in vitro* first.

In addition to the canonical siRNA structure described by Elbashir et al. (2001a), a range alternate structures have been reported (Bramsen et al., 2012). One of these, the Dicer-substrate siRNA, has been demonstrated in the current study to perform as well as, or in some cases better than its equivalent siRNA. Further investigation into the use of DsiRNA, or alternate structures such as those reviewed by Bramsen et al. (2012) may provide more potent RNAi-based inhibitors.

A number of the modifications described above are designed to reduce non-specific immunostimulation following treatment. Whilst this is clearly desirable for *in vitro* studies, in order to avoid confounding effects of treatment, and likely a good thing in many *in vivo* gene silencing applications, in the context of antiviral therapy a degree of immunostimulation triggered by the siRNA or its delivery vehicle could have a positive therapeutic effect. siRNAs designed specifically to result in immunostimulation have shown good efficacy in antiviral applications *in vitro* (Gantier et al., 2010). Investigation of these immunostimulatory siRNAs may be beneficial in the context of the current studies, however it should be considered that in the case of FCoV, given FIP is associated with significant immune dysregulation, it is possible these modifications may have untoward effects *in vivo*.

8.4.1.5. Further antiviral screening using the CPE inhibition assay

In addition to specific extensions of the work described herein, additional avenues for future research may arise from some of the methods and techniques developed during the course of this study. Perhaps the most important of these is the work in Chapter 3 describing the development of a robust and reliable CPE inhibition based assay for assessing compounds for antiviral effects against FCoV and FCV. In addition to excellent performance, the assay offers several practical benefits including minimal handling steps, low cost, and suitability for either fluorescence or colorimetric readout. In addition to screening for inhibitors of FCoV and FCV, the current assay could be easily modified, using the optimisation procedures outlined in Chapter 3, to screen for inhibitors of other viruses that replicate in CRFK cells such as canine and feline parvovirus, canine coronavirus, and feline herpesvirus.

Against FCoV and FCV there are a number of possibilities for the application of this assay in future research. Given the continually expanding field of antiviral research, particularly in the case of coronaviruses spurred by the emergence of MERS-CoV (Chan et al., 2013), this assay could be used for further directed screening using compounds with demonstrated antiviral properties against related viruses. Alternatively, a directed screening approach using chemical derivatives of the candidate compounds identified in this study may be useful to identify compounds with improved efficacy and toxicity profiles. This assay may also have a place in larger-scale screening, as based on the calculated Z'-factors the assay in its current form is amenable to HTS. Although expensive, screening of large compound libraries may identify additional novel agents for further research.

8.4.2. Therapeutic applications

The ultimate goal of the work described within this thesis is to develop safe and efficacious antiviral therapeutics for the treatment of FIP and serious FCV-associated disease. Whilst the studies presented herein have identified a number of potent antivirals, the decision as to when, and how to transition from *in vitro* to *in vivo* testing is complex. For animal welfare reasons there should be a body of evidence supporting the use of a drug prior to its therapeutic use, but this must be balanced against the current paucity of therapeutic options, especially considering the severity of the diseases to be treated. The drug development pathway for human therapeutics is well defined, with rigorous *in vitro* and animal model studies conducted prior to clinical trials in humans. In veterinary medicine the route from laboratory to clinical use is less clear; with the off-label use of compounds a commonly accepted practice in the absence alternative effective therapies.

The severity of the disease and the efficacy of currently available therapies may influence the rapidity and urgency with which the translation from *in vitro* to *in vivo* testing is made. For FIP, effectively an untreatable, uniformly fatal disease, there is clearly a large unmet need

which justifies the rapid clinical assessment of these compounds. Similarly, for more serious FCV-associated diseases, the current lack of effective therapeutics would argue for the testing of compounds identified in this thesis. For less serious disease manifestations, such as mild FCV-associated oro-respiratory disease or asymptomatic enteric FCoV infections, or for a condition such as FCGS in which a pathogenic role for chronic FCV infection is unproven, a risk benefit analysis may suggest a more cautious approach to *in vivo* testing.

Therapeutic testing will require studies in cats, as non-feline animal models of FCoV and FCV-associated disease are not available. Studies in experimentally infected laboratory cats would provide a well-controlled environment, however such studies are unlikely to perfectly mimic natural infections in terms of the viral strain, route of infection, and challenge dose used. It could also be argued from an ethical perspective that, in the case of FIP for example, given that the disease is currently untreatable and terminal, it would more appropriate to conduct studies in naturally infected cats. Testing in naturally infected cats clearly provides the most important and relevant measure of efficacy however it would be associated with increased experimental variability. This increased variability may arise due to animals presenting at various stages of disease and also the potential presence of co-morbidities. As a consequence, minor changes associated with treatment may be missed, however this is unlikely to be a problem in the first instance as changes of this magnitude are unlikely to be of therapeutic consequence. Without prior target animal safety studies in healthy cats, it would be difficult to assess the safety profile of the compounds when they are tested in diseased animals as it may not be possible to distinguish treatment-related and disease-related clinical signs.

8.4.2.1. Small molecule inhibitors

Chloroquine, one of the three small molecule inhibitors of FCoV identified in this study, has recently been tested *in vivo* in cats with FIP (Takano et al., 2013). This study, published following the conclusion of the experimental work described herein, used cats experimentally infected with FCoV FIPV1146. Overall the results of this study were disappointing, although chloroquine treatment did result in improved clinical scores and slightly prolonged, although not statistically significantly different, survival times. Whether the results reported by Takano et al. (2013) are an accurate reflection of the likely efficacy of chloroquine in the field is unclear. The challenge virus used, FCoV FIPV1146, is exceptionally virulent and may not be reflective of the viruses encountered in natural cases (Pedersen, 2009). The treatment regimen of 10 $mg.kg^{-1}$ every three days used in this study may have been insufficient to achieve therapeutic concentrations. Higher doses, and more frequent dosing of chloroquine has been reported in cats, with 50 $mg.kg^{-1}$ given for two years (dosing frequency not reported) (Gregory et al., 1970) and 20 $mg.kg^{-1}$ given five days per week for one year (Kuhn

et al., 1981). Unfortunately, as there was no detailed reporting of adverse effects at these doses, it is not possible to say how well they were tolerated. Additional testing in naturally infected cats, potentially using more frequent dosing, may provide a better indication of the antiviral efficacy of this drug. Drug monitoring during treatment would be helpful to determine the optimum treatment regimen, and to rule out sub-therapeutic concentrations as the cause of treatment failure. It is important to note that even in the absence of significant antiviral effects *in vivo*, chloroquine may have a role to play in the treatment of FIP, in combination with an effective antiviral, due to its immunomodulatory effects, in particular its antagonism of TNF-α (Savarino et al., 2003).

The other two small molecule inhibitors of FCoV, mefloquine and hexamethylene amiloride, have not been used in cats to the authors knowledge, and thus choosing an appropriate treatment regimen for studies is difficult. Simple allometric scaling may provide a reasonable starting point for calculating appropriate doses, but this approach does not take into account species differences in metabolism (Sharma and McNeill, 2009). Pharmacokinetic studies in cats to determine the maximum tolerable dose would provide the best information on which to base dosing. Whilst these studies are best performed in healthy animals, to avoid the confounding effects of disease on the measured parameters, pharmacokinetic studies in animals with FIP, or simple drug monitoring during treatment, would also provide useful information.

The same considerations detailed above are relevant for the use of mefloquine in treating serious FCV-associated disease. Additionally, given the *in vitro* results demonstrating concurrent treatment with rFeINF-ω and mefloquine results in additive effects, consideration should be given for combination therapy to potentially reduce the dose of mefloquine required, and therefore the risk of associated adverse effects. For FCGS, as an alternative to systemic therapy, topical application of mefloquine may provide therapeutic concentrations to infected tissue without the risk of systemic adverse effects, however the absorption of mefloquine from oral tissues has not been studied. Mefloquine is sparingly soluble in water, however as used in the current study, is soluble in DMSO. The successful use of DMSO as a drug delivery vehicle for topical antiviral therapy has been reported (Spruance et al., 1983) and thus formulation in DMSO may be appropriate. DMSO is also known to have antiinflammatory effects which may provide additional benefits in treating FCGS (Brayton, 1986).

8.4.2.2. siRNA

The results presented in this thesis clearly demonstrate potent and specific inhibition of viral replication for both FCoV and FCV by siRNAs. To harness this for therapeutic use requires the development of a suitable strategy for delivery to the target cells, perhaps the greatest

challenge facing the therapeutic application of RNAi. Systemic delivery would be required in many cases; however for FCGS topical mucosal delivery would likely be more suitable. Chemical or structural modifications as described in Section 8.4.1.4 may help to overcome some of the challenges associated with delivery, however for systemic applications, formulation with a delivery system is likely to provide the greatest efficacy. A variety of strategies have been used to encapsidate siRNAs into nanoparticles to facilitate delivery, using lipid or cationic-polymer based systems (Gao and Huang, 2009; Huang and Liu, 2011; Nguyen et al., 2008). Conjugation of siRNAs to cholesterol, antibodies, ligands, or aptamers has also been shown to facilitate delivery (Burnett and Rossi, 2012; Nguyen et al., 2008). An advantage of some of these approaches is that siRNAs can be targeted to specific tissue or cell types. This selective biodistribution to specific cells is the ultimate challenge of siRNA delivery. Delivery targeted in this manner maximises siRNA concentration in the desired cells to enhance efficacy, while minimising exposure, and therefore unwanted effects, in non-target cells. For treating FIP siRNAs should be targeted to monocytes and macrophages for maximum effect. Targeted *in vivo* delivery to monocytes has been demonstrated in mice using lipid nanoparticles (Leuschner et al., 2011), and a similar approach may be suitable in cats. If such selective targeting can be achieved in feline monocytes and macrophages, it may be possible to incorporate additional siRNAs targeting cellular factors, to modulate cytokine production from infected cells, and potentially minimise virus induced immune dysregulation.

Topical siRNA therapy using the anti-FCV siRNAs identified in this thesis may be a novel way to investigate the role of FCV in the aetiopathogenesis of FCGS, in addition to providing information on its potential as a therapeutic option for this common and difficult to treat condition. Such studies would need to be performed in naturally affected cats, as experimental recreation of the disease has not been possible. A placebo-controlled experiment, using topical application of either a combination of anti-FCV siRNAs or a combination of scrambled NSC siRNA, would be required to control for the potential off-target and immunostimulatory effects of siRNA treatment. As most cases of FCGS are bilateral, it is possible that a cat could act as its own control, with one side of the oral cavity treated with the active and the other treated with the scrambled NSC siRNAs. This approach would only be feasible if siRNAs were formulated into a gel or ointment that could remain localised once applied.

8.5. CONCLUSION

At the time of commencing the studies reported in this thesis there were no effective direct acting antiviral molecules for FCoV and FCV in clinical use. Sadly, as the concluding sentences are written, this situation has not changed. The identification, in this thesis, of a

number of potent small molecule and nucleic acid based antivirals provides important preliminary information on potential treatment options for infections associated with these viruses. In regards to FCoV, it is questionable as to whether antiviral therapy alone will be sufficient to control or cure FIP, given the immunopathological nature of the disease. As replication of virulent mutant FCoV is a triggering and perpetuating factor in the disease, there is little doubt that effective antiviral therapy will be a critical component of any successful therapeutic regimen. For FCV on the other hand, experience in experimental studies with antisense oligonucleotides has shown that antiviral therapy alone is sufficient to cure many infected cats (Smith et al., 2008). Thus, the successful translation of the *in vitro* success reported herein into a clinical setting would be significant advance for feline medicine, and have a dramatic effect on the treatment of these common infections. The potential benefits, in terms of feline health and welfare, should therefore encourage subsequent studies required to explore the potential of the identified compounds as antiviral therapeutics in treating FIP and FCV-associated disease.

References

Abd-Eldaim, M., Potgieter, L., Kennedy, M., 2005. Genetic analysis of feline caliciviruses associated with a hemorrhagic-like disease. Journal of Veterinary Diagnostic Investigation 17, 420-429.

Abrantes, J., van der Loo, W., Le Pendu, J., Esteves, P.J., 2012. Rabbit haemorrhagic disease (RHD) and rabbit haemorrhagic disease virus (RHDV): a review. Veterinary Research 43, 12.

Adachi, E., Koibuchi, T., Imai, K., Kikuchi, T., Koga, M., Nakamura, H., Miura, T., Iwamoto, A., Fujii, T., 2012. Favourable outcome of progressive multifocal leukoencephalopathy with mefloquine treatment in combination with antiretroviral therapy in an HIV-infected patient. International Journal of STD & AIDS 23, 603-605.

Adam, M. 2011. Multi-Level Complexities in Technological Development: Competing Strategies for Drug Discovery, In: Carrier, M., Nordmann, A. (Eds.) Science in the Context of Application. Springer Netherlands, 67-83.

Addie, D.D. 2012. Feline coronavirus infections, In: Greene, C.E. (Ed.) Infectious Diseases of the Dog and Cat. Elsevier, St Louis, Missouri, 92-108.

Addie, D.D., Jarrett, J.O., 1992a. Feline coronavirus antibodies in cats. Veterinary Record 131, 202-203.

Addie, D.D., Jarrett, O., 1992b. A study of naturally occurring feline coronavirus infections in kittens. Veterinary Record 130, 133-137.

Addie, D.D., Jarrett, O., 2001. Use of a reverse-transcriptase polymerase chain reaction for monitoring the shedding of feline coronavirus by healthy cats. Veterinary Record 148, 649-653.

Addie, D.D., Radford, A., Yam, P.S., Taylor, D.J., 2003a. Cessation of feline calicivirus shedding coincident with resolution of chronic gingivostomatitis in a cat. Journal of Small Animal Practice 44, 172-176.

Addie, D.D., Schaap, I.A.T., Nicolson, L., Jarrett, O., 2003b. Persistence and transmission of natural type I feline coronavirus infection. Journal of General Virology 84, 2735-2744.

Addie, D.D., Toth, S., Herrewegh, A.A.P.M., Jarrett, O., 1996. Feline coronavirus in the intestinal contents of cats with feline infectious peritonitis. Veterinary Record 139, 522-523.

Addie, D.D., Toth, S., Murray, G.D., Jarrett, O., 1995a. Risk of feline infectious peritonitis in cats naturally infected with feline coronavirus. American Journal of Veterinary Research 56, 429-434.

Addie, D.D., Toth, S., Murray, G.D., Jarrett, O., 1995b. The risk of typical and antibody enhanced feline infectious peritonitis among cats from feline coronavirus endemic households. Feline Practice 23, 24-26.

Akerstrom, S., Mirazimi, A., Tan, Y.-J., 2007. Inhibition of SARS-CoV replication cycle by small interference RNAs silencing specific SARS proteins, 7a/7b, 3a/3b and S. Antiviral Research 73, 219-227.

Aleksandrowicz, P., Marzi, A., Biedenkopf, N., Beimforde, N., Becker, S., Hoenen, T., Feldmann, H., Schnittler, H.-J., 2011. Ebola virus enters host cells by macropinocytosis and clathrin-mediated endocytosis. Journal of Infectious Diseases 204, S957-S967.

Allerson, C.R., Sioufi, N., Jarres, R., Prakash, T.P., Naik, N., Berdeja, A., Wanders, L., Griffey, R.H., Swayze, E.E., Bhat, B., 2005. Fully 2'-modified oligonucleotide duplexes with improved in vitro potency and stability compared

to unmodified small interfering RNA. Journal of Medicinal Chemistry 48, 901-904.
Almazan, F., Galan, C., Enjuanes, L., 2004. The nucleoprotein is required for efficient coronavirus genome replication. Journal of Virology 78, 12683-12688.
Amarzguioui, M., Lundberg, P., Cantin, E., Hagstrom, J., Behlke, M.A., Rossi, J.J., 2006. Rational design and in vitro and in vivo delivery of Dicer substrate siRNA. Nature Protocols 1, 508-517.
Amarzguioui, M., Rossi, J.J., 2008. Principles of Dicer substrate (D-siRNA) design and function. Methods in Molecular Biology 442, 3-10.
Amici, C., Di Coro, A., Ciucci, A., Chiappa, L., Castilletti, C., Martella, V., Decaro, N., Buonavoglia, C., Capobianchi, M.R., Santoro, M.G., 2006. Indomethacin has a potent antiviral activity against SARS coronavirus. Antiviral Therapy 11, 1021-1030.
An, W.F., Tolliday, N., 2010. Cell-based assays for high-throughput screening. Molecular Biotechnology 45, 180-186.
An, W.F., Tolliday, N.J., 2009. Introduction: cell-based assays for high-throughput screening. Methods in Molecular Biology 486, 1-12.
Anderson, J., Banerjea, A., Akkina, R., 2003. Bispecific short hairpin siRNA constructs targeted to CD4, CXCR4, and CCR5 confer HIV-1 resistance. Oligonucleotides 13, 303-312.
Anonymous n.d. alamarBlue® Assay, Invitrogen, ed.
Arrive, E., Newell, M.L., Ekouevi, D.K., Chaix, M.L., Thiebaut, R., Masquelier, B., Leroy, V., Van de Perre, P., Rouzioux, C., Dabis, F., Children, G.G.H.W., 2007. Prevalence of resistance to nevirapine in mothers and children after single-dose exposure to prevent vertical transmission of HIV-1: a meta-analysis. International Journal of Epidemiology 36, 1009-1021.
Baba, C., Yanagida, K., Kanzaki, T., Baba, M., 2005. Colorimetric lactate dehydrogenase (LDH) assay for evaluation of antiviral activity against bovine viral diarrhoea virus (BVDV) in vitro. Antiviral Chemistry & Chemotherapy 16, 33-39.
Bachmetov, L., Gal-Tanamy, M., Shapira, A., Vorobeychik, M., Giterman-Galam, T., Sathiyamoorthy, P., Golan-Goldhirsh, A., Benhar, I., Tur-Kaspa, R., Zemel, R., 2012. Suppression of hepatitis C virus by the flavonoid quercetin is mediated by inhibition of NS3 protease activity. Journal of Viral Hepatitis 19, e81-e88.
Bae, E.A., Han, M.J., Lee, M., Kim, D.H., 2000. In vitro inhibitory effect of some flavonoids on rotavirus infectivity. Biological & Pharmaceutical Bulletin 23, 1122-1124.
Bálint, Á., Farsang, A., Zádori, Z., Belák, S., 2014. Comparative In Vivo Analysis of Recombinant Type II Feline Coronaviruses with Truncated and Completed ORF3 Region. PLoS One 9, e88758.
Bálint, Á., Farsang, A., Zadori, Z., Hornyak, A., Dencso, L., Almazan, F., Enjuanes, L., Belak, S., 2012. Molecular characterization of feline infectious peritonitis virus strain DF-2 and studies on the role of ORF3abc in viral cell tropism. Journal of Virology.
Bannasch, M.J., Foley, J.E., 2005. Epidemiologic evaluation of multiple respiratory pathogens in cats in animal shelters. Journal of Feline Medicine and Surgery 7, 109-119.
Barlough, J.E., Scott, F.W., 1990. Effectiveness of three antiviral agents against FIP virus in vitro. Veterinary Record 126, 556-558.
Barlough, J.E., Shacklett, B.L., 1994. Antiviral studies of feline infectious peritonitis virus in vitro. Veterinary Record 135, 177-179.

Barnard, D.L., Hubbard, V.D., Burton, J., Smee, D.F., Morrey, J.D., Otto, M.J., Sidwell, R.W., 2004. Inhibition of severe acute respiratory syndrome-associated coronavirus (SARSCoV) by calpain inhibitors and beta-D-N4-hydroxycytidine. Antiviral Chemistry and Chemotherapy 15, 15-22.

Bauer, D.J., 1985. A history of the discovery and clinical application of antiviral drugs. British Medical Bulletin 41, 309-314.

Beaumont, S.L., Maggs, D.J., Clarke, H.E., 2003. Effects of bovine lactoferrin on in vitro replication of feline herpesvirus. Veterinary Ophthalmology 6, 245-250.

Behlke, M.A., 2006. Progress towards in Vivo Use of siRNAs. Molecular Therapy 13, 644-670.

Behlke, M.A., 2008. Chemical modification of siRNAs for in vivo use. Oligonucleotides 18, 305.

Belgard, S., Truyen, U., Thibault, J.C., Sauter-Louis, C., Hartmann, K., 2010. Relevance of feline calicivirus, feline immunodeficiency virus, feline leukemia virus, feline herpesvirus and Bartonella henselae in cats with chronic gingivostomatitis. Berliner und Munchener Tierarztliche Wochenschrift 123, 369-376.

Bell, E.T., Toribio, J.A., White, J.D., Malik, R., Norris, J.M., 2006. Seroprevalence study of feline coronavirus in owned and feral cats in Sydney, Australia. Australian Veterinary Journal 84, 74-81.

Benetka, V., Kubber-Heiss, A., Kolodziejek, J., Nowotny, N., Hofmann-Parisot, M., Mostl, K., 2004. Prevalence of feline coronavirus types I and II in cats with histopathologically verified feline infectious peritonitis. Veterinary Microbiology 99, 31-42.

Bennett, D., Gaskell, R.M., Mills, A., Knowles, J., Carter, S., Mcardle, F., 1989. Detection of Feline Calicivirus Antigens in the Joints of Infected Cats. Veterinary Record 124, 329-332.

Bentrivedi, A., Kitabatake, N., Doi, E., 1990. Toxicity of dimethyl-sulfoxide as a solvent in bioassay system with Hela-cells evaluated colorimetrically with 3-(4,5-dimethyl thiazol-2-Yl)-2,5-diphenyl-tetrazolium bromide. Agricultural and Biological Chemistry 54, 2961-2966.

Berg, A.L., Ekman, K., Belak, S., Berg, M., 2005. Cellular composition and interferon-gamma expression of the local inflammatory response in feline infectious peritonitis (FIP). Veterinary Microbiology 111, 15-23.

Bergman, S.J., Ferguson, M.K.C., Santanello, C., 2011. Interferons as Therapeutic Agents for Infectious Diseases. Infectious Disease Clinics of North America 25, 819-834.

Berkhout, B., Westerhout, E.M., Ooms, M., Vink, M., Das, A.T., 2005. HIV-1 can escape from RNA interference by evolving an alternative structure in its RNA genome. Nucleic Acids Research 33, 796-804.

Bhella, D., Gatherer, D., Chaudhry, Y., Pink, R., Goodfellow, I.G., 2008. Structural insights into calicivirus attachment and uncoating. Journal of Virology 82, 8051-8058.

Bhella, D., Goodfellow, I.G., 2011. The cryo-electron microscopy structure of feline calicivirus bound to junctional adhesion molecule A at 9-angstrom resolution reveals receptor-induced flexibility and two distinct conformational changes in the capsid protein VP1. Journal of Virology 85, 11381-11390.

Bilkei, G., 1988. Beitrag zur therapie der FIP. Tierärztl Umschau 43, 192-196.

Binns, S.H., Dawson, S., Speakman, A.J., Cuevas, L.E., Hart, C.A., Gaskell, C.J., Morgan, K.L., Gaskell, R.M., 2000. A study of feline upper respiratory tract disease with reference to prevalence and risk factors for infection with feline

calicivirus and feline herpesvirus. Journal of Feline Medicine and Surgery 2, 123-133.
Bitko, V., Barik, S., 2001. Phenotypic silencing of cytoplasmic genes using sequence-specific double-stranded short interfering RNA and its application in the reverse genetics of wild type negative-strand RNA viruses. BMC Microbiology 1, 34.
Bitko, V., Musiyenko, A., Shulyayeva, O., Barik, S., 2005. Inhibition of respiratory viruses by nasally administered siRNA. Nature Medicine 11, 50-55.
Boden, D., Pusch, O., Lee, F., Tucker, L., Ramratnam, B., 2003. Human immunodeficiency virus type 1 escape from RNA interference. Journal of Virology 77, 11531-11535.
Bos, E.C., Luytjes, W., van der Meulen, H.V., Koerten, H.K., Spaan, W.J., 1996. The production of recombinant infectious DI-particles of a murine coronavirus in the absence of helper virus. Virology 218, 52-60.
Bourinbaiar, A.S., Lee-Huang, S., 1995. The non-steroidal anti-inflammatory drug, indomethacin, as an inhibitor of HIV replication. FEBS Letters 360, 85-88.
Bowling, T., Mercer, L., Don, R., Jacobs, R., Nare, B., 2012. Application of a resazurin-based high-throughput screening assay for the identification and progression of new treatments for human African trypanosomiasis. International Journal for Parasitology: Drugs and Drug Resistance 2, 262-270.
Boyle, J.F., Pedersen, N.C., Evermann, J.F., McKeirnan, A.J., Ott, R.L., Black, J.W., 1984. Plaque assay, polypeptide composition and immunochemistry of feline infectious peritonitis virus and feline enteric coronavirus isolates. Advances in Experimental Medicine & Biology 173, 133-147.
Bradwell, K., Combe, M., Domingo-Calap, P., Sanjuan, R., 2013. Correlation between mutation rate and genome size in riboviruses: mutation rate of bacteriophage Qbeta. Genetics 195, 243-251.
Bramsen, J.B., Kjems, J., Bramsen, J., Kjems, J., 2012. Development of therapeutic-grade small interfering RNAs by chemical engineering. Frontiers in Genetics 3, 154.
Bramsen, J.B., Laursen, M.B., Nielsen, A.F., Hansen, T.B., Bus, C., Langkjaer, N., Babu, B.R., Hojland, T., Abramov, M., Van Aerschot, A., Odadzic, D., Smicius, R., Haas, J., Andree, C., Barman, J., Wenska, M., Srivastava, P., Zhou, C., Honcharenko, D., Hess, S., Muller, E., Bobkov, G.V., Mikhailov, S.N., Fava, E., Meyer, T.F., Chattopadhyaya, J., Zerial, M., Engels, J.W., Herdewijn, P., Wengel, J., Kjems, J., 2009. A large-scale chemical modification screen identifies design rules to generate siRNAs with high activity, high stability and low toxicity. Nucleic Acids Research 37, 2867-2881.
Brayton, C.F., 1986. Dimethyl sulfoxide (DMSO): a review. The Cornell Veterinarian 76, 61-90.
Brickelmaier, M., Lugovskoy, A., Kartikeyan, R., Reviriego-Mendoza, M.M., Allaire, N., Simon, K., Frisque, R.J., Gorelik, L., 2009. Identification and characterization of mefloquine efficacy against JC virus in vitro. Antimicrobial Agents and Chemotherapy 53, 1840-1849.
Brierley, I., 1995. Ribosomal frameshifting on viral RNAs. Journal of General Virology 76, 1885-1892.
Brown, M.A., Troyer, J.L., Pecon-Slattery, J., Roelke, M.E., O'Brien, S.J., 2009. Genetics and pathogenesis of feline infectious peritonitis virus. Emerging Infectious Diseases 15, 1445-1452.

Buckwold, V.E., Beer, B.E., Donis, R.O., 2003. Bovine viral diarrhea virus as a surrogate model of hepatitis C virus for the evaluation of antiviral agents. Antiviral Research 60, 1-15.

Burnett, J.C., Rossi, J.J., 2012. RNA-based therapeutics: current progress and future prospects. Chemistry & Biology 19, 60-71.

Buss, N., Cammack, N., 2001. Measuring the effectiveness of antiretroviral agents. Antiviral Therapy 6, 1-8.

Buyens, K., Lucas, B., Raemdonck, K., Braeckmans, K., Vercammen, J., Hendrix, J., Engelborghs, Y., De Smedt, S.C., Sanders, N.N., 2008. A fast and sensitive method for measuring the integrity of siRNA-carrier complexes in full human serum. Journal of Controlled Release 126, 67-76.

Calabrese, E., 2008. Hormesis: principles and applications for pharmacology and toxicology. American Journal of Pharmacology and Toxicology 3, 56-68.

Carpenter, A.E., Jones, T.R., Lamprecht, M.R., Clarke, C., Kang, I.H., Friman, O., Guertin, D.A., Chang, J.H., Lindquist, R.A., Moffat, J., Golland, P., Sabatini, D.M., 2006. CellProfiler: image analysis software for identifying and quantifying cell phenotypes. Genome Biology 7, R100.

Carstens, E.B., Ball, L.A., 2009. Ratification vote on taxonomic proposals to the International Committee on Taxonomy of Viruses (2008). Archives of Virology 154, 1181-1188.

Carter, M.J., Milton, I.D., Meanger, J., Bennett, M., Gaskell, R.M., Turner, P.C., 1992a. The complete nucleotide sequence of a feline calicivirus. Virology 190, 443-448.

Carter, M.J., Milton, I.D., Turner, P.C., Meanger, J., Bennett, M., Gaskell, R.M., 1992b. Identification and sequence determination of the capsid protein gene of feline calicivirus. Archives of Virology 122, 223-235.

Carvalho, O., Botelho, C., Ferreira, C., Ferreira, H., Santos, M., Diaz, M., Oliveira, T., Soares-Martins, J., Almeida, M., Silva Júnior, A., 2013. In vitro inhibition of canine distemper virus by flavonoids and phenolic acids: Implications of structural differences for antiviral design. Research in Veterinary Science.

Castanotto, D., Sakurai, K., Lingeman, R., Li, H., Shively, L., Aagaard, L., Soifer, H., Gatignol, A., Riggs, A., Rossi, J.J., 2007. Combinatorial delivery of small interfering RNAs reduces RNAi efficacy by selective incorporation into RISC. Nucleic Acids Research 35, 5154-5164.

Cerutti, H., Casas-Mollano, J., 2006. On the origin and functions of RNA-mediated silencing: from protists to man. Current Genetics 50, 81-99.

Chan, J.F., Chan, K.-H., Kao, R.Y., To, K.K., Zheng, B.-J., Li, C.P., Li, P.T., Dai, J., Mok, F.K., Chen, H., 2013. Broad-spectrum antivirals for the emerging Middle East respiratory syndrome coronavirus. Journal of Infection 67, 606-616.

Chang, C.I., Hong, S.W., Kim, S., Lee, D.-k., 2007. A structure–activity relationship study of siRNAs with structural variations. Biochemical & Biophysical Research Communications 359, 997-1003.

Chang, H.-W., de Groot, R.J., Egberink, H.F., Rottier, P.J.M., 2010. Feline infectious peritonitis: insights into feline coronavirus pathobiogenesis and epidemiology based on genetic analysis of the viral 3c gene. Journal of General Virology 91, 415-420.

Chang, H.W., Egberink, H.F., Halpin, R., Spiro, D.J., Rottier, P.J., 2012. Spike protein fusion Peptide and feline coronavirus virulence. Emerging Infectious Diseases 18, 1089-1095.

Chang, H.W., Egberink, H.F., Rottier, P.J., 2011. Sequence analysis of feline coronaviruses and the circulating virulent/avirulent theory. Emerging Infectious Diseases 17, 744-746.
Chang, K.O., George, D.W., Patton, J.B., Green, K.Y., Sosnovtsev, S.V., 2008. Leader of the capsid protein in feline calicivirus promotes replication of Norwalk virus in cell culture. Journal of Virology 82, 9306-9317.
Chen, D., Shien, J., Tiley, L., Chiou, S., Wang, S., Chang, T., Lee, Y., Chan, K., Hsu, W., 2010. Curcumin inhibits influenza virus infection and haemagglutination activity. Food Chemistry 119, 1346-1351.
Chen, F., Chan, K.H., Jiang, Y., Kao, R.Y., Lu, H.T., Fan, K.W., Cheng, V.C., Tsui, W.H., Hung, I.F., Lee, T.S., Guan, Y., Peiris, J.S., Yuen, K.Y., 2004. In vitro susceptibility of 10 clinical isolates of SARS coronavirus to selected antiviral compounds. Journal of Clinical Virology 31, 69-75.
Chen, L.L., Gui, C.S., Luo, X.M., Yang, Q.G., Gunther, S., Scandella, E., Drosten, C., Bai, D., He, X.C., Ludewig, B., Chen, J., Luo, H.B., Yang, Y.M., Yang, Y.F., Zou, J.P., Thiel, V., Chen, K., Shen, J.H., Xu, S., Jiang, H.L., 2005. Cinanserin is an inhibitor of the 3C-like proteinase of severe acute respiratory syndrome coronavirus and strongly reduces virus replication in vitro. Journal of Virology 79, 7095-7103.
Choi, H.-J., Kim, J.-H., Lee, C.-H., Ahn, Y.-J., Song, J.-H., Baek, S.-H., Kwon, D.-H., 2009a. Antiviral activity of quercetin 7-rhamnoside against porcine epidemic diarrhea virus. Antiviral Research 81, 77-81.
Choi, H.J., Song, J.H., Park, K.S., Kwon, D.H., 2009b. Inhibitory effects of quercetin 3-rhamnoside on influenza A virus replication. European Journal of Pharmaceutical Sciences 37, 329-333.
Choung, S., Kim, Y.J., Kim, S., Park, H.O., Choi, Y.C., 2006. Chemical modification of siRNAs to improve serum stability without loss of efficacy. Biochemical & Biophysical Research Communications 342, 919-927.
Cinatl, J., Morgenstern, B., Bauer, G., Chandra, P., Rabenau, H., Doerr, H.W., 2003. Glycyrrhizin, an active component of liquorice roots, and replication of SARS-associated coronavirus. The Lancet 361, 2045-2046.
Clarke, I.N., Estes, M.K., Green, K.Y., Hansman, G.S., Knowles, N.J., Koopmans, M.K., Matson, D.O., Meyers, G., Neill, J.D., Radford, A., Smith, A.W., Studdert, M.J., Thiel, H.J., Vinje, J. 2012. Family Caliciviridae, In: King, A.M.Q., Adams, M.J., Carstens, E.B., Lefkowitz, E.J. (Eds.) Virus taxonomy: Ninth Report of the International Committee on Taxonomy of Viruses. Elsevier, San Diego, 977-986.
Clarke, I.N., Lambden, P.R., 1997. The molecular biology of caliciviruses. Journal of General Virology 78 (Pt 2), 291-301.
Clemens, M.J., Jeffrey, I.W., 2006. Interferons and apoptosis–recent developments. The Interferons, 207-226.
Clifford, D.B., Nath, A., Cinque, P., Brew, B.J., Zivadinov, R., Gorelik, L., Zhao, Z., Duda, P., 2013. A study of mefloquine treatment for progressive multifocal leukoencephalopathy: results and exploration of predictors of PML outcomes. Journal of Neurovirology, 1-8.
Colgrove, D.J., Parker, A.J., 1971. Feline infectious peritonitis. Journal of Small Animal Practice 12, 225-232.
Cologna, R., Spagnolo, J., Hogue, B., 2000. Identification of nucleocapsid binding sites within coronavirus-defective genomes. Virology 277, 235-249.

Compton, S., Rogers, D., Holmes, K., Fertsch, D., Remenick, J., McGowan, J., 1987. In vitro replication of mouse hepatitis virus strain A59. Journal of Virology 61, 1814-1820.

Conneely, O.M., 2001. Antiinflammatory activities of lactoferrin. Journal of the American College of Nutrition 20, 389s-395s.

Corapi, W.V., Darteil, R.J., Audonnet, J.C., Chappuis, G.E., 1995. Localization of antigenic sites of the S glycoprotein of feline infectious peritonitis virus involved in neutralization and antibody-dependent enhancement. Journal of Virology 69, 2858-2862.

Cornelissen, E., Dewerchin, H., Van Hamme, E., Nauwynck, H., 2009. Absence of antibody-dependent, complement-mediated lysis of feline infectious peritonitis virus-infected cells. Virus Research 144, 285-289.

Court, M.H., 2013. Feline drug metabolism and disposition: pharmacokinetic evidence for species differences and molecular mechanisms. Veterinary Clinics of North America: Small Animal Practice 43, 1039.

Coutts, A.J., Dawson, S., Willoughby, K., Gaskell, R.M., 1994. Isolation of feline respiratory viruses from clinically healthy cats at UK cat shows. Veterinary Record 135, 555-556.

Coyne, K.P., Christley, R.M., Pybus, O.G., Dawson, S., Gaskell, R.M., Radford, A.D., 2012. Large scale spatial and temporal genetic diversity of feline calicivirus. Journal of Virology.

Coyne, K.P., Dawson, S., Radford, A.D., Cripps, P.J., Porter, C.J., McCracken, C.M., Gaskell, R.M., 2006a. Long-term analysis of feline calicivirus prevalence and viral shedding patterns in naturally infected colonies of domestic cats. Veterinary Microbiology 118, 12-25.

Coyne, K.P., Jones, B.R.D., Kipar, A., Chantrey, J., Porter, C.J., Barber, P.J., Dawson, S., Gaskell, R.M., Radford, A.D., 2006b. Lethal outbreak of disease associated with feline calicivirus infection in cats. Veterinary Record 158, 544-550.

Crandell, R.A., Fabricant, C.G., Nelson-Rees, W.A., 1973. Development, characterization, and viral susceptibility of a feline (Felis catus) renal cell line (CRFK). In Vitro 9, 176-185.

Croft, A.M., 2007. A lesson learnt: the rise and fall of Lariam and Halfan. Journal of the Royal Society of Medicine 100, 170-174.

Crotty, S., Cameron, C., Andino, R., 2002. Ribavirin's antiviral mechanism of action: lethal mutagenesis? Journal of Molecular Medicine 80, 86-95.

Cruz, D.J.M., Bonotto, R.M., Gomes, R.G.B., da Silva, C.T., Taniguchi, J.B., No, J.H., Lombardot, B., Schwartz, O., Hansen, M.A.E., Freitas-Junior, L.H., 2013. Identification of novel compounds inhibiting chikungunya virus-induced cell death by high throughput ccreening of a kinase inhibitor library. PLoS Neglected Tropical Diseases 7, e2471.

Cutler, B., Justman, J., 2008. Vaginal microbicides and the prevention of HIV transmission. The Lancet Infectious Diseases 8, 685-697.

Czekanska, E.M., 2011. Assessment of cell proliferation with resazurin-based fluorescent dye. Methods in Molecular Biology 740, 27-32.

Da Violante, G., Zerrouk, N., Richard, I., Provot, G., Chaumeil, J.C., Arnaud, P., 2002. Evaluation of the cytotoxicity effect of dimethyl sulfoxide (DMSO) on Caco2/TC7 colon tumor cell cultures. Biological & Pharmaceutical Bulletin 25, 1600-1603.

Danilov, L.L., Deeva, A.V., Kuritz, T., Maltsev, S.D., Narovlianskiy, A.N., Pronin, A.V., Sanin, A.V., Sosnovskaya, O.Y., Ozherelkov, S.V. 2003. Therapeutic composition and methods (United States).

Das, A.T., Brummelkamp, T.R., Westerhout, E.M., Vink, M., Madiredjo, M., Bernards, R., Berkhout, B., 2004. Human immunodeficiency virus type 1 escapes from RNA interference-mediated inhibition. Journal of Virology 78, 2601-2605.

Davies, W.L., Grunert, R.R., Haff, R.F., McGahen, J.W., Neumayer, E.M., Paulshock, M., Watts, J.C., Wood, T.R., Hermann, E.C., Hoffmann, C.E., 1964. Antiviral activity of 1-adamantanamine (amantadine). Science 144, 862-863.

Dawson, S., Bennett, D., Carter, S.D., Bennett, M., Meanger, J., Turner, P.C., Carter, M.J., Milton, I., Gaskell, R.M., 1994. Acute arthritis of cats associated with feline calicivirus infection. Research in Veterinary Science 56, 133-143.

Dawson, S., McArdle, F., Bennett, D., Carter, S.D., Bennett, M., Ryvar, R., Gaskell, R.M., 1993. Investigation of vaccine reactions and breakdowns after feline calicivirus vaccination. Veterinary Record 132, 346-350.

Day, M.J., Horzinek, M.C., Schultz, R.D., 2010. WSAVA guidelines for the vaccination of dogs and cats. Journal of Small Animal Practice 51, 338-356.

De Clercq, E., 2002. Strategies in the design of antiviral drugs. Nature Reviews Drug Discovery 1, 13-25.

De Clercq, E., 2006. Potential antivirals and antiviral strategies against SARS coronavirus infections. Expert review of Anti-Infective therapy 4, 291-302.

De Clercq, E., 2010. Antiviral therapy: quo vadis? Future Medicinal Chemistry 2, 1049-1053.

De Groot, R., Andeweg, A., Horzinek, M., Spaan, W., 1988. Sequence analysis of the 3'-end of the feline coronavirus FIPV 79-1146 genome: comparison with the genome of porcine coronavirus TGEV reveals large insertions. Virology 167, 370-376.

de Groot, R.J., Baker, S.C., Baric, R., Enjuanes, L., Gorbalenya, A.E., Holmes, K.V., Perlman, S., Poon, L., Rottier, P.J.M., Talbot, P.J., Woo, P.C.Y., Ziebuhr, J. 2012. Family Coronaviridae, In: King, A.M.Q., Adams, M.J., Carstens, E.B., Lefkowitz, E.J. (Eds.) Virus taxonomy: Ninth Report of the International Committee on Taxonomy of Viruses. Elsevier, San Diego, 806-828.

de Haan, C., Vennema, H., Rottier, P., 2000. Assembly of the coronavirus envelope: homotypic interactions between the M proteins. Journal of Virology 74, 4967-4978.

de Smet, M.D., Meenken, C.J., van den Horn, G.J., 1999. Fomivirsen - a phosphorothioate oligonucleotide for the treatment of CMV retinitis. Ocular Immunology and Inflammation 7, 189-198.

Dean, G.A., Olivry, T., Stanton, C., Pedersen, N.C., 2003. In vivo cytokine response to experimental feline infectious peritonitis virus infection. Veterinary Microbiology 97, 1-12.

Dean, R.T., Jessup, W., Roberts, C.R., 1984. Effects of exogenous amines on mammalian cells, with particular reference to membrane flow. Biochemical Journal 217, 27-40.

Decroly, E., Debarnot, C., Ferron, F., Bouvet, M., Coutard, B., Imbert, I., Gluais, L., Papageorgiou, N., Sharff, A., Bricogne, G., Ortiz-Lombardia, M., Lescar, J., Canard, B., 2011. Crystal structure and functional analysis of the SARS-coronavirus RNA Cap 2 '-O-methyltransferase nsp10/nsp16 complex. PLoS Pathogens 7.

Decroly, E., Imbert, I., Coutard, B., Bouvet, M.L., Selisko, B., Alvarez, K., Gorbalenya, A.E., Snijder, E.J., Canard, B., 2008. Coronavirus nonstructural

protein 16 is a cap-0 binding enzyme possessing (nucleoside-2'O)-methyltransferase activity. Journal of Virology 82, 8071-8084.
DeFilippis, V., Raggo, C., Moses, A., Früh, K., 2003. Functional genomics in virology and antiviral drug discovery. Trends in Biotechnology 21, 452-457.
Denison, M., Spaan, W., van der Meer, Y., Gibson, C., Sims, A., Prentice, E., Lu, X., 1999. The putative helicase of the coronavirus mouse hepatitis virus is processed from the replicase gene polyprotein and localizes in complexes that are active in viral RNA synthesis. Journal of Virology 73, 6862-6871.
Denison, M.R., Graham, R.L., Donaldson, E.F., Eckerle, L.D., Baric, R.S., 2011. Coronaviruses: an RNA proofreading machine regulates replication fidelity and diversity. RNA Biology 8, 270-279.
Desmarets, L.M., Theuns, S., Olyslaegers, D.A., Dedeurwaerder, A., Vermeulen, B.L., Roukaerts, I.D., Nauwynck, H.J., 2013. Establishment of feline intestinal epithelial cell cultures for the propagation and study of feline enteric coronaviruses. Veterinary Research 44, 71.
DeVincenzo, J., Lambkin-Williams, R., Wilkinson, T., Cehelsky, J., Nochur, S., Walsh, E., Meyers, R., Gollob, J., Vaishnaw, A., 2010. A randomized, double-blind, placebo-controlled study of an RNAi-based therapy directed against respiratory syncytial virus. Proceedings of the National Academy of Sciences 107, 8800-8805.
Dewerchin, H.L., Cornelissen, E., Nauwynck, H.J., 2005. Replication of feline coronaviruses in peripheral blood monocytes. Archives of Virology 150, 2483-2500.
Dewerchin, H.L., Cornelissen, E., Nauwynck, H.J., 2006. Feline infectious peritonitis virus-infected monocytes internalize viral membrane-bound proteins upon antibody addition. Journal of General Virology 87, 1685-1690.
Di Martino, B., Marsilio, F., 2010. Feline calicivirus VP2 is involved in the self-assembly of the capsid protein into virus-like particles. Research in Veterinary Science 89, 279-281.
Di Martino, B., Marsilio, F., Roy, P., 2007. Assembly of feline calicivirus-like particle and its immunogenicity. Veterinary Microbiology 120, 173-178.
Dick, C.P., Johnson, R.P., Yamashiro, S., 1989. Sites of persistence of feline calicivirus. Research in Veterinary Science 47, 367-373.
Diehl, K., Rosychuk, R.A., 1993. Feline gingivitis-stomatitis-pharyngitis. Veterinary Clinics of North America: Small Animal Practice 23, 139-153.
Dille, B.J., Johnson, T.C., 1982. Inhibition of vesicular stomatitis virus glycoprotein expression by chloroquine. Journal of General Virology 62, 91-103.
Doménech, A., Miró, G., Collado, V.M., Ballesteros, N., Sanjosé, L., Escolar, E., Martin, S., Gomez-Lucia, E., 2011. Use of recombinant interferon omega in feline retrovirosis: From theory to practice. Veterinary Immunology and Immunopathology.
Domingo, E., Baranowski, E., Ruiz-Jarabo, C.M., Martin-Hernandez, A.M., Saiz, J.C., Escarmis, C., 1998. Quasispecies structure and persistence of RNA viruses. Emerging Infectious Diseases 4, 521-527.
Domingo, E., Escarmis, C., Sevilla, N., Moya, A., Elena, S.F., Quer, J., Novella, I.S., Holland, J.J., 1996. Basic concepts in RNA virus evolution. FASEB Journal 10, 859-864.
Doultree, J.C., Druce, J.D., Birch, C.J., Bowden, D.S., Marshall, J.A., 1999. Inactivation of feline calicivirus, a Norwalk virus surrogate. Journal of Hospital Infection 41, 51-57.

Dowers, K.L., Hawley, J.R., Brewer, M.M., Morris, A.K., Radecki, S.V., Lappin, M.R., 2010. Association of Bartonella species, feline calicivirus, and feline herpesvirus 1 infection with gingivostomatitis in cats. Journal of Feline Medicine and Surgery 12, 314-321.

Drosten, C., Günther, S., Preiser, W., Van Der Werf, S., Brodt, H.-R., Becker, S., Rabenau, H., Panning, M., Kolesnikova, L., Fouchier, R.A., 2003. Identification of a novel coronavirus in patients with severe acute respiratory syndrome. New England Journal of Medicine 348, 1967-1976.

Du, Q., Thonberg, H., Wang, J., Wahlestedt, C., Liang, Z.C., 2005. A systematic analysis of the silencing effects of an active siRNA at all single-nucleotide mismatched target sites. Nucleic Acids Research 33, 1671-1677.

Dutta, D., Donaldson, J.G., 2012. Search for inhibitors of endocytosis: Intended specificity and unintended consequences. Cellular Logistics 2, 203-208.

Dye, C., Siddell, S.G., 2005. Genomic RNA sequence of Feline coronavirus strain FIPV WSU-79/1146. Journal of General Virology 86, 2249-2253.

Dye, C., Siddell, S.G., 2007. Genomic RNA sequence of feline coronavirus strain FCoV C1Je. Journal of Feline Medicine and Surgery 9, 202-213.

Dye, C., Temperton, N., Siddell, S.G., 2007. Type I feline coronavirus spike glycoprotein fails to recognize aminopeptidase N as a functional receptor on feline cell lines. Journal of General Virology 88, 1753-1760.

Echeverri, C.J., Perrimon, N., 2006. High-throughput RNAi screening in cultured cells: a user's guide. Nature Reviews Genetics 7, 373-384.

Eekels, J.J., Geerts, D., Jeeninga, R.E., Berkhout, B., 2011. Long-term inhibition of HIV-1 replication with RNA interference against cellular co-factors. Antiviral Research 89, 43-53.

Elbashir, S., Harborth, J., Lendeckel, W., Yalcin, A., Weber, K., Tuschl, T., 2001a. Duplexes of 21-nucleotide RNAs mediate RNA interference in cultured mammalian cells. Nature 411, 494-498.

Elbashir, S.M., Martinez, J., Patkaniowska, A., Lendeckel, W., Tuschl, T., 2001b. Functional anatomy of siRNAs for mediating efficient RNAi in Drosophila melanogaster embryo lysate. The EMBO journal 20, 6877-6888.

Ellis, T.M., 1981. Jaundice in a Siamese cat with in utero feline calicivirus infection. Australian Veterinary Journal 57, 383-385.

Elmen, J., Thonberg, H., Ljungberg, K., Frieden, M., Westergaard, M., Xu, Y., Wahren, B., Liang, Z., Orum, H., Koch, T., Wahlestedt, C., 2005. Locked nucleic acid (LNA) mediated improvements in siRNA stability and functionality. Nucleic Acids Research 33, 439-447.

Escors, D., Izeta, A., Capiscol, C., Enjuanes, L., 2003. Transmissible gastroenteritis coronavirus packaging signal is located at the 5' end of the virus genome. Journal of Virology 77, 7890-7902.

Evermann, J.F., Heeney, J.L., Roelke, M.E., McKeirnan, A.J., O'Brien, S.J., 1988. Biological and pathological consequences of feline infectious peritonitis virus infection in the cheetah. Archives of Virology 102, 155-171.

Ewart, G.D., Nasr, N., Naif, H., Cox, G.B., Cunningham, A.L., Gage, P.W., 2004. Potential new anti-human immunodeficiency virus type 1 compounds depress virus replication in cultured human macrophages. Antimicrobial Agents and Chemotherapy 48, 2325-2330.

Fan, Q., Wei, C., Xia, M., Jiang, X., 2013. Inhibition of Tulane virus replication in vitro with RNA interference. Journal of Medical Virology 85, 179-186.

Fastier, L.B., 1957. A new feline virus isolated in tissue culture. American Journal of Veterinary Research 18, 382-389.

Feld, J.J., Hoofnagle, J.H., 2005. Mechanism of action of interferon and ribavirin in treatment of hepatitis C. Nature 436, 967-972.
Ferraris, O., Kessler, N., Lina, B., 2005. Sensitivity of influenza viruses to zanamivir and oseltamivir: a study performed on viruses circulating in France prior to the introduction of neuraminidase inhibitors in clinical practice. Antiviral Research 68, 43-48.
Figlerowicz, M., Alejska, M., Kurzynska-Kokorniak, A., Figlerowicz, M., 2003. Genetic variability: The key problem in the prevention and therapy of RNA-based virus infections. Medicinal Research Reviews 23, 488-518.
Fiore, C., Eisenhut, M., Krausse, R., Ragazzi, E., Pellati, D., Armanini, D., Bielenberg, J., 2008. Antiviral effects of Glycyrrhiza species. Phytotherapy Research 22, 141-148.
Fire, A., Xu, S., Montgomery, M., Kostas, S., Driver, S., Mello, C., 1998. Potent and specific genetic interference by double-stranded RNA in Caenorhabditis elegans. Nature, 806-810.
Fischer, F., Stegen, C.F., Masters, P.S., Samsonoff, W.A., 1998. Analysis of constructed E gene mutants of mouse hepatitis virus confirms a pivotal role for E protein in coronavirus assembly. Journal of Virology 72, 7885-7894.
Fischer, Y., Ritz, S., Weber, K., Sauter-Louis, C., Hartmann, K., 2011. Randomized, placebo controlled study of the effect of propentofylline on survival time and quality of life of cats with feline infectious peritonitis. Journal of Veterinary Internal Medicine 25, 1270-1276.
Fluiter, K., Mook, O.R., Baas, F., 2009. The therapeutic potential of LNA-modified siRNAs: reduction of off-target effects by chemical modification of the siRNA sequence. Methods in Molecular Biology 487, 189-203.
Foley, J., Hurley, K., Pesavento, P.A., Poland, A., Pedersen, N.C., 2006. Virulent systemic feline calicivirus infection: local cytokine modulation and contribution of viral mutants. Journal of Feline Medicine and Surgery 8, 55-61.
Foley, J.E., Pedersen, N.C., 1996. The inheritance of susceptibility to feline infectious peritonitis in purebred catteries. Feline Practice 24, 14-22.
Foley, J.E., Poland, A., Carlson, J., Pedersen, N.C., 1997a. Patterns of feline coronavirus infection and fecal shedding from cats in multiple-cat environments. Journal of the American Veterinary Medical Association 210, 1307-1312.
Foley, J.E., Poland, A., Carlson, J., Pedersen, N.C., 1997b. Risk factors for feline infectious peritonitis among cats in multiple-cat environments with endemic feline enteric coronavirus. Journal of the American Veterinary Medical Association 210, 1313-1318.
Foley, J.E., Rand, C., Bannasch, M.J., Norris, C.R., Milan, J., 2002. Molecular epidemiology of feline bordetellosis in two animal shelters in California, USA. Preventive Veterinary Medicine 54, 141-156.
Ford, R.B., 1986. Biological response modifiers in the management of viral infection. Veterinary Clinics of North America: Small Animal Practice 16, 1191-1204.
Foster, D.J., Barros, S., Duncan, R., Shaikh, S., Cantley, W., Dell, A., Bulgakova, E., O'Shea, J., Taneja, N., Kuchimanchi, S., Sherrill, C.B., Akinc, A., Hinkle, G., White, A.C.S., Pang, B., Charisse, K., Meyers, R., Manoharan, M., Elbashir, S.M., 2012. Comprehensive evaluation of canonical versus Dicer-substrate siRNA in vitro and in vivo. RNA 18, 557-568.
Freiberg, A.N., Worthy, M.N., Lee, B., Holbrook, M.R., 2010. Combined chloroquine and ribavirin treatment does not prevent death in a hamster model of Nipah and Hendra virus infection. Journal of General Virology 91, 765-772.

French, J., Hurst, N., O'Donnell, M., Betts, W., 1987. Uptake of chloroquine and hydroxychloroquine by human blood leucocytes in vitro: relation to cellular concentrations during antirheumatic therapy. Annals of the Rheumatic Diseases 46, 42-45.

Fulton, R.W., Burge, L.J., 1985. Susceptibility of feline herpesvirus 1 and a feline calicivirus to feline interferon and recombinant human leukocyte interferons. Antimicrobial Agents and Chemotherapy 28, 698-699.

Gantier, M.P., Tong, S., Behlke, M.A., Irving, A.T., Lappas, M., Nilsson, U.W., Latz, E., McMillan, N.A.J., Williams, B.R.G., 2010. Rational design of immunostimulatory siRNAs. Molecular Therapy 18, 785-795.

Gao, K., Huang, L., 2009. Nonviral methods for siRNA delivery. Molecular Pharmaceutics 6, 651-658.

Gao, K., Huang, L., 2013. Achieving efficient RNAi therapy: progress and challenges. Acta Pharmaceutica Sinica B 3, 213-225.

Garrison, F.H., 1925. Alonzo Clark. Bulletin of the New York Academy of Medicine 1, i4-328.

Gaskell, R.M., Dawson, S., Radford, A. 2012. Feline respiratory disease, In: Greene, C.E. (Ed.) Infectious Diseases of the Dog and Cat. Elsevier, St Louis, Missouri, 151-162.

Gazina, E.V., Harrison, D.N., Jefferies, M., Tan, H., Williams, D., Anderson, D.A., Petrou, S., 2005. Ion transport blockers inhibit human rhinovirus 2 release. Antiviral Research 67, 98-106.

Gazina, E.V., Smidansky, E.D., Holien, J.K., Harrison, D.N., Cromer, B.A., Arnold, J.J., Parker, M.W., Cameron, C.E., Petrou, S., 2011. Amiloride is a competitive inhibitor of coxsackievirus B3 RNA polymerase. Journal of Virology 85, 10364-10374.

Ge, Q., McManus, M.T., Nguyen, T., Shen, C.-H., Sharp, P.A., Eisen, H.N., Chen, J., 2003. RNA interference of influenza virus production by directly targeting mRNA for degradation and indirectly inhibiting all viral RNA transcription. Proceedings of the National Academy of Sciences 100, 2718-2723.

Geisbert, T.W., Hensley, L.E., Kagan, E., Yu, E.Y.Z., Geisbert, J.B., Daddario-DiCaprio, K., Fritz, E.A., Jahrling, P.B., McClintock, K., Phelps, J.R., Lee, A.C.H., Judge, A., Jeffs, L.B., MacLachlan, I., 2006. Postexposure protection of guinea pigs against a lethal Ebola virus challenge is conferred by RNA interference. Journal of Infectious Diseases 193, 1650-1657.

Geisbert, T.W., Lee, A.C., Robbins, M., Geisbert, J.B., Honko, A.N., Sood, V., Johnson, J.C., De Jong, S., Tavakoli, I., Judge, A., 2010. Postexposure protection of non-human primates against a lethal Ebola virus challenge with RNA interference: a proof-of-concept study. The Lancet 375, 1896-1905.

Geissler, K., Schneider, K., Truyen, U., 2002. Mapping neutralizing and non-neutralizing epitopes on the capsid protein of feline calicivirus. Journal of Veterinary Medicine Series B 49, 55-60.

Ghareeb, B., 2008. RNAi inhibition of rabbit hemorrhagic disease virus (RHDV) gene expression in CHO cell line. An-Najah University Journal for Research 22, 145-165.

Gifford, G.E., 1963. Studies on the specificity of interferon. Journal of General Microbiology 33, 437-443.

Gitlin, L., Karelsky, S., Andino, R., 2002. Short interfering RNA confers intracellular antiviral immunity in human cells. Nature 418, 430-434.

Gitlin, L., Stone, J.K., Andino, R., 2005. Poliovirus escape from RNA interference: short interfering RNA-target recognition and implications for therapeutic approaches. Journal of Virology 79, 1027-1035.

Glaumann, H., Motakefi, A.M., Jansson, H., 1992. Intracellular distribution and effect of the antimalarial drug mefloquine on lysosomes of rat liver. Liver 12, 183-190.

Glenn, M., Radford, A.D., Turner, P.C., Carter, M., Lowery, D., DeSilver, D.A., Meanger, J., Baulch-Brown, C., Bennett, M., Gaskell, R.M., 1999. Nucleotide sequence of UK and Australian isolates of feline calicivirus (FCV) and phylogenetic analysis of FCVs. Veterinary Microbiology 67, 175-193.

Golovko, L., Lyons, L.A., Liu, H., Sørensen, A., Wehnert, S., Pedersen, N.C., 2013. Genetic susceptibility to feline infectious peritonitis in Birman cats. Virus Research 175, 58-63.

Gonon, V., Duquesne, V., Klonjkowski, B., Monteil, M., Aubert, A., Eloit, M., 1999. Clearance of infection in cats naturally infected with feline coronaviruses is associated with an anti-S glycoprotein antibody response. Journal of General Virology 80, 2315-2317.

Goodfellow, I., Chaudhry, Y., Gioldasi, I., Gerondopoulos, A., Natoni, A., Labrie, L., Laliberte, J.F., Roberts, L., 2005. Calicivirus translation initiation requires an interaction between VPg and eIF4E. EMBO Reports 6, 968-972.

Gosert, R., Kanjanahaluethai, A., Egger, D., Bienz, K., Baker, S., 2002. RNA replication of mouse hepatitis virus takes place at double-membrane vesicles. Journal of Virology 76, 3697-3708.

Govorkova, E.A., Webster, R.G., 2010. Combination chemotherapy for influenza. Viruses 2, 1510-1529.

Green, K.Y. 2007. Caliciviridae: The Noroviruses, In: Knipe, D.M., Howley, P.M. (Eds.) Fields Virology. Lippincott Williams & Wilkins, Philadelpia, 949-979.

Green, K.Y., Mory, A., Fogg, M.H., Weisberg, A., Belliot, G., Wagner, M., Mitra, T., Ehrenfeld, E., Cameron, C.E., Sosnovtsev, S.V., 2002. Isolation of enzymatically active replication complexes from feline calicivirus-infected cells. Journal of Virology 76, 8582-8595.

Green, N., Ott, R.D., Isaacs, R.J., Fang, H., 2008. Cell-based assays to identify inhibitors of viral disease. Expert Opinion on Drug Discovery 3, 671-676.

Gregory, M., Rutty, D., Wood, R., 1970. Differences in the retinotoxic action of chloroquine and phenothiazine derivatives. The Journal of Pathology 102, 139-150.

Gribbon, P., Sewing, A., 2003. Fluorescence readouts in HTS: no gain without pain? Drug Discovery Today 8, 1035-1043.

Grimm, D., Streetz, K.L., Jopling, C.L., Storm, T.A., Pandey, K., Davis, C.R., Marion, P., Salazar, F., Kay, M.A., 2006. Fatality in mice due to oversaturation of cellular microRNA/short hairpin RNA pathways. Nature 441, 537-541.

Groot-Mijnes, J.D.F.d., Dun, J.M.v., Most, R.G.v.d., Groot, R.J.d., 2005. Natural history of a recurrent feline coronavirus infection and the role of cellular immunity in survival and disease. Journal of Virology 79, 1036-1044.

Grove, J., Marsh, M., 2011. The cell biology of receptor-mediated virus entry. The Journal of Cell biology 195, 1071-1082.

Guidotti, L.G., Chisari, F.V., 2001. Noncytolytic control of viral infections by the innate and adaptive immune response. Annual Review of Immunology 19, 65-91.

Gunn-Moore, D.A., Gruffydd-Jones, T.J., Harbour, D.A., 1998. Detection of feline coronaviruses by culture and reverse transcriptase-polymerase chain reaction

of blood samples from healthy cats and cats with clinical feline infectious peritonitis. Veterinary Microbiology 62, 193-205.
Gunn-Moore, D.A., Gunn-Moore, F.J., Gruffydd-Jones, T.J., Harbour, D.A., 1999. Detection of FCoV quasispecies using denaturing gradient gel electrophoresis. Veterinary Microbiology 69, 127-130.
Guo, S., Kemphues, K.J., 1995. *par-1*, a gene required for establishing polarity in C. elegans embryos, encodes a putative Ser/Thr kinase that is asymmetrically distributed. Cell 81, 611-620.
Haagmans, B.L., Egberink, H.F., Horzinek, M.C., 1996. Apoptosis and T-cell depletion during feline infectious peritonitis. Journal of Virology 70, 8977-8983.
Haijema, B., Volders, H., Rottier, P., 2003. Switching species tropism: an effective way to manipulate the feline coronavirus genome. Journal of Virology 77, 4528-4538.
Haijema, B.J., Volders, H., Rottier, P.J.M., 2004. Live, attenuated coronavirus vaccines through the directed deletion of group-specific genes provide protection against feline infectious peritonitis. Journal of Virology 78, 3863-3871.
Haley, B., Zamore, P.D., 2004. Kinetic analysis of the RNAi enzyme complex. Nature Structural & Molecular Biology 11, 599-606.
Harbour, D.A., Howard, P.E., Gaskell, R.M., 1991. Isolation of feline calicivirus and feline herpesvirus from domestic cats 1980 to 1989. Veterinary Record 128, 77-80.
Harley, R., Gruffydd-Jones, T.J., Day, M.J., 2003. Salivary and serum immunoglobulin levels in cats with chronic gingivostomatitis. Veterinary Record 152, 125-129.
Harley, R., Gruffydd-Jones, T.J., Day, M.J., 2011. Immunohistochemical characterization of oral mucosal lesions in cats with chronic gingivostomatitis. Journal of Comparative Pathology 144, 239-250.
Harley, R., Helps, C.R., Harbour, D.A., Gruffydd-Jones, T.J., Day, M.J., 1999. Cytokine mRNA expression in lesions in cats with chronic gingivostomatitis. Clinical and Diagnostic Laboratory Immunology 6, 471-478.
Harpold, L.M., Legendre, A.M., Kennedy, M.A., Plummer, P.J., Millsaps, K., Rohrbach, B., 1999. Fecal shedding of feline coronavirus in adult cats and kittens in an Abyssinian cattery. Journal of the American Veterinary Medical Association 215, 948-951.
Harrison, D.N., Gazina, E.V., Purcell, D.F., Anderson, D.A., Petrou, S., 2008. Amiloride derivatives inhibit coxsackievirus B3 RNA replication. Journal of Virology 82, 1465-1473.
Hartmann, K., 2005. Feline infectious peritonitis. Veterinary Clinics of North America: Small Animal Practice 35, 39-79.
Hartmann, K., Donath, A., Kraft, W., 1995. AZT in the treatment of feline immunodeficiency virus infection Part 2. Feline Practice 23, 13-20.
Hartmann, K., Ritz, S., 2008. Treatment of cats with feline infectious peritonitis. Veterinary Immunology and Immunopathology 123, 172-175.
Harun, M.S., Kuan, C.O., Selvarajah, G.T., Wei, T.S., Arshad, S.S., Bejo, M.H., Omar, A.R., 2013. Transcriptional profiling of feline infectious peritonitis virus infection in CRFK cells and in PBMCs from FIP diagnosed cats. Virology Journal 10, 329.
Hashem, A.M., Flaman, A.S., Farnsworth, A., Brown, E.G., Van Domselaar, G., He, R., Li, X., 2009. Aurintricarboxylic acid is a potent inhibitor of influenza A and B virus neuraminidases. PLoS One 4, e8350.

Hayashi, T., Sasaki, N., Ami, Y., Fujiwara, K., 1983. Role of thymus-dependent lymphocytes and antibodies in feline infectious peritonitis after oral infection. Japanese Journal of Veterinary Science 45, 759-766.

He, L., Hannon, G.J., 2004. MicroRNAs: Small RNAs with a big role in gene regulation. Nature Reviews Genetics 5, 522-531.

He, L., Zhang, Y.-m., Dong, L.-j., Cheng, M., Wang, J., Tang, Q.-h., Wang, G., 2012. In vitro inhibition of transmissible gastroenteritis coronavirus replication in swine testicular cells by short hairpin RNAs targeting the ORF 7 gene. Virology Journal 9, 176.

He, M.L., Zheng, B., Peng, Y., Peiris, J.S.M., Poon, L.L.M., Yuen, K.Y., Lin, M.C.M., Kung, H., Guan, Y. 2003. Inhibition of SARS-associated coronavirus infection and replication by RNA interference (Am Med Assoc), 2665-2666.

He, M.L., Zheng, B.J., Chen, Y., Wong, K.L., Huang, J.D., Lin, M.C., Peng, Y., Yuen, K.Y., Sung, J.J.Y., Kung, H.F., 2006. Kinetics and synergistic effects of siRNAs targeting structural and replicase genes of SARS-associated coronavirus. FEBS Letters 580, 2414-2420.

He, M.L., Zheng, B.J., Chen, Y., Wong, K.L., Huang, J.D., Lin, M.C., Yuen, K.Y., Sung, J.J., Kung, H.F., 2009. Development of interfering RNA agents to inhibit SARS-associated coronavirus infection and replication. Hong Kong Medical Journal 15, 28-31.

He, R., Adonov, A., Traykova-Adonova, M., Cao, J., Cutts, T., Grudesky, E., Deschambaul, Y., Berry, J., Drebot, M., Li, X., 2004. Potent and selective inhibition of SARS coronavirus replication by aurintricarboxylic acid. Biochemical & Biophysical Research Communications 320, 1199-1203.

Healey, K.A., Dawson, S., Burrow, R., Cripps, P., Gaskell, C.J., Hart, C.A., Pinchbeck, G.L., Radford, A.D., Gaskell, R.M., 2007. Prevalence of feline chronic gingivo-stomatitis in first opinion veterinary practice. Journal of Feline Medicine and Surgery 9, 373-381.

Hean, J., Crowther, C., Ely, A., Ul Islam, R., Barichievy, S., Bloom, K., Weinberg, M.S., van Otterlo, W.A., de Koning, C.B., Salazar, F., Marion, P., Roesch, E.B., Lemaitre, M., Herdewijn, P., Arbuthnot, P., 2010. Inhibition of hepatitis B virus replication in vivo using lipoplexes containing altritol-modified antiviral siRNAs. Artificial DNA: PNA & XNA 1, 17-26.

Helps, C.R., Lait, P., Damhuis, A., Bjornehammar, U., Bolta, D., Brovida, C., Chabanne, L., Egberink, H., Ferrand, G., Fontbonne, A., Pennisi, M.G., Gruffydd-Jones, I., Gunn-Moore, D., Hartmann, K., Lutz, H., Malandain, E., Mostl, K., Stengel, C., Harbour, D.A., Graat, E.A.M., 2005. Factors associated with upper respiratory tract disease caused by feline herpesvirus, feline calicivirus, Chlamydophila felis and Bordetella bronchiseptica in cats: experience from 218 European catteries. Veterinary Record 156, 669-673.

Hennet, P.R., Camy, G.A., McGahie, D.M., Albouy, M.V., 2011. Comparative efficacy of a recombinant feline interferon omega in refractory cases of calicivirus-positive cats with caudal stomatitis: a randomised, multi-centre, controlled, double-blind study in 39 cats. Journal of Feline Medicine and Surgery 13, 577-587.

Herbert, T.P., Brierley, I., Brown, T.D., 1996. Detection of the ORF3 polypeptide of feline calicivirus in infected cells and evidence for its expression from a single, functionally bicistronic, subgenomic mRNA. Journal of General Virology 77 (Pt 1), 123-127.

Herbert, T.P., Brierley, I., Brown, T.D.K., 1997. Identification of a protein linked to the genomic and subgenomic mRNAs of feline calicivirus and its role in translation. Journal of General Virology 78, 1033-1040.
Herrewegh, A.A.P.M., Mahler, M., Hedrich, H.J., Haagmans, B.L., Egberink, H.F., Horzinek, M.C., Rottier, P.J.M., Groot, R.J.d., 1997. Persistence and evolution of feline coronavirus in a closed cat-breeding colony. Virology 234, 349-363.
Herrewegh, A.A.P.M., Smeenk, I., Horzinek, M.C., Rottier, P.J.M., Groot, R.J.d., 1998. Feline coronavirus type II strains 79-1683 and 79-1146 originate from a double recombination between feline coronavirus type I and canine coronavirus. Journal of Virology 72, 4508-4514.
Herrmann, E., Herrmann, J., 1977. A working hypothesis—virus resistance development as an indicator of specific antiviral activity. Annals of the New York Academy of Sciences 284, 632-637.
Hickerson, R.P., Vlassov, A.V., Wang, Q., Leake, D., Ilves, H., Gonzalez-Gonzalez, E., Contag, C.H., Johnston, B.H., Kaspar, R.L., 2008. Stability study of unmodified siRNA and relevance to clinical use. Oligonucleotides 18, 345-354.
Hickman, M.A., Morris, J.G., Rogers, Q.R., Pedersen, N.C., 1995. Elimination of feline coronavirus infection from a large experimental specific pathogen-free cat breeding colony by serologic testing and isolation. Feline Practice 23, 96-102.
Hilton, A., Mizzen, L., Macintyre, G., Cheley, S., Anderson, R., 1986. Translational control in murine hepatitis virus infection. Journal of General Virology 67, 923-932.
Hodge, A.V., Field, H.J., 2010. General mechanisms of antiviral resistance. Genetics and Evolution of Infectious Diseases, 339.
Hohdatsu, T., Izumiya, Y., Yokoyama, Y., Kida, K., Koyama, H., 1998. Differences in virus receptor for type I and type II feline infectious peritonitis virus. Archives of Virology 143, 839-850.
Hohdatsu, T., Nakamura, M., Ishizuka, Y., Yamada, H., Koyama, H., 1991a. A study of the mechanism of antibody-dependent enhancement of feline infectious peritonitis virus infection in feline macrophages by monoclonal antibodies. Archives of Virology 120, 207-217.
Hohdatsu, T., Okada, S., Ishizuka, Y., Yamada, H., Koyama, H., 1992. The prevalence of types I and II feline coronavirus infections in cats. Journal of Veterinary Medical Science 54, 557-562.
Hohdatsu, T., Okada, S., Koyama, H., 1991b. Characterization of monoclonal antibodies against feline infectious peritonitis virus type II and antigenic relationship between feline, porcine, and canine coronaviruses. Archives of Virology 117, 85-95.
Holen, T., Amarzguioui, M., Wiiger, M.T., Babaie, E., Prydz, H., 2002. Positional effects of short interfering RNAs targeting the human coagulation trigger Tissue Factor. Nucleic Acids Research 30, 1757-1766.
Holland, J., Spindler, K., Horodyski, F., Grabau, E., Nichol, S., VandePol, S., 1982. Rapid evolution of RNA genomes. Science 215, 1577-1585.
Holmes, E.C., 2009. The evolution and emergence of RNA viruses. Oxford University Press, New York.
Holst, B.S., Englund, L., Palacios, S., Renstrom, L., Berndtsson, L.T., 2006. Prevalence of antibodies against feline coronavirus and Chlamydophila felis in Swedish cats. Journal of Feline Medicine and Surgery 8, 207-211.
Holzworth, J., 1963. Some important disorders of cats. The Cornell Veterinarian 53, 157-160.

Hong, J., Huang, Y., Li, J., Yi, F., Zheng, J., Huang, H., Wei, N., Shan, Y., An, M., Zhang, H., Ji, J., Zhang, P., Xi, Z., Du, Q., Liang, Z., 2010. Comprehensive analysis of sequence-specific stability of siRNA. FASEB Journal 24, 4844-4855.

Hoopes, J.D., Driebe, E.M., Kelley, E., Engelthaler, D.M., Keim, P.S., Perelson, A.S., Rong, L., Went, G.T., Nguyen, J.T., 2011. Triple combination antiviral drug (TCAD) composed of amantadine, oseltamivir, and ribavirin impedes the selection of drug-resistant influenza A virus. PLoS One 6, e29778.

Hoover, E.A., Kahn, D.E., 1973. Lesions produced by feline picornaviruses of different virulence in pathogen-free cats. Veterinary Pathology 10, 307-322.

Hoover, E.A., Kahn, D.E., 1975. Experimentally induced feline calicivirus infection - clinical signs and lesions. Journal of the American Veterinary Medical Association 166, 463-468.

Hornung, V., Guenthner-Biller, M., Bourquin, C., Ablasser, A., Schlee, M., Uematsu, S., Noronha, A., Manoharan, M., Akira, S., de Fougerolles, A., 2005. Sequence-specific potent induction of IFN-alpha by short interfering RNA in plasmacytoid dendritic cells through TLR7. Nature Medicine 11, 263-270.

Horscroft, N., Lai, V.C.H., Cheney, W., Yao, N., Wu, J.Z., Hong, Z., Zhong, W., 2005. Replicon cell culture system as a valuable tool in antiviral drug discovery against hepatitis C virus. Antiviral Chemistry & Chemotherapy 16, 1-12.

Howett, M.K., Neely, E.B., Christensen, N.D., Wigdahl, B., Krebs, F.C., Malamud, D., Patrick, S.D., Pickel, M.D., Welsh, P.A., Reed, C.A., Ward, M.G., Budgeon, L.R., Kreider, J.W., 1999. A broad-spectrum microbicide with virucidal activity against sexually transmitted viruses. Antimicrobial Agents and Chemotherapy 43, 314-321.

Hsieh, L.E., Lin, C.N., Su, B.L., Jan, T.R., Chen, C.M., Wang, C.H., Lin, D.S., Lin, C.T., Chueh, L.L., 2010. Synergistic antiviral effect of Galanthus nivalis agglutinin and nelfinavir against feline coronavirus. Antiviral Research 88, 25-30.

Hu, W.Y., Myers, C.P., Kilzer, J.M., Pfaff, S.L., Bushman, F.D., 2002. Inhibition of retroviral pathogenesis by RNA interference. Current Biology 12, 1301-1311.

Huang, C.J., Hess, J., Gill, M., Hustead, D., 2010. A dual-strain feline calicivirus vaccine stimulates broader cross-neutralization antibodies than a single-strain vaccine and lessens clinical signs in vaccinated cats when challenged with a homologous feline calicivirus strain associated with virulent systemic disease. Journal of Feline Medicine and Surgery 12, 129-137.

Huang, L., Liu, Y., 2011. In vivo delivery of RNAi with lipid-based nanoparticles. Annual Review of Biomedical Engineering 13, 507-530.

Huang, Y.Y., Hong, J.M., Zheng, S.Q., Ding, Y., Guo, S.T., Zhang, H.Y., Zhang, X.Q., Du, Q.A., Liang, Z.C., 2011. Elimination pathways of systemically delivered siRNA. Molecular Therapy 19, 381-385.

Hughes, J., Rees, S., Kalindjian, S., Philpott, K., 2011. Principles of early drug discovery. British Journal of Pharmacology 162, 1239-1249.

Hurley, K.F., Pesavento, P.A., Pedersen, N.C., Poland, A.M., Wilson, E., Foley, J.E., 2004. An outbreak of virulent systemic feline calicivirus disease. Journal of the American Veterinary Medical Association 224, 241-249.

Hurley, K.F., Sykes, J.E., 2003. Update on feline calicivirus: new trends. Veterinary Clinics of North America: Small Animal Practice 33, 759-772.

Inglot, A.D., 1969. Comparison of the antiviral activity in vitro of some non-steroidal anti-inflammatory drugs. Journal of General Virology 4, 203-214.

Irwin, W., Jelic, D., Antolovic, R., 2008. Biomarkers for drug discovery: important aspects of in vitro assay design for HTS and HCS bioassays. Croatica Chemica Acta 81, 23-30.

Ishida, T., Shibanai, A., Tanaka, S., Uchida, K., Mochizuki, M., 2004. Use of recombinant feline interferon and glucocorticoid in the treatment of feline infectious peritonitis. Journal of Feline Medicine and Surgery 6, 107-109.

Iversen, P.W., Beck, B., Chen, Y., Dere, W., Devanarayan, V., Eastwood, B.J., Farmen, M.W., Iturria, S.J., Montrose, C., Moore, R.A., Weidner, J.S., Sittampalam, G.S. 2012. HTS assay validation. In Assay Guidance Manual, Sittampalam, G.S., Gal-Edd, N., Arkin, M., Auld, D., Austin, C., Bejcek, B., Glicksman, M., Inglese, J., Lemmon, V., Li, Z., McGee, J., McManus, O., Minor, L., Napper, A., Riss, T., Trask, O.J., Jr., Weidner, J.S., eds. (Bethesda, Eli Lilly & Company and the National Center for Advancing Translational Sciences).

Jackson, A.L., Burchard, J., Leake, D., Reynolds, A., Schelter, J., Guo, J., Johnson, J.M., Lim, L., Karpilow, J., Nichols, K., Marshall, W., Khvorova, A., Linsley, P.S., 2006a. Position-specific chemical modification of siRNAs reduces "off-target" transcript silencing. RNA 12, 1197-1205.

Jackson, A.L., Burchard, J., Schelter, J., Chau, B.N., Cleary, M., Lim, L., Linsley, P.S., 2006b. Widespread siRNA "off-target" transcript silencing mediated by seed region sequence complementarity. RNA 12, 1179-1187.

Jackson, A.L., Linsley, P.S., 2010. Recognizing and avoiding siRNA off-target effects for target identification and therapeutic application. Nature Reviews Drug Discovery 9, 57-67.

Jacobs, B.L., Langland, J.O., 1996. When two strands are better than one: the mediators and modulators of the cellular responses to double-stranded RNA. Virology 219, 339-349.

Jacobse-Geels, H.E., Daha, M.R., Horzinek, M.C., 1980. Isolation and characterization of feline C3 and evidence for the immune complex pathogenesis of feline infectious peritonitis. Journal of Immunology 125, 1606-1610.

Jensen, M., Mehlhorn, H., 2009. Seventy-five years of Resochin® in the fight against malaria. Parasitology Research 105, 609-627.

John, M., Constien, R., Akinc, A., Goldberg, M., Moon, Y.-A., Spranger, M., Hadwiger, P., Soutschek, J., Vornlocher, H.-P., Manoharan, M., Stoffel, M., Langer, R., Anderson, D.G., Horton, J.D., Koteliansky, V., Bumcrot, D., 2007. Effective RNAi-mediated gene silencing without interruption of the endogenous microRNA pathway. Nature 449, 745-747.

Jones, R., Kunsman, G., Levine, B., Smith, M., Stahl, C., 1994. Mefloquine distribution in postmortem cases. Forensic Science International 68, 29-32.

Judge, A.D., Sood, V., Shaw, J.R., Fang, D., McClintock, K., MacLachlan, I., 2005. Sequence-dependent stimulation of the mammalian innate immune response by synthetic siRNA. Nature Biotechnology 23, 457-462.

Jun, E.J., Nam, Y.R., Ahn, J., Tchah, H., Joo, C.H., Jee, Y., Kim, Y.K., Lee, H., 2008. Antiviral potency of a siRNA targeting a conserved region of coxsackievirus A24. Biochemical and Biophysical Research Communications 376, 389-394.

Jurgeit, A., McDowell, R., Moese, S., Meldrum, E., Schwendener, R., Greber, U.F., 2012. Niclosamide is a proton carrier and targets acidic endosomes with broad antiviral effects. PLoS Pathogens 8, e1002976.

Kahana, R., Kuznetzova, L., Rogel, A., Shemesh, M., Hai, D., Yadin, H., Stram, Y., 2004. Inhibition of foot-and-mouth disease virus replication by small interfering RNA. Journal of General Virology 85, 3213-3217.
Kahn, D.E., Hoover, E.A., Bittle, J.L., 1975. Induction of immunity to feline caliciviral disease. Infection and Immunity 11, 1003-1009.
Kanda, T., Yokosuka, O., Omata, M., 2013. Treatment of hepatitis C virus infection in the future. Clinical and Translational Medicine 2, 1-8.
Kang, M., Park, H., Kang, M.H., Park, H.M., 2011. Successful management of feline infectious peritonitis with human recombinant interferon-alpha and pentoxifylline in a cat. Journal of Veterinary Clinics 28, 427-430.
Kapadia, S.B., Brideau-Andersen, A., Chisari, F.V., 2003. Interference of hepatitis C virus RNA replication by short interfering RNAs. Proceedings of the National Academy of Sciences 100, 2014-2018.
Kapp, L.D., Lorsch, J.R., 2004. The molecular mechanics of eukaryotic translation. Annual Review of Biochemistry 73, 657-704.
Karakasiliotis, I., Chaudhry, Y., Roberts, L.O., Goodfellow, I.G., 2006. Feline calicivirus replication: requirement for polypyrimidine tract-binding protein is temperature-dependent. Journal of General Virology 87, 3339-3347.
Karbwang, J., White, N.J., 1990. Clinical pharmacokinetics of mefloquine. Clinical Pharmacokinetics 19, 264-279.
Kariko, K., Buckstein, M., Ni, H., Weissman, D., 2005. Suppression of RNA recognition by Toll-like receptors: the impact of nucleoside modification and the evolutionary origin of RNA. Immunity 23, 165-175.
Kass, P.H., Dent, T.H., 1995. The epidemiology of feline infectious peritonitis in catteries. Feline Practice 23, 27-32.
Katakowski, J.A., Palliser, D., 2010. siRNA-based topical microbicides targeting sexually transmitted diseases. Current Opinion in Molecular Therapeutics 12, 192.
Katakowski, J.A., Palliser, D., 2011. Optimizing siRNA delivery to the genital mucosa. Discovery Medicine 11, 124.
Katas, H., Alpar, H.O., 2006. Development and characterisation of chitosan nanoparticles for siRNA delivery. Journal of Controlled Release 115, 216-225.
Kennedy, M., Boedeker, N., Gibbs, P., Kania, S., 2001. Deletions in the 7a ORF of feline coronavirus associated with an epidemic of feline infectious peritonitis. Veterinary Microbiology 81, 227-234.
Keyaerts, E., Li, S., Vijgen, L., Rysman, E., Verbeeck, J., Van Ranst, M., Maes, P., 2009. Antiviral activity of chloroquine against human coronavirus OC43 infection in newborn mice. Antimicrobial Agents and Chemotherapy 53, 3416-3421.
Keyaerts, E., Vijgen, L., Maes, P., Neyts, J., Van Ranst, M., 2004. In vitro inhibition of severe acute respiratory syndrome coronavirus by chloroquine. Biochemical and Biophysical Research Communications 323, 264-268.
Keyaerts, E., Vijgen, L., Pannecouque, C., Van Damme, E., Peumans, W., Egberink, H., Balzarini, J., Van Ranst, M., 2007. Plant lectins are potent inhibitors of coronaviruses by interfering with two targets in the viral replication cycle. Antiviral Research 75, 179-187.
Khalil, I.A., Kogure, K., Akita, H., Harashima, H., 2006. Uptake pathways and subsequent intracellular trafficking in nonviral gene delivery. Pharmacological Reviews 58, 32-45.

Khan, A.A., Betel, D., Miller, M.L., Sander, C., Leslie, C.S., Marks, D.S., 2009. Transfection of small RNAs globally perturbs gene regulation by endogenous microRNAs. Nature Biotechnology 27, 549-555.

Khvorova, A., Reynolds, A., Jayasena, S.D., 2003. Functional siRNAs and miRNAs exhibit strand bias. Cell 115, 505-505.

Kim, D.-H., Behlke, M.A., Rose, S.D., Chang, M.-S., Choi, S., Rossi, J.J., 2005. Synthetic dsRNA Dicer substrates enhance RNAi potency and efficacy. Nature Biotechnology 23, 222-226.

Kim, S.-S., Peer, D., Kumar, P., Subramanya, S., Wu, H., Asthana, D., Habiro, K., Yang, Y.-G., Manjunath, N., Shimaoka, M., 2009. RNAi-mediated CCR5 silencing by LFA-1-targeted nanoparticles prevents HIV infection in BLT mice. Molecular Therapy 18, 370-376.

Kim, S.S., Ye, C., Kumar, P., Chiu, I., Subramanya, S., Wu, H., Shankar, P., Manjunath, N., 2010. Targeted delivery of siRNA to macrophages for anti-inflammatory treatment. Molecular Therapy 18, 993-1001.

Kipar, A., Baptiste, K., Barth, A., Reinacher, M., 2006a. Natural FCoV infection: cats with FIP exhibit significantly higher viral loads than healthy infected cats. Journal of Feline Medicine and Surgery 8, 69-72.

Kipar, A., Bellmann, S., Gunn-Moore, D.A., Leukert, W., Kohler, K., Menger, S., Reinacher, M., 1999. Histopathological alterations of lymphatic tissues in cats without feline infectious peritonitis after long-term exposure to FIP virus. Veterinary Microbiology 69, 131-137.

Kipar, A., Bellmann, S., Kremendahl, J., Kohler, K., Reinacher, M., 1998a. Cellular composition, coronavirus antigen expression and production of specific antibodies in lesions in feline infectious peritonitis. Veterinary Immunology and Immunopathology 65, 243-257.

Kipar, A., Kohler, K., Leukert, W., Reinacher, M., 2001. A comparison of lymphatic tissues from cats with spontaneous feline infectious peritonitis (FIP), cats with FIP virus infection but no FIP, and cats with no infection. Journal of Comparative Pathology 125, 182-191.

Kipar, A., Kremendahl, J., Addie, D.D., Leukert, W., Grant, C.K., Reinacher, M., 1998b. Fatal enteritis associated with coronavirus infection in cats. Journal of Comparative Pathology 119, 1-14.

Kipar, A., May, H., Menger, S., Weber, M., Leukert, W., Reinacher, M., 2005. Morphologic features and development of granulomatous vasculitis in feline infectious peritonitis. Veterinary Pathology 42, 321-330.

Kipar, A., Meli, M., 2014. Feline infectious peritonitis still an enigma? Veterinary Pathology 51, 505-526.

Kipar, A., Meli, M.L., Baptiste, K.E., Bowker, L.J., Lutz, H., 2010. Sites of feline coronavirus persistence in healthy cats. Journal of General Virology 91, 1698-1707.

Kipar, A., Meli, M.L., Failing, K., Euler, T., Gomes-Keller, M.A., Schwartz, D., Lutz, H., Reinacher, M., 2006b. Natural feline coronavirus infection: differences in cytokine patterns in association with the outcome of infection. Veterinary Immunology and Immunopathology 112, 141-155.

Kiss, I., Kecskemeti, S., Tanyi, J., Klingeborn, B., Belak, S., 2000. Prevalence and genetic pattern of feline coronaviruses in urban cat populations. Veterinary Journal 159, 64-70.

Kiss, I., Ros, C., Kecskemeti, S., Tanyi, J., Klingeborn, S.B., Belak, S., 1999. Observations on the quasispecies composition of three animal pathogenic RNA viruses. Acta Veterinaria Hungarica 47, 471-480.

Kittler, R., Surendranath, V., Heninger, A.K., Slabicki, M., Theis, M., Putz, G., Franke, K., Caldarelli, A., Grabner, H., Kozak, K., Wagner, J., Rees, E., Korn, B., Frenzel, C., Sachse, C., Sonnichsen, B., Guo, J., Schelter, J., Burchard, J., Linsley, P.S., Jackson, A.L., Habermann, B., Buchholz, F., 2007. Genome-wide resources of endoribonuclease-prepared short interfering RNAs for specific loss-of-function studies. Nature Methods 4, 337-344.

Kleyman, T.R., Cragoe, E.J., 1988. Amiloride and its analogs as tools in the study of ion transport. Journal of Membrane Biology 105, 1-21.

Knowles, J.O., Gaskell, R.M., Gaskell, C.J., Harvey, C.E., Lutz, H., 1989. Prevalence of feline calicivirus, feline leukaemia virus and antibodies to FIV in cats with chronic stomatitis. Veterinary Record 124, 336-338.

Knowles, J.O., Mcardle, F., Dawson, S., Carter, S.D., Gaskell, C.J., Gaskell, R.M., 1991. Studies on the role of feline calicivirus in chronic stomatitis in cats. Veterinary Microbiology 27, 205-219.

Koivusalo, M., Welch, C., Hayashi, H., Scott, C.C., Kim, M., Alexander, T., Touret, N., Hahn, K.M., Grinstein, S., 2010. Amiloride inhibits macropinocytosis by lowering submembranous pH and preventing Rac1 and Cdc42 signaling. The Journal of Cell biology 188, 547-563.

Kollaritsch, H., Karbwang, J., Wiedermann, G., Mikolasek, A., Na-Bangchang, K., Wernsdorfer, W., 2000. Mefloquine concentration profiles during prophylactic dose regimens. Wiener Klinische Wochenschrift 112, 441-447.

Korf, M., Jarczak, D., Beger, C., Manns, M.P., Krüger, M., 2005. Inhibition of hepatitis C virus translation and subgenomic replication by siRNAs directed against highly conserved HCV sequence and cellular HCV cofactors. Journal of Hepatology 43, 225-234.

Koyama, S., Ishii, K.J., Coban, C., Akira, S., 2008. Innate immune response to viral infection. Cytokine 43, 336-341.

Kramer, J.A., Sagartz, J.E., Morris, D.L., 2007. The application of discovery toxicology and pathology towards the design of safer pharmaceutical lead candidates. Nature Reviews Drug Discovery 6, 636-649.

Kreutz, L.C., Seal, B.S., 1995. The pathway of feline calicivirus entry. Virus Research 35, 63-70.

Kreutz, L.C., Seal, B.S., Mengeling, W.L., 1994. Early interaction of feline calicivirus with cells in culture. Archives of Virology 136, 19-34.

Kuhn, H., Keller, P., Kovacs, E., Steiger, A., 1981. Lack of correlation between melanin affinity and retinopathy in mice and cats treated with chloroquine or flunitrazepam. Albrecht von Graefe's Archive for Clinical and Experimental Ophthalmology 216, 177-190.

Kumar, P., Ban, H.S., Kim, S.S., Wu, H., Pearson, T., Greiner, D.L., Laouar, A., Yao, J., Haridas, V., Habiro, K., Yang, Y.G., Jeong, J.H., Lee, K.Y., Kim, Y.H., Kim, S.W., Peipp, M., Fey, G.H., Manjunath, N., Shultz, L.D., Lee, S.K., Shankar, P., 2008. T cell-specific siRNA delivery suppresses HIV-1 infection in humanized mice. Cell 134, 577-586.

Kummrow, M., Meli, M.L., Haessig, M., Goenczi, E., Poland, A., Pedersen, N.C., Hofmann-Lehmann, R., Lutz, H., 2005. Feline coronavirus serotypes 1 and 2: seroprevalence and association with disease in Switzerland. Clinical and Diagnostic Laboratory Immunology 12, 1209-1215.

Labro, M., Babin-Chevaye, C., 1988. Effects of amodiaquine, chloroquine, and mefloquine on human polymorphonuclear neutrophil function in vitro. Antimicrobial Agents and Chemotherapy 32, 1124-1130.

Lai, M., 1986. Coronavirus leader-RNA-primed transcription: an alternative mechanism to RNA splicing. Bioessays 5, 257-260.
Lai, M., Cavanagh, D., 1997. The molecular biology of coronaviruses. Advances in Virus Research 48, 1-100.
Lai, M.M.C., 1996. Recombination in large RNA viruses: Coronaviruses. Seminars in Virology 7, 381-388.
Lai, M.M.C., Patton, C.D., Stohlman, S.A., 1982. Further characterization of mRNAs of mouse hepatitis-virus - presence of common 5'-end nucleotides. Journal of Virology 41, 557-565.
Lam, J.K.-W., Liang, W., Chan, H.-K., 2012. Pulmonary delivery of therapeutic siRNA. Advanced Drug Delivery Reviews 64, 1-15.
Lamballerie, X.D., Boisson, V., Reynier, J.-C., Enault, S., Charrel, R.N., Flahault, A., Roques, P., Grand, R.L., 2008. On chikungunya acute infection and chloroquine treatment. Vector-Borne and Zoonotic Diseases 8, 837-840.
Lapps, W., Hogue, B., Brian, D., 1987. Sequence analysis of the bovine coronavirus nucleocapsid and matrix protein genes. Virology 157, 47-57.
Larson, R.A., Dai, D., Hosack, V.T., Tan, Y., Bolken, T.C., Hruby, D.E., Amberg, S.M., 2008. Identification of a broad-spectrum arenavirus entry inhibitor. Journal of Virology 82, 10768-10775.
Lauring, A.S., Andino, R., 2010. Quasispecies theory and the behavior of RNA viruses. PLoS Pathogens 6, e1001005.
Lauring, A.S., Frydman, J., Andino, R., 2013. The role of mutational robustness in RNA virus evolution. Nature Reviews Microbiology 11, 327-336.
Lee, H.S., Ahn, J., Jun, E.J., Yang, S., Joo, C.H., Kim, Y.K., Lee, H., 2009. A novel program to design siRNAs simultaneously effective to highly variable virus genomes. Biochemical & Biophysical Research Communications 384, 431-435.
Legendre, A., Bartges, J., 2009. Effect of Polyprenyl Immunostimulant on the survival times of three cats with the dry form of feline infectious peritonitis. Journal of Feline Medicine and Surgery 11, 624-626.
Legendre, A.M. 2012. Polyprenyl immunostimulant: adjunct for treatment of feline rhinotracheitis and feline infectious peritonitis. In: American College of Veterinary Internal Medicine Forum, New Orleans.
Leonard, J., Schaffer, D., 2005a. Antiviral RNAi therapy: emerging approaches for hitting a moving target. Gene Therapy 13, 532-540.
Leonard, J.N., Schaffer, D.V., 2005b. Computational design of antiviral RNA interference strategies that resist human immunodeficiency virus escape. Journal of Virology 79, 1645-1654.
Leuschner, F., Dutta, P., Gorbatov, R., Novobrantseva, T.I., Donahoe, J.S., Courties, G., Lee, K.M., Kim, J.I., Markmann, J.F., Marinelli, B., 2011. Therapeutic siRNA silencing in inflammatory monocytes in mice. Nature Biotechnology 29, 1005-1010.
Leuschner, P., Ameres, S., Kueng, S., Martinez, J., 2006. Cleavage of the siRNA passenger strand during RISC assembly in human cells. EMBO Reports 7, 314-320.
Levi, L.I., Gnädig, N.F., Beaucourt, S., McPherson, M.J., Baron, B., Arnold, J.J., Vignuzzi, M., 2010. Fidelity variants of RNA dependent RNA polymerases uncover an indirect, mutagenic activity of amiloride compounds. PLoS Pathogens 6, e1001163.
Leyssen, P., Balzarini, J., De Clercq, E., Neyts, J., 2005. The predominant mechanism by which ribavirin exerts its antiviral activity in vitro against

flaviviruses and paramyxoviruses is mediated by inhibition of IMP dehydrogenase. Journal of Virology 79, 1943-1947.
Li, B., Tang, Q., Cheng, D., Qin, C., Xie, F., Wei, Q., Xu, J., Liu, Y., Zheng, B., Woodle, M., 2005a. Using siRNA in prophylactic and therapeutic regimens against SARS coronavirus in Rhesus macaque. Nature Medicine 11, 944-951.
Li, S.-Y., Chen, C., Zhang, H.-Q., Guo, H.-Y., Wang, H., Wang, L., Zhang, X., Hua, S.-N., Yu, J., Xiao, P.-G., Li, R.-S., Tan, X., 2005b. Identification of natural compounds with antiviral activities against SARS-associated coronavirus. Antiviral Research 67, 18-23.
Li, T., Zhang, Y., Fu, L., Yu, C., Li, X., Li, Y., Zhang, X., Rong, Z., Wang, Y., Ning, H., 2005c. siRNA targeting the leader sequence of SARS-CoV inhibits virus replication. Gene Therapy 12, 751-761.
Li, Y., Larrimer, A., Curtiss, T., Kim, J., Jones, A., Baird-Tomlinson, H., Pekosz, A., Olivo, P.D., 2009. Influenza virus assays based on virus-inducible reporter cell lines. Influenza and Other Respiratory Viruses 3, 241-251.
Li, Y., Lu, J., Han, Y., Fan, X., Ding, S.-W., 2013. RNA interference functions as an antiviral immunity mechanism in mammals. Science 342, 231-234.
Liang, X.Y., 2008. CXCR4, inhibitors and mechanisms of action. Chemical Biology & Drug Design 72, 97-110.
Licitra, B.N., Millet, J.K., Regan, A.D., Hamilton, B.S., Rinaldi, V.D., Duhamel, G.E., Whittaker, G.R., 2013. Mutation in spike protein cleavage site and pathogenesis of feline coronavirus. Emerging Infectious Diseases 19.
Lin, C.W., Tsai, F.J., Tsai, C.H., Lai, C.C., Wan, L., Ho, T.Y., Hsieh, C.C., Chao, P.D., 2005. Anti-SARS coronavirus 3C-like protease effects of Isatis indigotica root and plant-derived phenolic compounds. Antiviral Research 68, 36-42.
Liu, Y., Wimmer, E., Paul, A.V., 2009a. *Cis*-acting RNA elements in human and animal plus-strand RNA viruses. Biochimica et Biophysica Acta (BBA)-Gene Regulatory Mechanisms 1789, 495-517.
Liu, Y.P., von Eije, K.J., Schopman, N.C., Westerink, J.T., ter Brake, O., Haasnoot, J., Berkhout, B., 2009b. Combinatorial RNAi against HIV-1 using extended short hairpin RNAs. Molecular Therapy 17, 1712-1723.
Lommer, M.J., Verstraete, F.J.M., 2003. Concurrent oral shedding of feline calicivirus and feline herpesvirus 1 in cats with chronic gingivostomatitis. Oral Microbiology and Immunology 18, 131-134.
Love, D.N., Baker, K.D., 1972. Sudden Death in Kittens Associated with a Feline Picornavirus. Australian Veterinary Journal 48, 643-&.
Lundholt, B.K., Scudder, K.M., Pagliaro, L., 2003. A simple technique for reducing edge effect in cell-based assays. Journal of Biomolecular Screening 8, 566-570.
Luo, J., Tannock, I., 1994. Inhibition of the regulation of intracellular pH: potential of 5-(N, N-hexamethylene) amiloride in tumour-selective therapy. British Journal of Cancer 70, 617.
Luria, B.J., Levy, J.K., Lappin, M.R., Breitschwerdt, E.B., Legendre, A.M., Hernandez, J.A., Gorman, S.P., Lee, I.T., 2004. Prevalence of infectious diseases in feral cats in Northern Florida. Journal of Feline Medicine and Surgery 6, 287-296.
Luttermann, C., Meyers, G., 2007. A bipartite sequence motif induces translation reinitiation in feline calicivirus RNA. Journal of Biological Chemistry 282, 7056-7065.

Luttermann, C., Meyers, G., 2009. The importance of inter- and intramolecular base pairing for translation reinitiation on a eukaryotic bicistronic mRNA. Genes & Development 23, 331-344.
Lyon, K.F., 2005. Gingivostomatitis. Veterinary Clinics of North America: Small Animal Practice 35, 891-+.
Macarron, R., Banks, M.N., Bojanic, D., Burns, D.J., Cirovic, D.A., Garyantes, T., Green, D.V., Hertzberg, R.P., Janzen, W.P., Paslay, J.W., 2011. Impact of high-throughput screening in biomedical research. Nature Reviews Drug Discovery 10, 188-195.
Mackenzie, A.H., 1983. Pharmacologic actions of 4-aminoquinoline compounds. The American Journal of Medicine 75, 5-10.
Madewell, B.R., Crow, S.E., Nickerson, T.R., 1978. Infectious peritonitis in a cat that subsequently developed a myeloproliferative disorder. Journal of the American Veterinary Medical Association 172, 169-172.
Maeda, K., Nakata, H., Ogata, H., Koh, Y., Miyakawa, T., Mitsuya, H., 2004. The current status of, and challenges in, the development of CCR5 inhibitors as therapeutics for HIV-1 infection. Current Opinion in Pharmacology 4, 447-452.
Maillard, P., Ciaudo, C., Marchais, A., Li, Y., Jay, F., Ding, S., Voinnet, O., 2013. Antiviral RNA interference in mammalian cells. Science 342, 235-238.
Makino, A., Shimojima, M., Miyazawa, T., Kato, K., Tohya, Y., Akashi, H., 2006. Junctional adhesion molecule 1 is a functional receptor for feline calicivirus. Journal of Virology 80, 4482-4490.
Manche, L., Green, S.R., Schmedt, C., Mathews, M.B., 1992. Interactions between double-stranded RNA regulators and the protein kinase DAI. Molecular and Cellular Biology 12, 5238-5248.
Mari, K.d., Maynard, L., Sanquer, A., Lebreux, B., Eun, H., de Mari, K., Eun, H.M., 2004. Therapeutic effects of recombinant feline interferon-omega on feline leukemia virus (FeLV)-infected and FeLV/feline immunodeficiency virus (FIV)-coinfected symptomatic cats. Journal of Veterinary Internal Medicine 18, 477-482.
Marques, J.T., Devosse, T., Wang, D., Zamanian-Daryoush, M., Serbinowski, P., Hartmann, R., Fujita, T., Behlke, M.A., Williams, B.R.G., 2006. A structural basis for discriminating between self and nonself double-stranded RNAs in mammalian cells. Nature Biotechnology 24, 559-565.
Marques, R.M., Teixeira, L., Águas, A.P., Ribeiro, J.C., Costa-e-Silva, A., Ferreira, P.G., 2014. Immunosuppression abrogates resistance of young rabbits to Rabbit Haemorrhagic Disease (RHD). Veterinary Research 45, 14.
Marra, M.A., Jones, S.J., Astell, C.R., Holt, R.A., Brooks-Wilson, A., Butterfield, Y.S., Khattra, J., Asano, J.K., Barber, S.A., Chan, S.Y., 2003. The genome sequence of the SARS-associated coronavirus. Science 300, 1399-1404.
Marsh, M., Helenius, A., 2006. Virus entry: open sesame. Cell 124, 729-740.
Martijn, P.C.M., 2009. Prevelence of feline calicivirus in cats with chronic gingivitis stomatitis and potential risk factors.
Martin, V., Najbar, W., Gueguen, S., Grousson, D., Eun, H.M., Lebreux, B., Aubert, A., 2002. Treatment of canine parvoviral enteritis with interferon-omega in a placebo-controlled challenge trial. Veterinary Microbiology 89, 115-127.
Martinez, M.A., Clotet, B., Este, J.A., Martinez, M.A., Clotet, B., Este, J.A., 2002. RNA interference of HIV replication. Trends in Immunology 23, 559-561.
Masters, P.S., 2006. The molecular biology of coronaviruses. Advances in Virus Research 66, 193-292.

McCann, K.B., Lee, A., Wan, J., Roginski, H., Coventry, M.J., 2003. The effect of bovine lactoferrin and lactoferricin B on the ability of feline calicivirus (a norovirus surrogate) and poliovirus to infect cell cultures. Journal of Applied Microbiology 95, 1026-1033.

McKeirnan, A.J., Evermann, J.F., Davis, E.V., Ott, R.L., 1987. Comparative properties of feline coronaviruses in vitro. Canadian Journal of Veterinary Research 51, 212-216.

McKeirnan, A.J., Evermann, J.F., Hargis, A., Miller, L.M., Ott, R.L., 1981. Isolation of feline coronaviruses from two cats with diverse disease manifestations. Feline Practice 11, 16...20.

McKinlay, M.A., Pevear, D.C., Rossmann, M.G., 1992. Treatment of the picornavirus common cold by inhibitors of viral uncoating and attachment. Annual Review of Microbiology 46, 635-654.

McSwiggen, J.A., Seth, S., 2008. A potential treatment for pandemic influenza using siRNAs targeting conserved regions of influenza A. Expert opinion on Biological Therapy 8, 299-313.

Meli, M., Kipar, A., Muller, C., Jenal, K., Gonczi, E., Borel, N., Gunn-Moore, D., Chalmers, S., Lin, F., Reinacher, M., Lutz, H., 2004. High viral loads despite absence of clinical and pathological findings in cats experimentally infected with feline coronavirus (FCoV) type I and in naturally FCoV-infected cats. Journal of Feline Medicine and Surgery 6, 69-81.

Mencke, N., Vobis, M., Mehlhorn, H., D Haese, J., Rehagen, M., Mangold-Gehring, S., Truyen, U., 2009. Transmission of feline calicivirus via the cat flea (Ctenocephalides felis). Parasitology Research 105, 185-189.

Meng, H., Cui, F., Chen, X., Pan, Y., 2007. Inhibition of gene expression directed by small interfering RNAs in infectious bronchitis virus. Acta Virologica 51, 265-269.

Mercer, J., Helenius, A., 2009. Virus entry by macropinocytosis. Nature Cell Biology 11, 510-520.

Meyer, A., Kershaw, O., Klopfleisch, R., 2011. Feline calicivirus-associated virulent systemic disease: not necessarily a local epizootic problem. Veterinary Record 168.

Meyers, G., Wirblich, C., Thiel, H.J., Thumfart, J.O., 2000. Rabbit hemorrhagic disease virus: genome organization and polyprotein processing of a calicivirus studied after transient expression of cDNA constructs. Virology 276, 349-363.

Minagawa, T., Ishiwata, K., Kajimoto, T., 1999. Feline interferon-omega treatment on canine parvovirus infection. Veterinary Microbiology 69, 51-53.

Minks, M.A., West, D.K., Benvin, S., Baglioni, C., 1979. Structural requirements of double-stranded RNA for the activation of 2',5'-oligo(A) polymerase and protein kinase of interferon-treated HeLa cells. Journal of Biological Chemistry 254, 10180-10183.

Minskaia, E., Hertzig, T., Gorbalenya, A.E., Campanacci, V., Cambillau, C., Canard, B., Ziebuhr, J., 2006. Discovery of an RNA virus 3'->5' exoribonuclease that is critically involved in coronavirus RNA synthesis. Proceedings of the National Academy of Sciences 103, 5108-5113.

Mizui, T., Yamashina, S., Tanida, I., Takei, Y., Ueno, T., Sakamoto, N., Ikejima, K., Kitamura, T., Enomoto, N., Sakai, T., Kominami, E., Watanabe, S., 2010. Inhibition of hepatitis C virus replication by chloroquine targeting virus-associated autophagy. Journal of Gastroenterology 45, 195-203.

Mochizuki, M., 1992. Different stabilities to bile among feline calicivirus strains of respiratory and enteric origin. Veterinary Microbiology 31, 297-302.

Mochizuki, M., Nakatani, H., Yoshida, M., 1994. Inhibitory effects of recombinant feline interferon on the replication of feline enteropathogenic viruses in vitro. Veterinary Microbiology 39, 145-152.
Mochizuki, M., Osawa, N., Ishida, T., 1999. Feline coronavirus participation in diarrhea of cats. The Journal of Veterinary Medical Science 61, 1071-1073.
Momattin, H., Mohammed, K., Zumla, A., Memish, Z.A., Al-Tawfiq, J.A., 2013. Therapeutic options for Middle East Respiratory Syndrome Coronavirus (MERS-CoV)–possible lessons from a systematic review of SARS-CoV therapy. International Journal of Infectious Diseases 17, e792-e798.
Monteiro, M.C., de la Cruz, M., Cantizani, J., Moreno, C., Tormo, J.R., Mellado, E., De Lucas, J.R., Asensio, F., Valiante, V., Brakhage, A.A., 2012. A new approach to drug discovery high-throughput screening of microbial natural extracts against Aspergillus fumigatus using resazurin. Journal of Biomolecular Screening 17, 542-549.
Moore, B.R., Page-Sharp, M., Stoney, J.R., Ilett, K.F., Jago, J.D., Batty, K.T., 2011. Pharmacokinetics, pharmacodynamics, and allometric scaling of chloroquine in a murine malaria model. Antimicrobial Agents and Chemotherapy 55, 3899-3907.
Muthyala, R., 2012. Orphan/rare drug discovery through drug repositioning. Drug Discovery Today 8, 71-76.
Naito, Y., Ui-Tei, K., Nishikawa, T., Takebe, Y., Saigo, K., 2006. siVirus: web-based antiviral siRNA design software for highly divergent viral sequences. Nucleic Acids Research 34, W448-W450.
Nakayama, G.R., Caton, M.C., Nova, M.P., Parandoosh, Z., 1997. Assessment of the Alamar Blue assay for cellular growth and viability in vitro. Journal of Immunological Methods 204, 205-208.
Napoli, C., Lemieux, C., Jorgensen, R., 1990. Introduction of a chimeric chalcone synthase gene into petunia results in reversible co-suppression of homologous genes in trans. The Plant Cell 2, 279-289.
Narayanan, K., Maeda, A., Maeda, J., Makino, S., 2000. Characterization of the coronavirus M protein and nucleocapsid interaction in infected cells. Journal of Virology 74, 8127-8134.
Narayanan, K., Makino, S. 2007. Coronavirus genome packaging, In: Thiel, V. (Ed.) Coronaviruses: Molecular and Cellular Biology. Caister Academic Press, Norflok, UK, 131-142.
Neill, J.D., 1992. Nucleotide sequence of the capsid protein gene of two serotypes of San Miguel sea lion virus: identification of conserved and non-conserved amino acid sequences among calicivirus capsid proteins. Virus Research 24, 211-222.
Neill, J.D., 2002. The subgenomic RNA of feline calicivirus is packaged into viral particles during infection. Virus Research 87, 89-93.
Neill, J.D., Reardon, I.M., Heinrikson, R.L., 1991. Nucleotide-sequence and expression of the capsid protein gene of feline calicivirus. Journal of Virology 65, 5440-5447.
Neuman, B.W., Adair, B.D., Yoshioka, C., Quispe, J.D., Milligan, R.A., Yeager, M., Buchmeier, M.J., 2006. Ultrastructure of SARS-CoV, FIPV, and MHV revealed by electron cryomicroscopy. Nidoviruses: Toward Control of Sars and Other Nidovirus Diseases 581, 181-185.
Neuman, B.W., Kiss, G., Kunding, A.H., Bhella, D., Baksh, M.F., Connelly, S., Droese, B., Klaus, J.P., Makino, S., Sawicki, S.G., Siddell, S.G., Stamou, D.G., Wilson, I.A., Kuhn, P., Buchmeier, M.J., 2011. A structural analysis of M

protein in coronavirus assembly and morphology. Journal of Structural Biology 174, 11-22.
Nguyen, T., Menocal, E.M., Harborth, J., Fruehauf, J.H., 2008. RNAi therapeutics: An update on delivery. Current Opinion in Molecular Therapeutics 10, 158-167.
Niles, A.L., Moravec, R.A., Riss, T.L., 2008. Update on in vitro cytotoxicity assays for drug development. Expert Opinion on Drug Discovery 3, 655-669.
Niles, A.L., Moravec, R.A., Riss, T.L., 2009. In vitro viability and cytotoxicity testing and same-well multi-parametric combinations for high throughput screening. Current Chemical Genomics 3, 33-41.
Ninomiya, H., Fukutome, A., Kabayashi, K., Shin, Y., Uchino, T., Motoyoshi, S. 1991. Effect of recombinant feline interferon on feline calicivirus infection. In: XVI World Small Animal Veterinary Association, Vienna, Austria.
Nobelprize.org, 2006. Press Release: The 2006 Nobel Prize in Physiology or Medicine. 2013.
Norris, J.M., Bosward, K.L., White, J.D., Baral, R.M., Catt, M.J., Malik, R., 2005. Clinicopathological findings associated with feline infectious peritonitis in Sydney, Australia: 42 cases (1990-2002). Australian Veterinary Journal 83, 666-673.
Novina, C.D., Murray, M.F., Dykxhoorn, D.M., Beresford, P.J., Riess, J., Lee, S.K., Collman, R.G., Lieberman, J., Shankar, P., Sharp, P.A., 2002. siRNA-directed inhibition of HIV-1 infection. Nature Medicine 8, 681-686.
O'Brien, J., Wilson, I., Orton, T., Pognan, F., 2000. Investigation of the Alamar Blue (resazurin) fluorescent dye for the assessment of mammalian cell cytotoxicity. European Journal of Biochemistry 267, 5421-5426.
O'Brien, S.J., Roelke, M.E., Marker, L., Newman, A., Winkler, C.A., Meltzer, D., Colly, L., Evermann, J.F., Bush, M., Wildt, D.E., 1985. Genetic basis for species vulnerability in the cheetah. Science 227, 1428-1434.
O'Brien, S.J., Troyer, J.L., Brown, M.A., Johnson, W.E., Antunes, A., Roelke, M.E., Pecon-Slattery, J., 2012. Emerging viruses in the felidae: shifting paradigms. Viruses 4, 236-257.
O'Brien, S.J., Wildt, D.E., Bush, M., Caro, T.M., FitzGibbon, C., Aggundey, I., Leakey, R.E., 1987. East African cheetahs: evidence for two population bottlenecks? Proceedings of the National Academy of Sciences 84, 508-511.
Ohe, K., Sakai, S., Sunaga, F., Murakami, M., Kiuchi, A., Fukuyama, M., Furuhata, K., Hara, M., Soma, T., Ishikawa, Y., Taneno, A., 2006. Detection of feline calicivirus (FCV) from vaccinated cats and phylogenetic analysis of its capsid genes. Veterinary Research Communications 30, 293-305.
Ohe, K., Takahashi, T., Hara, D., Hara, M., 2008. Sensitivity of FCV to recombinant feline interferon (rFeIFN). Veterinary Research Communications 32, 167-174.
Ohkuma, S., Poole, B., 1978. Fluorescence probe measurement of the intralysosomal pH in living cells and the perturbation of pH by various agents. Proceedings of the National Academy of Sciences 75, 3327-3331.
Olsen, C.W., Corapi, W.V., Ngichabe, C.K., Baines, J.D., Scott, F.W., 1992. Monoclonal antibodies to the spike protein of feline infectious peritonitis virus mediate antibody-dependent enhancement of infection of feline macrophages. Journal of Virology 66, 956-965.
Ooi, E.E., Chew, J., Loh, J.P., Chua, R., 2006. In vitro inhibition of human influenza A virus replication by chloroquine. Virology Journal 3, 39.
Orhan, D.D., Özçelik, B., Özgen, S., Ergun, F., 2010. Antibacterial, antifungal, and antiviral activities of some flavonoids. Microbiological Research 165, 496-504.

Ossiboff, R.J., Sheh, A., Shotton, J., Pesavento, P.A., Parker, J.S., 2007. Feline caliciviruses (FCVs) isolated from cats with virulent systemic disease possess in vitro phenotypes distinct from those of other FCV isolates. Journal of General Virology 88, 506-517.

Ossiboff, R.J., Zhou, Y., Lightfoot, P.J., Prasad, B.V., Parker, J.S., 2010. Conformational changes in the capsid of a calicivirus upon interaction with its functional receptor. Journal of Virology 84, 5550-5564.

Owen, A., Janneh, O., Hartkoorn, R.C., Chandler, B., Bray, P.G., Martin, P., Ward, S.A., Hart, C.A., Khoo, S.H., Back, D.J., 2005. In vitro synergy and enhanced murine brain penetration of saquinavir coadministered with mefloquine. Journal of Pharmacology and Experimental Therapeutics 314, 1202-1209.

Paeshuyse, J., Coelmont, L., Vliegen, I., Vandenkerckhove, J., Peys, E., Sas, B., Clercq, E.D., Neyts, J., 2006. Hemin potentiates the anti-hepatitis C virus activity of the antimalarial drug artemisinin. Biochemical & Biophysical Research Communications 348, 139-144.

Palliser, D., Chowdhury, D., Wang, Q.-Y., Lee, S.J., Bronson, R.T., Knipe, D.M., Lieberman, J., 2006. An siRNA-based microbicide protects mice from lethal herpes simplex virus 2 infection. Nature 439, 89-94.

Paltrinieri, S., Cammarata, M.P., Cammarata, G., Comazzi, S., 1998. Some aspects of humoral and cellular immunity in naturally occurring feline infectious peritonitis. Veterinary Immunology and Immunopathology 65, 205-220.

Paltrinieri, S., Ponti, W., Comazzi, S., Giordano, A., Poli, G., 2003. Shifts in circulating lymphocyte subsets in cats with feline infectious peritonitis (FIP): pathogenic role and diagnostic relevance. Veterinary Immunology and Immunopathology 96, 141-148.

Papazisis, K.T., Geromichalos, G.D., Dimitriadis, K.A., Kortsaris, A.H., 1997. Optimization of the sulforhodamine B colorimetric assay. Journal of Immunological Methods 208, 151-158.

Paragas, J., Whitehouse, C.A., Endy, T.P., Bray, M., 2004. A simple assay for determining antiviral activity against Crimean-Congo hemorrhagic fever virus. Antiviral Research 62, 21-25.

Parameswaran, P., Sklan, E., Wilkins, C., Burgon, T., Samuel, M.A., Lu, R., Ansel, K.M., Heissmeyer, V., Einav, S., Jackson, W., Doukas, T., Paranjape, S., Polacek, C., dos Santos, F.B., Jalili, R., Babrzadeh, F., Gharizadeh, B., Grimm, D., Kay, M., Koike, S., Sarnow, P., Ronaghi, M., Ding, S.W., Harris, E., Chow, M., Diamond, M.S., Kirkegaard, K., Glenn, J.S., Fire, A.Z., 2010. Six RNA viruses and forty-one hosts: viral small RNAs and modulation of small RNA repertoires in vertebrate and invertebrate systems. PLoS Pathogens 6.

Paredes, A., Alzuru, M., Mendez, J., Rodriguez-Ortega, M., 2003. Anti-Sindbis activity of flavanones hesperetin and naringenin. Biological & Pharmaceutical Bulletin 26, 108-109.

Park, K., Yeo, S., Baek, K., Cheon, D., Choi, Y., Park, J., Lee, S., 2011. Molecular characterization and antiviral activity test of common drugs against echovirus 18 isolated in Korea. Virology Journal 8, 516.

Paton, N.I., Lee, L., Xu, Y., Ooi, E.E., Cheung, Y.B., Archuleta, S., Wong, G., Smith, A.W., 2011. Chloroquine for influenza prevention: a randomised, double-blind, placebo controlled trial. The Lancet Infectious Diseases 11, 677-683.

Paul, S.M., Mytelka, D.S., Dunwiddie, C.T., Persinger, C.C., Munos, B.H., Lindborg, S.R., Schacht, A.L., 2010. How to improve R&D productivity: the pharmaceutical industry's grand challenge. Nature Reviews Drug Discovery 9, 203-214.

Pedersen, N.C., 1976. Serologic studies of naturally occurring feline infectious peritonitis. American Journal of Veterinary Research 37, 1449-1453.
Pedersen, N.C., 1995. An overview of feline enteric coronavirus and infectious peritonitis virus infections. Feline Practice 23, 7-19.
Pedersen, N.C., 2009. A review of feline infectious peritonitis virus infection: 1963-2008. Journal of Feline Medicine and Surgery 11, 225-258.
Pedersen, N.C., Allen, C.E., Lyons, L.A., 2008. Pathogenesis of feline enteric coronavirus infection. Journal of Feline Medicine and Surgery 10, 529-541.
Pedersen, N.C., Black, J.W., Boyle, J.F., Evermann, J.F., McKeirnan, A.J., Ott, R.L., 1984. Pathogenic differences between various feline coronavirus isolates. Advances in Experimental Medicine & Biology 173, 365-380.
Pedersen, N.C., Boyle, J.F., 1980. Immunologic phenomena in the effusive form of feline infectious peritonitis. American Journal of Veterinary Research 41, 868-876.
Pedersen, N.C., Boyle, J.F., Floyd, K., Fudge, A., Barker, J., 1981. An enteric coronavirus infection of cats and its relationship to feline infectious peritonitis. American Journal of Veterinary Research 42, 368-379.
Pedersen, N.C., Elliott, J.B., Glasgow, A., Poland, A., Keel, K., 2000. An isolated epizootic of hemorrhagic-like fever in cats caused by a novel and highly virulent strain of feline calicivirus. Veterinary Microbiology 73, 281-300.
Pedersen, N.C., Hawkins, K.F., 1995. Mechanisms for persistence of acute and chronic feline calicivirus infections in the face of vaccination. Veterinary Microbiology 47, 141-156.
Pedersen, N.C., Laliberte, L., Ekman, S., 1983. A transient febrile "limping" syndrome of kittens caused by two different strains of feline calicivirus. Feline Practice 13, 26-36.
Pedersen, N.C., Liu, H., Dodd, K.A., Pesavento, P.A., 2009. Significance of coronavirus mutants in feces and diseased tissues of cats suffering from feline infectious peritonitis. Viruses 1, 166-184.
Pedersen, N.C., Liu, H., Scarlett, J., Leutenegger, C.M., Golovko, L., Kennedy, H., Kamal, F.M., 2012. Feline infectious peritonitis: Role of the feline coronavirus 3c gene in intestinal tropism and pathogenicity based upon isolates from resident and adopted shelter cats. Virus Research.
Pedersen, N.C., Sato, R., Foley, J.E., Poland, A.M., 2004. Common virus infections in cats, before and after being placed in shelters, with emphasis on feline enteric coronavirus. Journal of Feline Medicine and Surgery 6, 83-88.
Perlman, S., Dandekar, A.A., 2005. Immunopathogenesis of coronavirus infections: implications for SARS. Nature Reviews Immunology 5, 917-927.
Perlman, S., Ries, D., Bolger, E., Lung-Ji, C., Stoltzfus, C., 1986. MHV nucleocapsid synthesis in the presence of cycloheximide and accumulation of negative strand MHV RNA. Virus Research 6, 261-272.
Pesavento, P.A., Chang, K.-O., Parker, J.S.L., 2008. Molecular virology of feline calicivirus. Veterinary Clinics of North America: Small Animal Practice 38, 775-786, vii.
Pesavento, P.A., Stokol, T., Liu, H., van der List, D.A., Gaffney, P.M., Parker, J.S., 2011. Distribution of the feline calicivirus receptor junctional adhesion molecule a in feline tissues. Veterinary Pathology 48, 361-368.
Pesteanu-Somogyi, L.D., Radzai, C., Pressler, B.M., 2006. Prevalence of feline infectious peritonitis in specific cat breeds. Journal of Feline Medicine and Surgery 8, 1-5.

Pham, Y., Nosten, F., Farinotti, R., White, N., Gimenez, F., 1999. Cerebral uptake of mefloquine enantiomers in fatal cerebral malaria. International Journal of Clinical Pharmacology and Therapeutics 37, 58.
Pillay, D., Zambon, M., 1998. Antiviral drug resistance. British Medical Journal 317, 660.
Pinto, L.H., Holsinger, L.J., Lamb, R.A., 1992. Influenza-virus M2 protein has iIon channel activity. Cell 69, 517-528.
Pinto, P., Wang, Q., Chen, N., Dubovi, E.J., Daniels, J.B., Millward, L.M., Buonavoglia, C., Martella, V., Saif, L.J., 2012. Discovery and genomic characterization of noroviruses from a gastroenteritis outbreak in domestic cats in the US. PLoS One 7, e32739.
Poland, A.M., Vennema, H., Foley, J.E., Pedersen, N.C., 1996. Two related strains of feline infectious peritonitis virus isolated from immunocompromised cats infected with a feline enteric coronavirus. Journal of Clinical Microbiology 34, 3180-3184.
Poncelet, L., Coppens, A., Peeters, D., Bianchi, E., Grant, C.K., Kadhim, H., 2008. Detection of antigenic heterogeneity in feline coronavirus nucleocapsid in feline pyogranulomatous meningoencephalitis. Veterinary Pathology 45, 140-153.
Porotto, M., Orefice, G., Yokoyama, C.C., Mungall, B.A., Realubit, R., Sganga, M.L., Aljofan, M., Whitt, M., Glickman, F., Moscona, A., 2009. Simulating henipavirus multicycle replication in a screening assay leads to identification of a promising candidate for therapy. Journal of Virology 83, 5148-5155.
Porter, C.J., Radford, A.D., Gaskell, R.M., Ryvar, R., Coyne, K.P., Pinchbeck, G.L., Dawson, S., 2008. Comparison of the ability of feline calicivirus (FCV) vaccines to neutralise a panel of current UKFCV isolates. Journal of Feline Medicine and Surgery 10, 32-40.
Poulet, H., Brunet, S., Soulier, M., Leroy, V., Goutebroze, S., Chappuis, G., 2000. Comparison between acute oral/respiratory and chronic stomatitis/gingivitis isolates of feline calicivirus: pathogenicity, antigenic profile and cross-neutralisation studies. Archives of Virology 145, 243-261.
Povey, R.C., 1978a. Effect of orally administered ribavirin on experimental feline calicivirus infection in cats. American Journal of Veterinary Research 39, 1337-1341.
Povey, R.C., 1978b. In vitro antiviral efficacy of ribavirin against feline calicivirus, feline viral rhinotracheitis virus, and canine parainfluenza virus. American Journal of Veterinary Research 39, 175-178.
Povey, R.C., Hale, C.J., 1974. Experimental infections with feline caliciviruses (Picornaviruses) in specific pathogen-free kittens. Journal of Comparative Pathology 84, 245-256.
Prasad, B.V., Matson, D.O., Smith, A.W., 1994. Three-dimensional structure of calicivirus. Journal of Molecular Biology 240, 256-264.
Premkumar, A., Wilson, L., Ewart, G.D., Gage, P.W., 2004. Cation-selective ion channels formed by p7 of hepatitis C virus are blocked by hexamethylene amiloride. FEBS Letters 557, 99-103.
ProMED 2014. MERS-CoV - Eastern Mediterranean (12): Saudi Arabia
Pussard, E., Verdier, F., 1994. Antimalarial 4-aminoquinolines: mode of action and pharmacokinetics. Fundamental & Clinical Pharmacology 8, 1-17.
Pyrc, K., Berkhout, B., van der Hoek, L., 2007. Antiviral strategies against human coronaviruses. Infectious Disorders - Drug Targets 7, 59-66.

Pyrc, K., Bosch, B.J., Berkhout, B., Jebbink, M.F., Dijkman, R., Rottier, P., van der Hoek, L., 2006. Inhibition of human coronavirus NL63 infection at early stages of the replication cycle. Antimicrobial Agents and Chemotherapy 50, 2000-2008.

Raaben, M., Groot Koerkamp, M., Rottier, P., de Haan, C., 2007. Mouse hepatitis coronavirus replication induces host translational shutoff and mRNA decay, with concomitant formation of stress granules and processing bodies. Cellular Microbiology 9, 2218-2229.

Radford, A.D., Bennett, M., McArdle, F., Dawson, S., Turner, P.C., Williams, R.A., Glenn, M.A., Gaskell, R.M., 1998. Quasispecies evolution of a hypervariable region of the feline calicivirus capsid gene in cell culture and persistently infected cats. Veterinary Microbiology 69, 67-68.

Radford, A.D., Coyne, K.P., Dawson, S., Porter, C.J., Gaskell, R.M., 2007. Feline calicivirus. Veterinary Research 38, 319-335.

Radford, A.D., Dawson, S., Coyne, K.P., Porter, C.J., Gaskell, R.M., 2006. The challenge for the next generation of feline calicivirus vaccines. Veterinary Microbiology 117, 14-18.

Radford, A.D., Gaskell, R.M., 2011. Dealing with a potential case of FCV-associated virulent systemic disease. Veterinary Record 168, 585-586.

Radford, A.D., Willoughby, K., Dawson, S., McCracken, C., Gaskell, R.M., 1999. The capsid gene of feline calicivirus contains linear B-cell epitopes in both variable and conserved regions. Journal of Virology 73, 8496-8502.

Reed, L., Muench, H., 1938. A simple method of estimating 50 per cent end-points. American Journal of Hygiene 27, 493-497.

Regan, A.D., Cohen, R.D., Whittaker, G.R., 2008a. Activation of p38 MAPK by feline infectious peritonitis virus regulates pro-inflammatory cytokine production in primary blood-derived feline mononuclear cells. Virology, 135-143.

Regan, A.D., Ousterout, D.G., Whittaker, G.R., 2010. Feline lectin activity is critical for the cellular entry of feline infectious peritonitis virus. Journal of Virology 84, 7917-7921.

Regan, A.D., Shraybman, R., Cohen, R.D., Whittaker, G.R., 2008b. Differential role for low pH and cathepsin-mediated cleavage of the viral spike protein during entry of serotype II feline coronaviruses. Veterinary Microbiology 132, 235-248.

Regan, A.D., Whittaker, G.R., 2008. Utilization of DC-SIGN for Entry of Feline Coronaviruses into Host Cells. Journal of Virology 82, 11992-11996.

Reid, G., Coppieters't Wallant, N., Patel, R., Antonic, A., Saxon-Aliifaalogo, F., Cao, H., Webster, G., Watson, J.D., 2009. Potent subunit-specific effects on cell growth and drug sensitivity from optimised siRNA-mediated silencing of ribonucleotide reductase. Journal of RNAi and Gene Silencing 5, 321.

Reubel, G.H., Hoffmann, D.E., Pedersen, N.C., 1992. Acute and chronic faucitis of domestic cats. A feline calicivirus-induced disease. Veterinary Clinics of North America: Small Animal Practice 22, 1347-1360.

Reynolds, B.S., Poulet, H., Pingret, J.L., Jas, D., Brunet, S., Lemeter, C., Etievant, M., Boucraut-Baralon, C., 2009. A nosocomial outbreak of feline calicivirus associated virulent systemic disease in France. Journal of Feline Medicine and Surgery 11, 633-644.

Ribeiro, R.M., Bonhoeffer, S., 2000. Production of resistant HIV mutants during antiretroviral therapy. Proceedings of the National Academy of Sciences 97, 7681-7686.

Rice, C.C., Kruger, J.M., Venta, P.J., Vilnis, A., Maas, K.A., Dulin, J.A., Maes, R.K., 2002. Genetic characterization of 2 novel feline caliciviruses isolated from cats with idiopathic lower urinary tract disease. Journal of Veterinary Internal Medicine 16, 293-302.

Riffkin, C.D., Chung, R., Wall, D.M., Zalcberg, J.R., Cowman, A.F., Foley, M., Tilley, L., 1996. Modulation of the function of human MDR1 P-glycoprotein by the antimalarial drug mefloquine. Biochemical Pharmacology 52, 1545-1552.

Ritz, S., Egberink, H., Hartmann, K., 2007. Effect of feline interferon-omega on the survival time and quality of life of cats with feline infectious peritonitis. Journal of Veterinary Internal Medicine 21, 1193-1197.

Robbins, M., Judge, A., Ambegia, E., Choi, C., Yaworski, E., Palmer, L., McClintock, K., MacLachlan, I., 2008. Misinterpreting the therapeutic effects of small interfering RNA caused by immune stimulation. Human Gene Therapy 19, 991-999.

Rocha Martins, L.R., Brenzan, M.A., Nakamura, C.V., Dias Filho, B.P., Nakamura, T.U., Ranieri Cortez, L.E., Garcia Cortez, D.A., 2011. In vitro antiviral activity from Acanthospermum australe on herpesvirus and poliovirus. Pharmaceutical Biology 49, 26-31.

Rohayem, J. 2010. Design of small-interfering RNA (Google Patents).

Rohayem, J., Bergmann, M., Gebhardt, J., Gould, E., Tucker, P., Mattevi, A., Unge, T., Hilgenfeld, R., Neyts, J., 2010. Antiviral strategies to control calicivirus infections. Antiviral Research 87, 162-178.

Rohrbach, B.W., Legendre, A.M., Baldwin, C.A., Lein, D.H., Reed, W.M., Wilson, R.B., 2001. Epidemiology of feline infectious peritonitis among cats examined at veterinary medical teaching hospitals. Journal of the American Veterinary Medical Association 218, 1111-1115.

Romano, N., Macino, G., 1992. Quelling: transient inactivation of gene expression in Neurospora crassa by transformation with homologous sequences. Molecular Microbiology 6, 3343-3353.

Romero, M.R., Serrano, M.A., Vallejo, M., Efferth, T., Alvarez, M., Marin, J.J., 2006. Antiviral effect of artemisinin from Artemisia annua against a model member of the Flaviviridae family, the bovine viral diarrhoea virus (BVDV). Planta Medica 72, 1169-1174.

Rose, S.D., Kim, D.-H., Amarzguioui, M., Heidel, J.D., Collingwood, M.A., Davis, M.E., Rossi, J.J., Behlke, M.A., 2005. Functional polarity is introduced by Dicer processing of short substrate RNAs. Nucleic Acids Research 33, 4140-4156.

Rossen, J.W.A., Horzinek, M.C., Rottier, P.J.M., 1995. Coronavirus infection of polarized epithelial cells. Trends in Microbiology 3, 486-490.

Rossen, J.W.A., Kouame, J., Goedheer, A.J.W., Vennema, H., Rottier, P.J.M., 2001. Feline and canine coronaviruses are released from the basolateral side of polarized epithelial LLC-PK1 cells expressing the recombinant feline aminopeptidase-N cDNA. Archives of Virology 146, 791-799.

Rottier, P.J.M., Nakamura, K., Schellen, P., Volders, H., Haijema, B.J., 2005. Acquisition of macrophage tropism during the pathogenesis of feline infectious peritonitis is determined by mutations in the feline coronavirus spike protein. Journal of Virology 79, 14122-14130.

Rozen, S., Skaletsky, H.J. 2000. Primer3 on the WWW for general users and biologist programmers, In: Krawetz, S., Misener, S. (Eds.) Bioinformatics Methods and Protocols: Methods in Molecular Biology. Humana Press, Totowa, NJ, 365-386.

Sadler, A.J., Williams, B.R., 2008. Interferon-inducible antiviral effectors. Nature Reviews Immunology 8, 559-568.
Salomon, W., Bulock, K., Lapierre, J., Pavco, P., Woolf, T., Kamens, J., 2010. Modified dsRNAs that are not processed by Dicer maintain potency and are incorporated into the RISC. Nucleic Acids Research 38, 3771-3779.
Sanjuán, R., Nebot, M.R., Chirico, N., Mansky, L.M., Belshaw, R., 2010. Viral mutation rates. Journal of Virology 84, 9733-9748.
Sarker, S.D., Nahar, L., Kumarasamy, Y., 2007. Microtitre plate-based antibacterial assay incorporating resazurin as an indicator of cell growth, and its application in the< i> in vitro</i> antibacterial screening of phytochemicals. Methods 42, 321-324.
Sato, R., Inanami, O., Tanaka, Y., Takase, M., Naito, Y., 1996. Oral administration of bovine lactoferrin for treatment of intractable stomatitis in feline immunodeficiency virus (FIV)-positive and FIV-negative cats. American Journal of Veterinary Research 57, 1443-1446.
Sato, Y., Ohe, K., Murakami, M., Fukuyama, M., Furuhata, K., Kishikawa, S., Suzuki, Y., Kiuchi, A., Hara, M., Ishikawa, Y., Taneno, A., 2002. Phylogenetic analysis of field isolates of feline calicivirus (FCV) in Japan by sequencing part of its capsid gene. Veterinary Research Communications 26, 205-219.
Satoh, R., Furukawa, T., Kotake, M., Takano, T., Motokawa, K., Gemma, T., Watanabe, R., Arai, S., Hohdatsu, T., 2011. Screening and identification of T helper 1 and linear immunodominant antibody-binding epitopes in the spike 2 domain and the nucleocapsid protein of feline infectious peritonitis virus. Vaccine 29, 1791-1800.
Savarino, A., Boelaert, J.R., Cassone, A., Majori, G., Cauda, R., 2003. Effects of chloroquine on viral infections: an old drug against today's diseases. The Lancet Infectious Diseases 3, 722-727.
Savarino, A., Gennero, L., Sperber, K., Boelaert, J., 2001. The anti-HIV-1 activity of chloroquine. Journal of Clinical Virology 20, 131-135.
Savarino, A., Lucia, M.B., Rastrelli, E., Rutella, S., Golotta, C., Morra, E., Tamburrini, E., Perno, C.F., Boelaert, J.R., Sperber, K., 2004. Anti-HIV effects of chloroquine: inhibition of viral particle glycosylation and synergism with protease inhibitors. Journal of Acquired Immune Deficiency Syndromes 35, 223-232.
Sawicki, S.G., Sawicki, D.L., 1995. Coronaviruses use discontinuous extension for synthesis of subgenome-length negative strands. Advances in Experimental Medicine & Biology 380, 499-506.
Sawicki, S.G., Sawicki, D.L., Siddell, S.G., 2007. A contemporary view of coronavirus transcription. Journal of Virology 81, 20-29.
Schaffer, D.V., Leonard, J.N., Shah, P.S., Burnett, J.C., 2008. HIV evades RNA interference directed at TAR by an indirect compensatory mechanism. Cell Host & microbe 4, 484-494.
Scholtissek, C., Müller, K., 1988. Effect of dimethylsulfoxide (DMSO) on virus replication and maturation. Archives of Virology 100, 27-35.
Schopman, N.C., ter Brake, O., Berkhout, B., 2010. Research anticipating and blocking HIV-1 escape by second generation antiviral shRNAs.
Schorr-Evans, E.M., Poland, A., Johnson, W.E., Pedersen, N.C., 2003. An epizootic of highly virulent feline calicivirus disease in a hospital setting in New England. Journal of Feline Medicine and Surgery 5, 217-226.

Schubert, S., Grunert, H.P., Zeichhardt, H., Werk, D., Erdmann, V.A., Kurreck, J., 2005. Maintaining inhibition: siRNA double expression vectors against coxsackieviral RNAs. Journal of Molecular Biology 346, 457-465.

Schulz, B.S., Hartmann, K., Unterer, S., Eichhorn, W., Majzoub, M., Homeier-Bachmann, T., Truyen, U., Ellenberger, C., Huebner, J., 2011. Two outbreaks of virulent systemic feline calicivirus infection in cats in Germany. Berliner und Munchener Tierarztliche Wochenschrift 124, 186-193.

Scott, F.W. 1988. Update on FIP, In: Proceedings of the Kal Kan Symposium for the Treatment of Small Animal Diseases. 43-47.

Scott, F.W., Olsen, C.W., Corapi, W.V., 1995. Antibody-dependent enhancement of feline infectious peritonitis virus infection. Feline Practice 23, 77-79.

Seal, B.S., Ridpath, J.F., Mengeling, W.L., 1993. Analysis of feline calicivirus capsid protein genes: identification of variable antigenic determinant regions of the protein. Journal of General Virology 74, 2519-2524.

Seto, D., 2010. Viral genomics and bioinformatics. Viruses 2, 2587-2593.

Severson, W.E., Shindo, N., Sosa, M., Fletcher, T., White, E.L., Ananthan, S., Jonsson, C.B., 2007. Development and validation of a high-throughput screen for inhibitors of SARS CoV and its application in screening of a 100,000-compound library. Journal of Biomolecular Screening 12, 33-40.

Shabalina, S., Koonin, E., 2008. Origins and evolution of eukaryotic RNA interference. Trends in Ecology & Evolution 23, 578-587.

Shafer, R., Vuitton, D., 1999. Highly active antiretroviral therapy (HAART) for the treatment of infection with human immunodeficiency virus type 1. Biomedicine & Pharmacotherapy 53, 73-86.

Shao, Y., Chan, C., Maliyekkel, A., Lawrence, C., Roninson, I., Ding, Y., 2007. Effect of target secondary structure on RNAi efficiency. RNA 13, 1631.

Sharma, V., McNeill, J.H., 2009. To scale or not to scale: the principles of dose extrapolation. British Journal of Pharmacology 157, 907-921.

Shi, J., Wang, M., Wang, J., Wang, S., Luo, E., 2011. Comparison of inhibitory efficacy of short interfering RNAs targeting different genes on Measles virus replication. Journal of Basic Microbiology.

Shim, M.S., Kwon, Y.J., 2010. Efficient and targeted delivery of siRNA in vivo. FEBS Journal 277, 4814-4827.

Shimizu, Y., Yamamoto, S., Homma, M., Ishida, N., 1972. Effect of chloroquine on the growth of animal viruses. Arch Gesamte Virusforsch 36, 93-104.

Shum, D., Smith, J.L., Hirsch, A.J., Bhinder, B., Radu, C., Stein, D.A., Nelson, J.A., Fruh, K., Djaballah, H., 2010. High-content assay to identify inhibitors of dengue virus infection. Assay and Drug Development Technologies 8, 553-570.

Sidahmed, A.M.E., Wilkie, B., 2010. Endogenous antiviral mechanisms of RNA interference: a comparative biology perspective. Methods in Molecular Biology 623, 3-19.

Sigma-Aldrich.

Simmonds, P., Karakasiliotis, I., Bailey, D., Chaudhry, Y., Evans, D.J., Goodfellow, I.G., 2008. Bioinformatic and functional analysis of RNA secondary structure elements among different genera of human and animal caliciviruses. Nucleic Acids Research 36, 2530-2546.

Simons, F.A., Vennema, H., Rofina, J.E., Pol, J.M., Horzinek, M.C., Rottier, P.J.M., Egberink, H.F., 2005. A mRNA PCR for the diagnosis of feline infectious peritonitis. Journal of Virological Methods 124, 111-116.

Simpson, J.A., Price, R., ter Kuile, F., Teja-Isavatharm, P., Nosten, F., Chongsuphajaisiddhi, T., Looareesuwan, S., Aarons, L., White, N.J., 1999. Population pharmacokinetics of mefloquine in patients with acute falciparum malaria&ast. Clinical Pharmacology & Therapeutics 66, 472-484.

Sioud, M., 2005. Induction of inflammatory cytokines and interferon responses by double-stranded and single-stranded siRNAs is sequence-dependent and requires endosomal localization. Journal of Molecular Biology 348, 1079-1090.

Sioud, M., Furset, G., 2006. Molecular basis for the immunostimulatory potency of small interfering RNAs. Journal of Biomedicine and Biotechnology.

Sittampalam, G.S., Gal-Edd, N., Arkin, M., Auld, D., Austin, C., Bejcek, B., Glicksman, M., Inglese, J., Lemmon, V., Li, Z., 2013. Cell Viability Assays.

Skehan, P., Storeng, R., Scudiero, D., Monks, A., McMahon, J., Vistica, D., Warren, J.T., Bokesch, H., Kenney, S., Boyd, M.R., 1990. New colorimetric cytotoxicity assay for anticancer-drug screening. Journal of the National Cancer Institute 82, 1107-1112.

Smith, A.W., Iversen, P.L., O'Hanley, P.D., Skilling, D.E., Christensen, J.R., Weaver, S.S., Longley, K., Stone, M.A., Poet, S.E., Matson, D.O., 2008. Virus-specific antiviral treatment for controlling severe and fatal outbreaks of feline calicivirus infection. American Journal of Veterinary Research 69, 23-32.

Smith, E.C., Blanc, H., Vignuzzi, M., Denison, M.R., 2013. Coronaviruses lacking exoribonuclease activity are susceptible to lethal mutagenesis: evidence for proofreading and potential therapeutics. PLoS Pathogens 9, e1003565.

Snead, N.M., Wu, X., Li, A., Cui, Q., Sakurai, K., Burnett, J.C., Rossi, J.J., 2013. Molecular basis for improved gene silencing by Dicer substrate interfering RNA compared with other siRNA variants. Nucleic Acids Research.

Snell, N.J., 2001. Ribavirin--current status of a broad spectrum antiviral agent. Expert Opinion on Pharmacotherapy 2, 1317-1324.

Sosnovtsev, S.V., Belliot, G., Chang, K.-O., Onwudiwe, O., Green, K.Y., 2005. Feline calicivirus VP2 is essential for the production of infectious virions. Journal of Virology 79, 4012-4024.

Sosnovtsev, S.V., Garfield, M., Green, K.Y., 2002. Processing map and essential cleavage sites of the nonstructural polyprotein encoded by ORF1 of the feline calicivirus genome. Journal of Virology 76, 7060-7072.

Sosnovtsev, S.V., Green, K.Y., 2000. Identification and genomic mapping of the ORF3 and VPg proteins in feline calicivirus virions. Virology 277, 193-203.

Sosnovtsev, S.V., Sosnovtseva, S.A., Green, K.Y., 1998. Cleavage of the feline calicivirus capsid precursor is mediated by a virus-encoded proteinase. Journal of Virology 72, 3051-3059.

Sousa, S.F., Cerqueira, N.M.F.S.A., Fernandes, P.A., Ramos, M.J., 2010. Virtual screening in drug design and development. Combinatorial Chemistry & High Throughput Screening 13, 442-453.

Southerden, P., Gorrel, C., 2007. Treatment of a case of refractory feline chronic gingivostomatitis with feline recombinant interferon omega. Journal of Small Animal Practice 48, 104-106.

Sparkes, A.H., Gruffydd-Jones, T.J., Howard, P.E., Harbour, D.A., 1992. Coronavirus serology in healthy pedigree cats. Veterinary Record 131, 35-36.

Spruance, S., McKeough, M., Cardinal, J., 1983. Dimethyl sulfoxide as a vehicle for topical antiviral chemotherapy. Annals of the New York Academy of Sciences 411, 28-33.

Stein, D.A., Skilling, D.E., Iversen, P.L., Smith, A.W., 2001. Inhibition of Vesivirus infections in mammalian tissue culture with antisense morpholino oligomers. Antisense and Nucleic Acid Drug Development 11, 317-325.
Stewart, C.R., Karpala, A.J., Lowther, S., Lowenthal, J.W., Bean, A.G., 2011. Immunostimulatory motifs enhance antiviral siRNAs targeting highly pathogenic avian influenza H5N1. PLoS One 6, e21552.
Stoddart, C.A., Scott, F.W., 1989. Intrinsic resistance of feline peritoneal macrophages to coronavirus infection correlated with in vivo virulence. Journal of Virology 63, 436-440.
Stoddart, M.E., Gaskell, R.M., Harbour, D.A., Gaskell, C.J., 1988. Virus shedding and immune responses in cats inoculated with cell culture-adapted feline infectious peritonitis virus. Veterinary Microbiology 16, 145-158.
Stuart, A.D., Brown, T.D.K., 2006. Entry of feline calicivirus is dependent on clathrin-mediated endocytosis and acidification in endosomes. Journal of Virology 80, 7500-7509.
Stuart, A.D., Brown, T.D.K., 2007. alpha 2,6-linked sialic acid acts as a receptor for Feline calicivirus. Journal of General Virology 88, 177-186.
Suikkanen, S., Antila, M., Jaatinen, A., Vihinen-Ranta, M., Vuento, M., 2003. Release of canine parvovirus from endocytic vesicles. Virology 316, 267-280.
Summerton, J., 1999. Morpholino antisense oligomers: the case for an RNase H-independent structural type. Biochimica et Biophysica Acta (BBA)-Gene Structure and Expression 1489, 141-158.
Sun, L., Hemgard, G.V., Susanto, S.A., Wirth, M., 2010. Caveolin-1 influences human influenza A virus (H1N1) multiplication in cell culture. Virology Journal 7, 108.
Tahara, S., Dietlin, T., Bergmann, C., Nelson, G., Kyuwa, S., Anthony, R., Stohlman, S., 1994. Coronavirus translational regulation: leader affects mRNA efficiency. Virology 202, 621-630.
Tahara, S.M., Dietlin, T.A., Nelson, G.W., Stohlman, S.A., Manno, D.J., 1998. Mouse hepatitis virus nucleocapsid protein as a translational effector of viral mRNAs. Advances in Experimental Medicine and Biology 440, 313-318.
Taharaguchi, S., Matsuhiro, T., Harima, H., Sato, A., Ohe, K., Sakai, S., Takahashi, T., Hara, M., 2012. Suppression of feline calicivirus replication using small interfering RNA targeted to its polymerase gene. Biocontrol Science 17, 87-91.
Taira, O., Suzuki, M., Takeuchi, Y., Aramaki, Y., Sakurai, I., Watanabe, T., Motokawa, K., Arai, S., Sato, H., Maehara, N., 2005. Expression of feline interferon-alpha subtypes in Esherichia coli, and their antiviral activity and animal species specificity. The Journal of Veterinary Medical Science 67, 543-545.
Takahashi, M., Nagai, C., Hatakeyama, H., Minakawa, N., Harashima, H., Matsuda, A., 2012. Intracellular stability of 2′-OMe-4′-thioribonucleoside modified siRNA leads to long-term RNAi effect. Nucleic Acids Research 40, 5787-5793.
Takano, T., Azuma, N., Hashida, Y., Satoh, R., Hohdatsu, T., 2009. B-cell activation in cats with feline infectious peritonitis (FIP) by FIP-virus-induced B-cell differentiation/survival factors. Archives of Virology 154, 27-35.
Takano, T., Hohdatsu, T., Hashida, Y., Kaneko, Y., Tanabe, M., Koyama, H., 2007a. A "possible" involvement of TNF-alpha in apoptosis induction in peripheral blood lymphocytes of cats with feline infectious peritonitis. Veterinary Microbiology 119, 121-131.
Takano, T., Hohdatsu, T., Toda, A., Tanabe, M., Koyama, H., 2007b. TNF-alpha, produced by feline infectious peritonitis virus (FIPV)-infected macrophages,

upregulates expression of type II FIPV receptor feline aminopeptidase N in feline macrophages. Virology 364, 64-72.
Takano, T., Katada, Y., Moritoh, S., Ogasawara, M., Satoh, K., Satoh, R., Tanabe, M., Hohdatsu, T., 2008a. Analysis of the mechanism of antibody-dependent enhancement of feline infectious peritonitis virus infection: aminopeptidase N is not important and a process of acidification of the endosome is necessary. Journal of General Virology 89, 1025-1029.
Takano, T., Katoh, Y., Doki, T., Hohdatsu, T., 2013. Effect of chloroquine on feline infectious peritonitis virus infection in vitro and in vivo. Antiviral Research.
Takano, T., Kawakami, C., Yamada, S., Satoh, R., Hohdatsu, T., 2008b. Antibody-dependent enhancement occurs upon re-infection with the identical serotype virus in feline infectious peritonitis virus infection. The Journal of Veterinary Medical Science 70, 1315-1321.
Talekar, A., Pessi, A., Glickman, F., Sengupta, U., Briese, T., Whitt, M.A., Mathieu, C., Horvat, B., Moscona, A., Porotto, M., 2012. Rapid Screening for Entry Inhibitors of Highly Pathogenic Viruses under Low-Level Biocontainment. PLoS One 7, e30538.
Tan, E.L.C., Ooi, E.E., Lin, C.-Y., Tan, H.C., Ling, A.E., Lim, B., Stanton, L.W., 2004. Inhibition of SARS coronavirus infection in vitro with clinically approved antiviral drugs. Emerging Infectious Diseases 10, 581-586.
Tanabe, T., Yamamoto, J.K., 2001. Feline immunodeficiency virus lacks sensitivity to the antiviral activity of feline IFN-gamma. Journal of Interferon & Cytokine Research 21, 1039-1046.
Taylor, W.R.J., White, N.J., 2004. Antimalarial drug toxicity. Drug Safety 27, 25-61.
Tekes, G., Hofmann-Lehmann, R., Bank-Wolf, B., Maier, R., Thiel, H., Thiel, V., 2010. Chimeric feline coronaviruses that encode Type II spike protein on type I genetic background display accelerated viral growth and altered receptor usage. Journal of Virology 84, 1326-1333.
Tekes, G., Hofmann-Lehmann, R., Stallkamp, I., Thiel, V., Thiel, H.J., 2008. Genome organization and reverse genetic analysis of a type I feline coronavirus. Journal of Virology 82, 1851-1859.
ter Brake, O., Karen't Hooft, Y.P.L., Centlivre, M., von Eije, K.J., Berkhout, B., 2008. Lentiviral vector design for multiple shRNA expression and durable HIV-1 inhibition. Molecular Therapy 16, 557-564.
ter Brake, O., Konstantinova, P., Ceylan, M., Berkhout, B., 2004. Silencing of HIV-1 with RNA interference: a multiple shRNA approach. Molecular Therapy 14, 883-892.
TerWee, J., Lauritzen, A.Y., Sabara, M., Dreier, K.J., Kokjohn, K., 1997. Comparison of the primary signs induced by experimental exposure to either a pneumotrophic or a 'limping' strain of feline calicivirus. Veterinary Microbiology 56, 33-45.
Thibaut, H.J., De Palma, A.M., Neyts, J., 2012. Combating enterovirus replication: state-of-the-art on antiviral research. Biochemical Pharmacology 83, 185-192.
Thomasy, S.M., Lim, C.C., Reilly, C.M., Kass, P.H., Lappin, M.R., Maggs, D.J., 2011. Evaluation of orally administered famciclovir in cats experimentally infected with feline herpesvirus type-1. American Journal of Veterinary Research 72, 85-95.
Thompson, R., Wilcox, G., Clark, W., Jansen, K., 1984. Association of calicivirus infection with chronic gingivitis and pharyngitis in cats. Journal of Small Animal Practice 25, 207-210.

Thumfart, J.O., Meyers, G., 2002. Feline calicivirus: recovery of wild-type and recombinant viruses after transfection of cRNA or cDNA constructs. Journal of Virology 76, 6398-6407.
Tompkins, S.M., Lo, C.-Y., Tumpey, T.M., Epstein, S.L., 2004. Protection against lethal influenza virus challenge by RNA interference in vivo. Proceedings of the National Academy of Sciences 101, 8682-8686.
Tong, T.R., 2009a. Therapies for coronaviruses. Part 2: Inhibitors of intracellular life cycle. Expert Opinion on Therapeutic Patents 19, 415-431.
Tong, T.R., 2009b. Therapies for coronaviruses. Part I of II - viral entry inhibitors. Expert Opinion on Therapeutic Patents 19, 357-367.
Tresnan, D.B., Levis, R., Holmes, K.V., 1996. Feline aminopeptidase N serves as a receptor for feline, canine, porcine, and human coronaviruses in serogroup I. Journal of Virology 70, 8669-8674.
Tricou, V., Minh, N.N., Van, T.P., Lee, S.J., Farrar, J., Wills, B., Tran, H.T., Simmons, C.P., 2010. A randomized controlled trial of chloroquine for the treatment of dengue in Vietnamese adults. PLoS Neglected Tropical Diseases 4, e785.
Truyen, U., Blewaska, S., Schultheiss, U., 2002. Antiviral potency of interferon-omega (IFN-omega) against selected canine and feline viruses. Praktische Tierarzt 83, 862-865.
Truyen, U., Geissler, K., Hirschberger, J., 1999. Tissue distribution of virus replication in cats experimentally infected with distinct feline calicivirus isolates. Berliner und Munchener Tierarztliche Wochenschrift 112, 355-358.
Tschuch, C., Schulz, A., Pscherer, A., Werft, W., Benner, A., Hotz-Wagenblatt, A., Barrionuevo, L., Lichter, P., Mertens, D., 2008. Off-target effects of siRNA specific for GFP. BMC Molecular Biology 9, 60.
Twigg, R., 1945. Oxidation-reduction aspects of resazurin. Nature 155, 401-402.
Umbach, J., Cullen, B., 2009. The role of RNAi and microRNAs in animal virus replication and antiviral immunity. Genes & Development 23, 1151.
van de Waterbeemd, H., Gifford, E., 2003. ADMET in silico modelling: Towards prediction paradise? Nature Reviews Drug Discovery 2, 192-204.
van der Meer, F.J., de Haan, C.A., Schuurman, N.M., Haijema, B.J., Peumans, W.J., Van Damme, E.J., Delputte, P.L., Balzarini, J., Egberink, H.F., 2007. Antiviral activity of carbohydrate-binding agents against Nidovirales in cell culture. Antiviral Research 76, 21-29.
van der Meer, Y., Snijder, E., Dobbe, J., Schleich, S., Denison, M., Spaan, W., Locker, J., 1999. Localization of mouse hepatitis virus nonstructural proteins and RNA synthesis indicates a role for late endosomes in viral replication. Journal of Virology 73, 7641-7657.
Van Hamme, E., Desmarets, L., Dewerchin, H.L., Nauwynck, H.J., 2011. Intriguing interplay between feline infectious peritonitis virus and its receptors during entry in primary feline monocytes. Virus Research 160, 32-39.
Van Hamme, E., Dewerchin, H., Cornelissen, E., Verhasselt, B., Nauwynck, H., 2008. Clathrin-and caveolae-independent entry of feline infectious peritonitis virus in monocytes depends on dynamin. Journal of General Virology 89, 2147-2156.
Van Hamme, E., Dewerchin, H.L., Cornelissen, E., Nauwynck, H.J., 2007. Attachment and internalization of feline infectious peritonitis virus in feline blood monocytes and Crandell feline kidney cells. Journal of General Virology 88, 2527-2532.
Van Marle, G., Luytjes, W., Van der Most, R., Van der Straaten, T., Spaan, W., 1995. Regulation of coronavirus mRNA transcription. Journal of Virology 69, 7851-7856.

Veldhoen, S., Laufer, S.D., Trampe, A., Restle, T., 2006. Cellular delivery of small interfering RNA by a non-covalently attached cell-penetrating peptide: quantitative analysis of uptake and biological effect. Nucleic Acids Research 34, 6561-6573.

Vennema, H., Godeke, G., Rossen, J., Voorhout, W., Horzinek, M., Opstelten, D., Rottier, P., 1996. Nucleocapsid-independent assembly of coronavirus-like particles by co-expression of viral envelope protein genes. The EMBO Journal 15, 2020-2028.

Vennema, H., Poland, A., Foley, J., Pedersen, N.C., 1998. Feline infectious peritonitis viruses arise by mutation from endemic feline enteric coronaviruses. Virology 243, 150-157.

Vichai, V., Kirtikara, K., 2006. Sulforhodamine B colorimetric assay for cytotoxicity screening. Nature Protocols 1, 1112-1116.

Vigerust, D.J., McCullers, J.A., 2007. Chloroquine is effective against influenza A virus in vitro but not in vivo. Influenza and Other Respiratory Viruses 1, 189-192.

Vigne, S., Duraffour, S., Andrei, G., Snoeck, R., Garin, D., Crance, J.-M., 2009. Inhibition of vaccinia virus replication by two small interfering RNAs targeting B1R and G7L genes and their synergistic combination with cidofovir. Antimicrobial Agents and Chemotherapy 53, 2579-2588.

Vincent, M.J., Bergeron, E., Benjannet, S., Erickson, B.R., Rollin, P.E., Ksiazek, T.G., Seidah, N.G., Nichol, S.T., 2005. Chloroquine is a potent inhibitor of SARS coronavirus infection and spread. Virology Journal 2, 69.

Voigt, W., 2005. Sulforhodamine B assay and chemosensitivity. Methods in Molecular Medicine 110, 39-48.

von Itzstein, M., 2007. The war against influenza: discovery and development of sialidase inhibitors. Nature Reviews Drug Discovery 6, 967-974.

Wang, K., Xie, S., Sun, B., 2011. Viral proteins function as ion channels. Biochimica et Biophysica Acta 1808, 510-515.

Wang, Q., Contag, C.H., Ilves, H., Johnston, B.H., Kaspar, R.L., 2005. Small hairpin RNAs efficiently inhibit hepatitis C IRES-mediated gene expression in human tissue culture cells and a mouse model. Molecular Therapy 12, 562-568.

Ward, V.K., Cooke, B.D., Strive, T. 2010. Rabbit haemorrhagic disease virus and other lagoviruses, In: Hansman, G.S., Jiang, X.J., Green, K.Y. (Eds.) Caliciviruses: Molecular and cellular virology. Caister Academic Press, Norfolk, UK, 223-245.

Wardley, R., Gaskell, R.M., Povey, R., 1974. Feline respiratory viruses—their prevalence in clinically healthy cats. Journal of Small Animal Practice 15, 579-586.

Wardley, R.C., Povey, R.C., 1977a. Aerosol transmission of feline calciciviruses. An assessment of its epidemiological importance. British Veterinary Journal 133, 504-508.

Wardley, R.C., Povey, R.C., 1977b. The clinical disease and patterns of excretion associated with three different strains of feline caliciviruses. Research in Veterinary Science 23, 7-14.

Watari, T., Kaneshima, T., Tsujimoto, H., Ono, K., Hasegawa, A., 1998. Effect of thromboxane synthetase inhibitor on feline infectious peritonitis in cats. The Journal of Veterinary Medical Science 60, 657-659.

Weber, F., Wagner, V., Rasmussen, S.B., Hartmann, R., Paludan, S.R., 2006. Double-stranded RNA is produced by positive-strand RNA viruses and DNA

viruses but not in detectable amounts by negative-strand RNA viruses. Journal of Virology 80, 5059-5064.
Wei, L., Huhn, J.S., Mory, A., Pathak, H.B., Sosnovtsev, S.V., Green, K.Y., Cameron, C.E., 2001. Proteinase-polymerase precursor as the active form of feline calicivirus RNA-dependent RNA polymerase. Journal of Virology 75, 1211-1219.
Weinberg, E.D., 2003. The therapeutic potential of lactoferrin. Expert Opinion on Investigational Drugs 12, 841-851.
Weiss, R., Scott, F.W., 1981a. Pathogenesis of feline infectious peritonitis: pathologic changes and immunofluorescence. American Journal of Veterinary Research 42, 2036-2048.
Weiss, R.C., 1995. Treatment of feline infectious peritonitis with immunomodulating agents and antiviral drugs: a review. Feline Practice 23, 103-106.
Weiss, R.C., Cox, N.R., 1989. Evaluation of immunity to feline infectious peritonitis in cats with cutaneous viral-induced delayed hypersensitivity. Veterinary Immunology and Immunopathology 21, 293-309.
Weiss, R.C., Cox, N.R., Boudreaux, M.K., 1993a. Toxicologic effects of ribavirin in cats. Journal of Veterinary Pharmacology and Therapeutics 16, 301-316.
Weiss, R.C., Cox, N.R., Martinez, M.L., 1993b. Evaluation of free or liposome-encapsulated ribavirin for antiviral therapy of experimentally induced feline infectious peritonitis. Research in Veterinary Science 55, 162-172.
Weiss, R.C., Cox, N.R., Oostrom-Ram, T., 1990. Effect of interferon or Propionibacterium acnes on the course of experimentally induced feline infectious peritonitis in specific-pathogen-free and random-source cats. American Journal of Veterinary Research 51, 726-733.
Weiss, R.C., Oostrom-Ram, T., 1989. Inhibitory effects of ribavirin alone or combined with human alpha interferon on feline infectious peritonitis virus replication in vitro. Veterinary Microbiology 20, 255-265.
Weiss, R.C., Scott, F.W., 1981b. Antibody-mediated enhancement of disease in feline infectious peritonitis: comparisons with dengue hemorrhagic fever. Comparative Immunology, Microbiology and Infectious Diseases 4, 175-189.
Wen, C.C., Kuo, Y.H., Jan, J.T., Liang, P.H., Wang, S.Y., Liu, H.G., Lee, C.K., Chang, S.T., Kuo, C.J., Lee, S.S., Hou, C.C., Hsiao, P.W., Chien, S.C., Shyur, L.F., Yang, N.S., 2007. Specific plant terpenoids and lignoids possess potent antiviral activities against severe acute respiratory syndrome coronavirus. Journal of Medicinal Chemistry 50, 4087-4095.
Wentworth, D.E., Holmes, K.V., 2001. Molecular determinants of species specificity in the coronavirus receptor aminopeptidase N (CD13): influence of N-linked glycosylation. Journal of Virology 75, 9741-9752.
Wentworth, D.E., Holmes, K.V. 2007. Coronavirus Binding and Entry, In: Thiel, V. (Ed.) Coronaviruses: Molecular and Cellular Biology. Caister Academic Press, Norflok, UK, 3-31.
Westerhout, E.M., Ooms, M., Vink, M., Das, A.T., Berkhout, B., 2005. HIV-1 can escape from RNA interference by evolving an alternative structure in its RNA genome. Nucleic Acids Research 33, 796-804.
White, L.K., Yoon, J.J., Lee, J.K., Sun, A.M., Du, Y.H., Fu, H., Snyder, J.P., Plemper, R.K., 2007. Nonnucleoside inhibitor of measles virus RNA-Dependent RNA polymerase complex activity. Antimicrobial Agents and Chemotherapy 51, 2293-2303.

White, S.D., Rosychuk, R.A., Janik, T.A., Denerolle, P., Schultheiss, P., 1992. Plasma cell stomatitis-pharyngitis in cats: 40 cases (1973-1991). Journal of the American Veterinary Medical Association 200, 1377-1380.
Whitehead, K.A., Langer, R., Anderson, D.G., 2009. Knocking down barriers: advances in siRNA delivery. Nature Reviews Drug Discovery 8, 129-138.
Wilhelmi, I., Roman, E., Sanchez-Fauquier, A., 2003. Viruses causing gastroenteritis. Clinical Microbiology and Infection 9, 247-262.
Wilkes, R.P., Kania, S.A., 2009. Use of interfering RNAs targeted against feline herpesvirus 1 glycoprotein D for inhibition of feline herpesvirus 1 infection of feline kidney cells. American Journal of Veterinary Research 70, 1018-1025.
Wilkes, R.P., Kania, S.A., 2010. Evaluation of the effects of small interfering RNAs on in vitro replication of feline herpesvirus-1. American Journal of Veterinary Research 71, 655-663.
Willoughby, K., 1989. Lameness in Kittens after Vaccination. Veterinary Record 125, 609-609.
Wilson, J.A., Richardson, C.D., 2005. Hepatitis C virus replicons escape RNA interference induced by a short interfering RNA directed against the NS5b coding region. Journal of Virology 79, 7050-7058.
Wilson, L., Gage, P., Ewart, G., 2006a. Hexamethylene amiloride blocks E protein ion channels and inhibits coronavirus replication. Virology 353, 294-306.
Wilson, L., Gage, P., Ewart, G., 2006b. Validation of coronavirus E proteins ion channels as targets for antiviral drugs. Advances in Experimental Medicine and Biology 581, 573-578.
Wlodawer, A., Vondrasek, J., 1998. Inhibitors of HIV-1 protease: a major success of structure-assisted drug design. Annual Review of Biophysics and Biomolecular Structure 27, 249-284.
Worthing , K.A., Wigney, D.I., Dhand, N.K., Fawcett, A., McDonagh, P., Malik, R., Norris, J.M., 2012. Risk factors for feline infectious peritonitis in Australian cats. Journal of Feline Medicine and Surgery 14, 405-412.
Wu, C., Huang, H., Liu, C., Hong, C., Chan, Y., 2005a. Inhibition of SARS-CoV replication by siRNA. Antiviral Research 65, 45-48.
Wu, C.J., Jan, J.T., Chen, C.M., Hsieh, H.P., Hwang, D.R., Liu, H.W., Liu, C.Y., Huang, H.W., Chen, S.C., Hong, C.F., Lin, R.K., Chao, Y.S., Hsu, J.T., 2004. Inhibition of severe acute respiratory syndrome coronavirus replication by niclosamide. Antimicrobial Agents and Chemotherapy 48, 2693-2696.
Wu, H.-L., Huang, L.-R., Huang, C.-C., Lai, H.-L., Liu, C.-J., Huang, Y.-T., Hsu, Y.-W., Lu, C.-Y., Chen, D.-S., Chen, P.-J., 2005b. RNA interference-mediated control of hepatitis B virus and emergence of resistant mutant. Gastroenterology 128, 708-716.
Wu, Y., Navarro, F., Lal, A., Basar, E., Pandey, R.K., Manoharan, M., Feng, Y., Lee, S.J., Lieberman, J., Palliser, D., 2009. Durable protection from Herpes Simplex Virus-2 transmission following intravaginal application of siRNAs targeting both a viral and host gene. Cell Host & Microbe 5, 84-94.
Wu, Y.S., Lin, W.H., Hsu, J.T., Hsieh, H.P., 2006. Antiviral drug discovery against SARS-CoV. Current Medicinal Chemistry 13, 2003-2020.
Wu, Z., Xue, Y., Wang, B., Du, J., Jin, Q., 2011. Broad-spectrum antiviral activity of RNA interference against four genotypes of Japanese encephalitis virus based on single microRNA polycistrons. PLoS One 6, e26304.
Ye, Y., Hogue, B.G., 2007. Role of the coronavirus E viroporin protein transmembrane domain in virus assembly. Journal of Virology 81, 3597-3607.

Yokomori, K., Lai, M.M., 1992. The receptor for mouse hepatitis virus in the resistant mouse strain SJL is functional: implications for the requirement of a second factor for viral infection. Journal of Virology 66, 6931-6938.

Yu, Z., Quinn, P., 1994. Dimethyl sulphoxide: a review of its applications in cell biology. Bioscience Reports 14, 259-281.

Zandi, K., Teoh, B.T., Sam, S.S., Wong, P.F., Mustafa, M.R., Abubakar, S., 2011. Antiviral activity of four types of bioflavonoid against dengue virus type-2. Virology Journal 8, 560.

Zeidner, N.S., Myles, M.H., Mathiason-DuBard, C.K., Dreitz, M.J., Mullins, J.I., Hoover, E.A., 1990. Alpha interferon (2b) in combination with zidovudine for the treatment of presymptomatic feline leukemia virus-induced immunodeficiency syndrome. Antimicrobial Agents and Chemotherapy 34, 1749-1756.

Zhang, J., Yamada, O., Sakamoto, T., Yoshida, H., Iwai, T., Matsushita, Y., Shimamura, H., Araki, H., Shimotohno, K., 2004. Down-regulation of viral replication by adenoviral-mediated expression of siRNA against cellular cofactors for hepatitis C virus. Virology 320, 135-143.

Zhang, J.H., Chung, T.D.Y., Oldenburg, K.R., 1999. A simple statistical parameter for use in evaluation and validation of high throughput screening assays. Journal of Biomolecular Screening 4, 67-73.

Zhang, W., Yang, H., Kong, X., Mohapatra, S., San Juan-Vergara, H., Hellermann, G., Behera, S., Singam, R., Lockey, R.F., Mohapatra, S.S., 2005. Inhibition of respiratory syncytial virus infection with intranasal siRNA nanoparticles targeting the viral NS1 gene. Nature Medicine 11, 56-62.

Zhou, J.-f., Hua, X.-g., Cui, L., Zhu, J.-g., Miao, D.-n., Zou, Y., He, X.-z., Su, W.-g., 2007. Effective inhibition of porcine transmissible gastroenteritis virus replication in ST cells by shRNAs targeting RNA-dependent RNA polymerase gene. Antiviral Research 74, 36-42.

Zhou, J., Huang, F., Hua, X., Cui, L., Zhang, W., Shen, Y., Yan, Y., Chen, P., Ding, D., Mou, J., 2010. Inhibition of porcine transmissible gastroenteritis virus (TGEV) replication in mini-pigs by shRNA. Virus Research 149, 51-55.

Zhou, J., Rossi, J.J., 2011. Aptamer-targeted RNAi for HIV-1 therapy. Methods in Molecular Biology 721, 355-371.

Zicola, A., Saegerman, C., Quatpers, D., Viandier, J., Thiry, E., 2009. Feline herpesvirus 1 and feline calicivirus infections in a heterogeneous cat population of a rescue shelter. Journal of Feline Medicine and Surgery 11, 1023-1027.

Ziebuhr, J., Snijder, E.J. 2007. The coronavirus replicase gene: Special enzymes for special viruses, In: Thiel, V. (Ed.) Coronaviruses: Molecular and Cellular Biology. Caister Academic Press, Norflok, UK, 33-63.

Appendix 1

2% carboxymethylcellulose (CMC)	CMC	4g
	Ultrapure water	200 ml

Add 4 g CMC to 100 ml ultrapure water and mix thoroughly. Autoclave to sterilise. Once cool add 100 ml sterile ultrapure water to bring concentration to 2%. Store at 4°C for maximum time of 6 weeks.

2 x DMEM	DMEM powder (D5523)	10 g
	$NaHCO_3$	3.7 g
	Sterile ultrapure water	500 ml
	HCl / NaOH	To pH

Add reagents to approximately 400 ml ultrapure water. Once dissolved make up volume to 500 ml with ultrapure water. pH at 7.15 (pH rises 0.2 to 0.3 units after filtration). Filter sterilise with 0.22 µm filter (Corning #431118). Store at 4°C in the dark for maximum time of 6 weeks.

CMC plaque assay overlay	2X DMEM	48 ml
	FBS	2 ml
	2% CMC	45 ml
	Sterile ultrapure water	5 ml

Warm all reagents to room temperature prior to mixing. Warm to 37°C prior to adding to wells.

Agarose plaque assay overlay	2X DMEM	48 ml
	FBS	2 ml
	2% agarose	50 ml

Warm DMEM / FBS to 40°C in water bath. Microwave 2% agarose to melt and equilibrate to 40°C in water bath. Immediately prior to use mix agarose and DMEM/FBS. Allow to cool slightly prior to adding to wells.

10 x PBS (Calcium and magnesium free)	NaCl	80 g
	KCl	2 g
	Na_2HPO_4	14.4 g
	KH_2PO_4	2.4 g
	Ultrapure water	Made up to 1 L
	HCl / NaOH	To pH

Dissolve reagents in approximately 800ml ultrapure water. Once dissolved make up to 1 L with ultrapure water. pH at 7.4. Autoclave to sterilise and store at room temperature.

1 x PBS (Calcium and magnesium free)	10X PBS	100 ml
	Ultrapure water	900 ml
	HCl / NaOH	To pH

pH at 7.4. Autoclave to sterilise and store at room temperature.

TAE buffer 50 x	Tris base	121 g
	Glacial acetic acid	28.55 ml
	0.5M EDTA	50 ml
	R/O water	Made up to 500 ml

Add reagents to 400 ml R/O water. Once dissolved make up to 500 ml with R/O water. Store room temperature.

TAE buffer 1 x	50X TAE buffer	20 ml
	R/O water	980 ml

Methanol-free 10% formalin in PBS	Paraformaldehyde	4 g
	10X PBS	10 ml
	R/O water	Made up to 100 ml
	HCl / NaOH	To pH

Add 4 g paraformaldehyde to approximately 80 ml R/O water. In fume cupboard heat to 59°C in water bath for 30 min. Add NaOH dropwise to dissolve and allow to cool to room temperature. Add 10 ml 10 x PBS and make up to 100 ml with R/O water. pH 7.4. Short term storage at 4°C (< 1 week). Long term storage aliquot and store at -20°C.

Appendix 2

FCoV – full and partial genome sequences accessed April 2009

Full: EU186072, DQ848678, DQ010921, AY994055, NC_002306

Partial: AB086902 (M and N ORF), Y13901 (M and N ORF), AB086881 (N ORF)

FCoV – full genome sequences accessed July 2013

EU186072, FJ938051, DQ286389, JQ408980, GQ152141, DQ848678, DQ010921, JN634064, FJ938060, FJ938061, FJ938054, FJ938056, FJ938053, FJ938055, FJ938062, FJ938059, FJ938052, FJ938057, FJ938058, HQ012367, HQ012368, HQ392470, HQ392471, HQ012369, GU553361, GU553362, HQ012370, HQ392472, HQ012371, HQ012372, HQ392469, JN183882, JN183883, AY994055, JQ408981

FCV – full genome sequences accessed July 2011

NC_001481, M86379, U13992, D31836, AY560118, AY560116, AY560117, AY560113, AY560114, AY560115, AF109465, AF479590, DQ424892, GU214989

FCV – full genome sequences accessed February 2014

JN210890, JN210889, NC_001481, JN210886, JN210885, JN210884, JN210887, JN210888, M86379, U13992, D31836, JX519214, JX519209, JX519210, JX519211, JX519212, JX519213, AY560118, AY560116, AY560117, AY560113, AY560114, AF109465, AF479590, KC835209, DQ424892, GU214989, L40021

Appendix 3

McDonagh, P., Sheehy, P.A., and Norris, J. *In vitro* inhibition of feline coronavirus by small interfering RNA. (2011) *Veterinary Microbiology* 150 (3-4) 220-229